frontiers | Research Topics

Perspectives for marine energy in the mediterranean area volume II

Edited by
Simone Bastianoni, Riccardo Maria Pulselli, Markos Damasiotis, Maria Vittoria Struglia and Hrvoje Mikulcic

Published in
Frontiers in Energy Research

ISSN 1664-8714
ISBN 978-2-83251-397-2
DOI 10.3389/978-2-83251-397-2

About Frontiers

Frontiers is more than just an open access publisher of scholarly articles: it is a pioneering approach to the world of academia, radically improving the way scholarly research is managed. The grand vision of Frontiers is a world where all people have an equal opportunity to seek, share and generate knowledge. Frontiers provides immediate and permanent online open access to all its publications, but this alone is not enough to realize our grand goals.

Frontiers journal series

The Frontiers journal series is a multi-tier and interdisciplinary set of open-access, online journals, promising a paradigm shift from the current review, selection and dissemination processes in academic publishing. All Frontiers journals are driven by researchers for researchers; therefore, they constitute a service to the scholarly community. At the same time, the *Frontiers journal series* operates on a revolutionary invention, the tiered publishing system, initially addressing specific communities of scholars, and gradually climbing up to broader public understanding, thus serving the interests of the lay society, too.

Dedication to quality

Each Frontiers article is a landmark of the highest quality, thanks to genuinely collaborative interactions between authors and review editors, who include some of the world's best academicians. Research must be certified by peers before entering a stream of knowledge that may eventually reach the public - and shape society; therefore, Frontiers only applies the most rigorous and unbiased reviews. Frontiers revolutionizes research publishing by freely delivering the most outstanding research, evaluated with no bias from both the academic and social point of view. By applying the most advanced information technologies, Frontiers is catapulting scholarly publishing into a new generation.

What are Frontiers Research Topics?

Frontiers Research Topics are very popular trademarks of the *Frontiers journals series*: they are collections of at least ten articles, all centered on a particular subject. With their unique mix of varied contributions from Original Research to Review Articles, Frontiers Research Topics unify the most influential researchers, the latest key findings and historical advances in a hot research area.

Find out more on how to host your own Frontiers Research Topic or contribute to one as an author by contacting the Frontiers editorial office: frontiersin.org/about/contact

Perspectives for marine energy in the mediterranean area volume II

Topic editors

Simone Bastianoni — University of Siena, Italy
Riccardo Maria Pulselli — University of Florence, Italy
Markos Damasiotis — Center for Renewable Energy Sources and Saving, Greece
Maria Vittoria Struglia — Italian National Agency for New Technologies, Energy and Sustainable Economic Development (ENEA), Italy
Hrvoje Mikulcic — University of Zagreb, Croatia

Citation

Bastianoni, S., Pulselli, R. M., Damasiotis, M., Struglia, M. V., Mikulcic, H., eds. (2023). *Perspectives for marine energy in the mediterranean area volume II*. Lausanne: Frontiers Media SA. doi: 10.3389/978-2-83251-397-2

Table of contents

frontiers | Frontiers in Energy Research

TYPE Editorial
PUBLISHED 09 January 2023
DOI 10.3389/fenrg.2022.1122265

OPEN ACCESS

EDITED AND REVIEWED BY
Uwe Schröder,
University of Greifswald, Germany

*CORRESPONDENCE
Riccardo Maria Pulselli,
riccardomaria.pulselli@unifi.it

SPECIALTY SECTION
This article was submitted to Sustainable Energy Systems and Policies, a section of the journal Frontiers in Energy Research

RECEIVED 12 December 2022
ACCEPTED 22 December 2022
PUBLISHED 09 January 2023

CITATION
Struglia MV, Pulselli RM, Damasiotis M, Mikulčić H and Bastianoni S (2023), Editorial: Perspectives for marine energy in the Mediterranean area Volume II. *Front. Energy Res.* 10:1122265. doi: 10.3389/fenrg.2022.1122265

Editorial: Perspectives for marine energy in the Mediterranean area Volume II

Maria Vittoria Struglia[1], Riccardo Maria Pulselli[2]*, Markos Damasiotis[3], Hrvoje Mikulčić[4] and Simone Bastianoni[5]

[1]Climate Modeling Laboratory, Division Model and Technologies for Risk Reduction, Department for Sustainability, ENEA, Rome, Italy, [2]Department of Architecture, University of Florence, Florence, Italy, [3]Center for Renewable Energy Sources and Saving, Pikermi, Greece, [4]Faculty of Mechanical Engineering and Naval Architecture, University of Zagreb, Zagreb, Croatia, [5]Department of Earth, Environmental and Physical Sciences, University of Siena, Siena, Italy

KEYWORDS

blue energy, marine energy, Mediterranean area, sustainable development, energy transition

Editorial on the Research Topic
Perspectives for marine energy in the Mediterranean area Volume II

The need to decisively and urgently address the transition to renewable sources of energy, and the awareness that offshore energy production is not only a possibility but a concrete EU strategy has stimulated us to take a new look at the situation of offshore energy in the Mediterranean, after 3 years since the publication of the first Research Topic on the *Perspectives for Marine Energy in the Mediterranean Area*.

If in the previous Research Topic the focus had been mainly on the level of development of the technologies available for the Mediterranean Sea, in this one we focus more on the way forward for an effective introduction of these technologies in a particularly fragile and complex context such as the Mediterranean Area. Marine Renewable Energies (MREs) are still under-deployed in the Mediterranean area for many reasons, including legislative constraints, social acceptance and a lower energy availability than in the Atlantic Ocean and Northern European seas.

In this volume, we have collected eight research articles and one perspective article centered on these very Research Topic. These papers mostly stem from the activities and synthesize the results of the BLUE DEAL project, that was conceived and implemented by 12 Mediterranean partners to tackle these Research Topic and set the route for blue energy (BE) deployment in the Mediterranean area.

Two research papers deal with the application of ocean numerical models in the BE sector (Carillo et al.; Napolitano et al.). Availability of detailed short-term forecasts of the ocean main characteristics (circulation and waves) is essential for the extraction of renewable energy. Activities aimed at harvesting energy from these sources require a detailed knowledge of the marine environment, both in terms of circulation and sea state, on a variety of time scales. Multi-decadal simulations are necessary to assess the resources and their variability, and consequently to choose the best technological solutions. On the other hand, the optimization and management of the devices being deployed requires the availability of detailed and reliable short-term forecasts. The maintenance of an operative wave forecast system has produced a 7-year dataset at high spatial and temporal resolution that has been analyzed together with site theoretical productivity for three state-of-the art WECs, showing interesting potential for future deployment in several target regions.

The energy transition is a complex process that mainly involves citizens, local communities and stakeholders and must reconcile the introduction of new technologies with the already existing economic activities, managing the possible conflicts among different productive sectors and complying with environmental legislation and the integrated maritime policy.

The implementation of integrated solutions to exploit MREs requires inclusive planning practices considering different aspects regarding climate and environmental impacts, landscape compatibility, interference with other marine activities, and social acceptance that can be tackled only with an interdisciplinary approach. Although each environment represents a *unicum*, it has been shown that a replicable BE planning framework can be developed and applied to very different test cases (Pulselli et al.).

As decarbonisation is the main driver towards the energy transition, energy planning must also include the environmental performance of offshore devices. In this volume we cover this aspect with two research papers: Life Cycle Assessment methodology was used to account for their potential environmental impact, in terms of carbon footprint (t CO_2eq) for both offshore wind (Pulselli et al.) turbines and WECs (Bruno et al.).

Besides these technical aspects (e.g., resource characterization, spatial planning, LCA) human factors are equally important to achieve an energy transition that includes offshore renewables. An appropriate participatory process including all actors (e.g., policymakers, firms, citizens, and researchers) is necessary for a correct path toward decarbonisation. The results of a survey that targeted about 3,000 persons in 12 Mediterranean sites are exposed and revealed that although BE is still relatively unknown to the general public (only 42% of respondents were aware of these technologies), there was a general willingness (70%) to host one or more such installations in their areas (Betti et al.). Not surprisingly, major concerns come from the environmental and visual impact of the new installations, and a new approach and a new paradigm should be considered as it is suggested in the perspective paper included in this Research Topic. Assuming that "protecting" means preserving without banning technological evolution, seascape protection and ecological transition are not alternatives because both converge toward sustainability (Paolinelli et al.).

The picture emerging from this Research Topic of papers is that a contribution to the decarbonisation of the power generation sector can be expected to come from offshore renewables and that offshore wind power will be the main driver of these transition in the next future, especially for the Mediterranean islands (Stančin et al.). While most of the attention is concentrated on new technologies for the production of electricity, we must keep in mind that important efforts must be expected also in other sectors, like energy efficiency and decarbonisation of buildings, and in coastal cities the sea still offers important opportunities to adopt new and effective mitigation measures, such as seawater based heat pump systems (Schibuola et al.).

Author contributions

MS drafted the paper that was improved by co-authors before submission.

All authors listed have made a substantial, direct and intellectual contribution to the work, and approved it for publication.

Acknowledgments

The Research Topic originated thanks to a project funded in the framework of the program Interreg Med (2014-2023): BLUE DEAL (Grant No. 5MED18_1.1_M23_072), project co-financed by the European Regional Development Fund.

Conflict of interest

The authors declare that the research was conducted in the absence of any commercial or financial relationships that could be construed as a potential conflict of interest.

Publisher's note

frontiers | Frontiers in Energy Research

ORIGINAL RESEARCH
published: 17 May 2022
doi: 10.3389/fenrg.2022.868334

Blue Energy Spearheading the Energy Transition: The Case of Crete

Hrvoje Stančin[1], Antun Pfeifer[1], Christoforos Perakis[2], Nikolaos Stefanatos[2], Marko Damasiotis[2], Stefano Magaudda[3], Federica Di Pietrantonio[3] and Hrvoje Mikulčić[1,4]**

[1]Faculty of Mechanical Engineering and Naval Architecture, University of Zagreb, Zagreb, Croatia, [2]Centre for Renewable Energy Sources and Saving, Pikermi, Greece, [3]U-SPACE ESPAÑA, Sevilla, Spain, [4]Department of Thermal Engineering, Xi'an Jiaotong University, Xi'an, China

Decarbonization of remote or isolated island communities represents a significant challenge nowadays. Nevertheless, the environmental, economic, and social benefits seek more attention. Lately, blue energy sources, particularly offshore wind power, are gaining momentum to take the lead in the energy transition process, simultaneously offering numerous benefits for local communities and potential investors. In this research, offshore wind power is considered the main driver of the energy transition for the case of the island of Crete. The energy systems' development scenarios are developed using an energy planning model EnergyPLAN, starting from a reference model developed for the year 2017. Since the island was recently isolated without connections to the mainland grid, integrating renewable energy sources was a challenging task that led to poor energy potential exploitation. The decarbonization of the power generation sector by offshore and onshore wind and photovoltaics can only partially reduce the import dependence on fossil fuels. At the same time, more significant efforts are expected in the transport and industry sectors. With the operational interconnections, 300 MW of offshore wind capacities can be deployed, averaging annual electricity production of 1.17 TWh, satisfying around 70% of total electricity demand.

Keywords: sustainable island, blue energy, offshore wind, RES integration, decarbonization

OPEN ACCESS

Edited by:
Adrian Ilinca,
Université du Québec à Rimouski, Canada

Reviewed by:
Raquel Segurado,
University of Lisbon, Portugal
Muhammad Sufyan Javed,
Jinan University, China

****Correspondence:***
Hrvoje Stančin
hrvoje.stancin@fsb.hr
Hrvoje Mikulčić
hrvoje.mikulcic@fsb.hr

Specialty section:
This article was submitted to Sustainable Energy Systems and Policies, a section of the journal Frontiers in Energy Research

Received: *02 February 2022*
Accepted: *14 April 2022*
Published: *17 May 2022*

Citation:
Stančin H, Pfeifer A, Perakis C, Stefanatos N, Damasiotis M, Magaudda S, Di Pietrantonio F and Mikulčić H (2022) Blue Energy Spearheading the Energy Transition: The Case of Crete. Front. Energy Res. 10:868334. doi: 10.3389/fenrg.2022.868334

INTRODUCTION

Energy transition of island communities is in particular focus of energy planning activities. This is important from an environmental point of view, but it is also interesting since the island energy systems are often isolated or not sufficiently connected to the mainland. Furthermore, seasonal variation in electricity demand due to high touristic activity makes this planning process even more complicated and requires energy storage installation or leads to oversizing of renewable energy source (RES) capacities (Marczinkowski and Barros, 2020). Overestimation of installed capacities coupled with insufficient infrastructure to utilize electricity production often results in critical excess electricity production (CEEP) and significant curtailments that are not beneficial from an energy and an economic point of view (Lund et al., 2017). Therefore, when it comes to planning smart energy systems based on renewables, it is inevitable to include either cross-border or cross-sector interconnectivity (Thellufsen and Lund, 2017). Cross-border interconnectivity might be more practical for isolated island energy systems since it is easier and cheaper to connect the island to the mainland by underwater cables than carrying out in-depth decarbonization that requires intra-sectoral interactions at the local or regional level (Bačeković and Østergaard, 2018). Moreover, in the case of isolated energy systems, higher penetration of RESs involves installing some form of energy

storage which increases the overall costs of transition. Groppi et al. (2021) carried out a detailed review of potential storage options for smart energy islands, emphasizing the importance of power-to-transport solutions.

Various energy transition strategies and analyses have been performed for island communities, from small communities like Gozo Region, Malta (Diane et al., 2019), to the whole archipelago like Kvarner, Croatia (Mimica et al., 2020). The analyses most often focus on integrating renewables into the energy system by examining the maximum potential that could be installed by observing the demand–production relations, while the technical and operational characteristics of distribution systems are not often investigated (Cabrera et al., 2018). In addition, particular focus is usually given to the decarbonization of the heating and cooling sectors due to the specifics related to island communities (Santamarta et al., 2021). These specifics arise from the significant seasonality of electricity demand, which significantly correlates with touristic activities. Finally, it is necessary to include other sectors into the analysis to close the sustainability loop. Kiviranta et al. (2020) and Calise et al. (2021) presented the methodology for energy planning of islands by moving the system boundaries from the power generation sector to industry and transport. Their work showed that the inevitable step is to electrify residential heating systems, industrial processes, and transportation, simultaneously introducing alternative fuels where electrification is not viable. Pfeifer et al. (2021) used the EnergyPLAN model to simulate the energy system's performance by analyzing different demand-response technologies. This work showed that significant savings could be achieved when demand-response technologies like vehicle-to-grid (V2G) are used, and the level of CEEP can be maintained in the acceptable range. Segurado et al. (2011) investigated the relation between renewables' penetration and desalinization plant as a storage solution for the case of Cape Verde. The analysis showed that approximately 30% of renewables could be incorporated into the grid, simultaneously providing 50% of water demand. Bačelić Medić et al. (2013) investigated the decarbonization potential of remote communities that are intensely dependable on fossil fuels and electricity imports. The analysis showed that an optimal mix of different technologies is required to avoid excess costs and reduce the environmental impact which might arise when one technology is preferred. The choice of technology to replace conventional, fossil-fuel–based energy sources requires the trade-off between environmental benefits and installation costs (Curto et al., 2020). In general, the energy transition of island communities has been widely investigated up to now (Krajačić et al., 2009; Rodrigues et al., 2014; Schallenberg -Rodriguez, 2014; Pfeifer et al., 2018) by using different approaches, methods, and decarbonization strategies. The common thing for all of them is that some form of energy storage or demand-response technology is used to maximize the penetration of variable RESs. Another common thing for the vast majority of the work is that only the potential of on-land renewable energy sources is investigated, while the energy of seas and oceans is often neglected. Lately, blue energy (BE) sources have arisen as the prominent technology to enhance the sustainability of the island energy systems. The most prominent technology seems to be offshore wind (Ashley et al., 2014). Offshore wind farms have significantly higher load factors than the rest of the considered renewables like wave energy or sea currents. Even more, they are only suitable options for the Mediterranean context at the moment (Soukissian et al., 2017). Nevertheless, when selecting a site for deployment of offshore wind farms, besides the energy potential, it is necessary to consider navigation routes, fishery, and visual impact (Stelzenmüller et al., 2021). Finally, the integration of variable renewable sources requires the smart operation of the energy system to maintain grid stability (Lund et al., 2021). The simulations and analysis on an hourly basis in the simulation models like EnergyPLAN (2022) or Dispaset (2022) can provide a valuable insight into system performance and viability to install RESs.

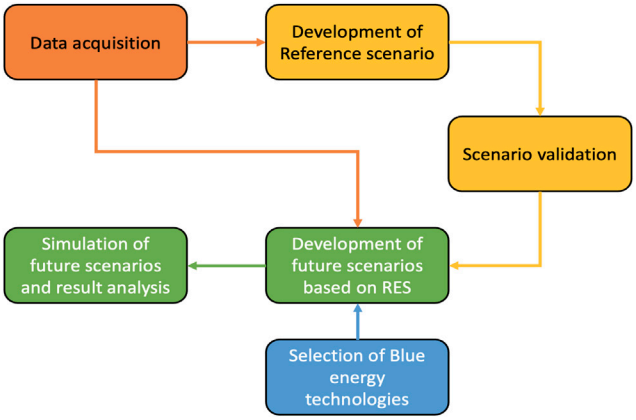

FIGURE 1 | Illustration of the applied methodology.

This work investigates the blue energy potential and its role in the energy transition for the case of Crete, Greece. Literature review showed a lack of similar analyses, where offshore wind is used as a primary driver for power production sector decarbonization. In addition, up to now, there is no clear pathway or strategy for the decarbonization of Crete Island. At the same time, a vast potential of renewables, especially offshore wind and photovoltaic (PV), remains unused. Therefore, this work aims to investigate the potential production from offshore wind farms that can be deployed near the island's coast and its influence on energy sector decarbonization. The simulations are carried out using the EnergyPLAN model, which was also used in similar studies. Additionally, simplified economic analysis is carried out to compare the cost of developed scenarios and evaluate their probability to be realized.

METHODOLOGY

Simulation of the energy system was performed using the planning model EnergyPLAN, as already mentioned above.

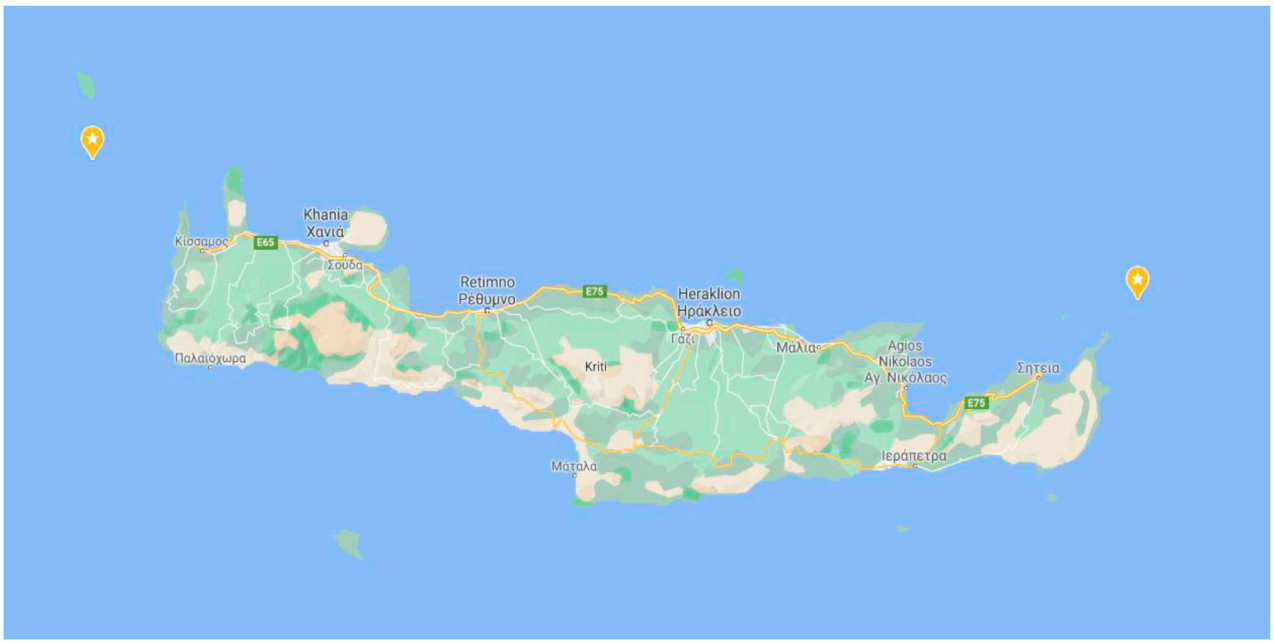

FIGURE 2 | Potential locations for offshore wind farms.

The software can carry out simulations on an hourly basis with various possibilities for input data. The model allows system analysis at a local, regional, or national level with an additional option to include all sectors or just the one of particular interest. The methodology applied in this work was already used to analyze similar systems in the previous works mentioned in the *Introduction*. The illustration of the applied methodological approach is presented in **Figure 1**. The first step is data acquisition, which consists of collecting the actual values and energy balances for the latest available period. Also, it includes a detailed analysis of the energy transition plan and strategies for the considered area. Based on data quality and accuracy, it is necessary to build a Reference scenario that should be validated with the actual values. In this work, the transport sector was left out from the analysis due to a lack of reliable data. Moreover, there are no data regarding the total primary energy supply (TPES) and carbon dioxide (CO_2) emissions which constrain the complete validation of the proposed Reference scenario. The energy transition plans and strategies are further used to develop future scenarios that include renewable energy sources and energy efficiency measures. Since the scope of this work was to investigate the potential of blue energy (BE) sources, an additional step was required. This is predominately related to selecting the appropriate technologies that have significant potential for the considered area. Once technologies are chosen, it is necessary to find suitable locations for their deployments. This is the most challenging step since it is necessary to consider other economic activities and avoid their interference. Selected areas resulted from an offshore wind energy potential analysis conducted in a GIS environment, based on open access geographical data on the environmental conditions and constraints relevant to the installation of offshore wind farms. Data processing within the GIS regarded a distance from the coast between 5 and 80 km and allowed for the following:

- The detection of the marine areas featuring the minimum environmental conditions required for the operation of floating offshore wind turbines, i.e., bathymetry between −400 m and −50 m and wind speed above 4 m/s at the sea level.
- The exclusion from these areas of sensitive environments (such as Natura2000 sites, GEA/GEN/GEETHA areas, and *Posidonia* meadows) and areas affected by navigation (such as shipping routes), which could interfere with offshore wind farms. Buffer zones were also proposed to minimize such interferences: a buffer of 2 km around environmentally sensitive areas and 5 km around the main navigation routes and the maneuvering areas of ports.

This resulted in the identification of marine areas eligible for installing floating offshore wind turbines. Such results were further refined, selecting only sites with wind speed ≥ 7 m/s at 100 m above the sea level, thus identifying the areas with the highest potential. Since the highest potential lies on the island's east side, this location is considered in this work (**Figure 2**). The maximum capacity that can be installed is obtained by considering dimensional requirements, cost of installation, and social factors such as the impact on tourism and visual effect. A full investigation of potential environmental impacts (especially

TABLE 1 | Installed capacities for power production facilities in 2019.

Energy source	Installed capacity* (MW)	Energy production* (TWh)
Thermal power plants	820	2.438
PV	96	0.162
Onshore wind	203	0.505
Small hydro	0.3	0

**Values are obtained directly from the system operator.*

TABLE 2 | Annual energy consumption by the type of fuel.

	TWh*
Electric demand	3.219
Electric cooling	0.402
Electric heating	0.123
Heating	0.86
LPG	0.092
Diesel	0.334
Biomass	0.233
Solar thermal	0.200
Industry and fuel	0.56
LPG	0.101
Diesel	0.102
Biomass	0.291
Heating oil	0.065
Gasoline	0.005

**Values are obtained directly from the system operator.*

on birds) was not carried out at this stage and will require additional data collection and processing.

Finally, the last step consists of gathering the hourly distribution curves for electricity demand, wind power potential, solar irradiation, and similar parameters depending on the input data. The hourly distribution curves for onshore wind and PV are obtained from the software Meteonorm (2022), while the values for electricity demand are obtained from the grid operator. The curve for offshore wind is obtained from Global Wind Atlas (2021), and the power potential is calculated using The PRISMI Wind Power Calculator Tool (PRISMI PLUS, 2021).

CASE STUDY ANALYSIS

Input Value for Energy Production and Consumption

In **Table 1**, the input values for installed energy production units at the island can be seen. The dominant electricity sources are thermal power plants that use fuel oil as an energy source. They account for approximately 2.48 TWh or 75% of electricity production. Moreover, there is notable production from onshore wind farms (0.505 TWh), while the PV potential remains mostly unused with a total installed capacity of only 96 MW and annual production of 0.162 TWh.

Table 2 presents the input values used when building a Reference scenario, which corresponds to current fuel consumption by an energy source. The data are directly obtained from Hellenic Electricity Distribution Network Operator. Electric heating and cooling are subtracted in the simulation due to seasonality, but the total electricity demand in 2017 was 3.219 TWh. **Figure 3** presents the annual electricity demand on an hourly basis in 2017 for the Crete case. As can be seen, the load is constant throughout the year, with several peaks

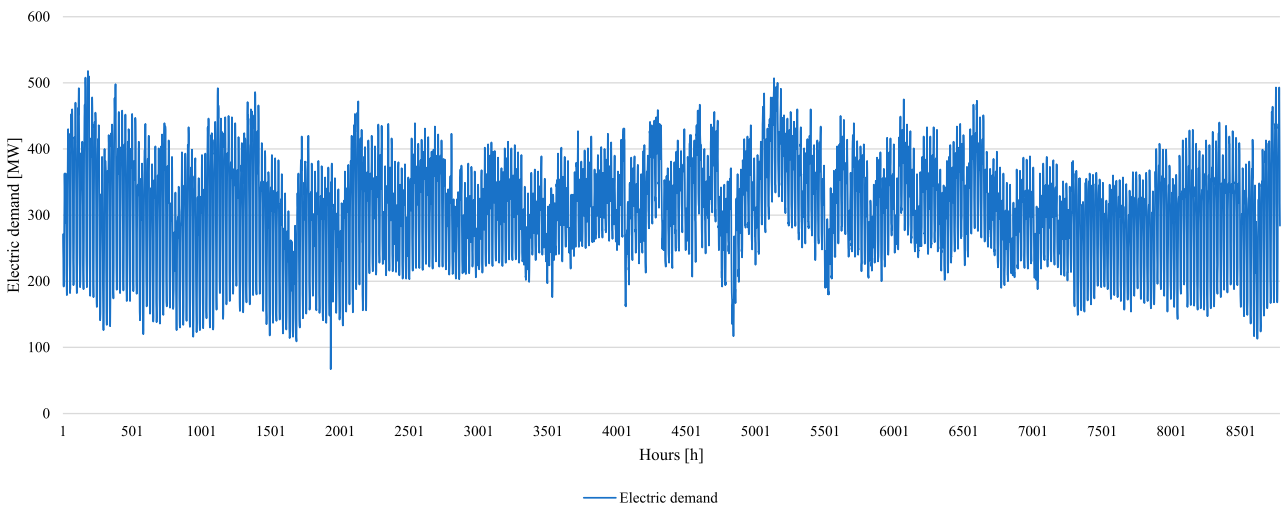

FIGURE 3 | Annual electric demand on an hourly basis.

TABLE 3 | Parameters investigated in considered scenarios.

Name of the scenario	Power plants	Offshore wind	Additional RES	Interconnection
Reference	+	-	-	-
Transition	+	+	-	400
Blue Energy	-	+	-	1,400
Renewable	-	+	+	1,400

in the summer and winter periods. The primary energy source is diesel in the residential sector, followed by renewable biomass and solar thermal primarily used for heating purposes. Various fossil fuels represent half of the consumption in the industry, while the other half is covered by biomass.

Modeling Future Scenarios

The precise, latest available data for 2017 and 2019 were used in the industry and power production sector. Nevertheless, when building future scenarios, fuel consumption for residential and industrial purposes did not change since the focus was on integrating renewable energy sources, especially offshore wind, when the island is connected to the mainland with interconnection cables. Therefore, there are four considered scenarios in this work. The first is the reference case where the island is an isolated system with thermal power plants, onshore wind, and photovoltaics. The second scenario considers the installation of a maximum of 300 MW of offshore wind on the east side of the island (**Figure 1**) and operating one interconnection cable of 400 MW capacity. In the third scenario, power plants are shut down, and the interconnection capacity is increased to 1400 MW. The last scenario considers the additional deployment of 480 MW of PV and onshore wind to reach the maximum capacity for the RES with a total interconnection capacity of 1400 MW. Interconnection capacities are obtained from the system and grid operator. According to the Greek national energy strategy, the shares of additional RES capacities are equally divided between PV and onshore wind (Hellenic Republic, 2019).

When building future scenarios, the following assumptions were used:

- The maximum offshore wind capacity is 300 MW.
- Interconnections will be fully operational by 2023.
- Power generation from thermal power plants is first reduced, and then they are entirely phased out.
- The additional renewable energy capacity that can be installed with fully operational interconnection is 480 MW.

An interconnection cable of 400 MW has been operational since the beginning of 2022, while an additional cable with 1000 MW will be deployed by the end of 2023. Thermal power plants, currently the backbone of the isolated energy system, will be shut down once interconnections are fully operational and the maximum capacity of renewable energy sources is installed. Interconnection of 1400 MW capacity allows for deployment of 300 MW offshore wind and an additional 480 MW of other RESs, which are equally divided on PV and onshore wind, following the guidelines from the national strategy (Hellenic Republic, 2019).

The future scenarios are named in the following manner: Reference (REF), Transition (TR), Blue Energy (BE), and Renewable (RE). Except for the Reference scenario, all others are investigating the potential of renewable sources in the context of interconnection with the mainland. **Table 3** presents the considered parameters for each investigated scenario.

RESULTS

First, the Reference scenario was validated by comparing the results from the EnergyPLAN model with actual values available. In the first place, this implies the production from thermal power plants, onshore wind, and PV. Obtained values for onshore wind and PV are almost identical to actual values when iterative correction factors are applied further in all scenarios. The application of correction factors is inevitable since there is no option to determine the operating conditions of installed technologies. Currently, thermal power plants are the primary electricity source with an installed capacity of 820 MW. On an annual basis, this accounts for 2.44 TWh of produced electricity, while simulation gives a result of 2.55 TWh which can be considered the correct value since the difference is less than 5%. Renewable capacities are 96 MW for PV and 203 MW for onshore wind. Their annual electricity production is 0.16 TWh for PV and 0.505 TWh for onshore wind. These data are summarized in **Table 1**.

Figure 4 presents the hourly production from all deployed electricity sources on the island in the case of the Reference scenario. Load factors of deployed RESs are an essential parameter to evaluate their applicability for the considered area. In the case of PV, the annual load factor is approximately 19%, with the highest output in June and July. The load factor is 29% for the onshore wind, with maximum production during the winter months, December and January. Validation of the Reference scenario regarding the CO_2 emissions and total primary energy supply (TPES) is impossible since there are no reference values for comparison, and the transport sector is not considered. Therefore, only the energy production sector is validated for its production, and the values correspond. Regarding the residential and industrial sectors, accurate available fuel consumption data (**Table 2**) are used and can be considered reliable.

Comparison of Scenarios With Operational Thermal Power Plants

In this subsection, Reference and Transition scenarios are compared more in-depth since they have operational thermal

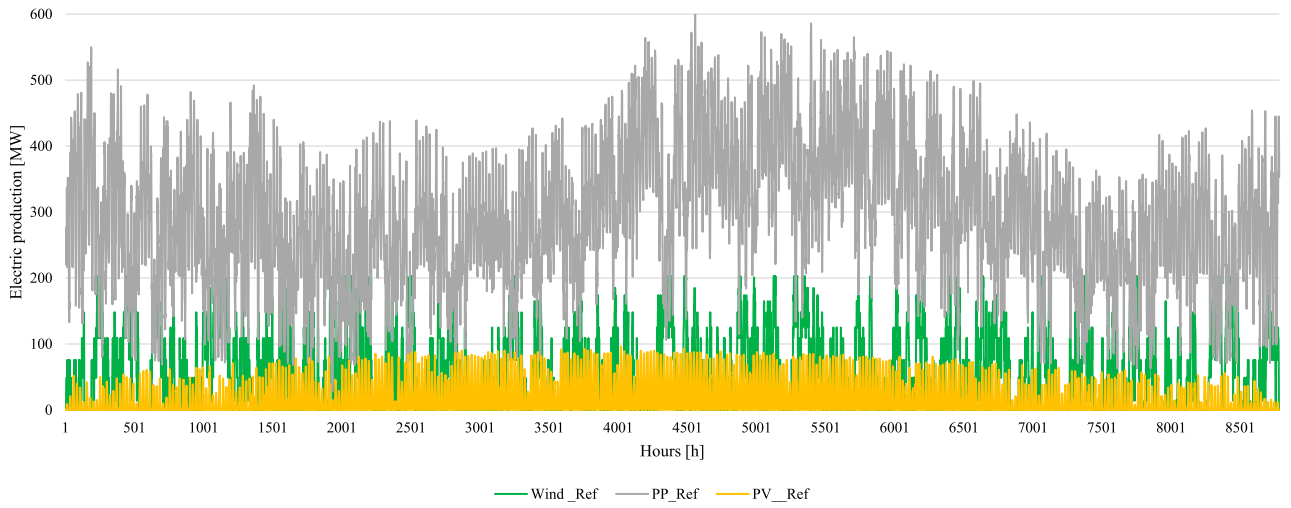

FIGURE 4 | Hourly electric production in a Reference scenario.

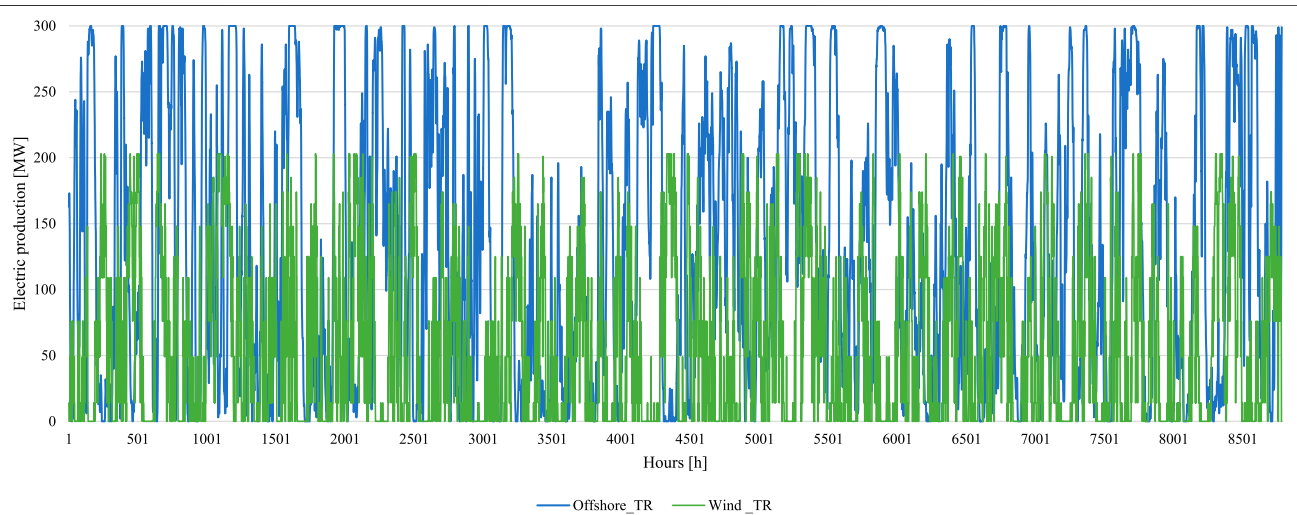

FIGURE 5 | Comparison of electricity production from offshore and onshore wind for a one-year period.

power plants included in the model. Moreover, this comparison shows the impact of offshore wind farms on energy system stability while there is no full connection to the mainland. There is no visible difference between the Reference and Transition scenarios in the case of PV and onshore wind electricity production. The power output remains the same in both cases, which is expected since the system is modeled to maximize renewables' production. Nevertheless, the introduction of offshore wind farms had a notable effect on power output from thermal power plants. The capacity of 300 MW ensures the annual production of 1.17 TWh of electricity from offshore wind, with an average load factor of 42%, and the highest production in August, even though winter months, in general, express better energy potential. Deployment of offshore wind directly reflects in power output from thermal power plants, which is reduced from 2.55 to 1.51 TWh. Moreover, offshore wind turbines and connection to the mainland with underwater cables allows some electricity export when production is higher than electricity demand. **Figure 5** presents the electricity production from offshore and onshore wind in a one-year period. It is evident that offshore wind has a significantly higher energy potential, resulting in higher load factors and electricity output. The production from the offshore wind farm is more than doubled compared to the onshore, even though the difference in considered capacity is less than 100 MW.

Figure 6 presents the monthly production from considered energy sources for these two scenarios. The figure shows that the introduction of offshore wind farms directly reduces output from thermal power plants, while the share of renewables is increasing.

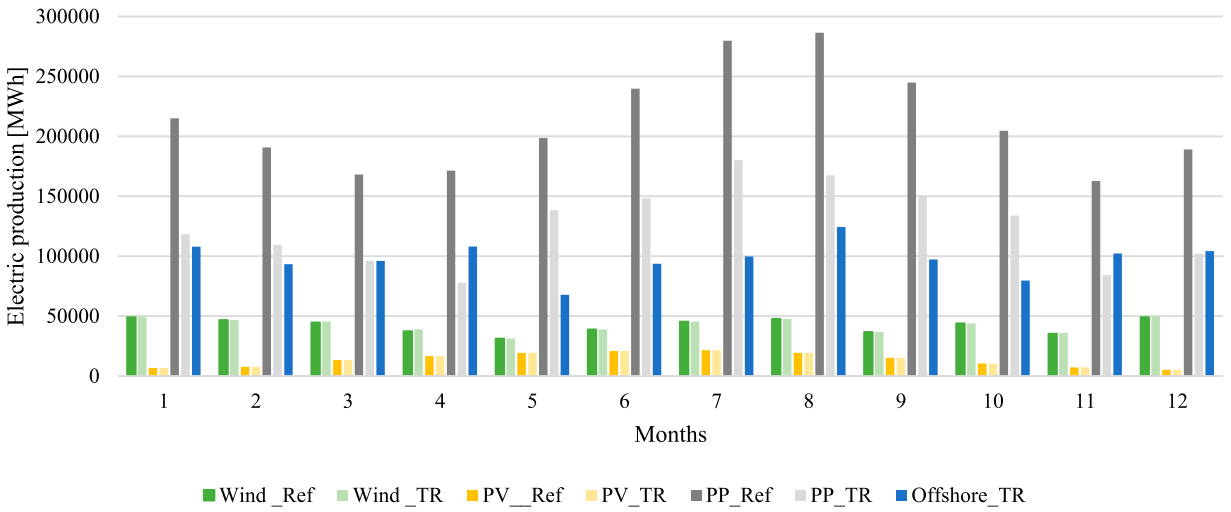

FIGURE 6 | Monthly production from electricity sources in Reference and Transition scenarios.

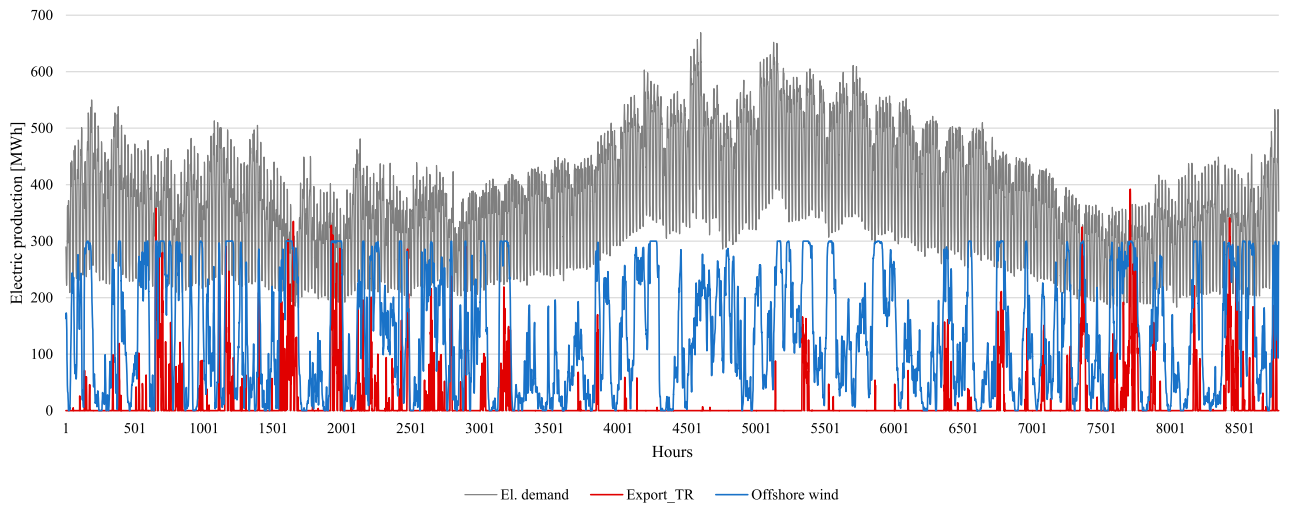

FIGURE 7 | Influence of the offshore wind farm on electricity export.

The analysis of results on an hourly basis gives a good insight into system components' interaction and reveals the potential spots where grid stability could be disturbed. With the operational thermal power plants, the supply side is stable since the production is following the demand side. The RESs are currently used to satisfy the peak demand, and the total share in the electricity mix is around 26%. The inclusion of offshore wind farms reduces the power output from thermal power plants, but even more, it opens the possibility for electricity export via the interconnection cable of 400 MW capacity. **Figure 7** presents the influence of offshore wind on electricity export. The figure shows that electricity export occurs only when the offshore wind farm is at its peak production. The export is around 130 GWh annually in the Transition scenario, which might be utilized on the island by introducing electric vehicles (EVs) or heat pumps for heating. Nevertheless, this would require cross-sectoral integration and a systematic approach to develop a decarbonization strategy.

Comparison of Scenarios Without Operational Thermal Power Plants

This section analyzes the energy system of Crete Island with fully operational interconnection cables with a capacity of 1400 MW and independent from fossil fuels for electricity production since the thermal power plants are phased out. The difference between Blue Energy and Renewable scenarios is in the total installed capacities of renewable energy sources. While the Blue Energy scenario considers offshore wind and currently installed PV and

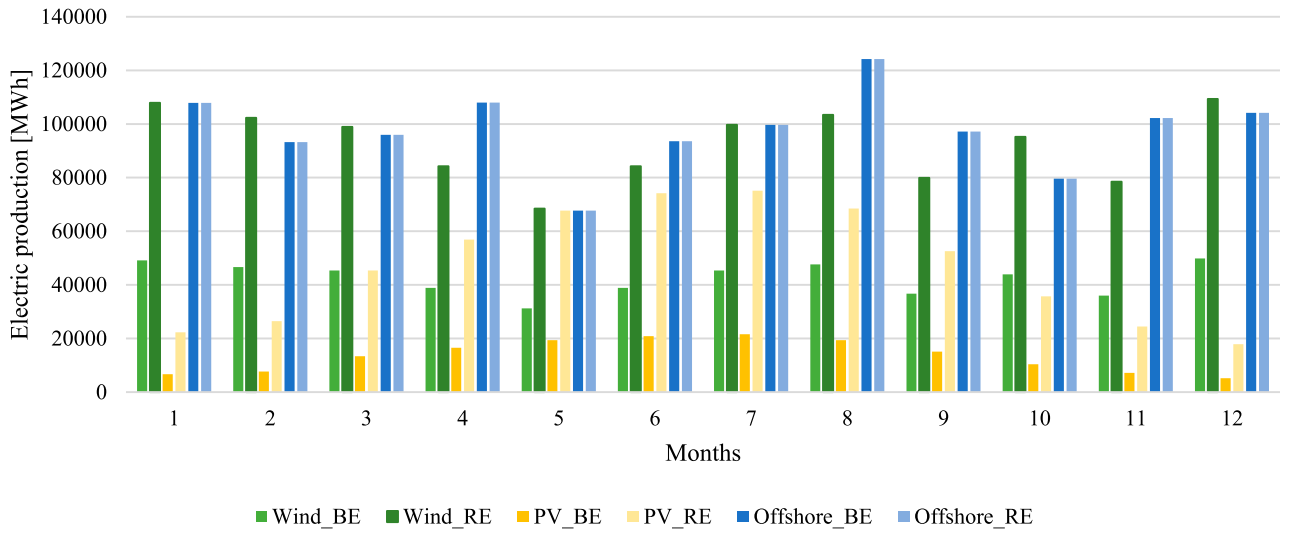

FIGURE 8 | Monthly production from electricity sources in Blue Energy and Renewable scenarios.

onshore wind capacities, an additional 480 MW of RES is added in the Renewable scenario. In total, 780 MW of renewables, compared to that in the Reference scenario, is the maximum capacity that could be installed with fully operational interconnection cables. Since the Greek energy strategy considers PV and onshore wind as the backbone of the future energy system, 480 MW is equally divided between these two sources. Therefore, the new capacity for PV is 336 MW, and the total capacity for onshore wind is 443 MW. It is necessary to ensure grid stability in both cases since installed renewables are strongly variable. The analysis shows that at least 25% of interconnection capacity needs to be used constantly for grid balancing to ensure undisrupted electricity supply to consumers. Moreover, to maintain grid stability in the Renewable scenario, it is necessary to ensure an operating grid stability strategy due to high-RES capacities. This can be done by electricity export, curtailment of the production from offshore and onshore wind farms, or utilizing electricity surplus to produce electrofuels. The exporting strategy was applied in this work, followed by the curtailment in extreme cases. Storing the electricity excess or utilization for electrofuel synthesis requires cross-sectoral coupling. This is not possible to assess with limited data or with the lack of a decarbonization strategy.

In the Blue Energy scenario, renewables can provide up to 57% (~1.8 TWh) of electricity demand on an annual basis, while the rest comes from import (~1.5 TWh). The electricity export accounts for 100 GWh on a yearly basis. Further increment of onshore renewables could theoretically cover up to 89% of electricity demand. Nevertheless, since the demand is not following the supply curve, a significant amount of electricity needs to be exported (~515 GWh). Due to that fact, import remains a vital part of the system operation and stability, and it accounts for 0.9 TWh or 27% of electricity demand. Monthly production for considered renewables is given in **Figure 8**. As can be seen, the power output from offshore wind farms remains at the same level for both scenarios, 1.17 TWh, and is the major contributor to the power production sector with a share of 36%. The offshore wind production in these scenarios is identical to that in the Transition scenario, which is expected since simulations are carried out to maximize the power output from offshore wind farms to enhance their economics. Therefore, this value represents the maximum theoretical potential of offshore wind energy with the current level of technology development. For the Renewable scenario, increment of installed capacity for onshore wind farms doubled the production from this source to 1.11 TWh, and its share is approximately 35%. An additional 240 MW of PV increases power output from this source to 0.57 TWh, accounting for 18% of electricity production.

Comparison of Energy Production and Fuel Consumption for Considered Scenarios

Figure 9 compares electricity supply by source for all considered scenarios. Currently, renewable electricity production is 0.67 TWh on an annual basis. Deployment of only 300 MW offshore wind turbines can increase this value to 1.85 TWh. Further increment in renewable capacities can increase renewable production on the island to 2.85 TWh, which corresponds to 89% of the current annual electricity demand. In terms of primary energy supply, fuel oil consumption for thermal power plants is 6.4 TWh for the Reference scenario, which can be reduced to 3.8 TWh in case that the offshore wind farm is installed. In general, the fuel oil used for power generation represents the vast majority of fossil fuels used on the island (~80%) when the transport sector is not considered. Energy consumption in the residential and industrial sectors is kept at the same level (~1.2 TWh) for all scenarios since electrification for heating, cooking, or industrial purposes is not considered.

In terms of fuel consumption, it should be emphasized once again that this analysis is done without the inclusion of the

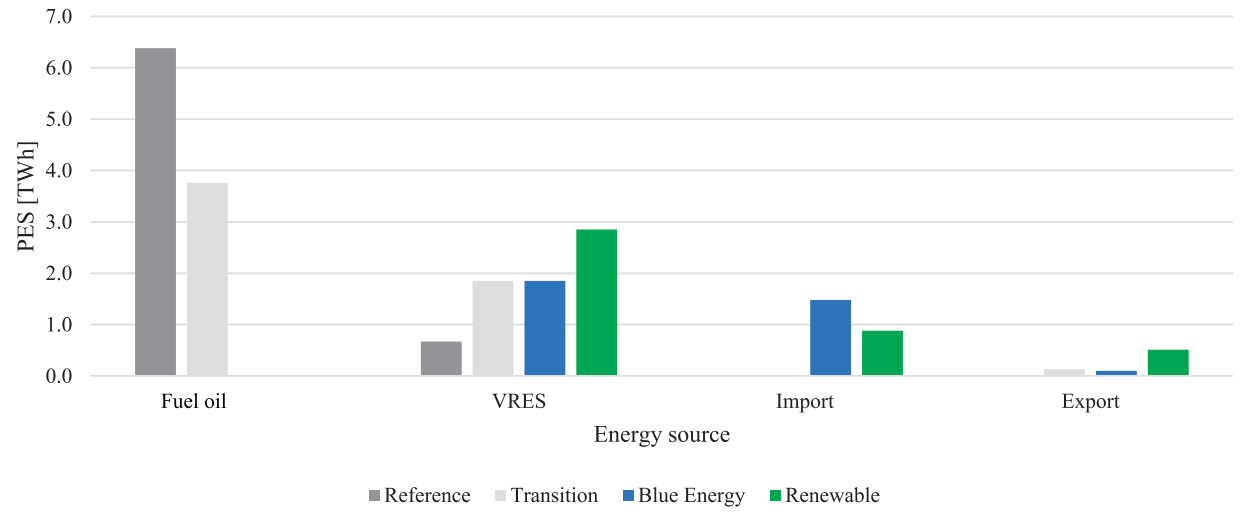

FIGURE 9 | Comparison of electricity supply for all scenarios.

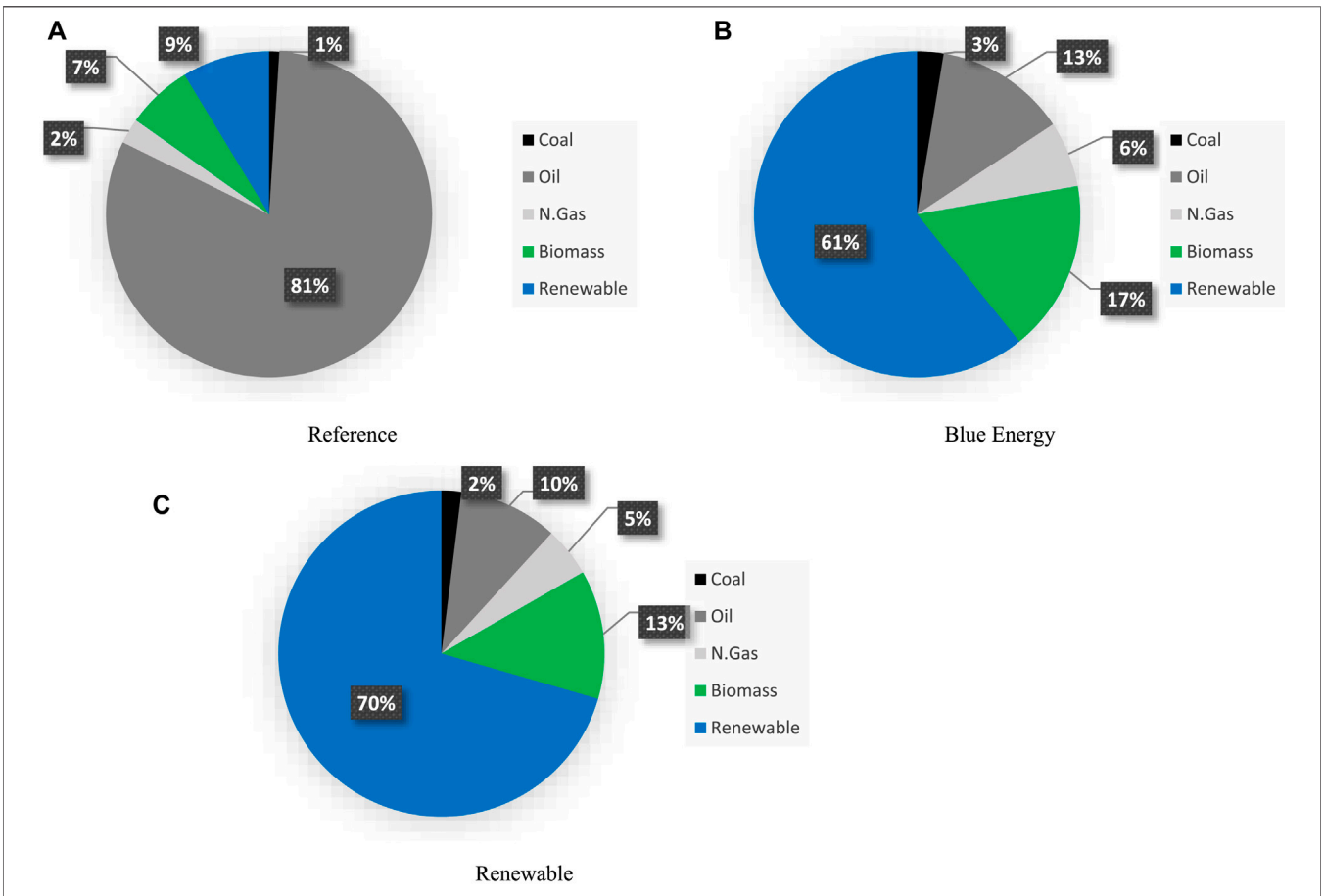

FIGURE 10 | Comparison of fuel consumption for Reference **(A)**, Blue Energy **(B)**, and Renewable **(C)** scenarios.

transport sector for which the data were not available. Having this in mind, it can be concluded that the introduction of offshore wind and the increase in other renewables' capacities can dramatically reduce the consumption of fossil fuels. As mentioned above, this is because the vast majority of fossil fuel consumption in considered sectors comes from thermal

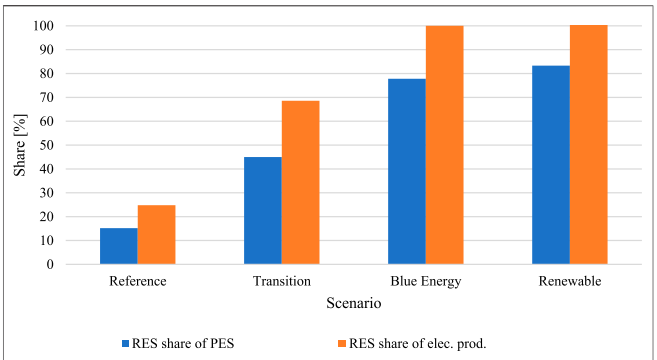

FIGURE 11 | Share of the RES in PES and electricity production.

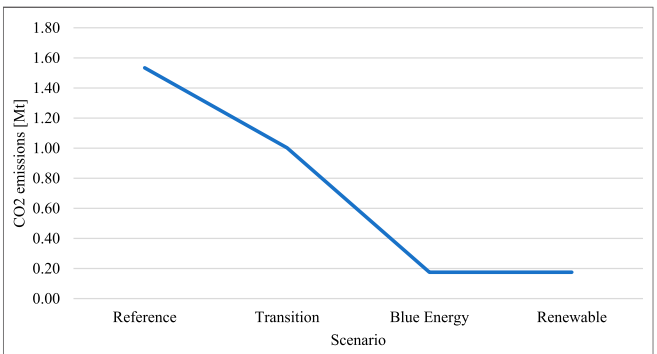

FIGURE 12 | CO_2 emissions for energy, residential, and industrial sectors.

power plants where fuel oil is used. The remaining share of fossil fuel consumption (coal, natural gas, and some oil) is still used for industries and households. Still, their overall share is dramatically reduced compared to the reference case. The results are given in **Figure 10**.

Figure 11 sums up the share of renewable energy sources in electricity production and primary energy supply for assessed sectors. The share of renewables in electricity production increases from 25 to 100% when the offshore wind is deployed in combination with additional PV and onshore wind capacities, and thermal power plants are phased out. Nevertheless, it should be emphasized that a significant amount of electricity comes from import in this case, for which the production source is not known. In terms of primary energy supply, the share of renewables, including biomass, increases from 15 to 83%. For the case of the Blue Energy scenario, it is noted that the percentage of renewables in PES surpasses the share in electricity production, which is a direct consequence of the dramatic drop in fuel oil consumption. For complete decarbonization, it is necessary to electrify heating and, where possible, industrial sector and include alternative renewable fuels (Stančin et al., 2020). With the inclusion of the transport sector into the assessment, the share of fossil fuels in TPES would dramatically increase. Therefore, it is necessary to establish a strategy for transport decarbonization, which is inevitably related to the power production system once when there is a high share of electric vehicles.

Estimation of CO_2 Emissions for Energy, Residential, and Industrial Sectors

Since there are no available data regarding the CO_2 emission for Crete Island, the results given in **Figure 12** can only be used as indicative values. Even more, this analysis is limited since the software cannot calculate the values of CO_2 emissions from imported electricity. For this reason, we have carried out a separate analysis to determine the level of emissions from imports, taking into account the average emission factor of Greek national systems, which is 487 $kgCO_2/MWh$. In this case, for the BE scenario, the imported emissions are 0.73 Mt, and for the case of the RE scenario, they are approximately 0.44 Mt. On the contrary, the emission generated at power plants reduces from reference 1.53 Mt to only 0.18 Mt. Only the introduction of offshore wind farms reduced the CO_2 emission by one-third to 1.0 Mt. From this preliminary analysis, it can be concluded that importing electricity from the mainland in combination with RES production at the island is a better solution than running thermal power plants.

Levelized Cost of Electricity

To evaluate the economic feasibility of proposed scenarios, the simplified levelized cost of electricity (LCOE) analysis is carried out. Simplified means that some rough estimations have been used, predominately on the investment side, due to the limited data availability. **Table 4** summarizes the data used for this economic assessment. All data regarding the technology costs are taken from the Danish Energy Agency (Technology Data, 2022). The weighted average cost of capital (WACC) is taken from the Energy Post platform (Energy Post, 2022), but for the onshore wind in the case of Greece, since the data for offshore are

TABLE 4 | Input data for LCOE analysis [1].

Technology	Installed capacity (MW)	Investment costs (EUR/MW)	Fixed O&M (EUR/MW)	Variable O&M (EUR/MWh)	Lifetime (years)	Electricity production (MWh/year)
Offshore wind	300	2,130,000	40,059	3	27	1,170,000
Onshore wind	240	1,120,000	14,000	1.5	27	600,000
PV	240	530,000	8,750	-	30	410,000
Interconnector	1,400	356,416,665*	-	-	-	-

*Total investment.

not available. The calculation also included the investment for interconnector cables, even though this investment would happen with or without deployment of considered RESs (Greece commissions Crete-Peloponnese power interconnection, 2022; Independent Power Transmission Operator, 2022).

The analysis shows that, in the case of TR or BE scenarios where only offshore wind and interconnector are considered, the LCOE is around 120 EUR/MWh. This value is in the range of LCOE values for offshore wind farms published in the study (Energy and Climate, 2022). When additional PV and onshore capacities are deployed, such as in the RE scenario, the LCOE is further reduced to 90 EUR/MWh. This reduction can be expected since the investment and operating and maintenance (O&M) costs are comparably lower for PV and onshore wind than offshore wind. The technology lifetime was considered 27 years, with the 12% WACC used to discount the costs and energy production. Once again, these values should only be taken as orientational values due to used approximations and uncertainties regarding the technology costs.

CONCLUSION

The analysis of the energy system of Crete Island shows excellent potential for deployment of renewable energy sources, especially offshore wind. The island is currently acting as an energy system with limited interconnections to the mainland, with thermal power plants as the primary electricity source and complete dependence on imported fossil fuels used for all sectors. Since the transport sector is not considered, the energy sector with thermal power plants is the biggest consumer of fossil fuels, specifically fuel oil. Deployment of underwater interconnection cables allows for higher penetration of RESs and opens the possibility of shutting down thermal power plants and turning to sustainable energy sources. Especially interesting might be an integration of offshore wind, which has tremendous potential with a power output of 1.17 TWh per year with 300 MW of installed capacity with an average load factor of 41%. Additional installation of 480 MW of RES, which is possible with interconnection cables, opens the possibility of completely phasing out fossil fuels in the power generation sector and using interconnection with the mainland to maintain grid stability. More than 70% of electricity demand could be satisfied by the installed capacities at the island, while the total share of RESs in the primary energy supply is around 80%. This also allows a significant reduction in CO_2 emissions, and even more, it opens the possibility to export excess electricity production. From the economic perspective, the calculated LCOE for TR and BE is 120 EUR/MWh. In comparison, this is further reduced to 90 EUR/MWh when additional RES capacities are deployed as in the RE scenario.

The transport sector should also be included in the analysis for future work. Moreover, an in-depth strategy for the electrification of the heating sector should be considered, especially seawater heat pumps as commercially available technology. This would require cross-sectoral coupling to minimize the losses and ensure a reliable, sustainable energy supply. Finally, it would be prudent to investigate the potential of offshore wind at the west location of the island to compare and make a trade-off between additional offshore and onshore capacities. Supplementary assessment of potential environmental impacts of offshore wind farms, especially on migratory birds, is also recommended.

DATA AVAILABILITY STATEMENT

The original contributions presented in the study are included in the article/Supplementary Material, further inquiries can be directed to the corresponding authors.

AUTHOR CONTRIBUTIONS

HS wrote and proofread the manuscript. HS and AP visualized the data. AP, HS, HM, and CP were involved in modeling the data. CP, FD, MD, NS, and SM were involved in data acquisition. MD, HM, and CP validated the results. HS interpreted the results.

FUNDING

This study was developed in the framework of the Interreg Med BLUE-DEAL (project number 5381) project co-financed by the European Regional Development Fund. Website: https://blue-deal.interreg-med.eu.

ACKNOWLEDGMENTS

The authors would like to thank the anonymous reviewers for their dedicated time and valuable comments that improved the quality of this work.

REFERENCES

Ashley, M. C., Mangi, S. C., and Rodwell, L. D. (2014). The Potential of Offshore Windfarms to Act as Marine Protected Areas - A Systematic Review of Current Evidence. *Mar. Policy* 45, 301–309. doi:10.1016/j.marpol.2013.09.002

Bačeković, I., and Østergaard, P. A. (2018). Local Smart Energy Systems and Cross-System Integration. *Energy* 151, 812–825.

Bačelić Medić, Z., Ćosić, B., and Duić, N. (2013). Sustainability of Remote Communities: 100% Renewable Island of Hvar. *J. Renew. Sustain. Energy* 5 (4). doi:10.1063/1.4813000

Cabrera, P., Lund, H., and Carta, J. A. (2018). Smart Renewable Energy Penetration Strategies on Islands: The Case of Gran Canaria. *Energy* 162, 421–443. doi:10.1016/j.energy.2018.08.020

Calise, F., Duic, N., Pfeifer, A., Vicidomini, M., and Orlando, A. M. (2021). Moving the System Boundaries in Decarbonization of Large Islands. *Energy Convers. Manag.* 234, 113956. doi:10.1016/j.enconman.2021.113956

Curto, D., Favuzza, S., Franzitta, V., Musca, R., Navarro Navia, M. A., and Zizzo, G. (2020). Evaluation of the Optimal Renewable Electricity Mix for Lampedusa Island: The Adoption of a Technical and Economical Methodology. *J. Clean. Prod.* 263, 121404. doi:10.1016/j.jclepro.2020.121404

Diane, C., Erika, M., Evangelos, R., Christoforos, P., Antun, P., Daniele, G., et al. (2019). "A Methodology for Energy Planning in Small Mediterranean Islands, the Case of the Gozo Region," in SyNERGY MED 2019 - 1st International Conference on Energy Transition in the Mediterranean Area, Cagliari, Italy (Institute of Electrical and Electronics Engineers Inc.). doi:10.1109/synergy-med.2019.8764131

Dispaset (2022). The Dispa-SET Model — Documentation [Internet]. Available from: http://www.dispaset.eu/en/latest/.

Energy and Climate (2022). Policy Implications of 2022 Cost-Effective Decarbonisation Study - Florence School of Regulation [Internet]. Available from: https://fsr.eui.eu/policy-implications-of-2022-cost-effective-decarbonisation-study/.

Energy Post (2022). Energy Post - the Best Thinkers on Energy - [Internet]. Available from: https://energypost.eu/.

EnergyPLAN (2022). Advanced Energy Systems Analysis Computer Model [Internet]. Available from: https://www.energyplan.eu/.

Global Wind Atlas (2021). Global Wind Atlas [Internet]. Available from: https://globalwindatlas.info/.

Greece commissions Crete-Peloponnese power interconnection (2022). Enerdata [Internet]. Available from https://www.enerdata.net/publications/daily-energy-news/greece-commissions-crete-peloponnese-power-interconnection.html.

Groppi, D., Pfeifer, A., Garcia, D. A., Krajačić, G., and Duić, N. (2021). A Review on Energy Storage and Demand Side Management Solutions in Smart Energy Islands. *Renew. Sustain. Energy Rev.* 135, 110183. doi:10.1016/j.rser.2020.110183

Hellenic Republic (2019). *Hellenic Republic M of the E and E. The National Energy and Climate Plan*. Athens: Ministry of the Environment and Energy.

Independent Power Transmission Operator (2022). Interconnection of Crete with Peloponnese IPTO [Internet]. Available from: https://www.admie.gr/en/erga/erga-diasyndeseis/diasyndesi-tis-kritis-me-tin-peloponniso.

Kiviranta, K., Thomasson, T., Hirvonen, J., and Tähtinen, M. (2020). Connecting Circular Economy and Energy Industry: A Techno-Economic Study for the Åland Islands. *Appl. Energy* 279, 115883. doi:10.1016/j.apenergy.2020.115883

Krajačić, G., Duić, N., and Carvalho, M. da. G. (2009). H2RES, Energy Planning Tool for Island Energy Systems - the Case of the Island of Mljet. *Int. J. Hydrogen Energy* 34 (16), 7015–7026. doi:10.1016/j.ijhydene.2008.12.054

Lund, H., Østergaard, P. A., Connolly, D., and Mathiesen, B. V. (2017). Smart Energy and Smart Energy Systems. *Energy* 137, 556–565. doi:10.1016/j.energy.2017.05.123

Lund, H., Thellufsen, J. Z., Østergaard, P. A., Sorknæs, P., Skov, I. R., and Mathiesen, B. V. (2021). EnergyPLAN - Advanced Analysis of Smart Energy Systems. *Smart Energy* 1, 100007. doi:10.1016/j.segy.2021.100007

Marczinkowski, H. M., and Barros, L. (2020). Technical Approaches and Institutional Alignment to 100% Renewable Energy System Transition of Madeira Island-Electrification, Smart Energy and the Required Flexible Market Conditions. *Energies* 13 (17). doi:10.3390/en13174434

Meteonorm (2022). Intro - Meteonorm (de) [Internet]. Available from: https://meteonorm.com/.

Mimica, M., Krajacic, G., Medved, D., and Jardas, D. (2020). "Digitalization and Smart Islands in the Kvarner Archipelago," in 2020 43rd International Convention on Information, Communication and Electronic Technology, MIPRO 2020 - Proceedings, Opatija, Croatia (Institute of Electrical and Electronics Engineers Inc.), 1837–1842. doi:10.23919/mipro48935.2020.9245328

Pfeifer, A., Herc, L., Batas Bjelić, I., and Duić, N. (2021). Flexibility Index and Decreasing the Costs in Energy Systems with High Share of Renewable Energy. *Energy Convers. Manag.* 240, 114258. doi:10.1016/j.enconman.2021.114258

Pfeifer, A., Dobravec, V., Pavlinek, L., Krajačić, G., and Duić, N. (2018). Integration of Renewable Energy and Demand Response Technologies in Interconnected Energy Systems. *Energy* 161, 447–455. doi:10.1016/j.energy.2018.07.134

PRISMI PLUS (2021). The PRISMI Wind Power Calculator Tool [Internet]. Available from: https://prismi.interreg-med.eu/news-events/news/detail/actualites/the-prismi-wind-power-calculator-tool/.

Rodrigues, E. M. G., Godina, R., Santos, S. F., Bizuayehu, A. W., Contreras, J., and Catalão, J. P. S. (2014). Energy Storage Systems Supporting Increased Penetration of Renewables in Islanded Systems. *Energy* 75, 265–280. doi:10.1016/j.energy.2014.07.072

Santamarta, J. C., García-Gil, A., Expósito, M. d. C., Casañas, E., Cruz-Pérez, N., Rodríguez-Martín, J., et al. (2021). The Clean Energy Transition of Heating and Cooling in Touristic Infrastructures Using Shallow Geothermal Energy in the Canary Islands. *Renew. Energy* 171, 505–515. doi:10.1016/j.renene.2021.02.105

Schallenberg-Rodriguez, J. (2014). Photovoltaic Techno-Economical Potential on Roofs in the Canary Islands. *J. Sustain. Dev. energy water Environ. Syst.* 2 (1), 68–87. doi:10.13044/j.sdewes.2014.02.0007

Segurado, R., Krajačić, G., Duić, N., and Alves, L. (2011). Increasing the Penetration of Renewable Energy Resources in S. Vicente, Cape Verde. *Appl. Energy* 88 (2), 466–472. doi:10.1016/j.apenergy.2010.07.005

Soukissian, T. H., Denaxa, D., Karathanasi, F., Prospathopoulos, A., Sarantakos, K., Iona, A., et al. (2017). Marine Renewable Energy in the Mediterranean Sea: Status and Perspectives. *Energies* 10 (10), 1–56. doi:10.3390/en10101512

Stančin, H., Mikulčić, H., Wang, X., and Duić, N. (2020). A Review on Alternative Fuels in Future Energy System. *Renew. Sustain. Energy Rev.* 128, 109927. doi:10.1016/j.rser.2020.109927

Stelzenmüller, V., Gimpel, A., Haslob, H., Letschert, J., Berkenhagen, J., and Brüning, S. (2021). Sustainable Co-location Solutions for Offshore Wind Farms and Fisheries Need to Account for Socio-Ecological Trade-Offs. *Sci. Total Environ.*, 776, 145918. doi:10.1016/j.scitotenv.2021.145918

Technology Data (2022). Technology Data Energistyrelsen [Internet]. Available from https://ens.dk/en/our-services/projections-and-models/technology-data.

Thellufsen, J. Z., and Lund, H. (2017). Cross-border versus Cross-Sector Interconnectivity in Renewable Energy Systems. *Energy* 124, 492–501. doi:10.1016/j.energy.2017.02.112

Conflict of Interest: The authors declare that the research was conducted in the absence of any commercial or financial relationships that could be construed as a potential conflict of interest.

Publisher's Note: All claims expressed in this article are solely those of the authors and do not necessarily represent those of their affiliated organizations, or those of the publisher, the editors, and the reviewers. Any product that may be evaluated in this article, or claim that may be made by its manufacturer, is not guaranteed or endorsed by the publisher.

frontiers | Frontiers in Energy Research

ORIGINAL RESEARCH
published: 30 June 2022
doi: 10.3389/fenrg.2022.902021

Benchmarking Marine Energy Technologies Through LCA: Offshore Floating Wind Farms in the Mediterranean

Riccardo Maria Pulselli[1,2], *Matteo Maccanti*[3]*, *Morena Bruno*[3], *Alessio Sabbetta*[2], *Elena Neri*[2], *Nicoletta Patrizi*[3] and *Simone Bastianoni*[3]

[1]Department of Architecture, University of Florence, Florence, Italy, [2]INDACO2 srl, Colle di Val d'Elsa, Italy, [3]Ecodynamics Group, Department of Physical, Earth and Environmental Science, University of Siena, Siena, Italy

Floating wind turbines are a valid option for offshore wind farms in the Mediterranean, where the sea-floor falls off rapidly with distance from the coastline. The present study concerns a Life Cycle Assessment of the environmental performance of two types of floating wind turbine. Greenhouse gas emissions of two standard models (raft-buoy and spar-buoy, 154 m rotor diameter, 6 MW installed power) were estimated in terms of Global Warming Potential (t CO_2eq) with the aim of determining a benchmark for evaluating the performance of similar offshore wind farms. Thus, the aim of the paper was to create a benchmark for the design of innovative technologies, such as those developed by specialist companies, and to verify the validity of new designs and technologies in terms of avoided greenhouse gas emissions. The results show that the Carbon Intensity of Electricity of a single floating wind turbine varies in the range 26–79 g CO_2eq·kWh^{-1}, averaging 49 g CO_2eq·kWh^{-1}, in line with other studies of offshore wind turbines and other renewable energy sources (such as onshore wind and photovoltaic). Extension of our study to the whole life cycle, including manufacturing, assembly and installation, maintenance and material replacement and a hypothetical decommissioning and end-of-life, showed that wind farms are among the most promising marine renewable energy technologies for the Mediterranean.

Keywords: raft-buoy wind turbine, spar-buoy wind turbine, carbon footprint, life cycle assessment, carbon intensity of electricity

Edited by:
Muyiwa S. Adaramola, Norwegian University of Life Sciences, Norway

Reviewed by:
Carlos Pérez-Collazo, University of Vigo, Spain
Davide Magagna, European Commission, Netherlands

***Correspondence:**
Matteo Maccanti
matteo.maccanti@unisi.it

Specialty section:
This article was submitted to Sustainable Energy Systems and Policies, a section of the journal Frontiers in Energy Research

Received: *22 March 2022*
Accepted: *09 June 2022*
Published: *30 June 2022*

Citation:
Pulselli RM, Maccanti M, Bruno M, Sabbetta A, Neri E, Patrizi N and Bastianoni S (2022) Benchmarking Marine Energy Technologies Through LCA: Offshore Floating Wind Farms in the Mediterranean. Front. Energy Res. 10:902021. doi: 10.3389/fenrg.2022.902021

INTRODUCTION

The European Union attributes strategic value to the development of offshore wind farms (European Commission, 2019; European Commission, 2020a; European Commission, 2020b; European Commission, 2021). The installed power of offshore wind turbines in Europe is 25 GW, 14.6 GW in EU-27 countries and 10.4 GW in extra-EU countries, principally the United Kingdom (Wind Europe, 2021) which has 45 MW of floating turbines which account for 70% of the world fleet (EC, 2020a). In 2020, the production of offshore wind energy in Europe was 83 TWh, 3% of the energy requirements of the continent (Wind Europe, 2021); this percentage could hopefully exceed 30% in 2050 (Ghigo et al., 2020).

European seas are estimated to have high potential for floating turbines: 4540 GW, of which at least 3000 GW could come from seas with depths in the range 100–1,000 m. The greatest wind potential is encountered in the North Sea and the Baltic Sea, but the Atlantic Ocean and Mediterranean Sea also offer opportunities for profitably exploiting wind energy (EC, 2020b). The aims of the EU are ambitious, with a goal of 450 GW installed offshore wind power by 2050, of which at least 48 GW is planned for the Mediterranean (Wind Europe, 2019). The webgis portal of the Interreg-MED MAESTRALE project indicates values of wind speeds which lie in the range 3–7 m/s in the Mediterranean (Maestrale, 2022). Among the advantages are the lower frequency and intensity of extreme weather events in this sea with respect to the Atlantic and the North Sea, which means that wind farms are less likely to be damaged. This carries over to greater security and lower investment risk. In more exposed contexts, the increase in extreme events linked to climate change may damage offshore wind farms (Diamond, 2012; Wang Q. et al., 2019; Kettle, 2020).

The predominant type of offshore wind farm at global level is the bottom-fixed wind turbine in shallow water (Pantusa et al., 2020). However, floating wind turbines are a more promising solution for offshore situations, since they can be installed with sea depths ranging from 50 to 500 m (Pantusa and Tomasicchio, 2019; Poujol et al., 2020). This aspect makes the Mediterranean context technically suitable for the exploitation of wind energy despite it has steep bathymetric slopes and deep waters near the coast (Chipindula et al., 2018; EC, 2020b; Staschus et al., 2020).

In February 2022 the first offshore wind turbine in the Mediterranean was completed in the waters of Taranto (Italy); this is the first of the ten 3 MW turbines that will make up the plant called "Beleolico". There are many other projects underway in the Mediterranean waters for both bottom-fixed and floating wind turbine plants (Palmiotti, 2022). In the Gulf of Lion (France), four floating wind turbines of 6 MW will be installed in the coming months (Poujol et al., 2020). The authorization process has begun for the construction of an energy hub in Ravenna (Italy) which will see 65 monopile wind turbines of 8 MW each and 100 MW floating photovoltaic panels for a total installed capacity of 620 MW (Dominelli, 2021). In Sardinia (Italy), a floating wind farm for a total power of around 450 MW is being planned (Palmiotti, 2022), while in Marsala (Italy), the construction of a floating wind farm 35 km from the coast, with 25 turbines of 10 MW is planned (Comelli, 2020). Moreover, an expression of interest in floating offshore wind farm with a configuration consisting of 27 turbines with a nominal power of 10 MW each, off the coast of Civitavecchia, was presented by the Lazio Region (Regione Lazio, 2021).

Floating offshore wind is considered to be among the main research and innovation priorities for opening the European market in new marine contexts (EC, 2020b). This paper is the result of a study that evaluates the use of offshore floating wind farms in the Mediterranean Sea, in the framework of the Interreg MED BLUE DEAL Project. In particular, the study estimates the Carbon Footprint (CF) of two types of floating wind turbine, having installed powers of 6 MW (EC, 2020b), by means of Life Cycle Assessment (LCA). In this regard, Pantusa and Tomasicchio (2019) conducted a study on the Mediterranean, assuming turbine between 3 and 6 MW. In addition, the study by Poujol et al. (2020), which carried out the first LCA analysis of a Mediterranean floating plant to be completed in the coming months, refers to a plant consisting of four 6 MW turbines. Although most of the literature for the Mediterranean assumes turbines with lower installed capacity, the current trend is to build turbines of increasing size; 10 MW turbines are available on the market and 20 MW units are forecasted by 2030 (International Renewable Energy Agency, 2019). Most of the floating plants planned in the Mediterranean area show values of 8–10 MW per unit.

The LCA methodology has already been used for the environmental assessment of floating offshore wind turbines in some specific applications, documented in the literature. Weinzettel et al. (2009) reported the first LCA of a spar-buoy wind turbine, a concept developed by Norwegian Sway Company. Its nominal power is 5 MW and installation was planned to be at a distance of 50 km from the coast. At the time of publication, it was not yet operating. The results obtained for the various impact categories of a floating wind farm proved to be in line with those of traditional monopile offshore turbines. Clearly, also, the use of recycled materials could further significantly reduce impacts.

Raadal et al. (2014) conducted LCA of greenhouse gas emissions of six different concepts of offshore turbine, using the same 5 MW model but considering different structures to support the tower. They evaluated five floating structures (tension-leg-spar, semi-submersible, spar-buoy, tension-leg-platform, tension-leg-buoy) and a bottom-fixed structure, type OC4 jacket. For each type they postulated a wind farm composed of 100 turbines (10 × 10 square layout) to install on the Doggerbank, 200 km off the coast of Britain in the North Sea. The study showed that the environmental performance of offshore wind turbines (both floating and bottom-fixed) can vary widely. The factors that most affect performance are: turbine lifetime, wind conditions, turbine size, the weight of steel in the platforms/foundations, distance from the coast, installation and decommissioning.

Tsai et al. (2016) reported a detailed LCA study of 20 scenarios for 3 MW floating offshore wind turbines (based on the Vestas V112-3.0 MW®) on the Great Lakes in the state of Michigan (United States). The scenarios reflect different spatial characteristics in relation to wind speed, water depth and distance from the electricity grid. Four different sites were considered with five different distances from the coast (5, 10, 15, 20, 30 km) and different types of foundation (floating and bottom-fixed: gravity-based foundation, tripod and monopile), depending on the type of bottom. The study showed that turbines closer to the coast have better environmental performance, because although turbines further offshore produce more (the theoretical productivity for 20 years of operation of a turbine was in the range 14.8–18.5 TWh, without significant differences between sites closer or more distant from the coast), the environmental load/burden associated with manufacturing, operating, maintaining and decommissioning is greater. It was also found that for all types of foundation, the weight of steel is relevant, making it crucial to reduce this parameter,

TABLE 1 | Carbon Intensity of Electricity (g CO_2eq kWh^{-1}) of onshore, offshore floating and bottom-fixed wind farms—literature review.

n	Nominal power Single turbine (MW)	Carbon intensity of electricity (g CO_2eq·kWh^{-1})	Lifetime (yr)	References	Type	LCA phases	Notes
1	5	12.2	25	Weinzettel et al. (2009)	Floating - Spar-Buoy	Manufacture: production of material components and transport (to assembly, final location and harbour); installation; maintenance; end of life (EoL)	Design: Norwegian Sway Company.The lifetime assumed in Weinzettel et al. (2009) is 25 years; the CIE is corrected for a 20-years lifetime (as suggested in Raadal et al., 2014). Outcomes: Impact categories: abiotic depletion, global warming (GWP100), human toxicity, fresh water, aquatic ecotoxicity, terrestrial ecotoxicity, photochemical oxidation, acidification, eutrophication
2	5	20.9	20	Raadal and Vold, 2012 Raadal et al., 2014	Floating - Tension-Leg-Spar (TLS)	Manufacture: production and transport of materials (turbine, platform, cables); installation: fuel for machinery; maintenance: fuel, production, and transport materials; EoL: fuel for decommissioning Sensitivity analysis variables: capacity factor and lifetime; - steel mass (in foundation/platforms); - fuel consumption during installation and decommissioning	Design: References turbine 5 MW rotor-nacelle-assembly model NREL, illustrated in Jonkman et al. (2009). Hub height 90 m, rotor diameter 126 m. Postulated depth: 200 m for floating turbines, 50 m bottom-fixed turbines. Outcomes: GHG emissions (by GWP); energy performance: energy payback ratio and energy payback time
3	5	31.4			Floating - Semi-Submersible		
4	5	25.3			Floating - Spar-Buoy		
5	5	19.2			Floating - Tension-Leg-Platform (TLP)		
6	5	18.0			Floating - Tension-Leg-Buoy (TLB)		
7	5	18.9			Bottom-Fixed OC4 Jacket		
8	3	40.9	20	Tsai et al. (2016)	Gravity-Based Foundation (GBF)	Manufacture: virgin materials and energy for manufacture of intermediate materials, components, modules and processing; transport of manufactured materials; installation: seabed preparation, foundations, substation, wind turbines and cables; maintenance (prevention and correction) and component replacement; decommissioning: disassembly, waste treatment; recycling scenarios	Design: turbines: Vestas V112-3.0 MW with different types of foundations. Installation hypothesised in four Michigan counties (US): n = 8–12 Berrien County (US-MI), n = 13–17 Ottawa County (US-MI); n = 18–22 Oceana County (US-MI); n = 23–27 Huron County (US-MI). Outcomes: GWP, acidification potential and cumulative energy demand
9	3	28			Monopile		
10	3	41.7			Tripod		
11	3	44.3			Tripod		
12	3	38.1			Floating		
13	3	25.7			Monopile		
14	3	32.9			Floating		
15	3	33			Floating		
16	3	33.8			Floating		
17	3	35.5			Floating		
18	3	25.6			Monopile		
19	3	40.5			Tripod		
20	3	33.1			Floating		
21	3	33.9			Floating		
22	3	35.5			Floating		
23	3	33.4			Gravity-based foundation (GBF)		
24	3	27.7			Monopile		
25	3	41.3			Tripod		
26	3	42			Tripod		
27	3	47.3			Tripod		
28	1	7.4	20	Chipindula et al. (2018)	Onshore	Extraction/Material Production and manufacturing; Installation; Operation/Maintenance; Transport of materials Disassembly, with EoL (and Recycle scenarios). Sensitivity Analysis variables: effect of changing the electricity source during extraction/processing stage	Design: hypothetical onshore (1, 2 and 2.3 MW), shallow water (2 and 2.3 MW), and deep-water (2.3 and 5 MW) wind farms Outcomes: 15 mid-point category: carcinogens, non-carcinogens, respiratory inorganics, ionizing radiation, ozone layer depletion, respiratory organics, aquatic ecotoxicity, terrestrial ecotoxicity, terrestrial acid/nutrification, land
29	2	7.1			Onshore		
30	2.3	5.8			Onshore		
31	2	9.5			Monopile		
32	2.3	6.5			Monopile		
33	2.3	7.9			Floating - Dutch Tri-Floater		
34	5	7.3			Floating - Dutch Tri-Floater		

(Continued on following page)

TABLE 1 | (*Continued*) Carbon Intensity of Electricity (g CO_2eq kWh^{-1}) of onshore, offshore floating and bottom-fixed wind farms—literature review.

n	Nominal power Single turbine (MW)	Carbon intensity of electricity (g CO_2eq·kWh^{-1})	Lifetime (yr)	References	Type	LCA phases	Notes
							occupation, aquatic acidification, aquatic eutrophication, global warming, non-renewable energy, mineral extraction
35	2	295.2	20	Wang S. et al. (2019)	Onshore	Manufacturing (turbine and transmission grid); transport and installation; operation and maintenance; dismantling and disposal. Sensitivity analysis variables: lifetime of wind turbine, energy production, degree of recycling, distance to wind farm site	Original values expressed in kg CO_2/MJ were converted to g CO_2/kWh. Outcomes: GHG emissions
36	2	468			Floating - Spar-Buoy		
37	6	22.3	20	Poujol et al. (2020)	Floating - Semi-Submersible	Materials and manufacture; transport of materials; installation of turbine and grid connection; maintenance; decommissioning. Sensitivity analysis variables: Model uncertainties and geographical variability linked to electricity estimates, - Parameter uncertainties and variability of foreground data, - Uncertainties in background data	Design: Four 6 MW turbines composing a 24 MW floating wind farm. Outcomes: Seven impact categories: climate change, resource depletion, water use, marine ecotoxicity, air quality, CED renewable, CED non-renewable

decommission correctly and increase the amount of recycled steel.

Chipindula et al. (2018) conducted LCA of hypothetical wind farms with wind turbines of different nominal power, onshore (1, 2 and 2.3 MW turbines) and offshore, in the latter case considering shallow-water (bottom-fixed 2 and 2.3 MW turbines) and deep-water (floating 2.3 and 5 MW turbines). Installation was contemplated in Texas (United States) and in the Gulf of Mexico. The study found that turbine size was crucial. Environmental performance improved with increasing turbine size. In general, turbines with lower environmental impact were onshore due to the smaller quantity of materials necessary, but in an offshore environment, floating turbines had much better performance than monopiles, and among floating turbines, 5 MW had better performance than 2.3 MW. The phase of extraction and processing of materials emerged as a critical factor and in the offshore environment accounted for up to 82% of total impact. Besides materials, the installation phase plays a primary role in the offshore environment: for floating turbines it accounts for 2% of total impact, against 30% for the classical monopile turbine, due to long processing requiring much machinery.

Wang S. et al., 2019 published an assessment of greenhouse gas emissions of a 2 MW turbine based on LCA, envisaging installation onshore and offshore (spar-buoy-type platform). The results are much higher than the unit and mean values of the rest of the literature. According to the report, the phase that weighs most on total emissions is transport and installation (>90% of total emissions), contrary to the rest of the literature. The authors show that the emissions of floating turbines are greater than those of onshore turbines due to a greater quantity of materials necessary for the foundations. It also emerges that turbine lifetime and productivity are among the factors that most influence environmental performance.

Poujol et al. (2020) reported a detailed study that included LCA of a real wind farm, installation of which should be complete in the coming months in the Gulf of Lion, south of France. The farm will consist of four turbines each with a nominal power of 6 MW, mounted on raft-buoy platforms, Heliande model 150. The farm will be installed 16 km off Leucate and productivity is estimated at 72 GWh/y and 1.45 TWh during the farm's estimated 20 years of life. The results show that materials (especially the floater) are responsible for the largest fraction of the impact. The other phases have a more marginal role, and for end-of-life the main contribution comes from fuel for transport in the decommissioning phase. Installation is envisaged in two coastal sites in Normandy and Brittany, where 14% and 25% reductions in impact per kWh seem possible, respectively. This underlines the importance of having site-specific estimates of energy productivity. It also emerged that structures with longer lifetimes have better environmental performance; the better productivity obtained makes up for the greater maintenance requirements of longer life. It is also demonstrated that the quantities of materials, especially steel, have a non-negligible impact on the final results and it is therefore important to have reliable background data.

Table 1 shows the Carbon Intensity of Electricity (CIE) values expressed in g CO_2eq·kWh^{-1}, obtained from the literature, of various types of onshore and offshore wind turbines, bottom-

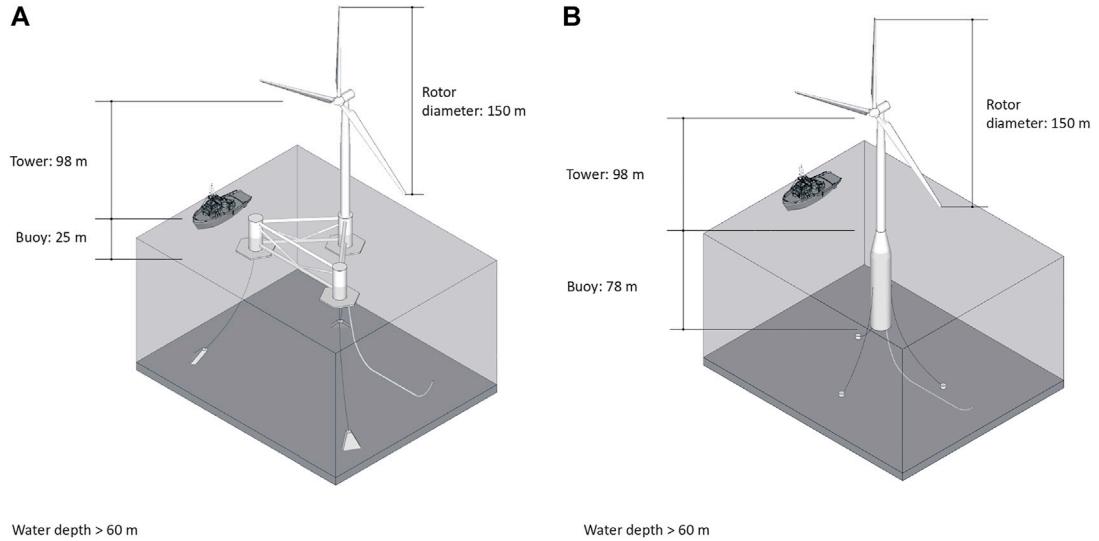

FIGURE 1 | Type and size of offshore floating wind turbines: raft-buoy **(A)** and spar-buoy **(B)**. Each one is composed by three main parts: rotor, tower, and buoy.

fixed and floating, with installed powers ranging from 1 to 6 MW. The table also gives information about the nominal power (in MW) of single turbines, the LCA phases and sensitivity analysis.

Although the case studies are highly varied in terms of subject and approach, results can be compared by considering relevant variables and indicators. For example, mean values of CIE by technology can be deduced: 6.8 g CO_2eq·kWh^{-1} for onshore wind turbines, 31.5 g CO_2eq·kWh^{-1} for bottom-fixed offshore wind turbines (including monopiles, OC4 jacket, tripod and gravity-based foundations) and 25.9 g CO_2eq·kWh^{-1} for offshore floating wind turbines (including spar-buoy, semi-submersible, tension-leg-spar, tension-leg-platform, tension-leg-buoy and Dutch tri-floater). The values of Wang S. et al., 2019 were not used to obtain these mean values because they were not coherent with the values published in the literature.

The aim of this paper is to evaluate the performance of two technological solutions of offshore floating wind turbines compared with studies from the literature. The generalisation in terms of type, size or installed power through a benchmark specifically designed, avoids reference to devices tested in a specific study or products of a specific company. It will help overcome differences between studies published in the literature and to interpret their results. The data complies with the 3D digital models of **Figure 1** which shows the main components and materials used. As a standard for widespread use, the models were constructed using realistic thicknesses and volumes, in line with the literature, ignoring technological details that show a variety of possible solutions but that do not significantly affect overall impact. Making reference to two simplified digital models instead of specific technologies with many variables, the two floating wind turbines offer a benchmark, namely two generic types, representative of a large range of specific technological solutions.

Once the models were created, inventory data were used for the analysis of environmental performance using the LCA methodology. The potential environmental impacts in terms of CF (t CO_2eq) were then quantified by the application of the Global Warming Potential (GWP 100a) characterization method. Thereafter, the analysis postulated the used of floating wind turbines to build wind farms in the Mediterranean by assuming the production potentials obtained in three sites: Crete (Greece), Split (Croatia) and Larnaca (Cyprus). In particular, values of energy production (MWh·yr^{-1}) refer to hypothetical offshore wind farms per each of the 6 MW units as documented by Pulselli et al. (2022). Using the results of GWP and electricity production per one turbine, we estimated the value of CIE in g CO_2eq·kWh^{-1} (Moro and Lonza, 2017). This indicator allowed for comparing values measured in the three sites examined with those of different wind farms reported in the literature, but also with values of other technologies exploiting renewable resources. Furthermore, the emission values of the electricity grid mix of different countries were compared with those emerging from the present analysis.

MATERIALS AND METHODS

The study analyses the components and processes of the life cycle of two types of floating wind turbine, raft-buoy and spar-buoy, both with 6 MW nominal power. The raft-buoy (**Figure 1A**) consists of a large, partly submerged triangular floating platform. Three columns at the apices of the platform contain ballast and horizontal anti-capsize plates. The tower of the turbine is mounted on one apex of the platform. The structure is anchored to the bottom with steel cables and specially designed and calibrated drag anchors (Robertson and Jonkman, 2011; Raadal et al., 2014). The spar-buoy (**Figure 1B**) consists of a long hollow vertical steel cylinder, ballasted in its lower part with water and cement conglomerate. The floating cylinder is half submerged and gives the system

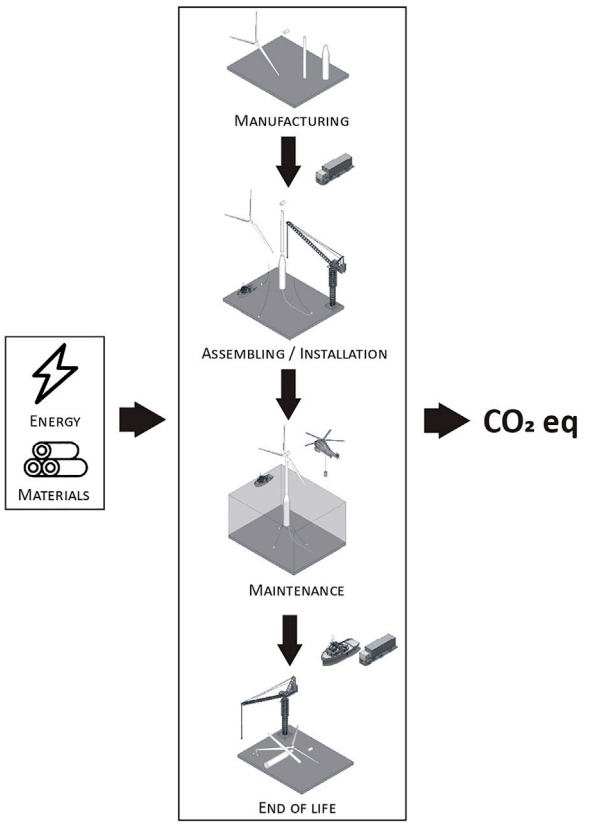

FIGURE 2 | Flow chart including the main life cycle phases of offshore floating wind turbines (raft-buoy model taken as example).

dynamic stability, maintaining a centre of gravity below the waterline (Tomasicchio et al., 2018; Ghigo et al., 2020). The size and characteristics of the rotor (fibreglass blades) and generator are the same for both devices. For an installed power of 6 MW and a rotor diameter of 154 m, the minimum requirements for installation indicate a minimum wind speed threshold of about 3 m/s (Pantusa and Tomasicchio, 2019).

The LCA was conducted in compliance with ISO 14040 (International Standard Organization, 2006) and 14044 (International Standard Organization, 2020). Four main phases were postulated: 1) manufacturing 2) assembly and installation 3) maintenance and material replacement 4) end of life (**Figure 2**). The system boundaries include the main processes of the life cycle from cradle to grave. The analysis considers the impacts of the life cycle of the main energy inputs and materials making up the technological components, starting with the weight of the material used and therefore ignoring the impact of the specific industrial processes used to produce each technological component in its final form (e.g., the impact of steel sheet is considered but not the process of creating the cylinder).

The functional unit (FU) is one year of operation of a 6 MW offshore floating wind turbine, assuming a lifetime of 20 years (Weinzettel et al., 2009; Huang et al., 2017; Chipindula et al., 2018; Wang S. et al., 2019). This made it possible to bring the impacts of the phases of manufacture, assembly-installation and end-of-life into line with the maintenance phase, e.g., regarding periodic replacement of parts subject to wear (i.e. for all elements having a lifetime of less than 20 years).

The inventory data was collected by combining 3D digital models and data from the literature, as reported in detail in **Table 2**. First of all, specific data on materials and energy necessary for Phase 1, manufacture of structural components, was estimated on a quantitative basis and considering the main components of each device.

For Phase 2, assembly-installation, the consumption of materials and energy (diesel for the crane, forklifts, generators, ships etc.), required for assembly on land or on site, is estimated (Chipindula et al., 2018). Emissions for transporting materials and construction components by truck for an assumed distance of 500 km are considered. This value is a precaution to consider the different realities of the Mediterranean basin. Not in all the possible locations for the implementation of the Turbines, in fact, there is the same level of development of the port, maritime, road and industrial infrastructures.

For Phase 3, maintenance, energy consumption of two boats (i.e., six trips per year of the transfer boat for small maintenance operations and one trip per year of the fast supply vessel with replacement components) and of a helicopter (one trip per year) for monitoring the farms, are considered in line with Weinzettel et al. (2009), Tsai et al. (2016) and Wang S. et al., 2019. Replacement of worn parts mostly concern factory pre-assembled technological components, such as the gearbox, which are transported to the site (in line with Bhattacharya et al., 2018; Chipindula et al., 2018; Wang S. et al., 2019).

For Phase 4, decommissioning and end-of-life, we postulated recycling and landfill disposal or waste-to-energy scenarios. Along the lines outlined in Chipindula et al. (2018), Raadal et al. (2014) and Tsai et al. (2016), we assumed the following destinations of the various materials: 90% recycling e 10% landfill for steel, aluminium and iron; 90% recycling and 10% waste-to-energy for copper, lead and zinc; 100% landfill for cement and 100% waste-to-energy for plastic polymers (PE, PP and other plastics), rubber, fibreglass, wood, alkyd paint and epoxy resin. Regarding recyclable metal components, we only counted emissions for their transport to a hypothetical waste management centre (300 km by boat and 200 km by truck). The impacts of subsequent management and recycling of metals to produce secondary raw material were assigned to the future process that would use those materials.

The exploded 3D models in **Figures 3**, **4** show the characteristics and dimensions of the devices. Based on the purpose to set the benchmark, the weights of steel and ballast materials were estimated entering realistic volumes and thicknesses in these models. Data on other materials used in specific components, such as the materials of the rotor blades or the internal parts of the nacelle, was obtained from the literature (Wang S. et al., 2019; Poujol et al., 2020). The composition of the 33 kV submarine cables was obtained from Birkeland (2011) and Tsai et al. (2016) (**Table 2**) postulating a wind farm with four turbines in 1 km^2 of sea and including the cables connecting the turbines to an underwater substation (750 m per turbine) and a cable connecting them to the coast (hypothetical distance of 12

TABLE 2 | Life Cycle Inventory of a 6 MW raft-buoy wind turbine and a 6 MW spar buoy wind turbine.

Element	Technical Specification	Unit	Raft-Buoy turbine		Spar-Buoy turbine		Lifetime (yr)	Notes and references
Phase 1—MANUFACTURING								
Turbine and Floating structure	steel	t	3,504.6	77.1%	3,450.5	33.6%	20	The data comes from 3D models developed in the study and from the literature. Rotor dimensions from Equinor (2021) based on the Hywind wind farm, Scotland; blade thickness and form from Nguyen-Thanh et al., 2016 and Wikantyoso et al. (2019); secondary rotor connection and coating elements from Vestas (2011; 2015; 2017; 2021); information on floating platforms from Antonutti et al. (2016), Les Eoliennes Flottantes du Golfe du Lion, 2018, Principle Power Inc (2022), Roddier et al. (2010) (for raft-buoy turbines), Ghigo et al. (2020) and Equinor (2021) (for spar-buoy turbines). Lifetime was assumed to be 20 years (see for example Huang et al., 2017; Chipindula et al., 2018; Wang S. et al., 2019) for all components except gearbox materials (steel, iron, and rubber)
	concrete	t	—	—	5,500	53.5%	20	
	fiberglass	t	211.3	4.6%	211.3	2.1%	20	
	cast iron	t	173.1	3.8%	173.1	1.7%	20	For components that cannot be obtained from a 3D model, real data from Poujol et al. (2020) was used. The input "other materials" was considered equivalent to steel; in fact, Poujol et al. (2020) indicates that this component is made of metal
	aluminium	t	71.5	1.6%	71.5	0.7%	20	
	plastics	t	65.8	1.4%	65.8	0.6%	20	
	other materials	t	42.8	0.9%	42.8	0.4%	20	
	copper	t	29.8	0.7%	29.8	0.3%	20	
	lead	t	23.5	0.5%	23.5	0.2%	20	
	alkyd paint	t	7.3	0.2%	7.3	0.07%	20	
	wood	t	4.8	0.1%	4.8	0.05%	20	
	zinc	t	4	0.1%	4	0.04%	20	
	epoxy	t	1.2	0.03%	1.2	0.01%	20	
	rubber	t	0.2	0.003%	0.2	0.001%	10	This component belongs to the gearbox
Subtotal	-	t	**4,139.6**	**91.0%**	**9,585.5**	**93.3%**	-	-
Anchor System	steel (chain)	t	180	4%	180	1.8%	20	Three anchorage chains each weighing 60 t were considered on the basis of Equinor (2021) and Vryhof (2018)
	steel (drag anchor/ suction pile)	t	45.0	1.0%	329.7	3.2%	20	Three Stevshark® type anchors measuring 6165 × 6645 mm and each weighing 15 t were considered for the raft-buoy turbine (Vryhof, 2018), as suggested by Golightly (2017). For the spar-buoy turbine, suction piles were modelled in 3D on the basis of the dimensions suggested by Golightly (2017) and Supachawarote (2006)
Subtotal	-	t	**225.0**	**4.9%**	**509.7**	**5%**	-	-
Submarine Power Cable (33 kV)	lead	t	50.4	1.1%	50.4	0.5%	20–40	A 33 kV submarine cable was chosen for connecting the turbines to the substation and for connection to the coast (Tsai et al., 2016); data from Birkeland (2011). Lifetime: 20 years for cables within the farm; 40 years for cables connecting to the national grid. The substation for cables within the farm was not considered in this study
	copper	t	37.8	0.8%	37.8	0.4%	20–40	
	polyethylene (PE)	t	12.6	0.3%	12.6	0.1%	20–40	
	steel	t	75.7	1.7%	75.7	0.7%	20–40	
	polypropylene (PP)	t	6.3	0.1%	6.3	0.06%	20–40	
Subtotal	-	t	**182.8**	**4%**	**182.8**	**1.8%**	-	-
Total Phase 1	-	t	**4,547.4**	**100%**	**10,278**	**100%**	-	-
Phase 2—ASSEMBLY and INSTALLATION								
Generator	diesel	t	2.8	37.9%	-	-	20	Equipment postulated on the basis of Chipindula et al. (2018). The raft-buoy turbine is assembled at the port and transported to the site: data for installation of an onshore turbine was used (without considering the machinery necessary for construction of the foundations: truck mixer, truck gravel and excavator) and sea transport for 22.2 km was considered. Data for installation of a deep-water wind turbine was used for the spar-
Crane	diesel	t	4.1	56.3%	4.1	38.5%	20	
Forklift	diesel	t	0.4	5.8%	0.4	4.0%	20	
Tugboat	diesel	t	-	-	4.2	39.0%	20	
Auxiliary boats	diesel	t	-	-	2.0	18.5%	20	

(Continued on following page)

TABLE 2 | (*Continued*) Life Cycle Inventory of a 6 MW raft-buoy wind turbine and a 6 MW spar buoy wind turbine.

Element	Technical Specification	Unit	Raft-Buoy turbine		Spar-Buoy turbine		Lifetime (yr)	Notes and references
								buoy. 8 h of work with the following hourly diesel consumption rate was assumed for all equipment: generator 418 L/h; crane 620.1 L/h; forklift 64 L/h; tugboat 628 L/h; auxiliary boat 297 L/h (Chipindula et al., 2018)
Total Phase 2	-	t	**7.4**	**100%**	**10.7**	**100%**	-	-
Phase 3—MAINTENANCE and MATERIAL REPLACEMENT								
Gearbox	cast iron	t	14.1	49.7%	14.1	49.7%	10	As suggested in Wang S. et al., 2019 and Chipindula et al. (2018), we assumed that the whole gearbox was replaced once in 20 years. Materials are from Wang S. et al., 2019 adjusted for a 6 MW turbine on the basis of rotor size (Bhattacharya et al., 2018 suggests a diameter of 100 m for a 2 MW turbine and 154 m for a 6 MW turbine)
	steel	t	14.1	49.7%	14.1	49.7%	10	
	rubber	t	0.2	0.5%	0.2	0.5%	10	
Subtotal Phase 3 (materials)	-	t	28.3	100%	28.3	100%	-	-
Transfer boat	diesel	t	2.4	14.6%	2.4	14.6%	1	As suggested by Tsai et al. (2016), 6 transfer boat trips per year (400 kg diesel/trip) and one FSV trip/year (29,000 kg diesel/trip) were considered, as well as one 4-h helicopter trip/year (as suggested in Weinzettel et al., 2009; Wang S. et al., 2019) which consumes 234 L/h kerosene (Swiss Helicopter, 2022)
Fast Supply Vessel (FSV)	diesel	t	13.2	79.8%	13.2	79.8%	1	
Helicopter	kerosene	t	0.9	5.7%	0.9	5.7%	1	
Subtotal Phase 3 (energy)	-	t	16.5	100%	16.5	100%	-	-
Phase 4—END OF LIFE								
Materials	Unit	Wind Raft Turbine			Spar Buoy Turbine			Notes and References
		Recycling	Landfill	Waste-to-energy	Recycling	Landfill	Waste-to-energy	
steel	t	3,450.0	380.6	-	3,657.6	403.7	-	Recycling 90% - Landfill 10%
concrete	t	-	-	-	-	5,500	-	Landfill 100%
fiberglass	t	-	-	211.3	-	-	211.3	Waste-to-energy 100%
cast iron	t	181.1	20.1	-	181.1	20.1	-	Recycling 90% - Landfill 10%
aluminium	t	64.4	7.2	-	64.4	7.2	-	Recycling 90% - Landfill 10%
plastics	t	-	-	65.8	-	-	65.8	Waste-to-energy 100%
other materials	t	38.5	4.3	-	38.5	4.3	-	Recycling 90% - Landfill 10%
copper	t	60.8	-	6.8	60.8	-	6.8	Recycling 90% - Waste-to-energy 10%
lead	t	66.5	-	7.4	66.5	-	7.4	Recycling 90% - Waste-to-energy 10%
alkyd paint	t	-	-	7.3	-	-	7.3	Waste-to-energy 100%
wood	t	-	-	4.8	-	-	4.8	Waste-to-energy 100%
zinc	t	3.6	-	0.4	3.6	-	0.4	Recycling 90% - Waste-to-energy 10%
epoxy resin	t	-	-	1.2	-	-	1.2	Waste-to-energy 100%
rubber	t	-	-	0.3	-	-	0.3	Waste-to-energy 100%
polyethylene (PE)	t	-	-	12.6	-	-	12.6	Waste-to-energy 100%
polypropylene (PP)	t	-	-	6.3	-	-	6.3	Waste-to-energy 100%

nautical miles, i.e., 22.2 km). **Figure 5** shows the wind farms layout for both models.

Table 2 shows the inventory data for the components and processes of the life cycle of raft-buoy and spar-buoy turbines. The table is a scheme of reference for the life cycle inventory of wind turbines, for replicating LCA or for showing differences in the calculation model. Lifetimes were differentiated to account for maintenance and replacement of certain construction elements. On the basis of the estimated lifetime of the structure (20 years) and the differentiated lifetimes, the table gives the values per FU, i.e., for one year of operation. The estimated lifetime of the electrical cables to the coast is 40 years, which is longer than the life of the wind farm, as suggested by Huang et al. (2017).

SimaPro 9.1.1 software (PRé Consultants, 2020) was used to model the inventory and do Life Cycle Impact Assessment. Ecoinvent v3.6 (Ecoinvent, 2022) is the database used as source of secondary data. We used the IPCC 2013 method of

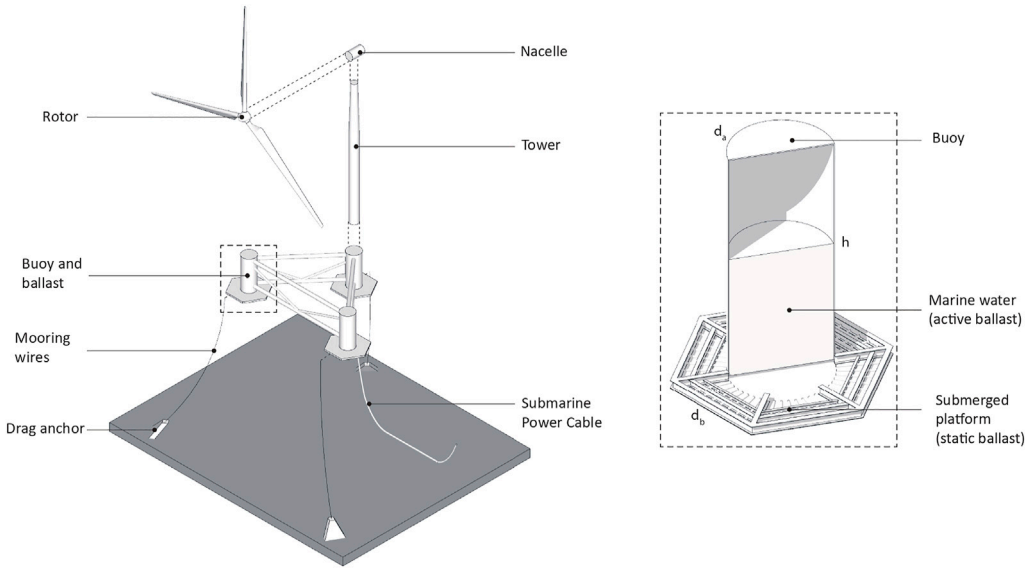

FIGURE 3 | Main construction elements of offshore raft-buoy wind turbine. Legend and values: d_a: 10 m, d_b: 21 m, h: 25 m.

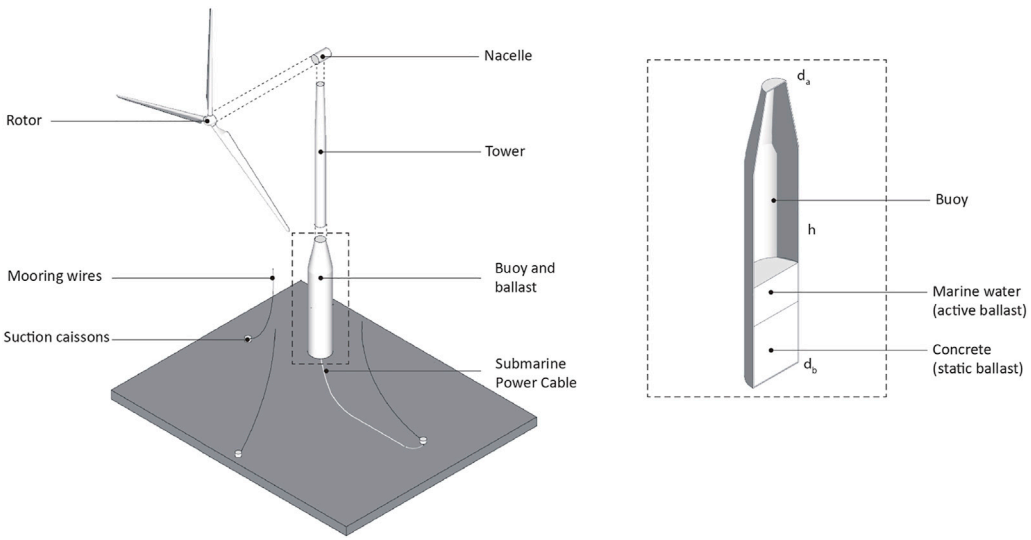

FIGURE 4 | Main construction elements of offshore spar-buoy wind turbine. Legend and values: d_a: 10 m, d_b: 14.5 m, h: 78 m.

characterisation and the impact category Global Warming Potential—GWP100a with a time horizon of 100 years (IPCC, 2013) to calculate greenhouse gas emissions via the Carbon Footprint indicator.

On the basis of the LCA results, we calculated the CIE per kWh generated by each turbine, assuming a reference energy production in three areas of the Mediterranean Sea with different energy potentials: a 300 MW wind farm installed in Crete (Greece) (50 × 6 MW wind turbines) is expected to generate 1.17 $TWh \cdot yr^{-1}$ (Stančin et al., 2022) or 23.4 $GWh \cdot yr^{-1}$ per turbine. Likewise, those in Split (Croatia) and Larnaca (Cyprus) are expected to generate 14.5 $GWh \cdot yr^{-1}$ and 9.6 $GWh \cdot yr^{-1}$ per turbine, respectively (Pulselli et al., 2022). Since this is an analysis aimed at creating a benchmark applicable in different contexts, the average value of the distance between the farm and the coast is the same for each area (22 km). This assumption makes the three systems comparable from the point of view of LCA; since, for example, the variation in the length of the connection cable to the electricity grid can significantly affect the result. Furthermore,

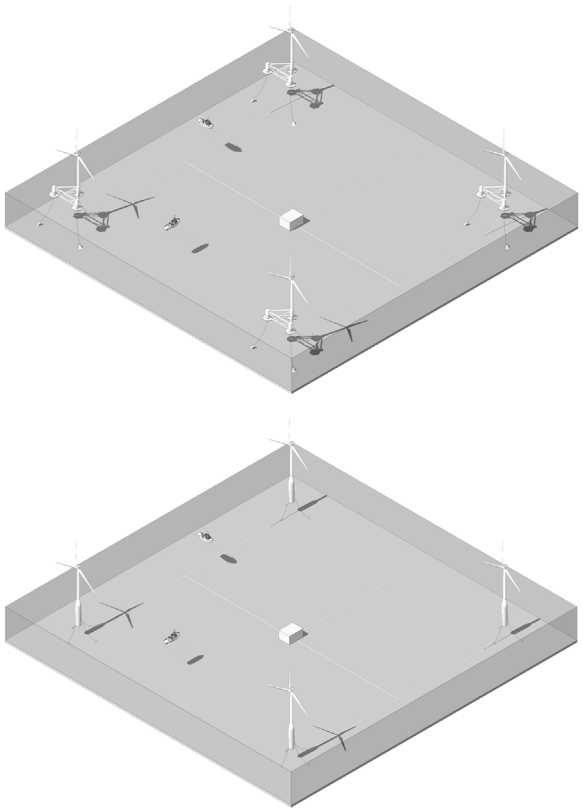

FIGURE 5 | The windfarm layout with four turbines in 1 km^2 (distance between turbines: 750 m) for raft-buoy (above) and spar-buoy (below) model.

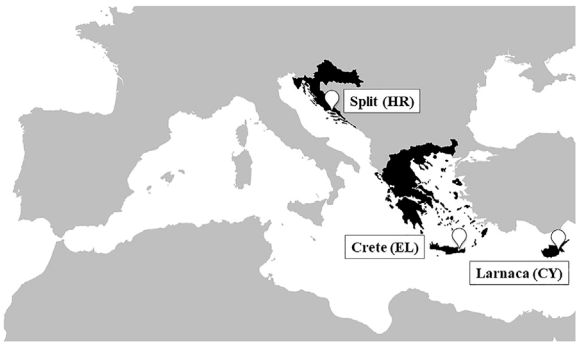

FIGURE 6 | Map of the Mediterranean Sea showing the three sites proposed for installation of wind farms: Crete (Greece), Split (Croatia) and Larnaca (Cyprus)—Map created with mapchart.net.

for the purposes of the study, the distance between the farm and a hypothetical port for the logistical management of the plant both during construction and maintenance, was assumed to coincide with that mentioned above. The three areas are shown in **Figure 6**. To estimate the productivity of the three areas, we considered wind energy potentials measured locally on yearly averaged values; the productivity values are site-specific since they also consider feasibility on the basis of the current energy balance of the national grids in the three sites (Pulselli et al., 2022). **Table 4** shows the productivity of a single wind turbine in the three sites.

RESULTS AND DISCUSSION

Table 3 shows the GWP (t CO_2eq) values of individual components and the total for the two devices. The life cycle of the two types of floating wind turbine (including the cables connecting them to the mainland) generates emissions of 12,242 t CO_2eq (i.e., 612 t CO_2eq per year of operation) in the case of the raft-buoy and 15,118 t CO_2eq (i.e., 756 t CO_2eq per year) in the case of the spar-buoy.

Figure 7 shows the main greenhouse gas emission sources by life cycle phase and process. The manufacturing phase that includes the materials constituting the turbines, the anchoring systems and the electric cables is the main source of emissions: over 75% for the raft-buoy (49% steel and 15.6% fiberglass); almost 70% for the spar-buoy (42.1% steel; 12.7% fiberglass); this is consistent with the results obtained in literature for other renewable energy sources, in which the manufacturing and installation phases dominate the impacts (Sacchi et al., 2019). According to Chipindula et al. (2018) for deep-water turbines, the manufacturing stage accounts for 81.5% of the total impact. Poujol et al. (2020) highlighted that around 80% of the climate change impact category are mainly due to the raw material extraction and manufacturing. Results obtained also agree with Raadaal et al. (2014), which showed that the turbine and foundation/platform materials (i.e., production, processing, transport and disposal of all the infrastructure material related to these elements production) contribute most to the overall GHG emissions (around 60%–80%). The difference between the two models is deduced principally from the mass balance: 4,547 t for the raft-buoy, of which 3,805 t (83.7%) steel; 10,278 t for the spar-buoy of which 4,036 t (39.3%) steel and 5,500 t (53.5%) cement. In alternative to cement, materials such as rubble could reduce emissions from cement production. The maintenance emissions can principally be attributed to the fuel used by motor vessels or craft (9.7% raft-buoy and 7.8% spar-buoy) necessary to replace gearbox components. Fuel for transport and assembly of components amounts to 7.5% and 17.7%, respectively.

The GWPs estimated for the two solutions were compared to the electrical productivity ($MWh{\cdot}yr^{-1}$) in the three sites, giving the CIE, expressed in g CO_2eq·kWh^{-1} (**Table 4**). The CIE values for production of electricity by the offshore floating wind farms fall in the range 26.1–78.7 g CO_2eq·kWh^{-1}. These results depend on the impacts measured for the two types of turbine, and are naturally influenced by the site-specific productivity of the marine areas selected: the intervals by type of turbine (raft-buoy and spar-buoy) are 26.1–32.2 g CO_2eq·kWh^{-1}, respectively, for Crete (EL), 42.1–52 g CO_2eq·kWh^{-1} for Split (HR) and 63.8–78.7 g CO_2eq·kWh^{-1} for Larnaca (CY). Mean values of 44 g CO_2eq·kWh^{-1} and 54.3 g CO_2eq·kWh^{-1} were recorded for raft-buoy and spar-buoy, respectively, in the eastern Mediterranean. The overall mean is 49.2 g

TABLE 3 | Life Cycle Analysis of a 6 MW raft-buoy wind turbine and a 6 MW spar buoy wind turbine.

Element	Technical Specification	Raft-Buoy turbine t CO_2eq	Raft-Buoy turbine%	Spar-Buoy turbine t CO_2eq	Spar-Buoy turbine%
Phase 1—MANUFACTURING					
Turbine and Floating structure	steel	278.7	45.5%	274.5	36.3%
	concrete	—	—	33.8	4.5%
	fiberglass	95.8	15.6%	95.8	12.7%
	cast iron	17.6	2.9%	17.6	2.3%
	aluminium	29.3	4.8%	29.3	3.9%
	plastics	9.5	1.5%	9.5	1.3%
	other materials	3.4	0.6%	3.4	0.4%
	copper	1.2	0.2%	1.2	0.2%
	lead	1.5	0.2%	1.5	0.2%
	alkyd paint	2.1	0.3%	2.1	0.3%
	wood	0.04	0.01%	0.04	0.005%
	zinc	1.0	0.2%	1.0	0.1%
	epoxy	0.3	0.04%	0.3	0.03%
	rubber	0.05	0.01%	0.05	0.01%
Subtotal		440.3	71.9%	469.9	62.2%
Anchor System	steel (chain)	14.3	2.3%	14.3	1.9%
	steel (drag anchor/suction pile)	3.6	0.6%	26.1	3.5%
Subtotal		17.8	2.9%	40.4	5.3%
Submarine Power Cable (33 kV)	lead	1.8	0.3%	1.8	0.2%
	copper	0.8	0.1%	0.8	0.1%
	polyethylene (PE)	0.6	0.1%	0.6	0.1%
	steel	3.4	0.5%	3.4	0.4%
	polypropylene (PP)	0.29	0.05%	0.3	0.04%
Subtotal		6.9	1.1%	6.9	0.9%
Total Phase 1		465.1	76%	517.2	68.4%
Phase 2—TRANSPORT, ASSEMBLY and INSTALLATION					
Generator	diesel	0.5	0.1%	-	-
Crane	diesel	0.8	0.1%	0.8	0.1%
Forklift	diesel	0.1	0.01%	0.1	0.01%
Tugboat	diesel	-	-	0.8	0.1%
Auxiliary boats	diesel	-	-	0.4	0.05%
Transport (truck)	-	43.3	7.1%	132	17.5%
Transport (boat)	-	1.1	0.2%	-	-
Total Phase 2		45.8	7.5%	134	17.7%
Phase 3—MAINTENANCE and MATERIAL REPLACEMENT					
Gearbox	cast iron	2.6	0.4%	2.6	0.4%
	steel	2.2	0.4%	2.2	0.3%
	rubber	0.05	0.01%	0.05	0.01%
Subtotal Phase 3 (materials)		4.9	0.8%	4.9	0.7%
Transfer boat	diesel	9.1	1.5%	9.1	1.2%
FSV vessel	diesel	49.7	8.1%	49.7	6.6%
Helicopter	kerosene	0.4	0.1%	0.4	0.1%
Subtotal Phase 3 (energy)		59.2	9.7%	59.2	7.8%
Phase 4—END OF LIFE					
Total Phase 4		37.1	6.1%	40.5	5.4%

CO_2eq·kWh^{-1} for a generic floating wind turbine installed in the eastern Mediterranean. The values obtained are in line with previous studies, as shown in **Table 1**. Particularly, in the case of Crete, the results obtained are consistent with the average values found in the literature for floating turbines (around 26 g CO_2eq·kWh^{-1} considering Weinzettel et al., 2009; Raadal et al., 2014; Tsai et al., 2016; Chipindula et al., 2018; Poujol et al., 2020).

In general, the CIE results indicate good environmental performance of floating wind turbines. They are in line with those of other renewable energy sources of electricity, such as onshore wind (10 g CO_2eq·kWh^{-1}) and photovoltaic (32 g CO_2eq·kWh^{-1}) (Pulselli et al., 2019) and are well below current CIE values of national electricity grids (Greece: 479 g CO_2eq·kWh^{-1}; Croatia: 134 g CO_2eq·kWh^{-1}; Cyprus: 621 g

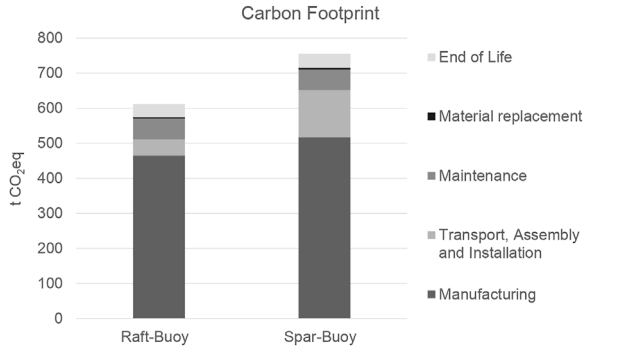

FIGURE 7 | Carbon Footprint (t CO_2eq) results for the two floating turbine models (raft-buoy and spar-buoy), in relation to different LCA phases.

CO_2eq·kWh^{-1}; data of 2020, source EEA, 2022). If the most suitable marine areas with good wind potential are chosen (e.g., Crete), the study shows that floating wind turbines in the Mediterranean are competitive in terms of environmental performance, with CIE values similar to those recorded in ocean contexts.

LCA is not the last word in evaluation of offshore technologies. Marine spatial planning should also consider other aspects, such as direct and indirect impact on flora and fauna, landscape compatibility, and interference with other marine activities like navigation, tourism and fisheries. The LCA method is useful to orientate decisions and to pinpoint solutions towards carbon neutrality. Although wind farms can have impacts on ecosystems and these need to be appropriately evaluated, several studies are showing that offshore wind farms can protect and even favour the proliferation of a wide range of marine species, such as fish, molluscs, crustaceans, seals and porpoises, that forage in these seas (Russell et al., 2014; Vattenfall, 2018).

With a view to future integration of renewable energy sources, floating systems offer a valid opportunity to integrate offshore wind with other renewable energies, such as floating photovoltaic, wave energy converters, aquaculture and hydrogen production (Buck et al., 2017; Lee et al., 2018; Roy et al., 2018; Fenu et al., 2020; SINN Power GmbH, 2022). LCA can be an auxiliary methodology for developing integrated systems, provided the results of different studies can be compared.

Sensitivity Analysis

To assess variations in terms of CF and consequently CIE, we conducted sensitivity analysis, postulating changes in a parameter that most influences the results of the study, namely the quantity of steel necessary to build the two types of turbine (46% CF for raft-buoy and 36% CF for spar-buoy). As indicated by the literature, steel is the predominant structural component of turbines (Poujol et al., 2020) and platforms/foundations (Raadal et al., 2014), besides being the greatest contributor to impacts in terms of emissions of greenhouse gases in the manufacturing phase (Phase 1). This applies to both systems, as seen above. Besides reducing the quantity of steel used, it turned out to be crucial to use recycled materials, which can significantly improve performance in terms of CF, as shown by Tsai et al. (2016) and Weinzettel et al. (2009).

We therefore considered three scenarios (S1, S2, S3) in which the quantity of steel used in the floating structure was reduced, and two scenarios in which recycled steel was used (S4 and S5). In the first three scenarios, steel was reduced by 5%, 10% and 15%, respectively. In S4 and S5, 30% and 50% of recycled metal was postulated for the turbine and the floating structure. The anchoring structure and the electric cables were not included in the evaluation.

The sensitivity analysis showed that for both models, scenarios S1 and S2 (with 5% and 10% reductions in the quantity of steel used) did not significantly improve impact (−0.3% and −0.5%, respectively), whereas scenario S3 (15% less steel) was associated with a 1% reduction in CF for both models. The CF of the raft-buoy model fell from 612 to 585 t CO_2eq, whereas the CF of the spar-buoy model dropped from 756 to 730 t CO_2eq. The mean CIE for the three sites declined from 44 to 42.1 g CO_2eq·kWh^{-1} for the raft-buoy and from 54.3 to 52.4 g CO_2eq·kWh^{-1} for the spar-buoy model.

These are only models. A reduction in the quantity of steel exceeding 15% would require further upstream engineering assessments. It is therefore reasonable to assume a life cycle perspective and to propose the use of recycled steel. On this question, the results for S4 and S5 showed that for both models, the scenario envisaging 50% recycled steel for the turbine is a critical variable (-1.3%). In particular, the CF of the raft-buoy drops from 612 to 566 t CO_2eq, whereas that of the spar-buoy goes from 756 to 710 t CO_2eq. Likewise for the CIE, the mean for the raft-buoy goes from 44 to 40.7 g CO_2eq·kWh^{-1} while that of the spar-buoy falls from 54.3 to 51 g CO_2eq·kWh^{-1}.

Sensitivity analysis showed minimal changes in the result obtained for GHG emissions and CIE with variations in the quantity and composition of the steel components. No significant change in the results were obtained by varying these parameters.

TABLE 4 | Electricity production yields and CIE of 6 MW wind turbines (raft-buoy and spar-buoy) and 24 MW wind farms in three Mediterranean marine areas, based on site-specific wind energy potentials.

Site	Electricity Production yield		Carbon intensity of electricity (CIE) g CO_2eq·kWh^{-1}	
	One wind turbine (GWh/yr)	1 km^2 farm - 4 turbines (TWh/20 years)	Raft-Buoy wind turbine	Spar-Buoy wind turbine
Crete, Greece	23.5	1.9	26.1	32.2
Split, Croatia	14.5	1.2	42.1	52
Larnaca, Cyprus	9.6	0.8	63.8	78.7

This observation lends reliability to the conclusions in relation to some of the assumptions made during the data inventory.

CONCLUSIONS

The marine renewable energy sector in Europe is growing and indicates offshore wind technologies to be among the most promising. The development of offshore floating wind farms is therefore strategic for the Mediterranean, where sea depth increases sharply with distance from the coast and does not permit the installation of bottom-fixed turbines. The present study documents the use of LCA to evaluate the environmental performance of two types of floating wind turbines, postulating their installation in three sites in the Mediterranean with different wind energy potentials. LCA has been used for similar studies, which have been used for comparison, highlighting different methodological assumptions (e.g., regarding life cycle processes or estimated electricity production) and the variety of technologies analysed and documented in the literature. Starting from theoretical 3D models for raft-buoy and spar-buoy models, we defined a benchmark, a generalisation useful for comparing the results obtained by more specific technologies, following homogeneous evaluation criteria. Any technology alternative to those presented, and presumably designed to improve performance, can be compared with the two basic solutions by a similar calculation procedure. Theoretically, a new offshore floating wind turbine technology, subject to LCA, should give better results than the two standard models in order to demonstrate its efficacy or should publish the factors that lead to different results (which could depend on more accurate inventory data or additional technological components).

The results show an interval of CIE values (range 26.1–78.7 g CO_2eq·kWh^{-1}), variations which depend largely on mass balance (materials used in the manufacturing and maintenance phases) and of course selection of marine areas with different wind energy potentials. The mean value of CIE recorded (49.2 g CO_2eq·kWh^{-1} for a generic floating wind turbine installed in the eastern Mediterranean) is in line with that of other renewable energy sources. Thus, the results show the competitivity of floating wind turbines in the Mediterranean and are useful to orientate the design of more efficient technologies. Sensitivity analysis reinforces the reliability of the evaluations and the assumptions made in the inventory phase. In line with other studies in the literature, it also showed that further research is necessary to conceive ways of reducing the quantity of steel needed to build floating wind turbines. It also shows that the use of recycled steel can improve the environmental performance of these devices.

DATA AVAILABILITY STATEMENT

The original contributions presented in the study are included in the article/Supplementary Material, further inquiries can be directed to the corresponding author.

AUTHOR CONTRIBUTIONS

RP, MM, MB, EN, and NP conceived the paper and processed and discussed data. AS elaborated the 3D models and extracted inventory data. RP and SB supervised writing of the paper. All authors discussed reviewer feedback and contributed to the final manuscript.

FUNDING

This study was conducted in the framework of the Interreg Med BLUE-DEAL (2019–2022) project, co-financed by the European Regional Development Fund. Website: https://blue-deal.interreg-med.eu.

REFERENCES

Antonutti, R., Peyrard, C., Johanning, L., Incecik, A., and Ingram, D. (2016). The Effects of Wind-Induced Inclination on the Dynamics of Semi-submersible Floating Wind Turbines in the Time Domain. *Renew. Energy* 88, 83–94. doi:10.1016/j.renene.2015.11.020

Bhattacharya, S., Nikitas, G., and Jalbi, S. (2018). "On the Use of Scaled Model Tests for Analysis and Design of Offshore Wind Turbines," in *Geotechnics for Natural and Engineered Sustainable Technologies* (Singapore: Springer), 107–129. doi:10.1007/978-981-10-7721-0_6

Birkeland, C. (2011). *Assessing the Life Cycle Environmental Impacts of Offshore Wind Power Generation and Power Transmission in the North Sea*. dissertation/master's thesis. Trondheim: Norwegian University of Science and Technology.

Buck, B. H., Krause, G., Pogoda, B., Grote, B., Wever, L., Goseberg, N., et al. (2017). "The German Case Study: Pioneer Projects of Aquaculture-Wind Farm Multi-Uses," in *Aquaculture Perspective of Multi-Use Sites in the Open Ocean* (Cham: Springer), 253–354. doi:10.1007/978-3-319-51159-7_11

Chipindula, J., Botlaguduru, V., Du, H., Kommalapati, R., and Huque, Z. (2018). Life Cycle Environmental Impact of Onshore and Offshore Wind Farms in Texas. *Sustainability* 10, 2022. doi:10.3390/su10062022

Comelli, E. (2020). Nascerà in Sicilia il primo parco eolico galleggiante del Mediterraneo. *Investimento da 740 milioni di euro della danese Cph. Offshore Partners al largo di Marsala tecnologia espansione*.

Diamond, K. E. (2012). Extreme Weather Impacts on Offshore Wind Turbines: Lessons Learned. *Nat. Resour. Environ.* 27 (2), 37–41.

Dominelli, C. (2021). Saipem: dalle turbine eoliche all'idrogeno, ecco l'hub energetico al largo delle coste di Ravenna. *Avviato il percorso Aut. il progetto oltre U. N. miliardo euro che Consent. il rilancio del distretto Ind. della città emiliana*.

Ecoinvent (2022). Ecoinvent. Available at: https://ecoinvent.org/(Accessed April 13, 2022).

Equinor (2021). How Hywind Works. Available at: https://www.equinor.com/en/what-we-do/floating-wind/how-hywind-works.html (Accessed April 13, 2022).

European Commission (2020a). *Communication from the Commission to the European Parliament, the Council, the European Economic and Social Committee and the Committee of the Regions - an EU Strategy to Harness the Potential of Offshore Renewable Energy for a Climate Neutral Future*. Brussels: European Commission.

European Commission (2021). *Communication from the Commission to the European Parliament, the Council, the European Economic and Social Committee and the Committee of the Regions - on a New Approach for a Sustainable Blue Economy in the EU Transforming the EU's Blue Economy for a Sustainable Future*. Brussels: European Commission.

European Commission (2019). *Communication from the Commission to the European Parliament, the Council, the European Economic and Social Committee, and the Committee of the Regions*. Brussels: The European Green Deal.

European Commission (2020b). The EU Blue Economy Report. Available at: https://op.europa.eu/it/publication-detail/-/publication/83843365-c18d-11ea-b3a4-01aa75ed71a1 (Accessed April 13, 2022).

European Environment Agency (EEA) (2022). Greenhouse Gas Emission Intensity of Electricity Generation in Europe. Available at: https://www.eea.europa.eu/ims/greenhouse-gas-emission-intensity-of-1 (Accessed April 13, 2022).

Fenu, B., Attanasio, V., Casalone, P., Novo, R., Cervelli, G., Bonfanti, M., et al. (2020). Analysis of a Gyroscopic-Stabilized Floating Offshore Hybrid Wind-Wave Platform. *Jmse* 8, 439. doi:10.3390/jmse8060439

Ghigo, A., Cottura, L., Caradonna, R., Bracco, G., and Mattiazzo, G. (2020). Platform Optimization and Cost Analysis in a Floating Offshore Wind Farm. *Jmse* 8, 835. doi:10.3390/jmse8110835

Golightly, C. R. (2017). GO-ELS Ltd. – Anchoring for Floating Wind Turbines Future Offshore Foundations. Available at: https://www.researchgate.net/publication/321011241 (Accessed April 13, 2022).

Huang, Y.-F., Gan, X.-J., and Chiueh, P.-T. (2017). Life Cycle Assessment and Net Energy Analysis of Offshore Wind Power Systems. *Renew. Energy* 102, 98–106. doi:10.1016/j.renene.2016.10.050

Intergovernmental Panel on Climate Change (IPCC) (2013). Fifth Assessment Report. The Physical Science Basis. Available at: https://www.ipcc.ch/report/ar5/wg1/(Accessed April 13, 2022).

International Renewable Energy Agency (IRENA) (2019). Future of Wind. Deployment, Investment, Technology, Grid Integration and Socio-Economic Aspects. Available at: https://www.irena.org/-/media/Files/IRENA/Agency/Publication/2019/Oct/IRENA_Future_of_wind_2019.pdf (Accessed April 13, 2022).

International Standard Organization (ISO) (2006). *Environmental Management and Life Cycle Assessment e principles and Framework, Goal and Scope Definition and Life Cycle Inventory Analysis, Life Cycle Impact Assessment and Life Cycle Interpretation*. Geneva: International Organization for Standardization.

International Standard Organization (ISO) (2020). *Environmental Management and Life Cycle Assessment e requirements and Guidelines*. Geneva: International Organization for Standardization.

Jonkman, J. M., Butterfield, S., Musial, W., and Scott, G. (2009). *Definition of a 5-MW Reference Wind Turbine for Offshore System Development*. Technical Report NREL/TP-500-38060. Golden, CO: National Renewable Energy Lab. (NREL). doi:10.2172/947422

Kettle, A. J. (2020). Storm Xaver over Europe in December 2013: Overview of Energy Impacts and North Sea Events. *Adv. Geosciences* 54, 137–147. doi:10.5194/adgeo-54-137-2020

Lee, H., Poguluri, S., and Bae, Y. (2018). Performance Analysis of Multiple Wave Energy Converters Placed on a Floating Platform in the Frequency Domain. *Energies* 11, 406. doi:10.3390/en11020406

Les Eoliennes Flottantes du Golfe du Lion (EFGL) (2018). Qu'est-ce que l'éolien flottant? Pourquoi au large de leucate et du barcarès? Available at: https://info-efgl.fr/wp-content/uploads/2021/05/EFGL_fiche_Eolien_flottant.pdf (Accessed April 13, 2022).

Maestrale (2022). Maestrale. Available at: https://maestrale.interreg-med.eu/ (Accessed April 13, 2022).

Moro, A., and Lonza, L. (2017). Electricity Carbon Intensity in European Member States: Impacts on GHG Emissions of Electric Vehicles. *Transp. Res. D. Transp. Environ.* 64, 5–14. doi:10.1016/j.trd.2017.07.012

Nguyen-Thanh, N., Zhou, K., Zhuang, X., Areias, P., Nguyen-Xuan, H., Bazilevs, Y., et al. (2016). Isogeometric Analysis of Large-Deformation Thin Shells Using RHT-Splines for Multiple-Patch Coupling. *Comput. Methods Appl. Mech. Eng.* 316, 1157–1178. doi:10.1016/j.cma.2016.12.002

Palmiotti, D. (2022). Taranto, il primo parco eolico offshore d'Italia va verso il completamento - Completata l'installazione della prima delle 10 turbe di Beleolico. *Nel Salento arrivo U. N. parco "galleggiante"*.

Pantusa, D., Francone, A., and Tomasicchio, G. R. (2020). Floating Offshore Renewable Energy Farms. A Life-Cycle Cost Analysis at Brindisi, Italy. *Energies* 13, 6150. doi:10.3390/en13226150

Pantusa, D., and Tomasicchio, G. R. (2019). Large-scale Offshore Wind Production in the Mediterranean Sea. *Cogent Eng.* 6, 1661112. doi:10.1080/23311916.2019.1661112

Poujol, B., Prieur-Vernat, A., Dubranna, J., Besseau, R., Blanc, I., and Pérez-López, P. (2020). Site-specific Life Cycle Assessment of a Pilot Floating Offshore Wind Farm Based on Suppliers' Data and Geo-located Wind Data. *J. Industrial Ecol.* 24, 248–262. doi:10.1111/jiec.12989

PRé Consultants (2020). SimaPro 9.1.1. Available at: https://simapro.com/ (Accessed April 13, 2022).

Principle Power INC (2022). Principle Power. Available at: https://www.principlepowerinc.com/en/home/interactive-windfloat (Accessed April 13, 2022).

Pulselli, R. M., Marchi, M., Neri, E., Marchettini, N., and Bastianoni, S. (2019). Carbon Accounting Framework for Decarbonisation of European City Neighbourhoods. *J. Clean. Prod.* 208, 850–868. doi:10.1016/j.jclepro.2018.10.102

Pulselli, R. M., Struglia, M. V., Maccanti, M., Bruno, M., Patrizi, N., Neri, E., et al. (2022). Integrated Blue Energy Planning Framework in the Mediterranean: Three Case Studies from the Interreg Med BLUE DEAL Project. *Front. Energy Res. - Sustain. Energy Syst. Policies*.

Raadal, H. L., and Vold, B. I. (2012). GHG Emissions and Energy Performance of Wind Power - LCA of Two Existing Onshore Wind Farms and Six Offshore Wind Power Conceptual Designs. Available at: https://norsus.no/wp-content/uploads/2412.pdf (Accessed April 13, 2022).

Raadal, H. L., Vold, B. I., Myhr, A., and Nygaard, T. A. (2014). GHG Emissions and Energy Performance of Offshore Wind Power. *Renew. Energy* 66, 314–324. doi:10.1016/j.renene.2013.11.075

Regione Lazio (2021). Eolico offshore per la transizione ecologica di Civitavecchia: sfide e opportunità. Position paper. Available at: https://www.lazioinnova.it/app/uploads/2022/02/Position-paper-Eolico-offshore-Civitavecchia.pdf (Accessed May 25, 2022).

Robertson, A. N., and Jonkman, J. M. (2011). Loads Analysis of Several Offshore Floating Wind Turbine Concepts. Available at: https://www.nrel.gov/docs/fy12osti/50539.pdf (Accessed April 13, 2022).

Roddier, D., Cermelli, C., Alexia Aubault, A., and Weinstein, A. (2010). WindFloat: A Floating Foundation for Offshore Wind Turbines. *J. Renew. Sustain. Energy* 2, 033104. doi:10.1063/1.3435339

Roy, A., Auger, F., Dupriez-Robin, F., Bourguet, S., and Tran, Q. T. (2018). Electrical Power Supply of Remote Maritime Areas: A Review of Hybrid Systems Based on Marine Renewable Energies. *Energies* 11, 1904. doi:10.3390/en11071904

Russell, D. J. F., Brasseur, S. M. J. M., Thompson, D., Hastie, G. D., Janik, V. M., Aarts, G., et al. (2014). Marine Mammals Trace Anthropogenic Structures at Sea. *Curr. Biol.* 24, R638. doi:10.1016/j.cub.2014.06.033

Sacchi, R., Besseau, R., Pérez-López, P., and Blanc, I. (2019). Exploring Technologically, Temporally and Geographically-Sensitive Life Cycle Inventories for Wind Turbines: A Parameterized Model for Denmark. *Renew. Energy* 132, 1238–1250. doi:10.1016/j.renene.2018.09.020

SINN Power GmbH. (2022). SINN Power. Available at: https://www.sinnpower.com/(Accessed April 13, 2022).

Stančin, H., Pfeifer, A., Perakis, C., Stefanatos, N., Damasiotis, M., Magaudda, S., et al. (2022). Blue Energy Spearheading the Energy Transition: The Case of Crete. *Front. Energy Res. - Sustain. Energy Syst. Policies* 10, 868334. doi:10.3389/fenrg.2022.868334

Staschus, K., Kielichowska, I., Ramaekers, L., Wouters, C., Vree, B., and Lejarreta, A. V. (2020). Study on the Offshore Grid Potential in the Mediterranean Region. Publications Office of the European Union. Available at: https://data.europa.eu/doi/10.2833/742284.

Supachawarote, C. (2006). *Inclined Load Capacity of Suction Caisson in Clay*. dissertation/Ph.D. thesis. Perth: University of Western Australia. https://research-repository.uwa.edu.au/files/3226499/Supachawarote_Chairat_2006.pdf.

Swiss helicopter (2022). Swiss Helicopter. Available at: https://www.swisshelicopter.ch/it/su-di-noi/flotta/agusta-a109e (Accessed April 13, 2022).

Tomasicchio, G. R., D'Alessandro, F., Avossa, A. M., Riefolo, L., Musci, E., Ricciardelli, F., et al. (2018). Experimental Modelling of the Dynamic

Behaviour of a Spar Buoy Wind Turbine. *Renew. Energy* 127, 412–432. doi:10.1016/j.renene.2018.04.061

Tsai, L., Kelly, J. C., Simon, B. S., Chalat, R. M., and Keoleian, G. A. (2016). Life Cycle Assessment of Offshore Wind Farm Siting: Effects of Locational Factors, Lake Depth, and Distance from Shore. *J. Industrial Ecol.* 20 (6), 1370–1383. doi:10.1111/jiec.12400

Vattenfall (2018). Offshore-Windpark – Ein Paradies für Muscheln. Available at: https://group.vattenfall.com/de/newsroom/blog/2018/01/offshore-windpark--ein-paradies-fur-muscheln (Accessed April 13, 2022).

Vestas (2021). 2 MW Platform. Available at: https://nozebra.ipapercms.dk/Vestas/Communication/Productbrochure/2MWTurbineBrochure/2mw-platform-brochure/?page=2 (Accessed April 13, 2022).

Vestas (2011). Life Cycle Assessment of Electricity Production from a V90-2.0 MW Gridstreamer Wind Plant. Available at: https://www.vestas.com/content/dam/vestas-com/global/en/sustainability/reports-and-ratings/lcas/LCA_V902MW_version1.pdf.coredownload.inline.pdf (Accessed April 13, 2022).

Vestas (2015). Life Cycle Assessment of Electricity Production from an Onshore V110-2.0 MW Wind Plant. Available at: https://www.vestas.com/content/dam/vestas-com/global/en/sustainability/reports-and-ratings/lcas/LCAV11020MW181215.pdf.coredownload.inline.pdf (Accessed April 13, 2022).

Vestas (2017). Life Cycle Assessment of Electricity Production from an Onshore V112-3.45 MW Wind Plant. Available at: https://www.vestas.com/content/dam/vestas-com/global/en/sustainability/reports-and-ratings/lcas/V1123%2045MW_Mk3a_ISO_LCA_Final_31072017.pdf.coredownload.inline.pdf (Accessed April 13, 2022).

Vryhof (2018). Vryhof Manual – the Guide to Anchoring. Available at: http://insights.vryhof.com/download-the-vryhof-manual (Accessed April 13, 2022).

Wang, Q., Yu, Z., Ye, R., Lin, Z., and Tang, Y. (2019). An Ordered Curtailment Strategy for Offshore Wind Power under Extreme Weather Conditions Considering the Resilience of the Grid. *IEEE Access* 7, 54824–54833. doi:10.1109/access.2019.2911702

Wang, S., Wang, S., and Liu, J. (2019). Life-cycle Green-House Gas Emissions of Onshore and Offshore Wind Turbines. *J. Clean. Prod.* 210, 804–810. doi:10.1016/j.jclepro.2018.11.031

Weinzettel, J., Reenaas, M., Solli, C., and Hertwich, E. G. (2009). Life Cycle Assessment of a Floating Offshore Wind Turbine. *Renew. Energy* 34, 742–747. doi:10.1016/j.renene.2008.04.004

Wikantyoso, F., Oktavitasari, D., Tjahjana, D. D. D. P., Hadi, S., and Pramujati, B. (2019). ""The Effect of Blade Thickness and Number of Blade to Crossflow Wind Turbine Performance Using 2D CFD Simulation"," in *International Journal of Innovative Technology and Exploring Engineering (IJITEE)* (Bhopal, INDIA: Blue Eyes Intelligence Engineering & Sciences Publication), 17–21.

Wind Europe (2019). Our Energy, Our Future: How Offshore Wind Will Help Europe Go Carbon-Neutral. Available at: https://windeurope.org/wp-content/uploads/files/about-wind/reports/WindEurope-Our-Energy-Our-Future.pdf (Accessed April 13, 2022).

Wind Europe (2021). Wind Energy in Europe in 2020-2020 Statistics and the Outlook for 2021-2025. Available at: https://windeurope.org/wp-content/uploads/files/about-wind/reports/WindEurope-Our-Energy-Our-Future.pdf (Accessed April 13, 2022).

Conflict of Interest: Authors AS and EN was employed by INDACO2 srl and author RP was employed by INDACO2 srl.

The remaining authors declare that the research was conducted in the absence of any commercial or financial relationships that could be construed as a potential conflict of interest.

Publisher's Note: All claims expressed in this article are solely those of the authors and do not necessarily represent those of their affiliated organizations, or those of the publisher, the editors and the reviewers. Any product that may be evaluated in this article, or claim that may be made by its manufacturer, is not guaranteed or endorsed by the publisher.

frontiers | Frontiers in Energy Research

ORIGINAL RESEARCH
published: 01 July 2022
doi: 10.3389/fenrg.2022.913411

Seawater Opportunities to Increase Heating, Ventilation, and Air Conditioning System Efficiency in Buildings and Urban Resilience

Luigi Schibuola, Chiara Tambani and Antonio Buggin*

Department of Architecture, University Iuav of Venice, Venice, Italy

In coastal cities, seawater heat pumps (SWHPs) can combine heat pump technology with the availability of seawater to produce the heat and the cold necessary for heating, ventilation, and air conditioning (HVAC) systems installed in buildings. In heating mode, the seawater is used as a cold source and provides the low-temperature heat needed for the operation of the machine. In cooling mode, the seawater removes the heat dissipated by the condenser of the heat pump working for air conditioning. This seawater application seems to be very promising since the temperature trend of the seawater appears to be more favorable than the alternative use of outdoor air, both in winter and in summer. In a case study in Trieste, the performance of a district heating/cooling network supplied with seawater and based on decentralized heat pumps is investigated. For this purpose, annual dynamic simulations were performed, modeling an urban area, the heat pumps, and the network. The energy efficiency evaluation shows a clear superiority of the SWHP solution compared to boilers and airsource heat pumps and thus the possibility to provide a significant contribution to the decarbonization of buildings. Moreover, the results highlight the ability of this GWHP network to reduce the urban heat island (UHI) phenomenon since the heat dissipated by the heat pumps during summer air conditioning is removed from the urban area. Therefore, SWHPs in coastal cities can be among the mitigation measures for UHI to increase outdoor comfort and heat wave resilience in urban areas.

Keywords: seawater heat pump, 5GDHC network, urban heat island mitigation, anthropogenic heat, decarbonization actions, city resilience, urban model

OPEN ACCESS

Edited by:
Riccardo Maria Pulselli,
University of Florence, Italy

Reviewed by:
Carla Balocco,
University of Florence, Italy
Hanan Al-Khatri,
Sultan Qaboos University, Oman

****Correspondence:***
Chiara Tambani
tambani@iuav.it

Specialty section:
This article was submitted to Sustainable Energy Systems and Policies, a section of the journal Frontiers in Energy Research

Received: *05 April 2022*
Accepted: *24 May 2022*
Published: *01 July 2022*

Citation:
Schibuola L, Tambani C and Buggin A (2022) Seawater Opportunities to Increase Heating, Ventilation, and Air Conditioning System Efficiency in Buildings and Urban Resilience. Front. Energy Res. 10:913411. doi: 10.3389/fenrg.2022.913411

INTRODUCTION

Decentralized Heat Pumps in District Heating and Cooling Networks

The use of heat pumps (HPs) can give an important contribution to achieving the decarbonization target in the building sector (Abbasi et al., 2021; Zuberi et al., 2021). It reduces energy consumption and CO_2 emissions and, on the other hand, increases the share of renewable energy (European Community, 2010). The best performance is possible when wasted heat or natural resources are available for HP use. The use of geothermal energy as a heat source/sink for heat pumps is of great interest due to the low seasonal temperature variations compared to the air source (Sarbu and Sebarchievici, 2014). There are several technologies based on the use of groundwater from wells,

surface water (lake, river, and sea), or direct coupling with the ground through a heat exchanger (Schibuola et al., 2013b). In general, the systematic installation of geothermal heat exchangers in existing urban areas is less feasible and geothermal heat exchangers may also release or extract heat in the first soil layers directly under the urban area. This fact leads to an increase in the subsurface of the UHI effect in summer and of cooling of the soil (Luo and Asproudi, 2015) in winter. The use of water offers significant advantages, such as low installation costs and no available land area and can therefore be a real alternative for buildings located near significant surface waters such as rivers, lakes, or seas (Chen et al., 2006; Nam and Ooka, 2010; Liang et al., 2011; Schibuola and Tambani, 2012) and is particularly tempting in coastal cities. Especially in the open sea, the presence of marine currents contributes to the rapid dissipation of the released heat from the coast in front of the urban area and the mixing of water with different temperature levels, which reduces the heating of the water compared to less extensive surface waters (ponds, lagoons). In the case of air conditioning, the energy advantages of these systems have been clearly highlighted (Song et al., 2007), and based on these results, numerous studies have been conducted on the economic and energy optimization of a large-scale application of the seawater heat pump (SWHP) for district heating and cooling (Li et al., 2010; Baik et al., 2014). From the first district heating systems, characterized by centralized plants injecting steam or water at high temperatures into the networks, this technology is gradually being transferred to the new generations of district heating systems distributing water at lower temperatures (Lund et al., 2014; Reiners et al., 2021). Recent studies focus, in detail, on the so-called 5th-generation district heating and cooling (5GDHC) systems, which operate at a temperature level close to that of the ground. In this case, the network water is used as a cold source/sink for decentralized HPs. The 5GDHC designation was first introduced as part of the EU FLEXYNETS project (Author Anonymous, 2020). 5GDHC offers numerous advantages, the most important of which are the elimination of heat losses in pipelines, the reduction of initial costs of centralized power generation systems, the possible contemporary use for heating and cooling services, increasing accessibility to use wasted heat (Wheatcroft et al., 2020), heat from geothermal heat exchangers (Foster et al., 2016; Prasanna et al., 2017), from solar systems (Pauschinger, 2016), and especially from locally available renewable energy sources such as underground and surface aquifers (Verhoeven et al., 2014; Pattijn and Baumans, 2017; Schibuola and Tambani, 2022), and in particular the sea (Stene and Eggen, 1995; Daikin, 2014; Schibuola and Tambani, 2020). In addition, decentralized electric HPs can spread the local use of electricity from photovoltaic systems and help a smart grid work together with the increasing proliferation of small generators/consumers (Schibuola et al., 2015; Schibuola et al., 2016; Lund et al., 2017; Chen et al., 2021). The lower temperature drop in the water loop is associated with larger flow rates and pipe sizes than previous hot water systems. However, the use of uninsulated polyethylene (PE) pipes reduces material and installation costs. The increase in pump consumption can be limited by variable flow rates based on the effective demand control.

Mitigating the Urban Heat Island Phenomenon

An important topic to explore is the relationship between 5GDHC and the urban heat island (UHI) effect, which affects both UHI mitigation and 5GDHC performance. The UHI effect is the best-known phenomenon of urban climate. It is characterized by the fact that ambient temperatures in urban areas are higher than in rural areas (Martin-Vide et al., 2015). Many studies (Santamouris, 2007; Santamouris, 2014; Manoli et al., 2019; Jain et al., 2020; Mosteiro-Romero et al., 2020; Hong et al., 2021) have clearly shown that UHI can significantly affect the energy consumption of buildings in different cities around the world. During the heating season in cold and temperate climates, the heat island reduces energy consumption in urban centers compared to that in suburban areas. On the other hand, in warm and hot climates without heating demand, the negative effect of UHI usually extends throughout the year and is not limited to summer. In fact, the urban temperature increment has a negative impact on the air conditioning of buildings due to the increased cooling demand, which negatively affects the efficiency of air conditioning systems and consequently increases the electrical load (Li et al., 2019; Shi et al., 2019). At the same time, high temperatures in cities reduce the cooling potential of techniques such as natural ventilation (Duan et al., 2019) and affect human comfort outdoors. In fact, energy consumption releases heat to the environment, influencing the intensity and temporal variability of urban climate (Cui et al., 2017; Sun et al., 2018). Therefore, action plans to reduce the UHI effect should also consider possible methods to reduce energy consumption (Ferrando et al., 2021), starting from a better understanding of the links between environmental impacts and energy system behavior (Wen and Lian, 2009; Doan et al., 2019), including UHI effects in thermal simulations (Guattari et al., 2018). Dynamic calculation programs based on climate data recorded in rural stations or airports are often used to simulate the energy efficiency of buildings. However, these weather records are inappropriate when used for different climatic conditions in urban environments and can lead to inaccurate predictions of energy demand. Two methods are commonly used to assess the impact of UHI on building energy use. The first uses on-site meteorological observations as input to energy simulation tools (Yang et al., 2019; Yang et al., 2020b), and the second uses meteorological files generated by urban climate modeling codes for simulation (Palme et al., 2017; Lauzet et al., 2019). One of the most commonly used simulation tools is the urban weather generator (UWG) (Bueno et al., 2013), a software based on EnergyPlus (U.S. Department of Energy, 2019a) that combines urban-scale assessments with a building simulation model. The UWG tool has been validated under different weather conditions (Salvati et al., 2017; Salvati et al., 2019; Mao et al., 2018; Martinez et al., 2021) and is widely used to study different urban contexts (Boccalatte et al., 2020; Liu et al., 2020). For this reason, it is used

in a wide range of use cases (Street et al., 2013; Mao et al., 2017; Santos et al., 2018; Lima et al., 2019). Measures to mitigate UHI typically focus on solutions that involve only the use of appropriate building geometries and surface materials with high albedo (Castellani et al., 2017; Morini et al., 2017) and a systematic increase in urban green space (Aram et al., 2019; Bisegna et al., 2019; Bevilacqua et al., 2020; MacLachlan et al., 2021). However, anthropogenic heat is often a driving force of the UHI phenomenon (Sailor and Fan, 2004; Smith et al., 2009; Luo et al., 2020; Mei and Yuan, 2021). As sensitivity studies have shown (Salvati et al., 2017), anthropogenic heat fluctuations can indeed significantly alter the UHI effect. This heat is mainly generated during the day and is largely due to human activities, traffic, and building air conditioning. For this reason, especially when air-cooled air conditioning systems are used systematically, the possibility of reducing the heat gain that is released to the outside by the HVAC system must always be considered. Consequently, implementing the 5GDHC technology in conjunction with the use of seawater can be an effective option.

A Performance Analysis of a Seawater-Fed 5th Generation District Heating and Cooling Networks

This study addresses the potential benefits of seawater for improving the energy performance of HVAC systems and reducing the UHI phenomenon. For this aim, a case study is investigated in the coastal city of Trieste, which is in the northeastern Italy on the Adriatic Sea. A retrofit action for an urban area based on the systematic introduction of decentralized HPs in a new 5GDHC network fed by seawater is proposed. Specifically, the analysis consists of 1) the elaboration of the specific retrofit project focusing on the 5GDHC to be installed in the area, 2) the application of the archetype procedure to model the urban area, 3) the evaluation of the UHI effect and its impact on the building heating and cooling demand, 4) the modeling of the 5GDHC network and HPs, and 5) the assessment of the benefits from the use of seawater in the 5GDHC compared to the alternative air source HPs (ASHP) or condensing boilers.

MATERIALS AND METHODS

Description of the Retrofit Action

The urban area selected as a case study is located near the old seaport and preserves the architectural setting from the time of the Austro-Hungarian Empire. A regular division into large building blocks, clearly recognizable because they are separated by streets, characterizes the architectural layout. The area is highlighted by a yellow line on the aerial photograph in **Figure 1A**. It is a rectangle with dimensions 402 m × 143 m and a total area of 57,486 m^2. **Figure 1B** shows a plan of the 16 blocks in the area, numbered in this study, as indicated at the bottom of the same figure. Each block consists of different buildings with diverse height and number of floors. **Figure 2** shows a photograph and plan of the existing buildings for each of the three blocks selected as examples. The total built-up area as a percentage of the total area is 79%, and the building density is 7.97 m^3/m^2. Most of the buildings are historic buildings built in the 19th and early 20th centuries, eventually with additional portions more recent. The remaining part dates back to the period between the 50s and 60 s of the last century. The buildings have usually retained the same features of the construction period. Since the thermal insulation of buildings was required by a national law starting in 1976, the building envelopes are uninsulated and only the windows have been changed from single to double glazing over the years.

Centralized heating systems of obsolete design with radiators and thermal power stations in each block are present. Air conditioning systems with air-cooled chillers are installed only for commercial and directional buildings. These refrigeration machines are located in courtyards or terraces; instead, the installation of autonomous air conditioners such as split systems, currently so widely used in residential buildings, is not possible here because the facades of these buildings do not have balconies and the presence of preservation orders affects the external perimeter walls. Therefore, air conditioning systems in residential buildings are very rare and may be present only in a few rooms.

In this context, an effective retrofit action must first provide for a substantial improvement in the thermal performance of the building envelope through the application of typical techniques. The insertion of a layer of insulation under the roof tiles, the replacement of the existing windows with higher performance products. In the presence of preservation orders, the external wall insulation must be applied on the inside instead of using it as an external thermal cladding. The goal is to achieve at least the thermal insulation level currently required by the national regulation (MISE, 2015). Therefore, this analysis considers the thermal transmittance coefficients (*U*-values) corresponding to the maximum value allowed by the national regulation for the climatic zone of Trieste (Zone E, 2102 HDD). The description of the multiple layers (from inside to outside) of the main building structures included in the building simulation models and their *U*-values is given in **Table 2**. Considering the increasing use of air conditioning, the adopted solution proposes the application of HP for both heating and air conditioning in all buildings. These two retrofit measures are fully aligned with the nearly zero-energy building (nZEB) goal. In fact, this level of insulation in building structures is one of the nZEB requirements in national legislation (MISE, 2015). Moreover, the nZEB definition (European Community, 2010) states that the low energy demand should be met to a very large extent by renewable energy. Heat pump technology can provide an important contribution to this purpose. The retrofit plan assumes the modern tendency to centralize the generation of heat and cold in the building blocks with individual energy accounting in order to optimize the management of the HVAC systems and, consequently, the energy consumption. Therefore, a centralized HP is considered for each block. The SWHP can be installed in a technical room and often in the existing thermal power station in the substitution of the boilers. The ASHP must be placed outdoors, possibly on flat roofs, terraces, or in courtyards. This is the solution already adopted for the existing air-cooled chillers for air conditioning of

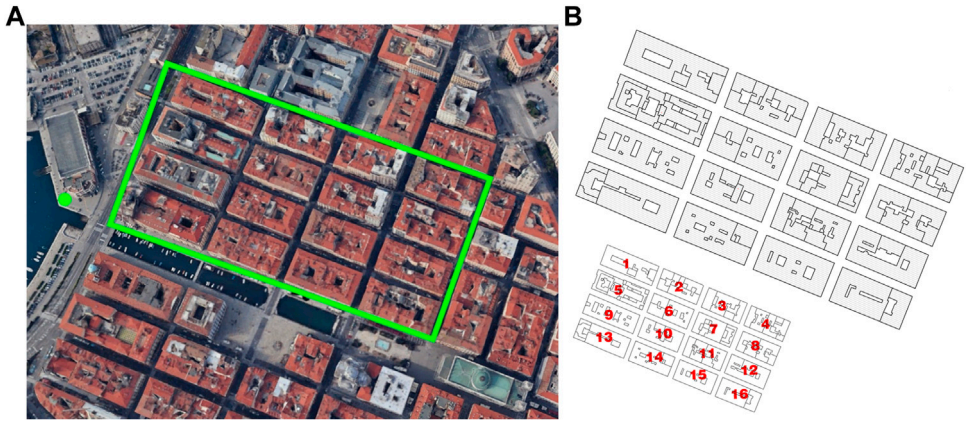

FIGURE 1 | The investigated area: a photograph **(A)** and a map of the blocks in the area, numbered as indicated in panel **(B)**.

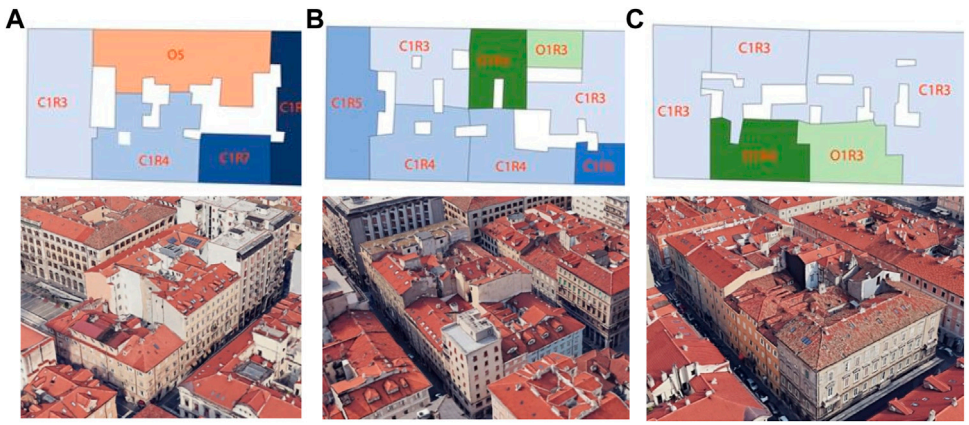

FIGURE 2 | Plan of buildings and photograph of block 3 **(A)**, block 4 **(B)**, and block 11 **(C)**.

the existing tertiary activities. Among the different options, the retrofit action foresees the installation of fan coils as terminal units, used for heating with a supply water temperature of 45°C and for air conditioning with a supply temperature of 7°C for both GWHP and ASHP.

The rural weather file used for the simulations was obtained from actual weather data collected from a meteorological station in a rural area near Trieste and therefore not affected by urban influences. The rural weather data were used to create the corresponding EnergyPlus weather (EPW) file according to the U.S. Department of Energy (2019b). In the figures, the rural weather data are indicated as S_rural in summer and W_rural in winter. Since in Trieste the heating season lasts from October to April, the winter period includes the months from January to April and then from October to December. The air conditioning, and therefore the summer period, lasts from June to September. The profile of outdoor air temperature is compared in **Figure 3A**, with the monthly average seawater temperatures in Trieste. These seawater temperatures come from a meteorological open data (Climate-data.org, 2022.), which provide the monthly average values of minimum, average, and maximum daily temperatures. These averages are shown in **Figure 3B** for the 12 months. **Figure 3B** shows a very limited thermal excursion of seawater temperature during each month with respect to the strong oscillation of outdoor air temperatures. The monthly average seawater temperature is effectively representative of the thermal level of the sea in a month, and this fact justifies the use of a linear interpolation between these averages to build an annual trend of the seawater temperatures, also reported in **Figure 3A**.

The Implementation of a Seawater District Heating and Cooling Networks

The intervention foresees the installation of centralized water-to-water HPs, one for each building block, connected to a two-pipe water network built in the studied area. Each HP withdraws the required amount of water from the delivery pipe of the network with a dedicated pump and gives it back to the return pipe. PE underground pipes are considered for this grid. The urban

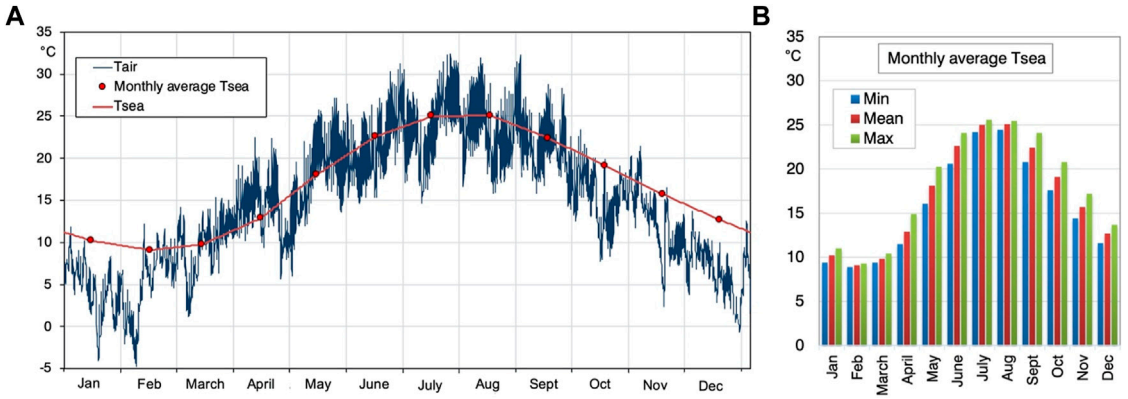

FIGURE 3 | Hourly trend of the outdoor air temperature (Tair) and monthly average seawater temperatures (Tsea) **(A)**. Monthly averages of the minimum, mean, and maximum daily seawater temperatures **(B)**.The linear interpolating trend of Tsea is also reported in panel **(A)**.

TABLE 1 | Main data of the district network.

Maximum simultaneous heating/cooling demand required from the network (kW)	6,303/5,872
Maximum water flow rate of the closed network (m^3/h)	1,141
Maximum tube sizes Di/De (mm) and maximum length of single closed loop circuit (m)	341/400–921
Maximum seawater flow rate (m^3/h)	1,901
Tube sizes Di/De (mm) and length of the well water circuit (m)	426/500–68
Peak electric load of the pumping system (kW)	98 kW

network forms a closed circuit connected to a technical station, which can be located in the immediate vicinity of the old warehouse next to the seaside and the study area. Here, two plate heat exchangers are considered, operating alternately to allow maintenance. They are interposed between the seawater circuit and the urban circuit to avoid fouling inside the evaporators and condensers of the HPs. Italian legislation (Author Anonymous, 1999) prohibits the thermal use of seawater with a temperature drop higher than 3°C and the temperature of the seawater returned must not exceed 35°C. The two heat exchangers are sized according to this worst permissible condition, i.e., in cooling mode, a temperature difference for the seawater of 32°C–35°C, which corresponds to a nominal water temperature drop of 35°C–40°C in the urban circuit. In heating mode, assuming the minimum seawater temperature of 11°C from **Figure3B**, the corresponding design temperature drops are 11°C–8°C for the seawater and 8°C–3°C for the urban loop. The sizing of the network is based on the simulation results regarding the building loads and the performances of HPs. The main network data can be found in **Table 1**.

The functional diagram of a typical seawater intake plant is shown in **Figure 4**. In the seawater circuit, a self-cleaning filter (**Figure 5A**) is recommended to reduce maintenance interventions on heat exchangers and filters. The location of the seawater intake station is proposed near the quay at a point indicated by a yellow dot in **Figure 1A**. A sketch of a typical station is shown in **Figure 5B**. The use of an underground space facilitates the operation of the hydraulic pumps, and the presence of a pre-chamber for the introduction of seawater reduces turbulence in the intake and the dirt sucked in. Of course, the pre-chamber must be accessible for maintenance, as shown in **Figure 5C**. To avoid interference, the water return to the sea can be placed 50 m away from the suction point at the tip of the same pier.

The pumping system is based on three pumps for both the closed loop of the district network and the open circuit of the seawater. A smart control of the pumping system is able to drastically reduce the power consumption, as the demand of the building varies greatly both in winter and in summer. Indeed, in the case of very frequent part loads, a reduced number of pumps can work alternatively. Moreover, a variable flow rate of the pumping system is achieved by controlling the speed of the electric motors of the pumps through the inverter technology. For this purpose, the control of the water flow rate is designed to keep the temperature difference between the return and supply water constant in both heating and cooling modes. This difference is 5°C for the urban network and 3°C for the seawater circuit. This control of pumping power is very performing. In the case study, the annual simulation shows a saving in the electricity consumption of the pumps of 71% compared to the case of constant flow rate. Normally, in this type of technical station, two heat exchangers are installed, working alternately to meet the maintenance requirements, as well as a filter for the seawater. The use of a self-cleaning filter through intermittent reversal cycles of the water flows can increase the life of the filter efficiency without maintenance stops. In addition, experience (Schibuola et al., 2017) with self-cleaning filters has shown that the heat

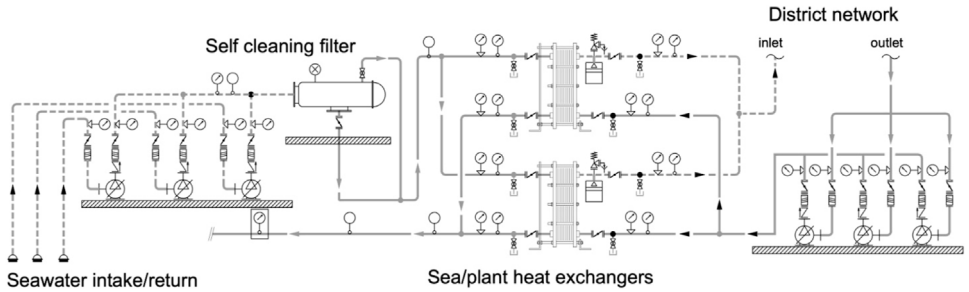

FIGURE 4 | A functional diagram of the seawater intake plant.

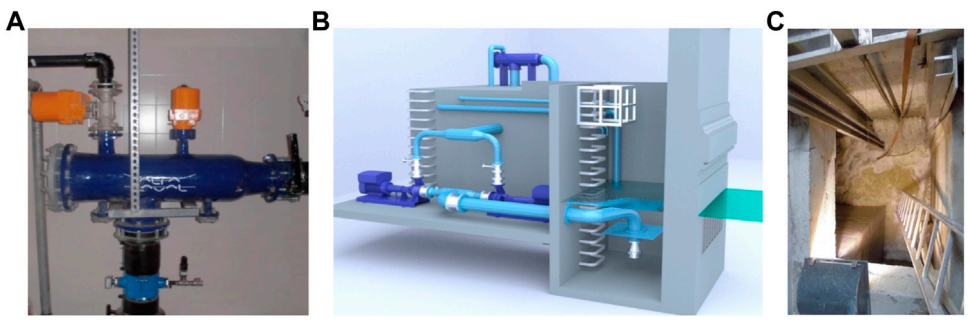

FIGURE 5 | A self-cleaning filter **(A)**, a sketch of a seawater intake station **(B)**, and a seawater intake prechamber **(C)**.

exchangers hardly foul even when the water is very dirty. This result suggests in many cases the possibility of using only one heat exchanger and limiting the cleaning of the exchanger to the end of the heating or cooling season.

Urban Area Modeling

The modeling of the investigated area is based on the data from GIS, which provides information about the building area, height, and use of each building in the blocks. The archetype modeling approach (Swan and Ugursal, 2009; Yang et al., 2020a) was used to calculate the heating and cooling demand of the buildings in the area. The entire building stock is categorized according to its characteristics that affect energy demand. The first step is to distinguish some basic building typologies. In this case study, four types were highlighted. Residential buildings where the ground floor rooms are not heated and are used as garages or storage rooms (type 1). Residential buildings, but whose ground floor is used by commercial establishments (type 2). Residential buildings whose ground floor is used for office purposes (type 3). Directional buildings that contain only offices (type 4). Based on these selected typologies, the second step is to distinguish all buildings into categories based on the use and number of floors. Each category is named by the initial letter of the use (garage, commercial, residential, office) followed by the number of floors. Thus, the categories of types 1 through 3 consist of two letters and two numbers. The categories of type 4 contain only the letter O followed by the number of floors. In **Figure 2**, different colors are used to indicate the categories in each block reported here. **Figure 6** shows the heated volume of the categories that belong to each type as a percentage of the total heated volume of the buildings of that type. In this way, it is possible to individuate the category that is to be considered representative of all buildings of that type on the basis of its volume significance in the total heated volume of that building typology. In **Figure 6**, the four selected categories are indicated by an arrow. A table in **Figure 6** also indicates the percentage volume of these selected categories with respect to the total building volume in the area. For each of these four categories, an archetype building is selected to characterize the category and thus all the types in the stock. The archetypes selected in this case study are listed in **Table 2**, which includes their main characteristics and simulation parameters. The hourly heating or cooling load profile of each archetype is calculated using the EnergyPlus code, a comprehensive and robust building simulation program. The EnergyPlus calculation is based on the contemporary solution of the global energy balance of each thermal zone of the building, taking into account the contribution of the HVAC system to maintain the thermal control setpoints (Yang et al., 2019). For each archetype, the hourly load is divided by the relative building volume to estimate an hourly load intensity that is adopted for all buildings belonging to the relative type. Consequently, the total load of a building typology is calculated by multiplying this load intensity by the corresponding total building volume.

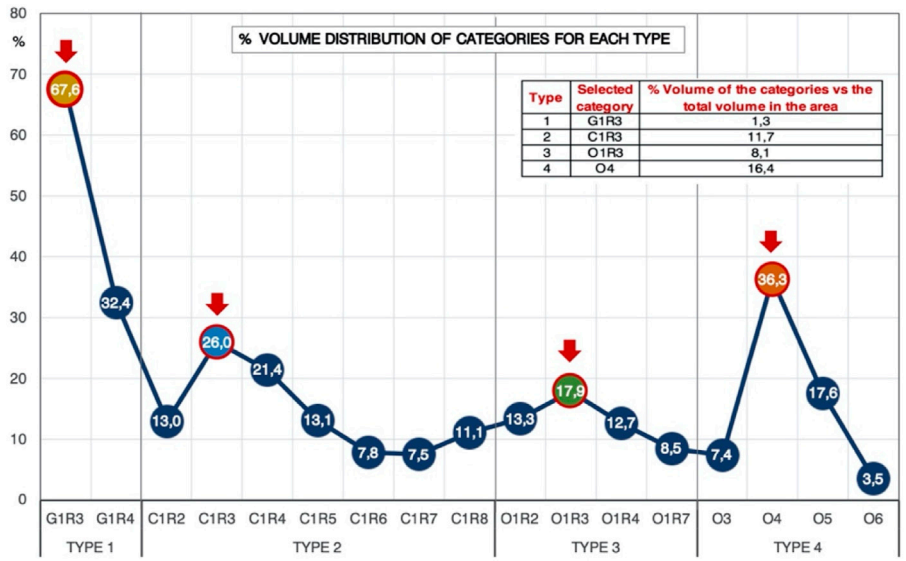

FIGURE 6 | Percentage volume distribution of categories and selected category for each type. The table shows the contribution of the selected categories to the total volume of buildings in the area.

Finally, the hourly demand profile of the entire building stock in the studied area is calculated by adding the four total loads for each building typology.

Urban Weather Generator Software to Simulate Urban Heat Island Effects

The UWG code calculates average hourly air temperatures within the urban canopy starting from a rural weather file. Its output is an urban weather file taking into account the UHI phenomenon and is in EPW format, so it can be used for EnergyPlus simulations. UWG requires an auxiliary file in XML format to proceed with parametric modeling of the urban area under study (MIT, 2014; Nakano et al., 2015). This XML file contains the values of the parameters used to build the urban model. These data are organized into four groups: information about the buildings, urban morphology, vegetation characteristics, and data about the reference site. UWG assumes that the air within the urban canopy layer is well mixed. Urban air temperatures are calculated using the heat balance method, taking into account the heat capacity of the air in the urban canyon. The energy balance of the urban canyon is based on heat fluxes from the building envelopes and the street, heat fluxes due to air exfiltration, waste heat from HVAC systems and other anthropogenic heat sources, convective heat exchange between the air of the urban canyon and the atmosphere, and the radiant heat exchange between the surfaces of the urban canyon and the sky.

Regarding building behavior, UWG uses EnergyPlus to simulate heat flows in buildings. Therefore, the required information about buildings is the same as that introduced in the EnergyPlus models. This includes building geometries and their structure characteristics, internal heat gains, and occupancy schedules. Consistent with the archetype approach adopted, the building data provided by the UWG model pertain only to the four archetypes representing all buildings present in the area and are the same as that used for the load calculations. These building data are summarized in **Table 2**. The other urban morphology information, mostly extracted from the data of GIS and introduced into the XML file, is shown in **Table 3**. A general typical albedo value of 0.2 is used for the building surfaces. For evaluation during the air conditioning period, the UWG requires an average chiller efficiency (EER) for each HVAC system. In this study, the seasonal EER values confirmed by the final outcomings were adopted and, more specifically, 3.6 in the case of the ASHPs and 4.5 for the SWHPs. Another important information requested by UWG in the XML file for each chiller is the value of the parameter "heat released to canyon," which can vary between 0 and 1. This is the fraction of waste heat from the chillers that is discharged to the urban area. A value of 1 is typical for ASHPs where all the heat from the condensers is released to the outside air in the canyon. A value of 0 means that the waste heat is not discharged into the canyon, which is the case with the SWHP technology. Consequently, by using these two different values for this parameter, two different urban EPW files were created for the summer. The first EPW, named S_UHI_A, was calculated with a value of 1 and was therefore used with the ASHPs. The second EPW, named S_UHI_B, was calculated with a value of 0 and used with the SWHPs.

During the heating season, UWG assumes the use of traditional boilers, while the use of HP is not currently planned. It is necessary to specify a boiler efficiency between 0 and 1. If you select a boiler efficiency of 1, no heat is released into the urban canopy by the HVAC system. This hypothesis is correct if the SWHPs are present. However, in the absence of a possible alternative calculation, it was also assumed in the case of ASHPs. Therefore, only one urban weather provided by UWG was used in winter and here named W_UHI. This fact leads to neglecting that

TABLE 2 | Characteristics and simulation parameters of the archetypes.

	Archetypes			
	Type 1	**Type 2**	**Type 3**	**Type 4**
Windows (%) of floor	12.5–20			
Total volume in the area (m^3)[a]	8,860	206839	108616	134025
Category	G1R3	C1R3	O1R3	O4
Total volume in the area (m^3)[b]	5,986	53,781	37,082	75,046
Building number[b]	1	7	5	2
Mean building volume (m^3)[b]	5,986	7,683	7,416	37,523
Reference Volume (m^3)[c]	6,465	8,221	7,861	41,651
Reference Surface (m^2)[c]	2,155	2,740	2,620	13,884
Occupancy (Pers/m^2)	0.035	0.035[d] or 0.1[e]	0.035[d] or 0.1[f]	0.1
Internal heat gain (W/m^2)	4	4[d] or 10[e]	4[d] or 16.5[f]	16.5
Heating set point temp. (°C)	20			
Cooling set point temp. (°C)	26			
Heating schedule (h)	7a.m.–9p.m.	7a.m.–9p.m.[d] or 7a.m.–7p.m.[e]	7a.m.–9p.m.[d] or 7a.m.–6p.m.[e]	7a.m.–6p.m.
Cooling schedule (h)	11a.m.–7a.m.	11a.m.–7p.m.[d] or 9a.m.–7p.m.[e]	11a.m.–7p.m.[d] or 8a.m.–6p.m.[e]	8a.m.–6p.m.
HVAC system schedule (day)	7	7[d] or 6[e]	7[d] or 5[e]	5
Air change rate (ACH)	0.5	0.5[d] or 1[e]	0.5[d] or 2[e]	2
Walls—*U*-value	Plaster (1.5 cm), polyurethane (12 cm), brick (40 cm), plaster (2 cm)—U = 0.22 W/m^2K			
Windows *U*-value	Double—pane clear glass—U = 1.3 W/m^2K—SHGC = 0.54 (-)			
Roof *U*-value	Plaster (1.5 cm), concrete (20 cm), polyurethane (14 cm), tiles (2 cm)—U = 0.20 W/ m^2K			

[a]*Referred to all the buildings of one type.*
[b]*Referred to all the buildings of the category.*
[c]*Referred to the simulated archetype.*
[d]*Dwellings.*
[e]*Commercial areas.*
[f]*Offices.*

TABLE 3 | Main parameters of the UWG model.

Urban area			
Average building height (m)	19.9	Vegetation albedo (-)	0.25
Site coverage ratio (-)	0.79	Vegetation start/end (month)	1/12
Facade to site ratio (-)	2.04	Daytime boundary layer height (m)	700
Tree coverage (-)	0	Nighttime boundary layer height (m)	80
Non-building sensible heat (W/m^2)	8	Reference height (m)	140
Non-building latent heat (W/m^2)	0	Road albedo (-)	0.165
Char length(m)	135	Road emissivity (-)	0.95
Tree latent (-)	0.7	Vegetation coverage (-)	0.001
Grass latent (-)	0.6	Material	Asphalt
Reference site			
Latitudine (°)	45.6	Temperature measurement height (m)	10
Longitudine (°)	13.8	Wind measurement height (m)	10

outdoor urban air is used as a cold source for ASHPs. By using W_UHI, the UHI effect in winter is overestimated in the case of ASHPs and consequently the heating load of the building is somewhat underestimated in this case. As quantified later by the simulation, the increase in urban temperature caused by the UHI phenomenon involves a useful reduction in heating demand. The UWG calculations take into account not only the outside anthropogenic heat but also the heat losses from the buildings that are transferred as heat to the urban canopy. However, in the case of ASHPs, the outdoor air is used as a cold source and a quota of the heat losses is returned to the interior of the buildings by the ASHPs. In detail, the heating capacity provided to a building by the ASHP is the sum of the contribution from the cold source and the energy consumed by the compressors. Therefore, for ASHPs, only a quota of the building's heat losses should be considered in the UWG calculation. For example, with a typical HP efficiency (COP) of 3, only 33% of the building's heat losses should be added to the external anthropogenic heat gains. The overestimation of heating demand reduction in the case of ASHPs is not considered a problem in this analysis. Since the purpose of this study is to evaluate the benefits of SWHPs as an alternative to ASHPs, the presence of a possible overestimation in the second case can be considered as a further motivation for an advantage in this comparison.

Decentralized Heat Pump Modeling

High performing machines are considered for both SWHPs and ASHPs. They are equipped with multiple scroll compressors,

stainless steel plate heat exchangers that serve as evaporators and condensers, and R410A brine. In the larger building blocks, HPs have two refrigerant circuits, each with two compressors. The only difference between ASHPs and SWHPs is that one heat exchanger of the ASHPs is an air coil. The performance of HP is characterized by two basic parameters, full capacity and efficiency. Full capacity is the maximum thermal power that the unit can provide in heating or cooling mode. Efficiency has a different expression in heating and cooling modes. In heating mode, this efficiency, called coefficient of performance (COP), is the ratio between the heating power provided and the electrical power consumption. In cooling mode, this efficiency, called energy efficiency ratio (EER), is the ratio between the cooling power provided and the electrical power consumption. These performances are greatly affected by the temperatures of the external fluids that exchange heat at the evaporator and the condenser. For this reason, performance data are normally provided by manufacturers as a function of these operating temperatures. Standard test methods (CEN, 2019) are used to obtain these data. Specifically, this information in this analysis comes from RHOSS (2019) for SWHPs and from RHOSS (2018) for ASHPs. As a result of choosing terminal units based on air handling units and fan coils for HVAC systems. The supply water temperatures are fixed at 45°C for heating and 7°C for cooling. Therefore, the performance of HP at full capacity varies only as a function of the outdoor air temperature for ASHPs and the water inlet temperature from the urban network for SWHPs. For ASHPs, the outdoor air is moved by fans installed in the machine, so the power consumption of the fans is included in the EER/COP calculation. Instead, the SWHPs' inlet water is pumped through the district grid and the consumption for pumping is calculated separately. For the simulated HPs, capacity control is based on a multi-stage control with two stages, 50% and 100% of total capacity, achieved by tandem compressors. A smart capacity control is fundamental for optimizing HP operation. In fact, the capacity control must modulate the actual capacity provided to balance the building load, which is highly variable and often very low relative to the full load capacity of the machine. This part-load operation can cause severe penalization in the absence of a proper control system. The use of tandem compressors installed in the same refrigerant circuit makes it possible to limit this degradation of performance thanks to the oversize of the evaporator and condenser when only one compressor is operating. In any case, for a correct evaluation of the effective HP efficiency, a correction part load factor (PLF) is used for the previously introduced COP/EER at full load. This procedure is validated by standards (CEN, 2018) and is usually used for a performance rating of HPs under real working conditions (Schibuola, 2000; Dongellini et al., 2015; In et al., 2015). PLF values are obtained by interpolating the manufacturer's data. Typically, the manufacturer provides part load ratings at 25%, 50%, 75%, and 100% of full load capacity, as determined by standard laboratory tests (CEN, 2018). Indeed, these data are available because they are needed to calculate seasonal efficiency indices such as the European Seasonal Energy Efficiency Ratio (ESEER), which is a weighted average of these four values (Marinhas, 2013). Based on these values, it is also possible to trace the curves of the corresponding PLF correction factor as a function of the part load level, which is the ratio between the actual capacity provided and the full load capacity of the HP (Schibuola et al., 2013a). For this HP modeling, a quasi-steady-state calculation procedure based on a spreadsheet-style model was used. In this case, at each time step, the hourly building load calculated by EnergyPlus is used to evaluate HP performance. At each time step, the actual HP capacity required is equal to the building load. In heating mode, the full load COP and heating capacity are determined as a function of the inlet water temperature for SWHPs or the outdoor air temperature for ASHPs. Based on the heat exchanger design, this inlet water temperature is estimated to be 3°C below the seawater temperature. The level of part load allows us to calculate the PLF. Finally, the actual COP is obtained by multiplying the full load COP by the PLF. The electricity consumption is the ratio between the actual heating capacity on the simultaneous COP. The monthly average COP is the ratio between the heating energy supplied in that month and the corresponding monthly electricity consumption. The same calculation at the seasonal level gives the seasonal average COP. In cooling mode, the same procedure is used, except that in this case EER and the cooling load are taken into account.

RESULTS

The Urban Heat Island Effect

The UHI effect is investigated by comparing the temperatures of the monitored rural weather and the two urban weathers calculated by the UWG code in the cases of using ASHPs or SWHPs. In summer, the weather condition is referred to as S_UHI_A in the first case and S_UHI_B in the second case. In winter, as mentioned earlier, only one urban weather condition is evaluated and is referred to as W_UHI. In general, these urban analyses highlight a UHI intensity equal to the difference between urban and rural temperatures at the same moment. **Figure 7** shows the air temperature trends of the rural weather and the two urban weather conditions, S_UHI_A and S_UHI_B, on 6 days in July. The corresponding UHI intensities are also indicated. The UHI behavior is clearly evident and always confirmed. The S_UHI_A temperatures are the highest, and the S_UHI_B temperatures are in between the other two. Building air conditioning degrades urban thermal conditions, but removal of heat from condensers in SWHPs reduces this degradation. High variability in UHI intensities is observed mainly during daytime hours, with a significant increase at night. In **Figure 7**, a table shows the average values of temperatures and UHI intensities on the 6 days for all day, daytime, and nighttime. The three average S_UHI_A intensities are greater than 1 degree, but these values are approximately halved in the S_UHI_B case. The same outcomes, based on 6 days in December, are reported in **Figure 8**. In this case, only one urban temperature trend is compared to that of the rural area. The UHI effect is again evident throughout the period, but the UHI intensities are lower than in summer. The high variability of UHI intensities and their largest values during the night are also confirmed in winter.

Figure 9A shows the total, daytime, and nighttime average air temperatures for the three weather conditions for each month and for the entire summer season, as well as the percent

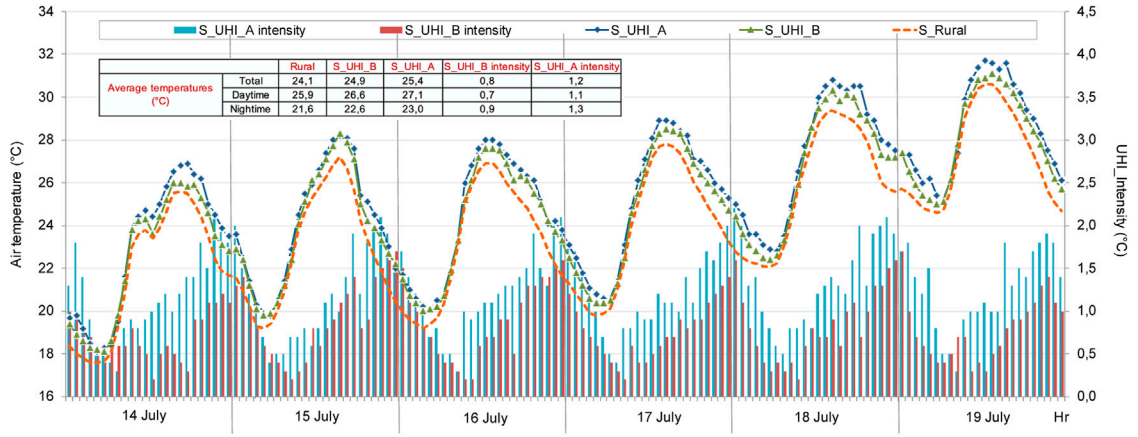

FIGURE 7 | Outdoor temperatures of rural and urban weather in case UHI_1 or UHI_2 on 6 days in July and corresponding UHI intensities. Their average values in the three daily periods are also shown.

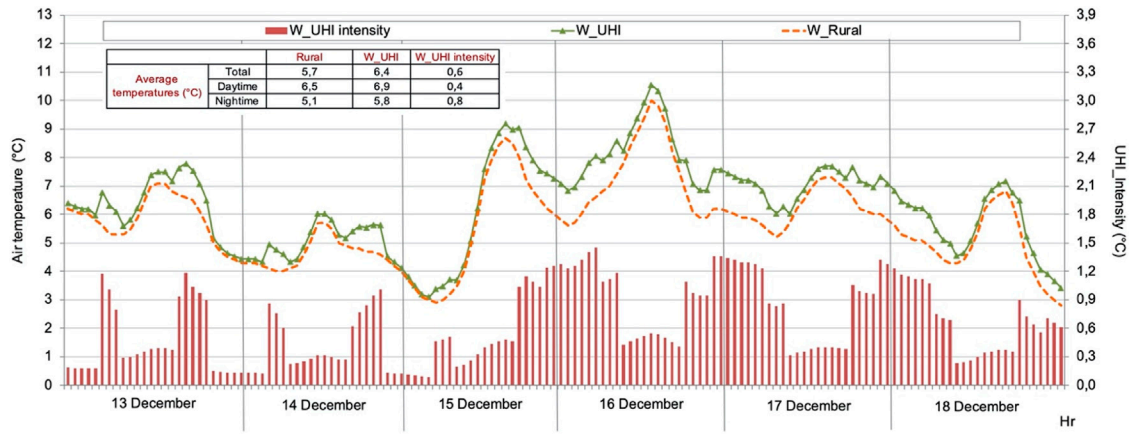

FIGURE 8 | Outdoor temperatures of rural and urban weather on 6 days in December and corresponding UHI intensities. Their average values in the three daily periods are also given.

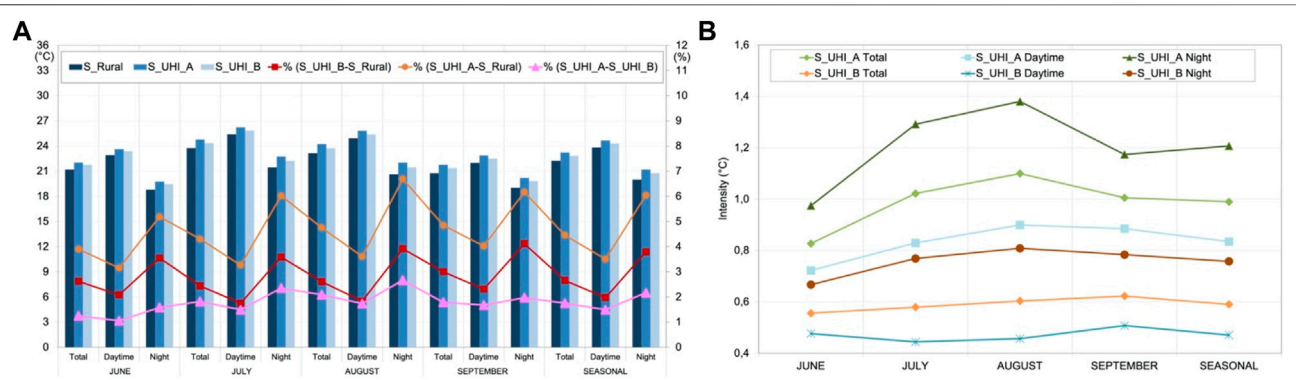

FIGURE 9 | Monthly and seasonal average air temperatures of rural and urban weather in case UHI_1 or UHI_2 in the three daily periods and their percent differences **(A)** in winter. The corresponding UHI intensities are shown in panel **(B)**.

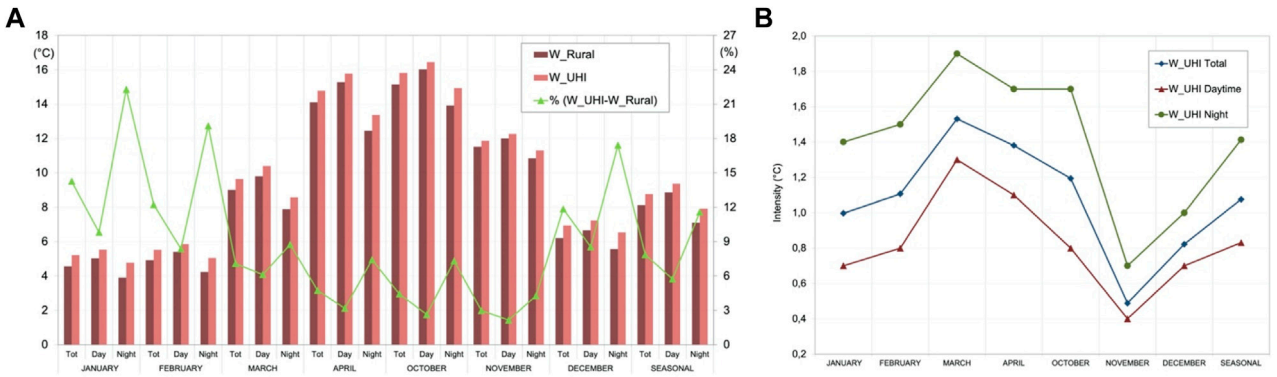

FIGURE 10 | Monthly and seasonal average air temperatures of rural and urban weather in case UHI_1 or UHI_2 in the three daily periods and their percent differences **(A)** in summer. The corresponding UHI intensities are shown in panel **(B)**.

differences in these temperatures. In all summer months, the UHI effect is anyway more relevant in case A than in case B. At the seasonal level, the percent increase in urban temperature in case A reaches 6% compared to that in rural temperature. In case B, this value is 3.8%. Thus, the SWHP option allows for a 36% reduction in this increase. **Figure 9B** shows the corresponding UHI intensities. In all months, the UHI effect depends strongly on the time of day. At the seasonal level, the average UHI related to the whole day is 1.0°C in case A and 0.6°C in case B. The same monthly and seasonal results for the winter period are shown in **Figure 10**. In winter, the UHI effect leads to an 11.6% increase in urban temperature compared to rural conditions. Of course, these percentage results also depend on the lower winter temperatures. The seasonal average UHI intensity is 1.1°C. The variability in monthly UHI intensities appears to be related to that of air temperatures and is therefore more pronounced in winter. In both seasons, the average monthly UHI effect is larger at night.

There are a few studies in the literature on the UHI phenomenon that also quantify the effect of heat released from the air cooled chillers (Bueno Unzeta, 2010; Salvati et al., 2017). The results found here are consistent with these previous evaluations. Nevertheless, these works do not address the question of how to eliminate this urban heat gain. Instead, this research evaluates the UHI mitigation benefits of a precise technology proposed to remove this heat from an urban area.

Heat Pump Performance Simulation

Figure 11A shows a comparison of the seasonal cooling and heating demand calculated by EnergyPlus with weather data for rural and urban areas for each building type. The percentage differences are also presented. Due to the significant variation in relative volumes in the area, the demand rates vary greatly between types, with types 2 and 4 being the largest contributors. However, the UHI phenomenon has an evident effect on the increase in cooling demand for all building types in summer but with a significant difference in the case of weather conditions S_UHI_A or S_UHI_B. Specifically, the percentage increase in cooling demand in the case of S_UHI_A ranges from 16.3% to 18.8%. In the case of S_UHI_B, this increase range is reduced between 6.9% and 7.4%. For all the types, the differences between these two increases vary to a limited extent between 8.1% and 9.6%, which is probably also related to the different cooling requirements of each type. The response to the UHI effect appears to be virtually the same for all building types. As for the reduction in heating demand, the response to the UHI effect is also similar among the four building types, varying between 9.5% and 11.0%. **Figure 11B** shows the monthly cooling and heating demands of the whole analyzed area calculated with the rural weather file. In the same histograms, the increase of cooling in the summer months with the two urban weather patterns and the reduction of heating thanks to the urban weather in the winter months are numerically expressed as percentages. The high variability of rural demand, especially in winter, results in considerable variation in these percentage increases or decreases on a monthly basis. In summer, however, the monthly differences between S_UHI_A and S_UHI_B are quite regular, ranging from 3.8% to 13.0%. In **Figures 11A,B**, the table shows the seasonal demands in rural areas and the corresponding percentage differences from the requirements resulting from urban weather conditions. At the seasonal level, the increase in cooling demand due to S_UHI_A in relation to rural weather is 17.3%, while for S_UHI_B, it is 8.7%. Therefore, the increase in cooling demand is reduced by 49.7% thanks to the SWHP technology. As for the seasonal heating demand, the calculation with the urban file indicates a reduction of 9.4% compared to the use of the rural file.

Figure 12A shows the monthly and seasonal averages of COPs relative to all SWHPs or ASHPs foreseen in the area. For SWHPs, these COPs, as well as the EERs that follow, also take into account the electrical absorption of pumping in the urban network and in the seawater loop. Due to careful control of the pumps, this electrical energy absorption is limited to 4.8% of the total annual electricity consumption of the SWHPs, with the same incidence on the corresponding electricity cost. On an annual basis, the electricity load of the seawater circuit including the filtration system is 32% of the total pumping consumption. The comparison highlights that the SWHPs perform best, especially in the coldest winter months, due to the more favorable thermal level of the sea compared to the outside air. However, the part load effect on COP is clearly observable. In the mid-season, the improvement in full-load performance due to the

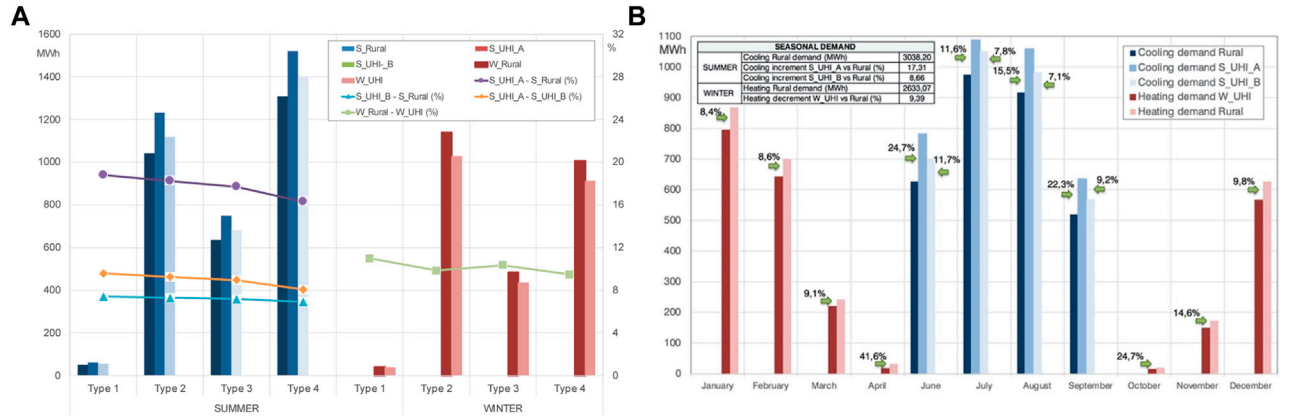

FIGURE 11 | SSeasonal heating or cooling demand of all buildings of each type calculated by rural or urban weather and corresponding percent differences **(A)**, total monthly and seasonal demand in rural weather, and corresponding changes in urban weather **(B)**.

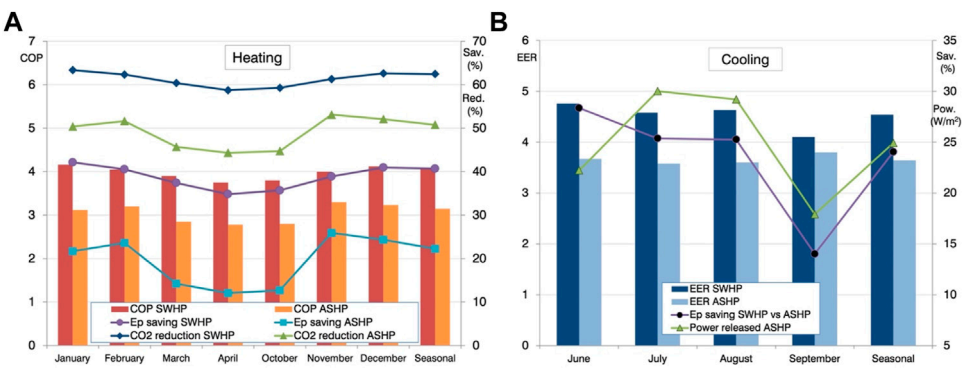

FIGURE 12 | Monthly and seasonal COP/EER of HPs during heating season **(A)** or cooling season **(B)**. In winter, both savings compared to using condensing boilers and CO_2 reductions. In summer, the savings are with SWHPs compared to those with ASHPs. The average specific heat power released by ASHPs in the area is also given in panel **(B)**.

higher thermal level of the cold source of the HP is counterbalanced by the part load penalization due to the reduction in building demand and the increase in the actual HP full-load capacity. High part load levels severely degrade HP efficiency. For this reason, the impact of part load must always be considered in the HP performance evaluation. On a seasonal basis, the average COP is 3.14 for the ASHPs and 4.08 for the SWHPs with a percentage increase of 29.8%. The advantage of adopting the HP technology as an alternative to the use of condensing boilers is investigated at the seasonal level in terms of primary energy consumption. For this purpose, the official Italian factor (DM 26 giugno 2015, 2015) 2.42 is used to convert the electrical energy consumption of HP to the corresponding primary energy. For the condensing boiler with a return water temperature of 40°C, an average seasonal efficiency of 1.01 from the national standard (UNI/TS 11300:2, 2014) is assumed. **Figure 12A** reports the percentage primary energy savings achieved with the HPs compared to the use of condensing boilers. The monthly trends are affected by the variability of the corresponding COPs. In any case, the net benefit of the HP technology is always evident for both ASHPs and SWHPs, although it is larger and more stable for SWHPs. Another important comparison term is the CO_2 emissions caused by the different heat generation systems. For the calculation of CO_2 emissions, the official data of Italy were used (Ispra, 2019). Specifically, 0.308 kg of CO_2 per electrical kWh consumed and 0.201 kg of CO_2 per kWh of primary energy consumed by a natural gas boiler were assumed as equivalences. **Figure 12A** shows the monthly and seasonal reductions by ASHPs and SWHPs in terms of CO_2 emissions compared to the case of a condensing boiler installation. At the seasonal level, ASHPs enable a reduction of 50.8%, while SWHPs achieve 62.4%. This remarkable result is the consequence of the different CO_2 emission rates for natural gas and electric energy and the better performances of the HPs, especially in the case of the SWHPs.

Figure 12B shows the monthly and seasonal average EERs for all area HPs in cooling mode. Primary energy savings achieved by SWHPs compared to consumption with ASHPs are also reported. In all summer months, the comparison points out the best performance of SWHPs due to the more favorable thermal level of seawater than outdoor air for cooling the HP condensers. In fact, the trend of the

seawater temperature is quite constant, while the outdoor air shows strong hourly variations, with the highest values during the air conditioning hours. The influence of part load is also evident in the EERs, but the fluctuations of the monthly trend are smaller in summer compared to those in winter months due to the smaller demand variations. The seasonal EERs are 3.63 and 4.54, respectively, with an increase of 24.6% for SWHPs. Lower cooling demand and better EER involve that the primary energy consumption for air conditioning is reduced thanks to SWHPs. On a seasonal level, this reduction is 24%. Since both ASHPs and SWHPs are electric-driven HPs, the percentage reduction in CO_2 emissions thanks to the use of seawater is equivalent to the percentage energy savings. HP performance assessment in cooling mode also provides the thermal power dissipated by condensers and removed in different ways with the two HP technologies. **Figure 12B** shows the thermal power released to outdoor urban air from ASHPs in terms of the monthly specific power per unit urban area, with a seasonal average value of 24.9 W/m^2. This high value underlines the importance of air conditioning systems in energy balances in terms of the UHI effect in the case of ASHPs. In the case of SWHPs, on the other hand, the relative condenser heat is removed from the urban area *via* the sea. As regards the thermal use of water from surface aquifers, the strict limitations of the above-mentioned national legislation were introduced to protect the outdoor environment. In particular, the maximum temperature difference of only 3°C between the water withdrawal and the return reduces the thermal stress, also considering possible problems for flora and fauna. In addition, in the case of the sea, the large thermal inertia, wave motion, and sea currents further contribute to eliminate the risks associated with the increase in water temperature. However, since the application of the SWHP technology in coastal areas is still at the beginning, there are no studies yet on its impact on the marine environment. In addition to performance monitoring, investigations on this topic are absolutely recommended. At the urban level, the possible negative impacts become negligible compared to the consequences of the total heat emission of the ASHPs in the immediate vicinity of the buildings.

The performance outcomes remedy the lack of studies on this technology. Indeed, a few 5GDHC systems are currently coupled with the use of seawater and little information is available (Buffa et al., 2019; Caputo et al., 2021). On the other hand, the current state of the literature focuses on the youth of the 5GDHC technology. Reviews on this topic emphasize the need for further development of design and simulation tools based on their application to real-case studies (Abugabbara et al., 2020; Lindhe et al., 2022).

DISCUSSION

This article addresses the environmental benefits of implementing a 5GDHC network in a coastal city using seawater as a heat source/sink as part of a retrofit action. Starting from the assessment of the UHI effect in the investigated area, the analysis highlights the deterioration of the UHI effect caused by the heat released by the traditional air conditioning systems in the urban area in summer, as well as the change in the urban climate in winter.

A first conclusion from the results is that building load simulations in urban areas should be performed considering the UHI phenomenon, instead of simply using rural weather data. However, the proposed technical solution is able to carry away from the city the heat dissipated by the chiller condensers. In this way, the results show a significant mitigation of the UHI effect in summer. Therefore, this option to mitigate the UHI effect can help to increase the resilience of cities, and the prediction of the future climate change scenario indicates that the potential benefits will increase during extreme events such as urban heat waves. Another fundamental study concerned the consequences of the introduction of the HP technology and the more favorable thermal level of seawater compared to outdoor air. For this purpose, during the heating season, the performance comparison has concerned not only the ASHPs and SWHPs but also the installation of condensing boilers as a possible alternative in the retrofit action. The findings show that the HP technology is superior in both increasing energy performance and reducing CO_2 emissions. However, the SWHP solution offers significantly better performance than the ASHP in both summer and winter. In terms of CO_2 emissions, even in summer, the savings in electricity consumption due to air conditioning in urban areas show a non-negligible overall reduction in CO_2 emissions. Indeed, the greenhouse gas footprint includes not only direct emissions in urban areas but also upstream emissions to produce goods and services for urban consumers. The main obstacle to the implementation of SWHP compared to other retrofit measures, and in particular to traditional urban heating/cooling networks, is the presence of a seawater access at an acceptable distance from the intervention area. This condition may limit the possibility of the expanded use of SWHP even in coastal areas. On the other hand, the availability of seawater provides the possibility to foster the benefits of including 5GDHC networks into retrofit actions to support current efforts to increase decarbonization and environmental resilience in urban areas.

DATA AVAILABILITY STATEMENT

The raw data supporting the conclusion of this article will be made available by the authors without undue reservation.

AUTHOR CONTRIBUTIONS

LS: conceptualization, methodology, writing—original draft preparation, and supervision. CT: data curation, methodology, software, investigation, writing—original draft preparation, and writing—review and editing. AB: investigation and writing.

REFERENCES

Abbasi, M. H., Abdullah, B., Ahmad, M. W., Rostami, A., and Cullen, J. (2021). Heat Transition in the European Building Sector: Overview of the Heat Decarbonisation Practices through Heat Pump Technology. *Sustain. Energy Technol. Assessments* 48, 101630. doi:10.1016/j.seta.2021.101630

Abugabbara, M., Javed, S., Bagge, H., and Johansson, D. (2020). Bibliographic Analysis of the Recent Advancements in Modeling and Co-simulating the Fifth-Generation District Heating and Cooling Systems. *Energy Build.* 224, 110260. doi:10.1016/j.enbuild.2020.110260

Aram, F., Higueras García, E., Solgi, E., and Mansournia, S. (2019). Urban Green Space Cooling Effect in Cities. *Heliyon* 5, e01339. doi:10.1016/j.heliyon.2019.e01339

Author Anonymous (2020). EU H2020 FLEXYNETS Project. Available online 〈 https://www.flexynets.eu.〉

Author Anonymous (1999). National Law Provisions on the Protection of the Waters from Pollution 'Disposizioni Sulla Tutela Delle Acque Dall'inquinamento. *Dlgs. N.* 152, 11. Italy.

Baik, Y.-J., Kim, M., Chang, K.-C., Lee, Y.-S., and Ra, H.-S. (2014). Potential to Enhance Performance of Seawater-Source Heat Pump by Series Operation. *Renew. Energy* 65, 236–244. doi:10.1016/j.renene.2013.09.021

Bevilacqua, P., Bruno, R., and Arcuri, N. (2020). Green Roofs in a Mediterranean Climate: Energy Performances Based on *In-Situ* Experimental Data. *Renew. Energy* 152, 1414–1430. doi:10.1016/j.renene.2020.01.085

Bisegna, F., Buggin, A., Peri, G., Rizzo, G., Scaccianoce, G., Scarpa, M., et al. (20192019). "Computing Methods for Resilience: Evaluating New Building Components in the Frame of SECAPs," in Proceedings - 2019 IEEE International Conference on Environment and Electrical Engineering and 2019 IEEE Industrial and Commercial Power Systems Europe. EEEIC/I and CPS Europe. doi:10.1109/EEEIC.2019.8783458

Boccalatte, A., Fossa, M., Gaillard, L., and Menezo, C. (2020). Microclimate and Urban Morphology Effects on Building Energy Demand in Different European Cities. *Energy Build.* 224, 110129. doi:10.1016/j.enbuild.2020.110129

Bueno, B., Norford, L., Hidalgo, J., and Pigeon, G. (2013). The Urban Weather Generator. *J. Build. Perform. Simul.* 6, 269–281. doi:10.1080/19401493.2012.718797

Bueno Unzeta, B. (2010). An Urban Weather Generator Coupling a Building, Simulation Program with an Urban Canopy Model. *Thesis-Massachusetts Institute of Technology.*

Buffa, S., Cozzini, M., D'Antoni, M., Baratieri, M., and Fedrizzi, R. (2019). 5th Generation District Heating and Cooling Systems: A Review of Existing Cases in Europe. *Renew. Sustain. Energy Rev.* 104, 504–522. doi:10.1016/j.rser.2018.12.059

Caputo, P., Ferla, G., Belliardi, M., and Cereghetti, N. (2021). District Thermal Systems: State of the Art and Promising Evolutive Scenarios. A Focus on Italy and Switzerland. *Sustain. Cities Soc.* 65, 102579. doi:10.1016/j.scs.2020.102579

Castellani, B., Morini, E., Anderini, E., Filipponi, M., and Rossi, F. (2017). Development and Characterization of Retro-Reflective Colored Tiles for Advanced Building Skins. *Energy Build.* 154, 513–522. doi:10.1016/j.enbuild.2017.08.078

CEN (2018). EN 14825:2018 Air Conditioners, Liquid Chilling Packages and Heat Pumps, with Electrically Driven, Compressors, for Space Heating and Cooling - Testing and Rating at Part Load Conditions and Calculation of Seasonal Performance.

Chen, S., Friedrich, D., and Yu, Z. (2021). Optimal Sizing of a Grid Independent Renewable Heating System for Building Decarbonisation. *Front. Energy Res.* 9. doi:10.3389/fenrg.2021.746268

Chen, X., Zhang, G., Peng, J., Lin, X., and Liu, T. (2006). The Performance of an Open-Loop Lake Water Heat Pump System in South China. *Appl. Therm. Eng.* 26, 2255–2261. doi:10.1016/j.applthermaleng.2006.03.009

Cui, Y., Yan, D., Hong, T., and Ma, J. (2017). Temporal and Spatial Characteristics of the Urban Heat Island in Beijing and the Impact on Building Design and Energy Performance. *Energy* 130, 286–297. doi:10.1016/j.energy.2017.04.053

Daikin (2014). *Innovative Engineering Preserves Venice Arsenal*. Ostend: press release.

DM 26 giugno 2015 (2015). *Applicazione delle metodologie di calcolo delle prestazioni energetiche e definizione delle prescrizioni e dei requisiti minimi degli edifici*.

Doan, V. Q., Kusaka, H., and Nguyen, T. M. (2019). Roles of Past, Present, and Future Land Use and Anthropogenic Heat Release Changes on Urban Heat Island Effects in Hanoi, Vietnam: Numerical Experiments with a Regional Climate Model. *Sustain. Cities Soc.* 47, 101479. doi:10.1016/j.scs.2019.101479

Dongellini, M., Naldi, C., and Morini, G. L. (2015). Seasonal Performance Evaluation of Electric Air-To-Water Heat Pump Systems. *Appl. Therm. Eng.* 90, 1072–1081. doi:10.1016/j.applthermaleng.2015.03.026

Duan, S., Luo, Z., Yang, X., and Li, Y. (2019). The Impact of Building Operations on Urban Heat/cool Islands under Urban Densification: A Comparison between Naturally-Ventilated and Air-Conditioned Buildings. *Appl. Energy* 235, 129–138. doi:10.1016/j.apenergy.2018.10.108

CEN (2019). *Air Conditioners, Liquid Chilling Packages and Heat Pumps for Space Heating and Cooling and Process Chillers, with Electrically Driven Compressors Part 3*. Tests Methods.

European Community (2010). *Energy Performance Building Directive*. EPBD.

Ferrando, M., Hong, T., and Causone, F. (2021). A Simulation-Based Assessment of Technologies to Reduce Heat Emissions from Buildings. *Build. Environ.* 195, 107772. doi:10.1016/j.buildenv.2021.107772

Foster, S., Love, J., Walker, I., and Crane, M. (2016). *Heat Pumps in District Heating: Case Studies*. LondonUK Government: Department of Energy & Climate Change.

Guattari, C., Evangelisti, L., and Balaras, C. A. (2018). On the Assessment of Urban Heat Island Phenomenon and its Effects on Building Energy Performance: A Case Study of Rome (Italy). *Energy Build.* 158, 605–615. doi:10.1016/j.enbuild.2017.10.050

Hong, T., Xu, Y., Sun, K., Zhang, W., Luo, X., and Hooper, B. (2021). Urban Microclimate and its Impact on Building Performance: A Case Study of San Francisco. *Urban Clim.* 38, 100871. doi:10.1016/j.uclim.2021.100871

In, S., Cho, K., Lim, B., and Lee, C. (2015). Partial Load Performance Test of Residential Heat Pump System with Low-GWP Refrigerants. *Appl. Therm. Eng.* doi:10.1016/j.applthermaleng.2015.04.013

Ispra (2019). *Greenhouse Gas Emission Factors in the National Electricity Sector and in the Main European Countries*. report 303.

Jain, R., Luo, X., Sever, G., Hong, T., and Catlett, C. (2020). Representation and Evolution of Urban Weather Boundary Conditions in Downtown Chicago. *J. Build. Perform. Simul.* 13, 182–194. doi:10.1080/19401493.2018.1534275

Lauzet, N., Rodler, A., Musy, M., Azam, M.-H., Guernouti, S., Mauree, D., et al. (2019). How Building Energy Models Take the Local Climate into Account in an Urban Context - A Review. *Renew. Sustain. Energy Rev.* 116, 109390. doi:10.1016/j.rser.2019.109390

Li, X.-l., Duanmu, L., and Shu, H.-w. (2010). Optimal Design of District Heating and Cooling Pipe Network of Seawater-Source Heat Pump. *Energy Build.* 42, 100–104. doi:10.1016/j.enbuild.2009.07.016

Li, X., Zhou, Y., Yu, S., Jia, G., Li, H., and Li, W. (2019). Urban Heat Island Impacts on Building Energy Consumption: A Review of Approaches and Findings. *Energy* 174, 407–419. doi:10.1016/j.energy.2019.02.183

Liang, J., Yang, Q., Liu, L., and Li, X. (2011). Modeling and Performance Evaluation of Shallow Ground Water Heat Pumps in Beijing Plain, China. *Energy Build.* 43, 3131–3138. doi:10.1016/j.enbuild.2011.08.007

Lima, I., Scalco, V., and Lamberts, R. (2019). Estimating the Impact of Urban Densification on High-Rise Office Building Cooling Loads in a Hot and Humid Climate. *Energy Build.* 182, 30–44. doi:10.1016/j.enbuild.2018.10.019

Lindhe, J., Javed, S., Johansson, D., and Bagge, H. (2022). A Review of the Current Status and Development of 5GDHC and Characterization of a Novel Shared Energy System. *Sci. Technol. Built Environ.* 0, 1–15. doi:10.1080/23744731.2022.2057111

Liu, Y., Li, Q., Yang, L., Mu, K., Zhang, M., and Liu, J. (2020). Urban Heat Island Effects of Various Urban Morphologies under Regional Climate Conditions. *Sci. Total Environ.* 743, 140589. doi:10.1016/j.scitotenv.2020.140589

Lund, H., Østergaard, P. A., Connolly, D., and Mathiesen, B. V. (2017). Smart Energy and Smart Energy Systems. *Energy* 137, 556–565. doi:10.1016/j.energy.2017.05.123

Lund, H., Werner, S., Wiltshire, R., Svendsen, S., Thorsen, J. E., Hvelplund, F., et al. (2014). 4th Generation District Heating (4GDH). *Energy* 68, 1–11. doi:10.1016/j.energy.2014.02.089

Luo, X., Vahmani, P., Hong, T., and Jones, A. (2020). City-scale Building Anthropogenic Heating during Heat Waves. *Atmosphere* 11, 1206. doi:10.3390/atmos11111206

Luo, Z., and Asproudi, C. (2015). Subsurface Urban Heat Island and its Effects on Horizontal Ground-Source Heat Pump Potential under Climate Change. *Appl. Therm. Eng.* 90, 530–537. doi:10.1016/j.applthermaleng.2015.07.025

MacLachlan, A., Biggs, E., Roberts, G., and Boruff, B. (2021). Sustainable City Planning: A Data-Driven Approach for Mitigating Urban Heat. *Front. Built Environ.* 6. doi:10.3389/fbuil.2020.519599

Manoli, G., Fatichi, S., Schläpfer, M., Yu, K., Crowther, T. W., Meili, N., et al. (2019). Magnitude of Urban Heat Islands Largely Explained by Climate and Population. *Nature* 573, 55–60. doi:10.1038/s41586-019-1512-9

Mao, J., Fu, Y., Afshari, A., Armstrong, P. R., and Norford, L. K. (2018). Optimization-aided Calibration of an Urban Microclimate Model under Uncertainty. *Build. Environ.* 143, 390–403. doi:10.1016/j.buildenv.2018.07.034

Mao, J., Yang, J. H., Afshari, A., and Norford, L. K. (2017). Global Sensitivity Analysis of an Urban Microclimate System under Uncertainty: Design and Case Study. *Build. Environ.* 124, 153–170. doi:10.1016/j.buildenv.2017.08.011

Marinhas, S. (2013). Eurovent Chiller Certification Key Stones and Future Challenges. *REHVA J.*, 31–33.

Martin-Vide, J., Sarricolea, P., and Moreno-GarcÃa, M. C. (2015). On the Definition of Urban Heat Island Intensity: the Â€œruralâ€ Reference. *Front. Earth Sci.* 3. doi:10.3389/feart.2015.00024

Martinez, S., Machard, A., Pellegrino, A., Touili, K., Servant, L., and Bozonnet, E. (2021). A Practical Approach to the Evaluation of Local Urban Overheating- A Coastal City Case-Study. *Energy Build.* 253, 111522. doi:10.1016/j.enbuild.2021.111522

Mei, S.-J., and Yuan, C. (2021). Analytical and Numerical Study on Transient Urban Street Air Warming Induced by Anthropogenic Heat Emission. *Energy Build.* 231, 110613. doi:10.1016/j.enbuild.2020.110613

MISE (2015). *national decree, Requisiti tecnici per l'accesso alle detrazioni fiscali per la riqualificazione energetica degli edifici, annex E.* Ministry of Economic Development. 6 August 2020.

MIT (2014). Urban Weather Generator. Available at: http://urbanmicroclimate.scripts.mit.edu/uwg.php.

Morini, E., Castellani, B., Presciutti, A., Anderini, E., Filipponi, M., Nicolini, A., et al. (2017). Experimental Analysis of the Effect of Geometry and Façade Materials on Urban District's Equivalent Albedo. *Sustainability* 9, 1245. doi:10.3390/su9071245

Mosteiro-Romero, M., Maiullari, D., Pijpers-van Esch, M., and Schlueter, A. (2020). An Integrated Microclimate-Energy Demand Simulation Method for the Assessment of Urban Districts. *Front. Built Environ.* 6. doi:10.3389/fbuil.2020.553946

Nakano, A., Bueno, B., Norford, L., and Reinhart, C. F. (2015). "Urban Weather Generator - A Novel Workflow for Integrating Urban Heat Island Effect within Urban Design Process," in 14th International Conference of IBPSA - Building Simulation 2015, BS 2015, Conference Proceedings.

Nam, Y., and Ooka, R. (2010). Numerical Simulation of Ground Heat and Water Transfer for Groundwater Heat Pump System Based on Real-Scale Experiment. *Energy Build.* 42, 69–75. doi:10.1016/j.enbuild.2009.07.012

Palme, M., Inostroza, L., Villacreses, G., Lobato-Cordero, A., and Carrasco, C. (2017). From Urban Climate to Energy Consumption. Enhancing Building Performance Simulation by Including the Urban Heat Island Effect. *Energy Build.* 145, 107–120. doi:10.1016/j.enbuild.2017.03.069

Pattijn, I. P., and Baumans, A. (2017). Fifth-generation Thermal Grids and Heat Pumps: A Pilot Project in Leuven, Belgium. *HPT Mag.*

Pauschinger, T. (2016). *Advanced District Heating and Cooling (DHC) Systems.*

Prasanna, A., Dorer, V., and Vetterli, N. (2017). Optimisation of a District Energy System with a Low Temperature Network. *Energy* 137, 632–648. doi:10.1016/j.energy.2017.03.137

Reiners, T., Gross, M., Altieri, L., Wagner, H.-J., and Bertsch, V. (2021). Heat Pump Efficiency in Fifth Generation Ultra-low Temperature District Heating Networks Using a Wastewater Heat Source. *Energy* 236, 121318. doi:10.1016/j.energy.2021.121318

RHOSS (2019). TCHEY-THHEY 245÷2187, technical bulletin K20325EN ed.11.

RHOSS (2018). THAEY 105÷111, technical bulletin K20151IT ed.7.

Sailor, D. J., and Fan, H. (2004). *The Importance of Including Anthropogenic Heating in Mesoscale Modeling of the Urban Heat Island.* Bulletin of the American Meteorological Society.

Salvati, A., Monti, P., Coch Roura, H., and Cecere, C. (2019). Climatic Performance of Urban Textures: Analysis Tools for a Mediterranean Urban Context. *Energy Build.* 185, 162–179. doi:10.1016/j.enbuild.2018.12.024

Salvati, A., Palme, M., and Inostroza, L. (2017). Key Parameters for Urban Heat Island Assessment in A Mediterranean Context: A Sensitivity Analysis Using the Urban Weather Generator Model. *IOP Conf. Ser. Mat. Sci. Eng.* 245, 082055. doi:10.1088/1757-899X/245/8/082055

Santamouris, M. (2007). Heat Island Research in Europe: The State of the Art. *Adv. Build. Energy Res.* 1, 123–150. doi:10.1080/17512549.2007.9687272

Santamouris, M. (2014). On the Energy Impact of Urban Heat Island and Global Warming on Buildings. *Energy Build.* 82, 100–113. doi:10.1016/j.enbuild.2014.07.022

Santos, L. G. R., Afshari, A., Norford, L. K., and Mao, J. (2018). Evaluating Approaches for District-wide Energy Model Calibration Considering the Urban Heat Island Effect. *Appl. Energy* 215, 31–40. doi:10.1016/j.apenergy.2018.01.089

Sarbu, I., and Sebarchievici, C. (2014). General Review of Ground-Source Heat Pump Systems for Heating and Cooling of Buildings. *Energy Build.* 70, 441–454. doi:10.1016/j.enbuild.2013.11.068

Schibuola, L. (2000). Heat Pump Seasonal Performance Evaluation: A Proposal for a European Standard. *Appl. Therm. Eng.* doi:10.1016/S1359-4311(99)00041-1

Schibuola, L., Scarpa, M., and Tambani, C. (2015). Demand Response Management by Means of Heat Pumps Controlled via Real Time Pricing. *Energy Build.* 90, 15–28. doi:10.1016/j.enbuild.2014.12.047

Schibuola, L., Scarpa, M., and Tambani, C. (2018). Innovative Technologies for Energy Retrofit of Historic Buildings: An Experimental Validation. *J. Cult. Herit.* 30, 147–154. doi:10.1016/J.CULHER.2017.09.011

Schibuola, L., Scarpa, M., and Tambani, C. (2013a). "Modelling of HVAC System Components for Building Dynamic Simulation," in Proceedings of BS 2013: 13th Conference of the International Building Performance Simulation Association.

Schibuola, L., Scarpa, M., and Tambani, C. (2016). Parametric Study on the Financial Performance of Battery-Supported Photovoltaic Systems Connected to Smart Grids in Current and Future Market Scenarios. *Sci. Technol. Built Environ.* 22, 751–765. doi:10.1080/23744731.2016.1197717

Schibuola, L., and Tambani, C. (2022). Environmental Impact and Energy Performance of Groundwater Heat Pumps in Urban Retrofit. *Energy Build.* 261, 111964. doi:10.1016/j.enbuild.2022.111964

Schibuola, L., and Tambani, C. (2020). Performance Assessment of Seawater Cooled Chillers to Mitigate Urban Heat Island. *Appl. Therm. Eng.* 175, 115390. doi:10.1016/j.applthermaleng.2020.115390

Schibuola, L., and Tambani, C. (2012). Renewable Energy Sources for Historic Buildings: The Crucifers Convent in Venice. *WIT Trans. Ecol. Environ.* 165. doi:10.2495/ARC120301

Schibuola, L., Tambani, C., Zarrella, A., and Scarpa, M. (2013b). Ground Source Heat Pump Performance in Case of High Humidity Soil and Yearly Balanced Heat Transfer. *Energy Convers. Manag.* 76, 956–970. doi:10.1016/j.enconman.2013.09.002

Shi, L., Luo, Z., Matthews, W., Wang, Z., Li, Y., and Liu, J. (2019). Impacts of Urban Microclimate on Summertime Sensible and Latent Energy Demand for Cooling in Residential Buildings of Hong Kong. *Energy* 189, 116208. doi:10.1016/j.energy.2019.116208

Smith, C., Lindley, S., and Levermore, G. (2009). Estimating Spatial and Temporal Patterns of Urban Anthropogenic Heat Fluxes for UK Cities: The Case of Manchester. *Theor. Appl. Climatol.* 98, 19–35. doi:10.1007/s00704-008-0086-5

Song, Y.-h., Akashi, Y., and Yee, J.-J. (2007). Effects of Utilizing Seawater as a Cooling Source System in a Commercial Complex. *Energy Build.* 39, 1080–1087. doi:10.1016/j.enbuild.2006.11.011

Stene, J., and Eggen, G. (1995). *Heat Pump System with Distribution at Intermediate Temperature at the University of Bergen*. Norway.

Street, M., Reinhart, C., Norford, L., and Ochsendorf, J. (2013). "Urban Heat Island in Boston - an Evaluation of Urban Airtemperature Models for Predicting Building Energy Use," in *n*.Proceedings of BS 2013: 13th Conference of the International Building Performance Simulation Associatio

Sun, R., Wang, Y., and Chen, L. (2018). A Distributed Model for Quantifying Temporal-Spatial Patterns of Anthropogenic Heat Based on Energy Consumption. *J. Clean. Prod.* 170, 601–609. doi:10.1016/j.jclepro.2017.09.153

Swan, L. G., and Ugursal, V. I. (2009). Modeling of End-Use Energy Consumption in the Residential Sector: A Review of Modeling Techniques. *Renew. Sustain. Energy Rev.* 13, 1819–1835. doi:10.1016/j.rser.2008.09.033

UNI/TS 11300:2 (2014). *Energy Performance of Buildings*. Technical Specification. Italian standard.

U.S. Department of Energy (2019b). EnergyPlus. Available at: https://energyplus.net/.

U.S. Department of Energy (2019a). EnergyPlus Version 9.2.0, Documentation-Auxiliary Programs. https://energyplus.net/sites/all/modules/custom/ nrel_custom/pdfs/pdfs_v9.2.0/AuxiliaryPrograms.pdf.

Verhoeven, R., Willems, E., Harcouët-Menou, V., De Boever, E., Hiddes, L., Veld, P. O. t., et al. (2014). Minewater 2.0 Project in Heerlen the Netherlands: Transformation of a Geothermal Mine Water Pilot Project into a Full Scale Hybrid Sustainable Energy Infrastructure for Heating and Cooling. *Energy Procedia* 46, 58–67. Energy Procedia. doi:10.1016/j.egypro.2014.01.158

Wen, Y., and Lian, Z. (2009). Influence of Air Conditioners Utilization on Urban Thermal Environment. *Appl. Therm. Eng.* 29, 670–675. doi:10.1016/j.applthermaleng.2008.03.039

Wheatcroft, E., Wynn, H., Lygnerud, K., Bonvicini, G., and Leonte, D. (2020). The Role of Low Temperature Waste Heat Recovery in Achieving 2050 Goals: A Policy Positioning Paper. *Energies* 13, 2107. doi:10.3390/en13082107

Yang, X., Hu, M., Heeren, N., Zhang, C., Verhagen, T., Tukker, A., et al. (2020a). A Combined GIS-Archetype Approach to Model Residential Space Heating Energy: A Case Study for the Netherlands Including Validation. *Appl. Energy* 280, 115953. doi:10.1016/j.apenergy.2020.115953

Yang, X., Peng, L. L. H., Jiang, Z., Chen, Y., Yao, L., He, Y., et al. (2020b). Impact of Urban Heat Island on Energy Demand in Buildings: Local Climate Zones in Nanjing. *Appl. Energy* 260, 114279. doi:10.1016/j.apenergy.2019.114279

Yang, X., Yao, L., Peng, L. L. H., Jiang, Z., Jin, T., and Zhao, L. (2019). Evaluation of a Diagnostic Equation for the Daily Maximum Urban Heat Island Intensity and its Application to Building Energy Simulations. *Energy Build.* 193, 160–173. doi:10.1016/j.enbuild.2019.04.001

Zuberi, M. J. S., Chambers, J., and Patel, M. K. (2021). Techno-economic Comparison of Technology Options for Deep Decarbonization and Electrification of Residential Heating. *Energy Effic.* 14, 75. doi:10.1007/s12053-021-09984-7

Conflict of Interest: The authors declare that the research was conducted in the absence of any commercial or financial relationships that could be construed as a potential conflict of interest.

Publisher's Note: All claims expressed in this article are solely those of the authors and do not necessarily represent those of their affiliated organizations, or those of the publisher, the editors, and the reviewers. Any product that may be evaluated in this article, or claim that may be made by its manufacturer, is not guaranteed or endorsed by the publisher.

frontiers | Frontiers in Energy Research

ORIGINAL RESEARCH
published: 15 August 2022
doi: 10.3389/fenrg.2022.939961

Integrating Blue Energy in Maritime Spatial Planning of Mediterranean Regions

Riccardo Maria Pulselli[1,2], Maria Vittoria Struglia[3], Matteo Maccanti[4], Morena Bruno[4], Nicoletta Patrizi[4], Elena Neri[2], Adriana Carillo[3], Ernesto Napolitano[3], Nikolaos Stefanatos[5], Christoforos Perakis[6], Markos Damasiotis[6], Federica Di Pietrantonio[7], Stefano Magaudda[8], Venturo Madalena[8], Hrvoje Stančin[9], Hrvoje Mikulčić[9,10], Vasilis Petrou[11], Konstantinos Smagas[11], Eleni Valari[11], Louisa Marie Shakou[12] and Simone Bastianoni[4]*

[1]Department of Architecture, University of Florence, Florence, Italy, [2]Indaco2 srl, Colle Val d'Elsa (SI), Italy, [3]Climate Modeling Laboratory, Division Model and Technologies for Risk Reduction, Department for Sustainability, ENEA, Rome, Italy, [4]Department of Physical, Earth and Environmental Sciences, University of Siena, Siena, Italy, [5]Division of Renewable Energy Sources, Centre for Renewable Energy Sources and Saving—CRES, Pikermi, Greece, [6]Division of Development Programs, Centre for Renewable Energy Sources and Saving—CRES, Pikermi, Greece, [7]Department of Architecture, University of Roma Tre, Rome, Italy, [8]U-space sl, Sevilla, Spain, [9]Faculty of Mechanical Engineering and Naval Architecture, University of Zagreb, Zagreb, Croatia, [10]MOE Key Laboratory of Thermo-Fluid Science and Engineering, Xi'an Jiaotong University, Xi'an, China, [11]Geoimaging Ltd, Nicosia, Cyprus, [12]Climate Change and Environment Department, Cyprus Energy Agency, Nicosia, Cyprus

OPEN ACCESS

Edited by:
Biagio Fernando Giannetti, Paulista University, Brazil

Reviewed by:
Alessio Tei, University of Genoa, Italy
Hale Özgit, Cyprus International University, Cyprus
Maxim A. Dulebenets, Agricultural and Mechanical University, United States

***Correspondence:**
Riccardo Maria Pulselli
riccardomaria.pulselli@unifi.it

Specialty section:
This article was submitted to Sustainable Energy Systems and Policies, a section of the journal Frontiers in Energy Research

Received: *09 May 2022*
Accepted: *21 June 2022*
Published: *15 August 2022*

Citation:
Pulselli RM, Struglia MV, Maccanti M, Bruno M, Patrizi N, Neri E, Carillo A, Napolitano E, Stefanatos N, Perakis C, Damasiotis M, Di Pietrantonio F, Magaudda S, Madalena V, Stančin H, Mikulčić H, Petrou V, Smagas K, Valari E, Shakou LM and Bastianoni S (2022) Integrating Blue Energy in Maritime Spatial Planning of Mediterranean Regions. Front. Energy Res. 10:939961. doi: 10.3389/fenrg.2022.939961

Blue Energy (BE) is expected to play a strategic role in the energy transition of Europe, particularly toward the 2050 horizon. It refers to a set of Marine Energy Sources (MES), including offshore wind, waves, tides, marine currents, sea thermal energy, salinity gradients, and marine biomass, which are exploited by different BE technologies. Nevertheless, the implementation of integrated solutions to exploit MES in marine areas does not just concern technological issues; it requires inclusive planning practices considering different aspects regarding climate and environmental impacts, landscape compatibility, interference with other marine activities (such as shipping, fishing, and tourism), and social acceptance. A replicable BE planning framework has been developed based on interdisciplinary knowledge in three Mediterranean sites in Greece, Croatia, and Cyprus, under the scope of the Interreg Med BLUE DEAL project. It has been implemented by some interdisciplinary experts through a collaborative and iterative process of data elaboration, mapping, evaluation, and visualization. Results concern the localization of suitable sites to install BE plants and the estimation of potential energy production and avoided emissions in selected scenarios. Together with visual simulations, this study shows the potential effects of the implementation of BE in specific marine areas, with a special focus on the most promising offshore floating wind farms and wave energy converters (WECs), as basic information for participative design and stakeholder engagement initiatives, including public authorities, businesses, and citizens.

Keywords: marine energy sources, offshore wind farms (OWFs), wave energy converters (WECs), stakeholders engagement, energy transition

INTRODUCTION

The Sixth Assessment Report of the IPCC highlights climate change impacts and risks emphasizing the interdependence of climate and human societies. The recognition of climate risks, especially in the Mediterranean, one of the world's hotspots in terms of temperature increase, is expected to strengthen mitigation and adaptation actions and accelerate transitions to a more resilient state (IPCC, 2022). In particular, the risks of climate change give rise to a timebound imperative to transform modern energy systems into low-carbon alternatives (Fries, 2021). This will require multiple efforts to implement necessary measures, including high penetration of renewable energy, development of distributed and integrated energy systems, management of inherent intermittency of renewable sources, real-time supply-demand balancing, innovation and testing of alternative low-carbon technologies in initial markets, and selection of the ones best suited to customer needs (Petit, 2018; Helm and Miller, 2021; Zhao et al., 2021).

Especially in Europe, the wide deployment of renewable energy sources is a necessary condition to meet the EU targets of greenhouse-gas emission reduction by at least 55% by 2030 (compared to the 1990 levels) and carbon neutrality by 2050. Among other Marine Energy Sources (MES), offshore wind energy is expected to become the European largest source of electricity generation, with an increase of the offshore wind power in Europe from 12 GW to 60 GW by 2030 and 300 GW by 2050. These targets (COM, 2020) demand for a commitment by the Member States to include MES in their future planning and actions. The EU Commission considers that a diversified approach is required, tailored to the different contexts, in which specific policy solutions are adapted to the different levels of development of available technologies and regional contexts, particularly as different technological solutions suit different sea basins. The Interreg Med BLUE DEAL project (BLUE DEAL, 2022) gives a broader interpretation of the energy transition as a complex process that mainly involves citizens, local communities, and stakeholders, which should be carefully supervised by local public authorities to ensure that the introduction of new technologies harmonizes with already existing economic activities, and that possible conflicts among different productive sectors are managed while complying with environmental legislation and integrated maritime policy (Bastianoni et al., 2020).

The major instrument to do this is to develop early Maritime Spatial Plans (MPSs) that identify suitable areas for the deployment of offshore energy farms (Soukissian et al., 2017). While several European countries in the Northern Seas have already implemented their own ocean planning that includes MES, mainly offshore wind, in the Southern Seas, such a process has been hindered by both technical difficulties and administrative and consent limitations (Pisacane et al., 2018). A recent review (Quero Garcia et al., 2020) compared the MSPs of Southern Countries and analyzed their impact on the Blue Energy (BE) sector: the authors found that Spain, Italy, Greece, and Malta have explicitly considered offshore renewables among their energy policies; nevertheless, a qualitative assessment of the progress of MSP with respect to BE in these countries still shows low and medium levels of development. The influence of national regulatory frameworks concerning MSP on the development of BE has been analyzed by Salvador et al. (2019) with a focus on Portugal. The authors highlight the importance of flexible planning systems, setting criteria for the prioritization of marine uses, incorporating trade-off mechanisms, and regulating pilot zones. These measures can help streamline licensing processes, avoid and resolve conflicts with other sea users, and adapt planning instruments to the rapid development of new BE technologies. Howells and Ramirez-Monsalve (2022) investigated the Danish approach to governing land-sea interactions, exploring the impacts of various institutional and procedural factors on the MSP practice. The authors notice a lack of integration between the maritime and terrestrial planning systems, which are differentiated in terms of institutional responsibility and scale, thus creating conflicts at the coastline. First, they recommend the cooperation of local authorities and experts to improve the governance and build consensus around decisions, especially if carried out at an earlier stage in the planning process. Second, they support the need to move toward marine planning processes at the regional or municipal level rather than purely national. Nevertheless, in this perspective, MSP practices still look immature. Kyvelou (2017) argued that improved governance and capacity building is necessary considering that there are no generalized solutions and that each managed area requires a customized and specialized design approach. Geographically explicit examination of areas susceptible to change and suitable development locations is an essential part of any evidence-based planning and decision-making process. In this regard, González et al. (2020) reviewed available web mapping tools that can contribute to anticipating and avoiding land and marine-use conflicts, comparing planning alternatives, and forecasting the impacts of planning decisions. According to the authors, the value of spatial data exploration is to support analytical planning practices through robust, systematic, and consistent means, assuring transparent and informed decisions.

Considering the increasing demand for multiuse of marine space, at least between uses that show reasonable compatibility, Kyriazi et al. (2016) mentioned several parameters to consider, starting from the involvement of players affected by the decision-making process. In general, to guarantee an efficient, fair, and acceptable spatial coexistence, parties interested in the same area should negotiate the terms of co-use (Grip and Blomqvist, 2021; Moodie and Sielker, 2022). Therefore, maximizing spatial efficiency and minimizing conflicts of use should not be seen as one-off management decisions but as a dynamic integrated MSP process that needs to respond to actual developments in the use of marine space. Stakeholder processes in MSP and their effects are interpreted as crucial actions (Twomey and O'Mahony, 2019; Zaucha and Kreiner, 2021) to encourage ownership of the plan, engendering trust among stakeholders and decision-makers; improve understanding of the complexity (spatial, temporal) and human influences of the marine management area; develop a mutual and shared understanding about the problems and challenges, as well as perceptions and interests

that stimulate the integration of policies; examine existing and potential compatibility and/or conflicts of multiple-use objectives; aid the generation of new options and solutions that may not have been considered individually; and expand the capacity of the planning team, in particular by acquiring new information.

Therefore, a set of gaps emerge from the literature on MSP, not yet properly solved. The main improvements and recommendations concern the release of specifically addressed regulatory frameworks; the resolution of conflicts between responsible institutions, especially due to different sectors and spatial scales of competence; the development of regional and local planning practices rather than national; the need for capacity building and informed design practices, particularly taking advantage of available web tools to address choices; and the stakeholders' engagement to guarantee transparent, fair, and widely shared decision-making, especially regarding the coexistence of marine uses. This is particularly true looking at the growing interest in MES, especially in the offshore wind sector. Due to the different maturity levels of BE technologies, with some of them still at an early stage of technical development, their inclusion in MSP requires the definition of a proper planning methodology, which is able, through scientific and technological skills, to fill knowledge gaps and promote the inclusion of these technologies in future energy plans.

How can MSP strategies consider MES and embed BE technologies to support their deployment? The present study shows a systematic procedure of BE planning to identify suitable sites for different BE plants; determine their possible location and size against environmental, physical, legal, or social constraints; evaluate potential effects in terms of energy production and carbon emission mitigation; and visualize possible configurations in relation to coastal landscapes. The BE planning framework involves multidisciplinary experts and exploits available web tools to address choices as part of MSP in regional and local contexts; it has been demonstrated in three workshops, namely, BLUE DEAL Labs (BLUE DEAL, 2022) in Crete (Greece), Split (Croatia), and Larnaca (Cyprus). The procedure has been conceived as a practical guide to start and support new MSP initiatives, including MES, to hypothesize possible scenarios for further integration of BE plants, discuss limits and opportunities, and foster public–private cooperation for BE deployment in Mediterranean regions by engaging public authorities, businesses, and citizens in participative design processes. Rather than being definitive or exhaustive, results concern reliable scenarios and allow for bringing a set of solutions to the table and leading the discussion toward concrete questions, instead of hypothetical purposes, to attract interest from a wide number of audiences and players and raise awareness of specific themes. Based on the BE planning action, the Labs are intended as kick-off initiatives to start a proactive debate around MES in target regions.

MATERIALS AND METHODS

The BE planning framework presented here combines interdisciplinary knowledge to integrate BE into strategic and operational plans in compliance with physical, regulatory, environmental, technical, and social constraints that necessarily emerge in the Mediterranean area. The planning procedure is structured into several iterative processes grouped into a sequence of six main stages: Stage 1—identification of BE potentials; Stage 2—identification of suitable BE technologies; Stage 3—identification of potential sites; Stage 4—energy assessment; Stage 5—carbon footprint mitigation assessment; and Stage 6—visual impact assessment (VIA). **Table 1** outlines the planning framework and the methodological stages, outputs, and used tools. The final outcome consists of a comprehensive BE plan with possible scenarios of BE deployment and quantitative estimates. The resulting maps and assessments aim to support the narrative and make the process easily understandable to a wide audience.

Necessary information for the implementation of the planning process is collected from sources at a regional or local level (e.g., government departments and agencies; other research projects; research and academia), if available, or otherwise taken from official databases at a national or EU level. More detailed data allow for more accurate elaboration, but general databases can be useful anyhow to draft coherent scenarios and start a proactive discussion on their feasibility and concrete implementation. Any outcome from the planning process can be further investigated, finetuned, and changed.

Identification of Blue Energy Potentials

Different tools can be used for the analysis of BE potentials in the Mediterranean, with different levels of accuracy (Stage 1). The MAESTRALE webgis (2018) provides access to open geographical data on BE potentials, including offshore wind, wave, tides, marine currents, and salinity gradients. It was first developed under the scope of the Interreg Med MAESTRALE project (MAESTRALE, 2019) to support researchers, decision-makers, and investors in setting the basis for the development of BE initiatives in the Mediterranean. From this general overview, it emerges that, in general, MES in the Mediterranean have lower potential with respect to the Northern Sea and the Atlantic ocean, but there is evidence of high availability that can eventually be exploited for profit. The highest potentials are those related to offshore wind and wave energy; marine currents are not intensive sources, except for specific hotspots in the Strait of Messina and Gibraltar, and tides are almost irrelevant; seawater thermal energy, salinity gradients, and marine biomass are valuable options in specific contextual circumstances.

The MAESTRALE webgis is a practical tool that can be used in Stage 3 of the procedure; nevertheless, besides this general overview of the Mediterranean basin, site-specific data, when available, are also necessary to investigate scenarios of BE installations at the regional and local levels making the analysis in Stage 4 more robust and exhaustive, especially concerning offshore wind and wave energy (Carillo et al., 2022). In particular, climatological atlases are the primary instrument to be used to establish whether a particular technology is worth being installed in a specific location or not. However, they can be enriched with complementary information from operational oceanographic models, which allow for the construction of long time series of high spatial and temporal resolution data characterizing MES in the Mediterranean. This

TABLE 1 | Stages of the BE planning framework, methodological approach, data sources and tools, and references for methodological insights.

Stage n	Action outcome	Methodological processes and references	Data sources and tools
Stage 1	Identification of BE potentials	Analysis of BE potentials, first at the Mediterranean scale and then at the regional scale, regarding different MES, including offshore wind, wave energy (more details in Carillo et al., 2022), and marine currents (more details in Napolitano et al., 2022)	MAESTRALE webgis Global wind atlas PRISMI tool WAVES tool MITo tool
Stage 2	Identification of suitable BE technologies	Literature and technical review of available BE technologies classified into different types per exploited MES, operational areas (onshore, near-shore, offshore), and technological solutions with details on size and basic requirements for installation	Dataset on BE technologies basic requirements (**Table 2**)
Stage 3	Identification of potential sites	GIS-based elaboration of maps through the combination, merging, and overlaying of geographical datasets (most relevant variables are listed in **Table 3**) with marine energy potentials and BE technological requirements. Once data are processed, eligible sites for the installation of each type of technology are identified by subtraction, detecting areas where good BE potentials combine with the absence of exclusion zones	Global wind atlas for offshore wind energy EMODnet for bathymetry, seabed habitats, and physics Natura 2000 for protected natural sites Marine vessel traffic for shipping routes Other site-specific open-access geodatabases locally available
Stage 4	Energy assessment	Energy modeling for the integration of the identified BE technologies in the electricity grid mix and estimated power. Considered variables concern current and forecasted annual energy production of planned BE plants and energy consumption in different sectors (more details in Stančin et al., 2022)	EnergyPLAN tool
Stage 5	Carbon footprint mitigation assessment	Assessment of avoided emission by replacing electricity from the national grid mix with electricity generated by planned BE plants. Values of the carbon intensity of electricity (CIE: g CO_2eq/kWh) are assessed based on the LCA of offshore floating wind turbines (more details in Pulselli et al., 2022) and WECs (more details in Bruno et al., 2022)	Life-cycle assessment (LCA) EEA European Environment Agency, 2022 for National CIE values
Stage 6	Visual impact assessment	Development of a digital visualization including 3D models of BE technologies and 3D terrain of surrounding sites. The latter takes elevation and texture data from Bing Maps API to create a terrain object in real-life dimensions. Data elaboration is performed to achieve the realism of landscape visualizations and faster rendering for the real-time interactive tool	Blender 3D computer graphics software toolset Real-world terrain and unity game engine

information is relevant for designing, tuning, and optimizing the production of different BE technologies in specific marine areas and for the planning of monitoring activities of any kind of device deployed at sea.

For assessing wind potentials, representative wind speed time series for the selected sites were established through the use of the PRISMI tool along with the data collected from open wind data (Global Wind Atlas, 2015). The PRISMI tool is based on the long-term MERRA data for defining the yearly and diurnal wind speed variations that are accordingly scaled against either measured or calculated yearly averaged values. The defined yearly time series are consequently transformed into wind power time series *via* a representative offshore wind turbine power curve.

For the assessment of wave energy potentials, the WAVES tool was used. It is based on the spectral model WAM (version 4.5.3) and implemented over the Mediterranean Sea with a spatial resolution of 1/32° (approximately 3.5 km). Forecast outputs are released hourly over a 5-day simulation and have been used to build a dataset of significant wave height, energy, peak period, and wave direction. The model is forced with winds produced by the SKIRON forecast model (Kallos, 1997) and has been validated over the years against *in situ* measurements (buoy data) and satellite data (Carillo et al., 2013; Carillo et al., 2014; Carillo et al., 2015). For the regions targeted in this study, a detailed statistical analysis of wave energy has been done, relying on the database constructed on the hourly outputs of the wave operational forecast system, daily operating since 2014 at the *ENEA* Climate and Impact Modeling Laboratory.

Similarly, the MITO tool is based on an innovative three-dimensional numerical model of marine circulation implemented in the Mediterranean (Napolitano et al., 2022) and Black Seas; it includes the main tidal effects, both produced by local forcing and coming from the Atlantic boundary (Palma et al., 2020) with a horizontal detail of 1/48° (about 2 km)—twice as high as the current operating models available of the Mediterranean (CMEMS-Copernicus)—which increases further up to a few hundred meters, in the region of the Strait of Gibraltar and the Strait of the Dardanelles. Looking at the mean kinetic energy related to currents along the entire Mediterranean basin, marine currents are not a valuable source of energy, but a few hotspots for energy harvesting can be identified anyhow. The Messina strait and Gibraltar strait are the areas with the highest energy potential of marine currents in the Mediterranean.

Identification of Suitable Blue Energy Technologies

The energy potential analysis from marine sources above (Stage 1) allows understanding the most promising options in the

TABLE 2 | Technical requirements of BE technologies.

Location	BE technology	Requirements	Estimated electricity production	References
Onshore	**Wave energy converter (WEC)**			
	Oscillating Water Column (OWC)	***Physical requirements***	250–500 MWh/yr per unit	Arena et al. (2013)
		Wave height: 0.5–3.5 m		
		Bathymetry: 2.5–15 m		Curto et al. (2021)
		Size unit (16–24 devices)		Falcão and Henriques (2016)
		N° chambers: 16–24 (4–6 m in length each)		Faÿ et al. (2020)
		Emerged height: 7–10 m		Ibarra-Berastegi et al. (2018), Ibarra-Berastegi et al. (2021)
		Submerged height: 2.5–15 m		Malara et al. (2017)
		Width: 2–6 m		Spanos et al. (2018)
		Pier length: 100 m		
	Overtopping Breakwater	***Physical requirements***	200–250 MWh/yr per unit	Buccino et al. (2016)
		Wave energy power: 2.5 kW/m		Contestabile et al. (2016)
		Bathymetry: 2–10 m		Contestabile et al. (2017)
		Size unit (20 devices)		Patrizi et al. (2019)
		N° modules: 20		
		Height: 3–5 m		
		Width: 8–15 m		
		Pier length: 100 m		
	Oscillating Floaters	***Physical requirements***	200–800 MWh/yr per unit	Curto et al. (2021)
		Wave height: 0.5–3 m		EWP Eco Wave Power (2019), EWP Eco Wave Power (2022)
		Wave power: 1–9 kW/m		Marchesi et al. (2020)
		Size unit (15 devices)		Negri and Malavasi (2018)
		N° floater: 15		Tethys (2022)
		Floater width: 2–5 m		
		Floater length: 4–6 m		
		Arm length: 4–10 m		
		Interaxle spacing: ~3 m		
		Pier length: 100 m		
Onshore	**Osmotic gradient converter**			
	Reverse Electro Dialysis (RED)	***Physical requirements***	~3 MWh/yr per unit	Tedesco et al., 2015; Tedesco et al., 2016, Tedesco et al., 2017
		NaCl solution: 0.7–215 mS/cm		
		Flow rate: 16–38 l/min		
		Size unit (1 device)		
		Building surface area: 20 m^2		
		Stacks volume: ~1.5 m^3		
		Cell surface area: 400 m^2		
Onshore	**Heat exchangers**			
	Seawater heat pump	***Physical requirements***	—	Stival (2014)
		Low seasonal temperature oscillation		Xuejing et al. (2014)
		Accessible intake of seawater (direct intake or a well)		ENERCOAST (2014)
		Size unit (1 device)		MAESTRALE (2019)
		Intake distance from the shore: 10–100 m		Nordic Heat Pump (2017)
		Suction depth: at least 10 m, intake elevated from the sea surface		
Nearshore	**Wave energy converter (WEC)**			
	Seabed-based Buoy	***Physical requirements***	40–60 MWh/yr per unit	Babarit et al. (2012)
		Minimum wave height: 0.5 m		Bozzi et al. (2013, 2018)
		Bathymetry: ≤ 25 m		Chatzigiannakou et al. (2015), Chatzigiannakou et al. (2017)
		Size unit (1 device)		Rémouit et al. (2018)
		Minimum buoy distance: 25 m		Strömstedt et al. (2012)
		Height cylinder: 3.5–7 m		
		Height buoy: 1.5–2.5 m		
		Width: 3–5 m		

(Continued on following page)

TABLE 2 | (*Continued*) Technical requirements of BE technologies.

Location	BE technology	Requirements	Estimated electricity production	References
Nearshore	**Marine biomass treatment**			
	Algae farm	***Physical requirements***	470–2,260 m^3 methane per unit	Barbot et al. (2016)
		Seaweed: green macroalgae	2,200–4,700 kg ethanol per unit	Bastianoni et al. (2008)
		Bathymetry: SL—15 m		Migliore et al. (2012)
		Size unit (1 farm)		Offei et al. (2018)
		Length of headline: 220 m		Seghetta et al. (2016)
		Height of U-shaped seeded line: 2.5 m		
Offshore	**Wave energy converter (WEC)**			
	Oscillating Buoy	***Physical requirements***	12–250 MWh/yr per unit	Bonfanti et al. (2020)
		Minimum wave height: <1–1.6 m		Bozzi et al. (2013), Bozzi et al. (2018)
		Bathymetry: 35–50 m		Mattiazzo (2019)
		Size unit (1 device)		Vannucchi & Cappietti (2016)
		Distance: > 30 m		
		Width: 5–8 m		
	Oscillating attenuator	***Physical requirements***	20–53 MWh/yr per unit	Bozzi et al. (2018)
		Wave energy: 3.5–5 kW/m		Parker et al. (2007)
		Wave height: 0.5–2.5 m		Thomson et al. (2011), Thomson et al. (2019)
		Bathymetry: 50–100 m		Vannucchi & Cappietti (2016)
		Size unit (1 device)		SWEL Sea Wave Energy Ltd. (2022)
		Length: 30–120 m		
		Diameter: 0.9–3.5 m		
Offshore	**Marine currents converter**			
	Underwater Helix	***Physical requirements***	300 MWh/yr per unit	Coiro et al. (2013), Coiro et al. (2017), Coiro et al. (2018)
		Current speed: 1.5–4.5 m/s		Seapower scrl (2022)
		Bathymetry: 9.8–15 m		
		Size unit (1 device)		
		Height: 5.2 m		
		Width: 10.4 m		
		Width (three-blade) rotor: 3 m		
Offshore	**Wind energy converter**			
	Offshore floating wind	***Physical requirements***	10–25 GWh/yr per unit	Chipindula et al. (2018)
		Mean wind speed: 3–7 m/s		Pantusa et al. (2020)
		Bathymetry: 50–500 m		Pantusa and Tomasicchio (2019)
		Distance from the coast: > 5 Miles		Poujol et al. (2020)
		Size unit (1 device)		Raadal et al. (2014)
		Hub heights: 80–140 m		Tsai et al. (2016)
		Rotor diameter: 110–150 m		Weinzettel et al. (2009)
		N° blades: 3		

Mediterranean Sea for implementing BE technologies. Stage 2 is based on a survey of available BE technologies classified into different types, depending on the MES exploited, operational areas (onshore, near-shore, offshore), and technological solutions referring to the physical principle exploited. The observation of available BE technologies allowed for identifying the main characteristics to inform the planning process, such as nominal power, size, basic requirements for installation, and technology readiness level.

Offshore wind turbines are the best-known technology available in terms of production yields and technology readiness level. They are classified into two main categories: bottom-fixed and floating windmills. Wave Energy Converters (WECs) are promising solutions to harvest wave energy; their three main categories include Oscillating Water Column (OWC), Overtopping Breakwater Systems (OBS), and Floating Buoy Systems (FBS). Moreover, WECs are classified into onshore devices fixed on piers and docks or other coastal infrastructures; near-shore, including oscillating buoys connected to generators fixed on the seabed; and offshore, including buoys taken by a mooring system. Other BE technologies include biorefineries for biofuel or biogas production from marine biomass, Reverse Electro Dialysis (RED) to exploit salinity gradients combined with desalinating plants and underwater turbines exploiting marine currents in very specific locations. Seawater-based heat exchange combined with heat pumps for climate conditioning of buildings is among the most mature BE technologies.

TABLE 3 | Types of data needed for BE planning.

Required data	Description and notes
Bathymetry	Map of sea depths, preferably with bathymetry lines every 20 m
Wind speed	Map(s) displaying information on wind speed at a national/regional scale
Navigation routes	Map(s) showing the position and layout of harbor approach routes and navigation routes, including the buffer zone (exclusion zone) around them where the installation of BE plants is not allowed
Birds migration routes	Map(s) showing the paths of the migration of birds at the Mediterranean and/or a national/regional scale
Aquaculture areas	Map(s) showing the position and boundaries of aquaculture farms
Strategic infrastructure—1	Map(s) showing the locations of facilities close to the sea, such as business hubs, ports and marinas, waterfronts, large hotels/tourist resorts
Strategic infrastructure—2	Map(s) showing the locations of facilities close to the sea, such as desalination plants (if existing) and sewage/wastewater treatment plants
Protected natural and landscape areas	Map(s) including the perimeters/boundaries of natural protected areas (both marine and terrestrial): Natura 2000 areas, national and regional parks, areas of landscape protection, etc. Information on the level of protection (total, partial, etc.).
Posidonia oceanica distribution	Maps of the distribution and boundaries of *Posidonia oceanica* meadows along the coast and in the marine waters
Sea waves	Maps displaying graphical information on wave height, direction, and frequency at a national/regional scale
Altimetry	Map of contours on land in the study area (and especially of the coastal area), with curves as close as possible

In **Table 2**, basic requirements have been determined per each type of technology based on data from the literature or private companies, concerning the size of devices, distance from the shore, distance from devices, water depth, relevant physical or legal constraints, optimal working regime (e.g., minimum wind speed or wave high), and mean potential production yields.

Identification of Potential Sites

The identification of sites suitable for the installation of BE plants is a GIS-based procedure that entails the production of maps through the combination, merging, and overlaying of relevant geographical datasets (Stage 3). It starts from the combination of data concerning BE potentials (Stage 1) and the basic requirements of BE technologies (Stage 2) (i.e., technical and environmental conditions, such as sea depth, wave height, and wind speed) needed to ensure their operability. This allows for identifying marine and coastal areas that, fulfilling such conditions, are theoretically suitable for their installation.

This procedure also introduces additional variables corresponding to supplementary datasets and GIS layers, which contribute to determining zones with physical or legal restrictions. The objective is twofold: on the one hand, to minimize the disturbance of environmentally sensitive areas and the interference with other maritime activities and, on the other hand, to assess the presence of coastal infrastructure (i.e., buildings and other facilities) that can host/incorporate BE systems and/or consume the energy produced.

The additional variables introduced belong to three main categories: 1) environmentally sensitive areas: protected natural areas (both marine and terrestrial), reserves, and sensitive marine ecosystems (such as Posidonia meadows); 2) spatial footprint of other maritime activities: navigation routes, ports and ships' maneuvering areas, military areas, aquaculture plants; and 3) large energy consumers along the coast (desalination plants, public buildings, large hotels, and tourist resorts, etc.). A short checklist of the most relevant variables used in this analysis is shown in **Table 3** and corresponds to the datasets to be provided for each target area.

All groups of datasets undergo the same processing, albeit with some adjustment depending on the energy source considered (wind and waves) and on the distance from shore of the BE technology analyzed (onshore, near-shore, or offshore). The basic steps are the following:

a. Matching the map of marine energy potentials relevant to the specific BE technologies considered (e.g., wind speed, wave height, and wave power) with the minimum requirements for these technologies to operate efficiently, including water depth (bathymetry map);
b. Uniting the boundaries of environmentally sensitive areas, thus producing a map of ecological constraints;
c. Uniting the tracks of the main navigation routes with the boundaries of ports, marinas, and ships maneuvering areas and/or military areas to avoid interferences;
d. Mapping aquaculture farms to avoid interferences and identify possible synergies (i.e., collection of marine biomass for energy purposes) and/or potential BE consumers;
e. Mapping desalination plants (to eventually host BE systems based on salinity gradient) and wastewater treatment plants (to incorporate algae cultivations for energy purposes).

Overlapping and union of the maps resulting from steps *b* to *d* determine the exclusion areas, that is, areas unsuitable for the installation of the type of technology considered. Buffer areas around them are also excluded, their size depending on international and national laws and the type of technology considered.

When datasets are available, these results are further refined by producing additional maps of the following:

- Coastal public/private infrastructure with intense energy use, as potential developers of BE systems for energy self-consumption;
- Tourist infrastructure (diving centers, etc.) to avoid interference with;
- Bird migration routes, essential to identify unsuitable areas for offshore wind turbines;

TABLE 4 | Data input for energy planning in the case of Crete.

Type of data	Units
Annual electric demand	3.22 TWh
Annual electric heating and cooling demand	0.53 TWh
Other fuel types used for heating on an annual basis	**TWh**
• Biomass	0.23
• Diesel	0.33
• Solar thermal	0.20
• Solar thermal	0.10
Transmission lines capacities and interconnections	1,400 MW
Installed power plant and renewable capacities and annual energy generation	**MW/TWh**
• Thermal power plants	820/2.44
• PV	96/0.16
• Onshore wind	203/0.51
• Small hydro	0.3/—
Fuel consumption in the industry sector	**TWh**
• LPG	0.10
• Diesel	0.10
• Biomass	0.29
• Heating oil	0.10
• Gasoline	0.01
Planned additional renewable capacities	**MW**
• PV	240
• Onshore wind	240
• Offshore wind	300

Bold represents the unit of the following list of values.

- Submarine archaeological sites to avoid interference with cultural heritage.

Data collection involves local stakeholders and institutions that are more likely to possess detailed and up-to-date information: public authorities (at the national, regional, and local levels) in charge of spatial planning, energy planning and environmental protection, port authorities, universities and research centers, and environmental associations. In order to speed up the process, data are required in formats (shp, geoJSON, geoTIFF, gdb, and spatialite) that can be easily treated even by open-source GIS software.

Once the data are processed, the marine areas eligible for the installation of each type of technology can be identified by subtraction, detecting the areas where a good BE potential combines with the absence of exclusion zones. The procedure ends with a further selection of the eligible areas with the highest energy potential, finally proposed as "pilot areas."

It is worth stressing the preliminary and indicative nature of these results: further in-depth analysis is needed (at a smaller scale and considering site-specific restrictions from the environmental and legal standpoint) to verify the eligibility of the chosen sites. Moreover, energy potential analysis should be further refined because the range values used as a starting point only represent the minimum requirements for each type of technology and not the optimal ones for a specific device.

Assessment of the Energy Production of the Blue Energy Plans

Once available sites for the installation of BE plants have been identified (Stage 3), effective energy production can be estimated considering site-specific and operational energy system characteristics (Stage 4). Therefore, a specific energy modeling for the integration of BE in the regional energy system is developed (Stančin et al., 2022 for details). In the first place, this is related to the annual energy demand for power generation, residential, industry, and transport sectors. Moreover, it is necessary to include in the analysis all the energy sources, baseload, and intermittency to investigate their interaction and identify potential spots that might disrupt system stability. The latter concerns the capability of the existing grid to integrate electricity generated by intermittent renewable sources, such as BE.

Through the EnergyPLAN tool, the energy modeling for evaluating the integration of the identified BE technologies in the electricity mix considers a set of variables that covers the current and forecasted annual energy production and consumption in all considered sectors. The modeling is performed on an hourly basis for an average 1-year period (long-term time-series data provided in Stage 1), which allows for the identification of peak loads, a lack or excess in electricity production from renewables, energy imports and exports, and spots for better inter-sectoral integration.

First, a reference scenario of the energy system is determined and validated based on the available data from statistics or grid operators, which is done using the data in **Table 4**. Then, existing energy strategies are checked to identify future system capacities and energy demand. These strategies and plans serve as a backbone for building up different scenarios in which BE are included. Finally, the scenario that shows the most promising renewable energy potential and does not express disruptions with the inclusion of BE is chosen for further analysis to determine an optimal size for BE devices such as offshore wind farms (OWFs) and WECs.

TABLE 5 | Carbon footprint mitigation effect of BE plans.

	Data	CIE	CF
	TWh/year	kg CO_2eq/KWh	t CO_2eq/year
Crete			
Reference scenario: current electricity demand from the grid	3.22	0.479	1,542,380
Transition scenario: electricity by offshore wind farm	1.17	0.029	33,930
Transition scenario: residual electricity from the grid	2.05	0.479	981,950
Transition scenario	3.22	**0.315**	**1,015,880**
Avoided GHG emission		–34.1%	–526,500
Croatia			
Reference scenario: current electricity demand from the grid	19	0.134	2,546,000
Transition scenario: electricity by offshore wind farm	4.35	0.047	204,450
Transition scenario: residual electricity from the grid	14.65	0.134	1,963,100
Transition scenario	19	**0.114**	**2,167,550**
Avoided GHG emission		–14.9%	–378,450
Cyprus			
Reference scenario: current electricity demand from the grid	4.6	0.621	2,856,600
Transition scenario: electricity by offshore wind farm	0.5	0.071	35,500
Transition scenario: electricity by WECs	0.001	0.126	126
Transition scenario: residual electricity from the grid	4.099	0.621	2,545,479
Transition scenario	4.6	**0.561**	**2,581,105**
Avoided GHG emission		–9.6%	–275,495

Bold values are the results of the assessment.

Assessment of the Carbon Footprint Mitigation Effect of the Blue Energy Plan

Based on the estimate of energy production from MES in selected scenarios, the reduction of GHG emissions in the studied areas is assessed to highlight how BE can contribute to the European goal of carbon neutrality (Stage 5). The values of the carbon intensity of electricity (CIE: g CO_2eq/kWh) are used to assess the avoided emission due to the replacement of electricity from the national grid mix (Pulselli et al., 2018) with electricity generated by OWFs and WECs. The first has been assessed by Pulselli et al. (2022) based on a life-cycle assessment (LCA) of floating wind mills, including the phases of manufacturing, installation, maintenance, and end of life. Results show different intervals of values in Crete, Croatia, and Cyprus depending on the different site-specific wind energy potentials and two different floating wind turbines: spar buoy and raft buoy. The latter was assessed by Bruno et al. (2022) based on the life-cycle assessment of various devices: onshore fixed floating buoys (i.e., 93–372 g CO_2eq/kWh) and near-shore buoys (i.e., 101–151 g CO_2eq/kWh). **Table 5** shows values of CIE for the national grid mix in Crete, Croatia, and Cyprus (EEA European Environment Agency, 2022), for OWFs and WECs (taking interval values for both onshore and near-shore devices).

Assessment of the Visual Impact of the Blue Energy Plan

Tools for 3D modeling and virtual touring have been used to visualize the installations forecasted in BE plans, involve the stakeholders engaged in BLUE DEAL Labs, and stimulate discussions, contributing to a more open, transparent, and inclusive planning process (Stage 6). The simulated virtual environments have been created to show the characteristics of selected BE technologies and their interaction with the landscape, considering the physical and infrastructural configurations of shores and the most relevant viewpoints along the coast. These allowed introducing elements of VIA as a systematic analysis of potential impacts to landscapes.

The VIA takes inspiration from a set of references. Molina-Ruiz et al. (2011) predicted and evaluated, before construction, the visual impact of wind farms placed on mountains from different observation points; a Digital Elevation Model (DEM) with a 20 m retail was produced for an area and transformed into Triangulated Irregular Network (TIN) by way of 3D ArcGIS Analyst to create the 3D terrain and 50 m high cones, with 20 m of diameter, placed to simulate the wind turbines in photographs. Molnarova et al. (2012) used a set of 18 photographs (with a basic focal length of 50 mm) that included landscapes of varying aesthetic value in the Czech Republic, with and without wind turbines. These were included in questionnaires, and respondents were asked to evaluate the aesthetic value of the landscapes. Takacs and Goulden (2019) used photomontage to add turbines on a photograph of a landscape for VIA and noticed that camera lens focal length affects the perception of the scale of wind turbines; results show that panoramic photomontages are perceived as the least accurate, whereas images taken at 75 mm focal length in full-frame format are perceived as the most accurate form of representation of the scale and visual impact of wind turbines focal length. Maslov et al. (2017) developed a methodology to assess the degree of visibility of an offshore wind farm from an observer located along the coast; an index of horizon occupation was determined by considering the projection of several distinguishable turbines (installed in Saint-Nazaire in Northwest France) on a plane perpendicular to the sight direction. Sklenickaa and Zouhar (2018) evaluated public visual preferences using photos taken on days with clear weather conditions using a digital camera with a focal length of 50 mm and a tripod set to a height of approximately

170 cm (an "adult man's eye view"). A wind farm was digitally added with 10 wind turbines into each photo. Kokologos et al. (2014) showcased a realistic 3D simulation of a study area before and after construction by importing orthophotomaps, which, together with field observation of the area, allowed the simulation of elements such as trees and houses; finally, wind turbines were designed and imported in the 3D model at their exact dimensions.

In this study, the composition of a wind park scenery uses two basic elements: the various 3D models of BE technologies and the 3D terrain of the surrounding site. Blender 3D computer graphics software toolset has been used to manually design each technology model based on images. All the 3D terrains were created inside the Unity Game Engine using the real-world terrain asset. This asset uses elevation and texture data from Bing Maps API to create a terrain object in real-life dimensions. An API key can be issued from the Bing Maps Dev Center. Then, a high spatial resolution is used for the terrain near the installed technologies and a lower one for the terrain that is visible but not near to achieving both realism and faster rendering, especially for the real-time interactive tool.

The activity of visualizing BE devices and plants in a realistic environment was realized through an online interactive tool developed to increase the engagement of stakeholders participating in the planning process. To allow replicability of this "experience," an open-access tool for 3D visualization of BE technologies in real contexts has been provided, including interactive elements for gamification that can also contribute to increasing the engagement level. A game engine was selected to allow users to interact with the scene, go around, see how technologies function, and simulate the scenery from every angle and location the viewer could choose. To enhance realism in user experience, Ceto Ocean System has been used to simulate the sea in the scene, and objects were given physics rules such as buoyancy, which is available in the Ceto package, and gravity, which is available in Unity. Accuracy of the location of the installed technologies is achieved by loading and aligning the GIS software analysis layers (Stage 3) as an image depicting the eligible area of each technology on top of the Unity terrain area. During the design phase, a grid available in Unity's scene environment is used to assure that every technology has the right dimensions and sets the correct distance between objects. Full atmospheric visibility is assumed in all scenarios, and all objects further than a predefined distance from the camera plane are clipped (50 km for the wind turbines scene, 25 km for the rest). The project has been exported into a WEBGL format to be integrated into the web platform and be easily accessible by anyone. The Earth curvature effect was also implemented in the developed tool, especially for scenarios with turbines placed far from shore (the cases of Croatia and Cyprus). Due to the curvature of the Earth, objects placed further than the horizon, for a specific observation point, tend to have their lower part obscured. The height of the obscured part of the object was calculated in real time, and this phenomenon was simulated in Unity according to the altitude of the camera and the distance of the arc between the camera and any object.

RESULTS

The BE planning framework has been tested and demonstrated in three case study areas. Although not exhaustive, outcomes from the planning process show the basic ingredients of a comprehensive BE plan to inform and address the next MSP initiatives in the area. The general information on MES potentials (Stage 1) and BE technologies (Stage 2) is followed by a site-specific analysis and proposal, showing selected marine areas (Stage 3), potential energy production and integration within the regional energy system (Stage 4), potential effects of mitigation of carbon emissions (Stage 5), and hypothetical views of installed BE plants in specific sites with proper infrastructures and landscape (Stage 6). In particular, the analyses presented here have focused on offshore wind and wave energy, considered the most promising MES.

Blue Energy Plan in Crete

In Crete, the identification of eligible and possible pilot sites started from the definition of main variables and the check of available data. The analysis of BE potentials (Stage 1) has been built on geographical datasets from the MAESTRALE webgis integrated into the GIS-based procedure. Technological requirements then allowed for mapping suitable areas per each type of BE technology (Stage 2). Coherently with technical requirements in **Table 2**, some assumptions derived from a preliminary consultation with local stakeholders: for OWFs, the distance from the coast was considered from 5 to 80 km, given that wire connection would not be cost-effective beyond that limit; for WECs, a maximum bathymetric depth of 100 m limited the field within 20 km from the shore. After matching the map of BE potentials with that representing the operational requirements of each technology, the analysis was restricted to five types of BE technologies, more suitable for installation in the target region: offshore floating wind turbines and the following WECs: OWC, oscillating floaters, Seabed-based buoys, and oscillating buoys.

The exclusion zones concern the boundaries of areas of high ecological value (sites included in the Natura2000 network, Greek protected areas classified as GEA/GEN/GEETHA Areas, and Posidonia meadows) and areas interested by navigation routes and ports assuming a buffer zone ranging from 0.5 to 5 km depending on the type of technology. For inclusion in the GIS-based procedure, open data have been downloaded from a set of web portals regarding offshore wind energy potential (Global Wind Atlas, 2015); bathymetry, seabed habitats, and ocean physics (EMODnet, 2021); sites belonging to the Natura 2000 network (Natura 2000); shipping routes (Marine Vessel Traffic, 2017) and bird migration routes (Hellenic Ornithological Society, 1982); site-specific basic maps and open-access geodata (Geofabrik, 2007; Greek Government Geodata, 2018; Greek Ministry of Maritime Affairs, 2020).

The combination of the energy potential maps and the exclusion zones derived from the analysis led to the identification, by subtraction, of the eligible areas and the two most appropriate pilot sites for each type of technology (Stage 3). **Figure 1** shows the sequence of variables made spatially explicit

FIGURE 1 | Sequence of maps showing the process for the identification of potential sites for the installation of offshore wind turbines in Crete: a. Combination of bathymetry (50–400 m) and wind speed (>4 m/s); b. Exclusion zones: the union of areas with high ecological value (2 km buffer zone), main navigation routes, and maneuvering areas of ports (5 km buffer zone); c. Eligible areas (in light red) from the combination of the two previous maps and pilot sites (optimal wind speed ≥7 m/s at 100 m above sea level).

and overlaid to determine exclusion zones and identify the most suitable sites for the installation of BE plants.

Figure 2 summarizes the results achieved for all the considered technologies. It is worth mentioning that the optimal pilot areas for the installation of offshore wind turbines (e.g., with wind speed ≥7 m/s at 100 m above sea level) are located off both the eastern and western extremities of Crete Island, whereas potential sites for WECs are concentrated along its southern coastline.

Being the BE planning an iterative process, additional observations have determined further restrictions, especially concerning the installation of WECs. An assessment of wave resources has been made in specific locations in the Cretan Sea based on the dataset built on the hourly outputs of the wave operational forecast system at the ENEA Climate and Impact Modeling Laboratory (Stage 1).

Figure 3 shows the map of the yearly mean value of the significant wave height, computed over the whole period of

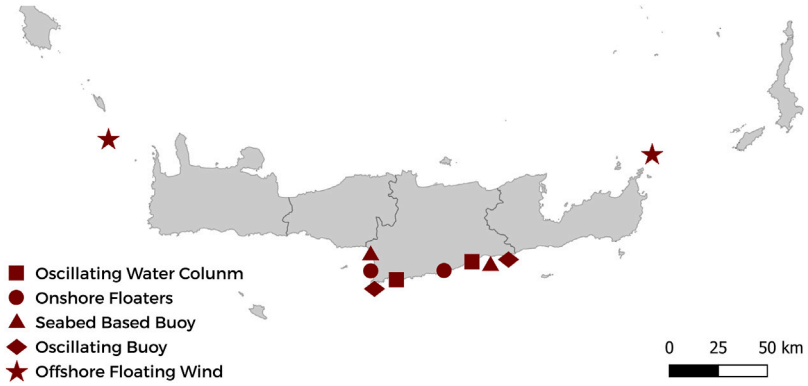

FIGURE 2 | Synthetic map with the identified potential pilot areas for the installation of wind and wave energy plants in Crete.

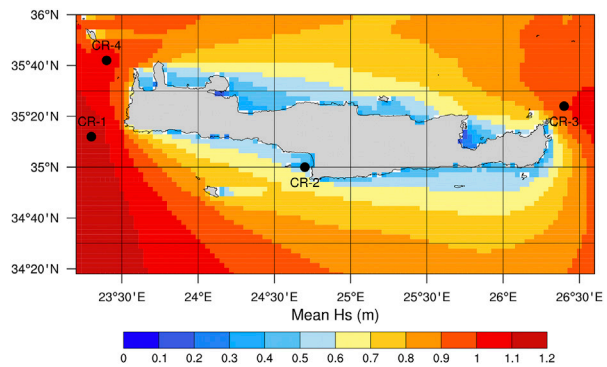

FIGURE 3 | Mean wave height Hs (m) over the period 2014–2020. Dots indicate locations monitored in detail.

2014–2020. The mean value of the significant wave height (Hs) in this subdomain ranges from 0.5 to 1.2 m. The westernmost zone of Crete Island is the most productive, as it is exposed to the waves propagating from the Ionian Sea and those generated by the northerly winds. Also, the eastern part of the island is characterized by waves exceeding 1 m in height on average and can be considered eligible for wave energy harvesting. The black dots in the figure show the sites for which a more detailed analysis has been done: CR-1 has been selected as an example of a location, on the western flank of the Crete Island, with high wave potential; CR-2 instead had been selected through the BE-planning approach for wave energy devices applied to the Heraklion county; and CR-3 and CR-4 correspond to the locations identified as suitable for the installation of WECs. For each location, the distribution of yearly average energy in terms of the mean period (Te) and of Hs has been evaluated over 7 years simulation period. Contribution to the total energy given by individual sea states is lumped together in 0.25 s intervals of Te and 0.25 m intervals of Hs. Wave power contributions of individual 1 h sea states obtained from the model output are calculated using the power equation. **Table 6** summarizes the mean power and the yearly average for each point together with the bathymetric depth among the variables mentioned in the technology requirements.

As a result, the CR-2 location, a representative for most of the sites identified through the mapping procedure, does not show exploitable potential. The most energetic site is CR-1. The sites CR-3 and CR-4 are also suitable for the installation of offshore WECs. Nevertheless, the bathymetric values do not allow for a favorable and cost-effective installation at the moment, except for the eventual integration of WECs in the structure of floating wind farms.

Stančin et al. (2022) demonstrated how different scenarios for integrating BE plants into the energy system of the study areas are examined by determining the electricity production and their share in the electricity production mix (Stage 4). Precisely, four different scenarios were considered for the case of Crete, starting from the Referent scenario: the transition scenario concerns 300 MW of offshore wind with 400 MW of interconnection capacity to the mainland; the BE scenario considers the complete phase-out of thermal power plants and the interconnection with the mainland in full capacity of 1,400 MW. Finally, the renewable scenario implies an additional 480 MW of installed capacities, equally divided between PV and onshore wind. The information about the maximum potential of 480 MW of additional renewables that can be integrated is directly obtained by the system distributor. Because the National Energy Strategy implies PV and wind as the backbone of the decarbonized energy system, the maximum potential is distributed as explained above.

This analysis showed that the maximum production from OWFs of 300 MW of installed capacity is 1.17 TWh per year, with an average load factor of 41%. Therefore, in the case of the transition scenario where thermal power plants are still operating, and there is interconnection to the mainland, the offshore wind farm allows for a reduction of oil for power generation by more than 1 TWh on an annual basis. Furthermore, with the installation of additional renewable capacities in PV and onshore wind, the production of electricity on the island can cover up to more than 70% of annual demand. The rest of the electricity demand is met by importing from the mainland through the interconnector, of which 25% of nominal capacity

TABLE 6 | Mean wave energy for the selected points around Crete.

Site	Bathymetric depth	Mean power (kW/m)	Annual mean (MWh/m)
CR-1	2,200	5.85	51.25
CR-2	48	0.82	7.22
CR-3	387	3.80	33.33
CR-4	404	5.32	46.56

is continuously used for grid balancing. Besides, a significant amount of production excess can be exported to the mainland, which improves the wind farm economics. Finally, a complete phase-out of the thermal power plant can achieve savings of 6.4 TWh in terms of heating oil consumption. Better intersectoral integration, especially electrification of transport, heating, and industry sectors, could allow for even greater penetration of the MES, especially of offshore wind, which also shows good potential on the west side of the island.

This analysis is then further developed with an assessment of how the integration of BE technologies can result in a reduction of greenhouse gas (GHG) emissions and support the goal of a carbon-neutral energy system through carbon footprint and life-cycle assessment evaluations (Stage 5). In the reference scenario for Crete, electricity (3.22 TWh demand per year) is assumed as taken from the grid (479 g CO_2eq/kWh), and the corresponding greenhouse gas emission is, therefore, 1,542,380 t CO_2eq/year. The 1.17 TWh (36%) per year produced by the offshore wind farm (average 29 g CO_2eq/kWh of carbon intensity) in the transition scenario would decrease the emission to 1,015,880 t CO_2eq/year with 526,500 t CO_2eq/year of avoided emission (−34%). The new value for CIE of the grid mix would decrease to 315 g CO_2eq/kWh (**Table 5**).

The interactive visual tool developed during the Crete BLUE DEAL Lab (Bluedealmed visual-too-Cyprus, 2022) contains a fully 3D virtual world where the user can navigate and look at the BE plants with location and size determined in Stage 3 and Stage 4, respectively. The selected area for the offshore wind farm in Crete is localized to the northeast of the island, as shown in **Figure 1** and **Figure 2**; this has been modeled for 3D visualization. When the interactive visual tool is loaded, on the top right of the user interface, three buttons allow the user to navigate the area (**Figure 4**) using a drone or a boat and obtain a view from shore. Using the drone camera, the user can go anywhere in the environment, even underwater, which is very helpful to see parts of the submerged technologies. With the use of direction keys (ASDW keys), the user can navigate, control vehicle speed, and rotate the viewing camera. The user can freely navigate the different locations and technologies using the top-left dropdown menu. On the bottom right, a virtual map depicts the current location. Selecting the map allows viewing the whole area. A compass is also available on screen to help the viewer with the scene orientation. The settings button on the bottom left lets the users set the graphics quality, monitor frames per second, and adjust the wind levels, which simulates waves, particularly useful when observing buoys. Advised graphics quality is set to at least 25 frames per second for a better and smooth experience.

Blue Energy Plan in Croatia

Similarly, results have been obtained in two other locations: the marine areas of Split (Croatia) and Larnaca (Cyprus).

In Croatia, the process for the identification of pilot sites regarded the marine area of the Split-Dalmatia County and, in particular, the internal waters and territorial seas, thus excluding international waters (farther than 12 nautical miles from the coastline) whose energy exploitation could imply additional permitting issues. Moreover, for offshore wind energy, only areas more than 10 km from the coast were considered to avoid visual impact (and hence potential public acceptance issues) in an area rich in small islands and strongly devoted to tourism. As regards the types of technologies, ten different technologies were considered, also excluding seawater heat pumps, which are already a well-established technology in Croatia.

Figure 5 summarizes the results achieved in terms of eligible and pilot areas for the above-mentioned technologies. It is worth mentioning that no potential whatsoever was detected for overtopping breakwaters, oscillating attenuators, and tidal turbines, thus cutting the technologies applicable in the region down to seven. These are mostly concentrated in the northern part of the region and, for wind energy, in two offshore areas: one situated between the islands of Vis and Korčula and the other located northwest of Vis.

Given that Split-Dalmatia County was selected as a pilot site, the energy consumption and production were observed firstly only on the county level and then given in the perspective of the whole Croatian energy system. The simulated scenarios include the referent case and a transition scenario. In 2018, the electricity demand in Croatia was 19 TWh, of which is mostly supplied by hydropower plants (7.7 TWh), thermal power plants (3.7 TWh), and onshore wind (1.3 TWh). There is also a net import of about 6.3 TWh per year.

In the analysis, only the area of Split Dalmatia County was observed for the deployment of OWFs. At two selected sites (north and south), the maximum potential is 1,590 MW and 204 MW, respectively. If the nominal capacity of each unit is considered as 6 MW (technology is still in development), this will account for 265 and 34 wind turbines per site. With those installed capacities, electricity production from the north wind farm would be 3.85 TWh/year and 0.5 TWh/year for the south site. The average load factors for both wind farms would be 28%. Together, OWFs could contribute with 4.35 TWh to the national grid, which is around 22% of annual electricity demand, making offshore wind the second most important energy source. The small drawback might represent the fact that offshore wind production does not correlate with demand. Therefore, the lowest output is during the summer months, whereas the highest production is noted during the winter months.

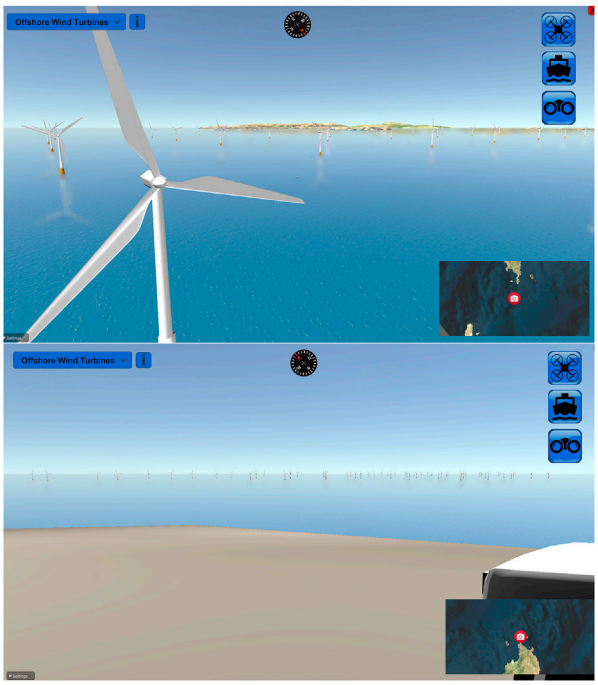

FIGURE 4 | Wind farm visualization in Crete, view from the sea and the shore.

As a testing case, the wave energy potential was analyzed for Split Dalmatia County for 2050. At the selected testing sites, approximately 267 devices of oscillating buoys of 100 kW were considered. On an annual basis, such devices with the current level of development could provide around 1 GWh of electricity. This represents an almost negligible share of total demand; therefore, this technology was considered not promising for the Adriatic coast. This was expected since the Adriatic Sea is a semi-closed sea with poor wave resources.

In Croatia, electricity (19 TWh demand per year) from the grid has a low emission factor due to a high share of renewables (134 g CO_2eq/kWh) and the corresponding greenhouse gas emission is therefore 2,546,000 t CO_2eq/year. The 4.35 TWh per year produced by the OWFs (average 47 g CO_2eq/kWh of carbon intensity) would decrease the emission to 2,167,5500 t CO_2eq/year with 378,450 t CO2eq/year of avoided emission (−15%). The new value for CIE of the grid mix would decrease to 114 g CO_2eq/kWh (**Table 5**).

After the results of eligible and pilot areas from the analyses were available, the interactive visual tool was developed for this scenario (Bluedealmed visual-tool-Croatia, 2022). Nearby 3D terrains were generated, and the technologies were placed in the pilot areas accordingly. **Figure 6** showcases the 3D simulation for the cases of wind turbines accordingly, as seen from the drone camera in the tool.

Blue Energy Plan in Cyprus

In Cyprus, the process for the identification of pilot sites regarded all marine areas belonging to the internal waters, territorial seas, and contiguous zones, thus excluding international waters. Moreover, for Croatia, only areas more than 10 km from the coast were considered for offshore wind energy to avoid the visual impact of turbines.

Figure 7 summarizes the results achieved in terms of eligible and pilot areas. It is worth mentioning that no potential whatsoever was detected for overtopping breakwaters, oscillating attenuators, and tidal turbines. The potential pilot areas for the remaining technologies are concentrated in the southern and northwestern parts of the island, with a suitable site for the installation of an offshore floating wind farm off the southern coast between Larnaca and Limassol.

The energy system of Cyprus is mostly dependent on fossil fuels and expresses an evident seasonality in terms of electricity consumption due to the notable touristic activity. In 2018, less than 10% of electricity was from renewable sources, mainly PV and onshore wind. The transition scenario with the inclusion of MES is built for 2030, according to the national strategy to increase the share of renewables. From the perspective of MES, offshore wind is considered with 300 MW, and wave energy with the 30 MW of installed capacity. Wave energy capacities are equally divided between OWCs, onshore floaters,

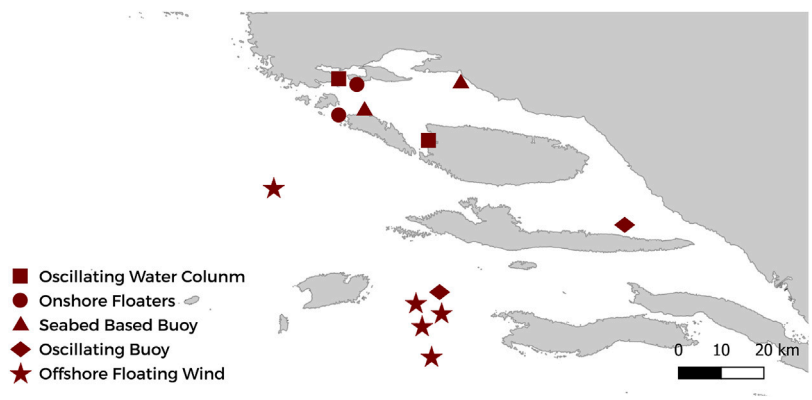

FIGURE 5 | Synthetic map with the identified potential pilot areas for the installation of wind and wave energy plants in Croatia.

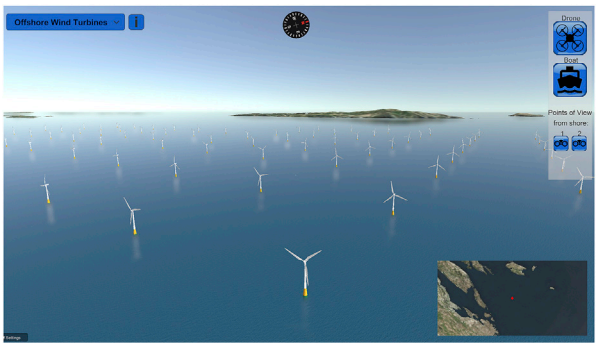

FIGURE 6 | Wind farm visualization Croatia, view from the sea.

and seabed buoys at two selected sites. Additionally, it was assumed that the interconnection cable will be operational by 2030, with a capacity of 1200 MW which is essential for higher penetration of RES.

Offshore wind could produce around 0.5 TWh of electricity per year, accounting for only 10% of annual demand (4.6 TWh), with a quite poor load factor of 18%. This low load factor is partially derived from the fact that the energy system is heavily based on baseload power plants. Therefore, the maximum potential cannot be exploited. Electricity production from WECs is almost negligible and accounts for 10 GWh per year, with a poor load factor of only 2%. This implies that wave energy has a long road ahead before becoming a significant part of the energy system. Finally, the deployment of additional onshore renewable sources, mostly PV, and offshore wind farm could increase the share of renewables in total primary fuel consumption from 5% to 11%. Even more, in such a case for 2030, the share of renewables in the electricity mix would be around 45%, with an annual production of 1.9 TWh. For more in-depth decarbonization, it is necessary to include seawater heat pumps for heating and cooling in both household and service sectors and carry out electrification of the transport sector, which would allow even higher penetration of renewables from the perspective of grid balancing strategy.

In Cyprus, electricity (4.6 TWh demand per year) from the grid has a high emission factor due to a high share of fossil sources (621 g CO_2eq/kWh), and the corresponding greenhouse gas emission is therefore 2,856,600 t CO_2eq/year. The 0.5 TWh (11%) per year produced by the OWFs (average 71 g CO_2eq/kWh of carbon intensity) and 10 GWh (0.2%) per year produced by WECs (average 126 g CO_2eq/kWh of carbon intensity for near-shore buoys) would decrease the emission to 2,581,105.t CO_2eq/year with 275,495.t CO_2eq/year of avoided emission (almost −10%). The new value for CIE of the grid mix would decrease to 561 g CO_2eq/kWh (**Table 5**).

In **Figure 8**, the image above shows the offshore wind turbine park, which is placed 39,868 m from this observation point on the shore near Pervolia Area and can be seen through a zoomed virtual camera. In this implementation of the tool (Bluedealmed visual-too-Cyprus, 2022) in the bottom left of the UI, users can monitor the average distance of the turbines from the camera, the elevation of the camera, and the average obscured height of the turbines in the park. The image below showcases oscillating buoys in Pomos Paphos area, as seen from the drone camera in the tool.

DISCUSSION

Experts from partner institutions of the BLUE DEAL project have developed the different phases of the planning process according to their specialized knowledge and finally provided a BE plan for each target area. The plan was graphically displayed and presented, combining different representations and visualization tools to make it “readable” to a general audience. Given the innovative nature of BE technologies and their dependency on a wide range of conditions (environmental, administrative, and technical) that cannot be fully and consciously handled, the role of the experts was crucial to process, summarize, and transfer scientific data and information that can be used as a basis for discussion, policymaking, and action planning.

Despite assumptions and approximations, the BE planning framework provides a reliable result with concrete information on potential locations for BE plants and estimated benefits. Given that accuracy can be improved based on more accurate data sources, the BE plan presented anyhow provides concrete subjects for an open consultation with local stakeholders, which brings to a constructive discussion on solutions for the energy transition. In particular, results have been presented and used to address the discussion on BE development in target regions during public workshops: BLUE DEAL Labs.

In the BLUE DEAL Lab, the preliminary work of experts providing a comprehensive, integrated BE plan is the pre-requisite to launch a participative design process by engaging local stakeholders with a double aim, which is to validate results according to their expertise and eventually contribute to improve and fine-tune the planning process and to acquire knowledge on opportunities and requirements in order to start a process of capitalization.

Stakeholders engaged in Labs are expected to take vision of the proposed solutions and act as developers of the planned initiatives that will necessarily involve public and private actors throughout the value chain of BE technologies and plans. These include the following:

- Public authorities in charge of regional planning: first, these can provide specific information and ensure full access to main data sources, including geographical data on restrictions preventing the installation of BE devices, for example, regional/local protected areas not included in the Natura 2000 network (information not available on EU platforms). Then, these can support the inclusion of BE plants in the next MPSs or regional energy plans.
- Public authorities in charge of ports management: first, these can provide information on restrictions preventing the

FIGURE 7 | Synthetic map with the identified potential pilot areas for the installation of wind and wave energy plants in Cyprus.

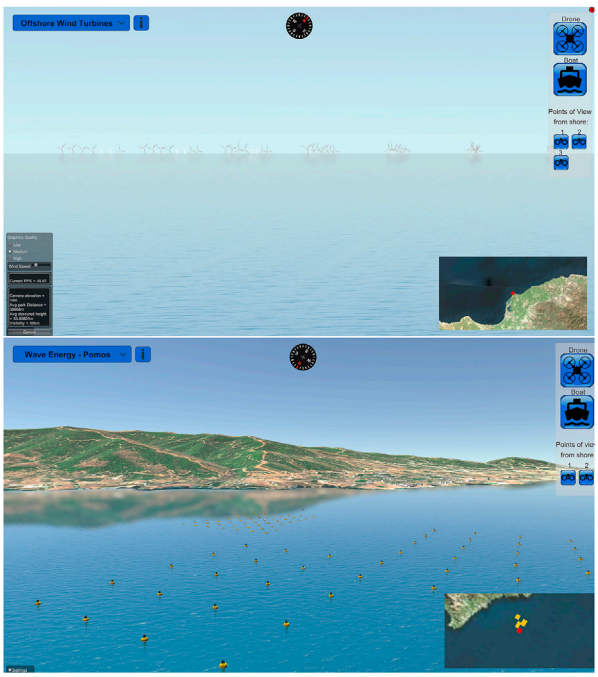

FIGURE 8 | Offshore wind park including 50 spar buoys wind turbines (250 MW), view from Pervolia Area in Cyprus (above) and Oscillating buoys in Pomos Paphos area in Cyprus including 50 seabed-based buoys, 750 m minimum distance (below).

installation of BE devices, for example, due to requisites for ports operations, navigation routes, and other spaces that can be subject to the provisions of local laws and regulations. Then, these can support the inclusion of BE technologies in new port master plans, for example, in new or renewed infrastructures.

- Public authorities in charge of environmental protection and environmental associations of citizens: first, these can provide information regarding the spatial distribution of vulnerable species and habitats (i.e., Posidonia meadows) or birds' migration routes and other information on marine wildlife. Then, these can play a role in supporting initiatives for the energy transition and sustainable development of local communities.
- Public authorities in charge of tourism and private stakeholders, such as associations of hotels, entrepreneurs, and SMEs, to identify tourist facilities along the coast willing to invest in BE technologies: together with the association of citizens, these can play a role as end-users, for example, in the case of energy communities supplied by renewable MES.
- Private stakeholders, such as SMEs or investors interested in new start-up initiatives to evaluate business opportunities in prototyping, installing, and maintaining BE plants in target regions.

Further work can be done in the future to improve the BE planning framework presented here and related tools, such as visual tools for public consultation.

Regarding the identification of BE potentials (Stage 1), MES in the Mediterranean have lower potentials compared to oceans and the North Sea, but minimum requisites are often satisfied, for example, regarding wind speed and wave energy. Results of electricity generation (Stage 4) show that wind farms would have different production yields in selected sites in Crete, Croatia, and Cyprus due to different wind potentials; the identification of suitable sites depending on maximum available potentials at the regional level allowed for maximizing efficiency and provided profitable results in each of the three case studies, meaning that offshore wind represents a profitable solution for increasing renewable rates of energy systems. Wave energy is not as easily exploitable as wind, especially in near-shore areas (only the case of Cyprus shows interesting results compared to negligible outcomes in Crete and Croatia); waves can eventually represent a valuable source of energy in the case of offshore solutions, such as in combination with wind farms (e.g., hybrid floating platforms), where there is evidence of higher potentials. The methodological approach in Stage 1 for assessing BE potentials is crucial in BE planning. Open-access tools, such as the MAESTRALE website, can be used for a preliminary estimate. Nevertheless, the development of site-specific analysis is always recommended at the regional level and needs specific competencies of experts and advanced models to be implemented.

Regarding the identification of BE technologies (Stage 2), offshore wind is currently the most profitable MES, but, considering the bathymetric slope in the Mediterranean Sea, floating wind turbines are a mandatory choice in most cases. Although floating platforms have not been widely tested yet at full scale, floating wind farms have been interpreted by stakeholders during Labs as the most profitable solution. WECs show a lower TRL, but several innovative solutions are under study. Despite the lower potential, the interest of stakeholders, such as Port Authorities, is mainly addressed to onshore and near-shore WEC devices that, for example, can be included in plans of port expansion to make harbors and marinas energy self-sufficient. In the future, the advancement of TRL values would likely increase the performance and applicability of WECs and allow for their effective inclusion in BE planning. In Stage 2 of the methodology, the basic requirements of BE technologies derive from the most recent survey and should be taken as general indications to address planning activities rather than mandatory prescriptions; the survey should be periodically updated because of the fast innovation trends and technological development in this sector.

Regarding the identification of potential sites (Stage 3), maps have been provided in the three case studies, including possible locations for wind farms and WECs and options for technologies coupled with aquacultural systems (marine biomass), desalinating plants (salinity gradients), and touristic infrastructures (seawater heat-cold exchange). Besides seawater-based heat pumps that are already widely used, most of these combined solutions would require extensive innovation and investments for prototyping and testing, and their production yields are still uncertain. The procedure in Stage 3 depends on data availability and accuracy. Far from being an exhaustive spatial plan, results provide matter for a debate with local stakeholders and lay the basis for a discussion on regional MSP that would need deeper and more accurate investigations. Cooperation with experts and negotiations with local stakeholders regarding data sources and their interpretation are recommended for finetuning the spatial analysis. Additional variables, besides those mentioned in the case studies, should be added to inform the mapping process according to site-specific characteristics and needs of target regions.

Energy assessment (Stage 4) faces the problem of temporal intermittence of renewable energy, such as wind and wave energy, that must suit the local energy grid with no dysfunction. The connection with broader grids, such as the national electricity grids, has been forecasted in the hypothesized scenarios as a factor of stability for integrated energy systems. Isolated sites, such as remote islands, would need a deeper analysis to introduce energy storage facilities and production-consumption interactions with other sectors. In Stage 4, a set of progressively improved scenarios, also in combination with other renewable energy sources, with increasing renewable rates, is recommended to guarantee the coherence of interventions and plan the required technical improvements of grids with proper production-consumption-storage balance.

The assessment of carbon footprint mitigation effects (Stage 5) by different BE technologies is based on the various sources used for energy production in target regions (national electricity grid mix). The CIE from local grids are different in the three case studies and, consequently, the contribution of MES in terms of avoided emission. Values of CIE of BE technologies, specifically offshore floating wind farms and WECs, derive from LCA-based assessments, considering the main lifecycle processes of the devices, from manufacturing to maintenance, use, and end of life. Therefore, results open an additional debate, engaging local stakeholders to be actively involved in the value chain with potential effects in terms of climate action (CIE), economic growth (investments, services), and job opportunities. In Stage 5, wider research on the impacts of BE technologies, other than greenhouse gas emission, would improve the accuracy of results, allow for cost-effective organization of lifecycle processes throughout the production chain of BE plants by decreasing impacts and maximizing efficiency (lower CIE values), and increase the capacity to plan fair and sustainable interventions.

VIA (Stage 6) plays a crucial role in the interaction with local stakeholders, especially in engaging non-technical audiences. It can help build social acceptance and better understand impacts and benefits in terms of landscape compatibility and land-use change. An innovative conceptual approach to the problem of the visual impact of renewable energy systems was introduced by Paolinelli et al., 2022; rather than minimizing the visual impact by moving offshore devices as far away as possible from the shore, their expressiveness can eventually be enhanced and interpreted as an added value. In Stage 6, the web tools for visualization of BE plants can contribute to supporting the discussion in this field. More realistic effects can eventually be rendered. For example, even though the terrain of the nearest shore is created using real DEM and texture data, it is very poor in terms of elements such as trees and buildings, which are essential to identify the region; a drone can be used to create an exact 3D model of the landscape containing all the above elements and then it can be imported in the Unity project. Although the environment is in 3D, it is very easy to underestimate or overestimate the dimensions due to various facts, including the camera's focal length and the fact that screens are flat and vary in dimensions. The perception will change if we experience the tool through a laptop screen, a PC monitor, or a larger TV screen. A virtual reality version of the tool would contribute to making this action even more effective for citizen engagement, and their early assessment of BE plans through immersive experiences.

Table 7 provides a synthetic description of key findings and methodological recommendations to improve the BE planning methodology and facilitate its replicability. The implementation of BLUE DEAL Labs provided an opportunity to build a narrative, that is, a story, of what BE technologies are and how they can provide clean energy and new job opportunities in the region. Currently, in the Mediterranean region, there is a narrative that BE potential is very low and that the technologies suitable for deployment in the region are limited. At the same time, there are concerns by other marine users and the general public that such technologies may have negative impacts. An alternative narrative can be presented to local stakeholders through appropriate means, which can spark their imagination. Building an alternative positive narrative can be achieved through storytelling in which existing BE technologies

TABLE 7 | List of main findings per each stage and recommendations for methodological improvement and replication of the BE planning framework.

Stage n	General findings	Methodological recommendations
Stage 1	Variable wind energy potentials in Mediterranean regions; low near-shore wave energy potentials; higher offshore wave energy potentials (e.g., the opportunity for hybrid platforms)	Site-specific BE potentials analysis is needed to increase the accuracy of regional BE plans
Stage 2	Floating wind turbines are the optimal solution in the Mediterranean; offshore wind is the most profitable technology with higher TRL; WECs have low TRL; stakeholders (port authorities) show interest in near-shore WEC devices	The survey on BE technologies and datasets on their basic requirements should be periodically updated
Stage 3	Spatial mapping concerns different MES, depending on potentials, technological requisites, and physical and legal restrictions; interferences with other marine activities have also been considered in maps and give matter for negotiation with stakeholders; BE technologies coupled with existing infrastructures (e.g., aquaculture, desalination plants) have uncertain effects but are options for future development	Identified sites, rather than definitive results, need a consultation with local stakeholders both for validating reference data and for interpreting outcomes; additional relevant variables should be introduced, besides those mentioned, to inform the mapping process according to site-specific characteristics and needs
Stage 4	BE production can suit local energy grids with no dysfunction; connection wires with broader grids have been hypothesized as a factor of stability for integrated energy systems; isolated islands need a deeper analysis to guarantee energy production-consumption-storage balance	Energy assessments should concern short-medium-long term scenarios, also in combination with other renewable energy sources, forecasting increasing renewable rates
Stage 5	Carbon mitigation effects of BE plants are consistent in the three case studies; CIE values of national electricity grids are variable in Mediterranean regions; CIE values of BE plants are calculated based on LCA and energy production yields of BE devices; in general, OWFs have low CIE values, variable with energy production in different sites; WECs still need improvements in terms of energy production and CIE values	The optimization of lifecycle processes throughout the production chain of BE plants would contribute to decreasing climate impacts and maximizing efficiency (lower CIE values); besides carbon emission and CIE values, additional impact categories can help understand the environmental performance of BE plants
Stage 6	Social acceptance is one of the main obstacles to the implementation of BE plants in the Mediterranean; visualization tools play a crucial role in the interaction with local stakeholders, especially citizens; two options can be discussed, minimizing visual impacts and enhancing the expressiveness of energy plants	It is easy to underestimate or overestimate the dimensions of BE plants due to various factors, e.g., camera focal length and flat screens; a virtual reality version of the visualization tool would improve effectiveness in citizen engagement

and BE future technologies are presented to demonstrate the variety of solutions and broaden the concept of BE.

CONCLUSION

The BE planning framework described in this study has been developed under the scope of the Interreg Med BLUE DEAL project to promote the deployment of BE technologies in the Mediterranean region and support their inclusion in regional Energy Plans and Marine Spatial Planning initiatives.

The proposed methodology has been demonstrated during three BLUE DEAL Labs in Crete, Croatia, and Cyprus to preliminarily identify the areas that are eligible for the deployment of blue energies, dimension possible interventions, and assess potential outputs and impacts. In general, results from the three case studies confirm that BE can consistently contribute to the energy transition of Mediterranean regions, especially in the case of offshore floating wind farms, depending on site-specific potentials. WECs are still at an early stage of development and currently show low efficiency compared to other renewable sources, but technological improvements may likely allow for profitably harvesting wave energy in the next future. While thermal energy already represents a valuable option, exploitable through seawater-based heat pumps, limited and still uncertain potentials are associated with marine biomass, in combination with aquaculture, and salinity gradients, coupled with desalinating plants. Marine currents are not significant enough in the Mediterranean except for a few hotspots.

A sequence of clearly defined stages is provided to release an early integrated BE plan to exploit different MES in specific marine areas. This takes into consideration local BE potentials (Stage 1), characteristics, and minimum requirement of technologies to ensure their operability (Stage 2), and the combination with physical, environmental, and legal restrictions in the area, as well as other maritime activities (e.g., shipping, fishing, and tourism) (Stage 3). Moreover, the hypothesized scenarios are evaluated by assessing the impact of the penetration into the local energy grid mix (Stage 4), the effects in terms of carbon footprint mitigation of BE plants, and renewable energy systems (Stage 5). The last stage concerns the visualization of the planned BE plants in contextual landscapes through digital simulations (Stage 6). Limitations of the procedure have been systematically highlighted in this study per each stage, with recommendations to improve accuracy and increase the reliability of results. Besides the suggested datasets and tools, additional data sources, models and tools, variables analyzed, visualization and communication techniques, and other complementary competencies, such as economic estimates and financial issues, would contribute in the future to advance the planning methodology, building on more robust knowledge and transparent and widely shared information.

The procedure, initially based on open-access web tools and datasets, can be performed by an interdisciplinary group of experts in a few working days to transfer scientific and technical knowledge to a broad range of stakeholders.

Although assumptions and approximations can determine inaccurate outcomes, the resulting BE plans provide matter for discussion within participatory forums through which the interested parties can learn how to profitably implement BE technologies in target regions, collaborate to sign cooperation agreements, and take action. In particular, national and regional public authorities can be informed to decide whether and where to support BE deployment in their marine areas.

The Blue Energy Planning framework can be a valuable tool to facilitate dialog and discussions among local administrators, industry, and civil society. Through open consultation, it can help anticipate possible causes of resistance against the deployment of Blue Energies and proactively address emerging problems, thus making a step forward in the social acceptance of these new technologies. Although each test case had its own characteristics and specificities, the replicability of the proposed method in different regions of the Mediterranean can contribute to promoting and accelerating an effective and fair energy transition based on marine energy and boost regional and transnational cooperation for a sustainable blue economy.

DATA AVAILABILITY STATEMENT

The original contributions presented in the study are included in the article. Further inquiries can be directed to the corresponding author.

AUTHOR CONTRIBUTIONS

RP: research coordinator, main curator, and writer. SB: general supervisor and project coordinator. Co-authors: writers of specific sections, all involved in the cooperative work.

FUNDING

This study has been developed in the framework of the Interreg Med BLUE-DEAL (2019–2022) project co-financed by the European Regional Development Fund (Ref. 5381). Website: https://blue-deal.interreg-med.eu.

REFERENCES

Hellenic Ornithological Society (1982). Hellenic Ornithological Society. Available at: http://www.ornithologiki.gr.

Arena, F., Romolo, A., Malara, G., and Ascanelli, A. (2013). "On Design and Building of a U-Owc Wave Energy Converter in the Mediterranean Sea: A Case Study," in Proceedings of the ASME 2013 32nd International Conference on Ocean, Offshore and Arctic Engineering, Nantes, France, June 9-14, 2013. OMAE2013. doi:10.1115/OMAE2013-11593

Babarit, A., Hals, J., Muliawan, M. J., Kurniawan, A., Moan, T., and Krokstad, J. (2012). Numerical Benchmarking Study of a Selection of Wave Energy Converters. *Renew. Energy* 41, 44–63. doi:10.1016/j.renene.2011.10.002

Barbot, Y., Al-Ghaili, H., and Benz, R. (2016). A Review on the Valorization of Macroalgal Wastes for Biomethane Production. *Mar. Drugs* 14 (6), 120. doi:10.3390/md14060120

Bastianoni, S., Coppola, F., Tiezzi, E., Colacevich, A., Borghini, F., and Focardi, S. (2008). Biofuel Potential Production from the Orbetello Lagoon Macroalgae: A Comparison with Sunflower Feedstock. *Biomass Bioenergy* 32, 619–628. doi:10.1016/j.biombioe.2007.12.010

Bastianoni, S., Praticò, C., Damasiotis, M., and Pulselli, R. M. (2020). Editorial: Perspectives for Marine Energy in the Mediterranean Area. *Front. Energy Res.* 8. article 09 September 2020. doi:10.3389/fenrg.2020.00209

BLUE DEAL (2022). Interreg Med Project Official Website. Available at: https://blue-deal.interreg-med.eu.

Bluedealmed visual tool Crete (2022). Bluedealmed Visual Tool Crete. Available at: https://bluedealmed.eu/visual-tool.

Bluedealmed visual tool Croatia (2022). Bluedealmed Visual Tool Croatia. Available at: https://bluedealmed.eu/visual-tool-croatia.

Bluedealmed visual tool Cyprus (2022). Bluedealmed Visual Tool Cyprus. Available at: https://bluedealmed.eu/visual-tool-cyprus.

Bonfanti, M., Hillis, A., Sirigu, S. A., Dafnakis, P., Bracco, G., Mattiazzo, G., et al. (2020). Real-Time Wave Excitation Forces Estimation: An Application on the ISWEC Device. *Jmse* 8 (10), 825. doi:10.3390/jmse8100825

Bozzi, S., Besio, G., and Passoni, G. (2018). Wave Power Technologies for the Mediterranean Offshore: Scaling and Performance Analysis. *Coast. Eng.* 136, 130–146. doi:10.1016/j.coastaleng.2018.03.001

Bozzi, S., Miquel, A., Antonini, A., Passoni, G., and Archetti, R. (2013). Modeling of a Point Absorber for Energy Conversion in Italian Seas. *Energies* 6, 3033–3051. doi:10.3390/en6063033

Bruno, M., Maccanti, M., Sabbetta, A., Neri, E., Patrizi, N., Pulselli, R. M., et al. (2022). Benchmarking Marine Energy Technologies through LCA: Wave Energy Converters in the Mediterranean. *Front. Energy Res.* In press (this research topic).

Buccino, M., Dentale, F., Salerno, D., Contestabile, P., and Calabrese, M. (2016). The Use of CFD in the Analysis of Wave Loadings Acting on Seawave Slot-Cone Generators. *Sustainability* 8, 1255. doi:10.3390/su8121255

Carillo, A., Lombardi, E., and Sannino, G. (2013). *Report di sintesi sulla realizzazione di un sistema operativo per la previsione dell'energia da moto ondoso*. RdS/2013/085.

Carillo, A., Lombardi, E., and Sannino, G. (2014). *Validazione del sistema operativo per la previsione del moto ondoso nel Mediterraneo*. RdS/PAR2014/238.

Carillo, A., Pisacane, G., and Struglia, M. V. (2022). Exploitation of an Operative Wave Forecast System for Energy Resource Assessment in the Mediterranean Sea. *Front. Energy Res.* In press (this research topic).

Carillo, A., Sannino, G., and Lombardi, E. (2015). Wave Energy Potential: A Forecasting System for the Mediterranean Basin. *Energ. Ambiente Innov.* 61 (special n. 2), 16–21.

Chatzigiannakou, M. A., Dolguntseva, I., and Ekström, R. L. (2015)). "Offshore Deployment of Marine Substation in the Lysekil Research Site," in Proceedings of the Twenty-fifth (2015) International Ocean and Polar Engineering Conference Kona, Hawaii, USA, June 21-26, 2015. Big Island. ISBN 978-1-880653-89-0; ISSN 1098-6189.

Chatzigiannakou, M., Dolguntseva, I., and Leijon, M. (2017). Offshore Deployments of Wave Energy Converters by Seabased Industry AB. *Jmse* 5, 15. doi:10.3390/jmse5020015

Chipindula, J., Botlaguduru, V., Du, H., Kommalapati, R., and Huque, Z. (2018). Life Cycle Environmental Impact of Onshore and Offshore Wind Farms in Texas. *Sustainability* 10, 2022. doi:10.3390/su10062022

Coiro, D. P., Troise, G., and Bizzarrini, N. (2018). Experiences in Developing Tidal Current and Wave Energy Devices for Mediterranean Sea. *Front. Energy Res.* 6, 136. doi:10.3389/fenrg.2018.00136

Coiro, D. P., Troise, G., Ciuffardi, T., and Sannino, G. (2013). "Tidal Current Energy Resource Assessment: the Strait of Messina Test Case," in 2013 International Conference on Clean Electrical Power, Alghero, Italy (ICCEP), 213–220. doi:10.1109/ICCEP.2013.6586992

Coiro, D. P., Troise, G., Scherillo, F., De Marco, A., Calise, G., and Bizzarrini, N. (2017). Development, Deployment and Experimental Test on the Novel Tethered System GEM for Tidal Current Energy Exploitation. *Renew. Energy* 114, 323–336. doi:10.1016/j.renene.2017.01.040

COM (2020). *An EU Strategy to Harness the Potential of Offshore Renewable Energy for a Climate Neutral Future*. Brussels, Belgium: EU Commission. Brussels. 741.

Contestabile, P., Di Lauro, E., Buccino, M., and Vicinanza, D. (2017). Economic Assessment of Overtopping BReakwater for Energy Conversion (OBREC): a Case Study in Western Australia. *Sustainability* 9, 51. doi:10.3390/su9010051

Contestabile, P., Ferrante, V., Di Lauro, E., and Vicinanza, D. (2016). "Prototype Overtopping Breakwater for Wave Energy Conversion at Port of NaplesProceedings of the Twenty-Sixth," in *International Ocean and Polar Engineering Conference* (Rhodes, Greece. 978-1-880653-88-3. June 26-July 1, 2016ISSN 1098-6189.

Curto, D., Franzitta, V., and Guercio, A. (2021). Sea Wave Energy. A Review of the Current Technologies and Perspectives. *Energies* 14, 6604. doi:10.3390/en14206604

EEA European Environment Agency (2022). Greenhouse Gas Emission Intensity of Electricity Generation in Europe. Published: 18 November 2021. Available at: https://www.eea.europa.eu/ims/greenhouse-gas-emission-intensity-of-1.

EMODnet (2021). EMODnet. Available at: https://emodnet.ec.europa.eu/.

ENERCOAST (2014). "Renewable Energies in the Marine-Coastal Areas of the Adriatic-Ionian Region," in *Project Deliverable "Technical, Environmental and Economic Analysis of Low and Medium Size of Solar Cooling Systems, Heat Pumps with Sea Water, Wind Turbines and Tidal Current Technologies*. Available at: https://bib.irb.hr/datoteka/784638.ENERCOAST_Technology_data.pdf (Accessed on April 01, 2022).

EWP Eco Wave Power (2022). How it Works. Available at: https://www.ecowavepower.com/our-technology/how-it-works/(accessed on March 29, 2022).

EWP Eco Wave Power (2019). *Invitation to Subscribe for Shares in EWPG Holding AB (Publ)*. Review Report. Stockholm, June 26, 2019. Available at: https://www.ecowavepower.com/wp-content/uploads/2019/07/EWP_prospekt_EN.pdf (Accessed on March 29, 2022).

Falcão, A. F. O., and Henriques, J. C. C. (2016). Oscillating-water-column Wave Energy Converters and Air Turbines: A Review. *Renew. Energy* 85, 1391–1424. doi:10.1016/j.renene.2015.07.086

Faÿ, F.-X., Henriques, J. C., Kelly, J., Mueller, M., Abusara, M., Sheng, W., et al. (2020). Comparative Assessment of Control Strategies for the Biradial Turbine in the Mutriku OWC Plant. *Renew. Energy* 146, 2766–2784. doi:10.1016/j.renene.2019.08.074

Fries, S. (2021). *Transforming Energy Systems: Economics, Policies and Change*. Cheltenham, United Kingdom: Edward Elgar Publishing.

Geofabrik (2007). Geofabrik. Available at: https://www.geofabrik.de.

Global Wind Atlas (2015). Global Wind Atlas. Available at: https://globalwindatlas.info/.

González, A., Kelly, C., and Rymszewicz, A. (2020). Advancements in Web-mapping Tools for Land Use and Marine Spatial Planning. *Trans. GIS* 24 (2), 253–267.

Greek Government Geodata (2018). Greek Government Geodata. Available at: http://geodata.gov.gr/.

Greek Ministry of Maritime Affairs (2020). Greek Ministry of Maritime Affairs. Available at: https://www.ynanp.gr/.

Grip, K., and Blomqvist, S. (2021). Marine Spatial Planning: Coordinating Divergent Marine Interests. *Ambio* 50 (6), 1172–1183. doi:10.1007/s13280-020-01471-0

Helm, C., and Mier, M. (2021). Steering the Energy Transition in a World of Intermittent Electricity Supply: Optimal Subsidies and Taxes for Renewables and Storage. *J. Environ. Econ. Manag.* 109, 102497. doi:10.1016/j.jeem.2021.102497

Howells, M., and Ramírez-Monsalve, P. (2022). Maritime Spatial Planning on Land? Planning for Land-Sea Interaction Conflicts in the Danish Context. *Plan. Pract. Res.* 37 (2), 152–172. doi:10.1080/02697459.2021.1991656

Ibarra-Berastegi, G., Sáenz, J., Ulazia, A., Serras, P., Esnaola, G., and Garcia-Soto, C. (2018). Electricity Production, Capacity Factor, and Plant Efficiency Index at the Mutriku Wave Farm (2014-2016). *Ocean. Eng.* 147, 20–29. doi:10.1016/j.oceaneng.2017.10.018

Ibarra-Berastegi, G., Ulazia, A., Sáenz, J., Serras, P., González Rojí, S. J., Esnaola, G., et al. (2021). The Power Flow and the Wave Energy Flux at an Operational Wave Farm: Findings from Mutriku, Bay of Biscay. *Ocean. Eng.* 227, 108654. doi:10.1016/j.oceaneng.2021.108654

IPCC (2022). *Climate Change 2022 Impacts, Adaptation and Vulnerability. Contribution of Working Group II to the Sixth Assessment Report of the Intergovernmental Panel on Climate Change*.

Kallos, G. (1997)). "The Regional Weather Forecasting System SKIRON," in *Proceedings, Symposium on Regional Weather Prediction on Parallel Computer Environments*, 15–17.

Kokologos, D., Tsitoura, I., Kouloumpis, V., and Tsoutsos, T. (2014). Visual Impact Assessment Method for Wind Parks: A Case Study in Crete. *Land Use Policy* 39, 110–120. doi:10.1016/j.landusepol.2014.03.014

Kyriazi, Z., Maes, F., and Degraer, S. (2016). Coexistence Dilemmas in European Marine Spatial Planning Practices. The Case of Marine Renewables and Marine Protected Areas. *Energy Policy* 97, 391–399. doi:10.1016/j.enpol.2016.07.018

Kyvelou, S. (2017). Maritime Spatial Planning as Evolving Policy in Europe: Attitudes, Challenges, and Trends. *Eur. Q. Political Attitudes Ment.* 6 (3), 1–13.

MAESTRALE (2019). Interreg Med Project Official Website. Available at: https://maestrale.interreg-med.eu.

MAESTRALE webgis (2018). MAESTRALE Webgis. Available at: http://maestrale-webgis.unisi.it.

Malara, G., Romolo, A., Fiamma, V., and Arena, F. (2017). On the Modelling of Water Column Oscillations in U-OWC Energy Harvesters. *Renew. Energy* 101, 964–972. doi:10.1016/j.renene.2016.09.051

Marchesi, E., Negri, M., and Malavasi, S. (2020). Development and Analysis of a Numerical Model for a Two-Oscillating-Body Wave Energy Converter in Shallow Water. *Ocean. Eng.* 214, 107765. doi:10.1016/j.oceaneng.2020.107765

Marine Vessel Traffic (2017). Marine Vessel Traffic. Available at: https://www.marinevesseltraffic.com/.

Maslov, N., Claramunt, C., Wang, T., and Tang, T. (2017). Evaluating the Visual Impact of an Offshore Wind Farm. *Energy Procedia* 105, 3095–3100. doi:10.1016/j.egypro.2017.03.649

Mattiazzo, G. (2019). State of the Art and Perspectives of Wave Energy in the Mediterranean Sea: Backstage of ISWEC. *Front. Energy Res.* 7, 114. doi:10.3389/fenrg.2019.00114

Migliore, G., Alisi, C., Sprocati, A. R., Massi, E., Ciccoli, R., Lenzi, M., et al. (2012). Anaerobic Digestion of Macroalgal Biomass and Sediments Sourced from the Orbetello Lagoon, Italy. *Biomass Bioenergy* 42, 69–77. doi:10.1016/j.biombioe.2012.03.030

Molina-Ruiz, J., Martínez-Sánchez, M. J., Pérez-Sirvent, C., Tudela-Serrano, M. L., and García Lorenzo, M. L. (2011). Developing and Applying a GIS-Assisted Approach to Evaluate Visual Impact in Wind Farms. *Renew. Energy* 36, 1125–1132. doi:10.1016/j.renene.2010.08.041

Molnarova, K., Sklenicka, P., Stiborek, J., Svobodova, K., Salek, M., and Brabec, E. (2012). Visual Preferences for Wind Turbines: Location, Numbers and Respondent Characteristics. *Appl. Energy* 92, 269–278. doi:10.1016/j.apenergy.2011.11.001

Moodie, J. R., and Sielker, F. (2022). Transboundary Marine Spatial Planning in European Sea Basins: Experimenting with Collaborative Planning and Governance. *Plan. Pract. Res.* 37 (3), 317–332. doi:10.1080/02697459.2021.2015855

Napolitano, E., Iacono, R., Palma, M., Sannini, G., Carillo, A., Lombardi, E., et al. (2022). MITO: a New Operational Model for the Forecasting of the Mediterranean Sea Circulation. *Front. Energy Res.* In press (this research topic).

Natura (2000). Natura. Available at: https://natura2000.eea.europa.eu/.

Negri, M., and Malavasi, S. (2018). Wave Energy Harnessing in Shallow Water through Oscillating Bodies. *Energies* 11, 2730. doi:10.3390/en11102730

Nordic Heat Pump (2017). *How Low Can Nordic Heat Pumps Go?* Available at: https://www.nordicghp.com/2017/01/heat-pump-effective-temperature-range/ (Accessed on April 01, 2022).

Offei, F., Mensah, M., Thygesen, A., and Kemausuor, F. (2018). Seaweed Bioethanol Production: A Process Selection Review on Hydrolysis and Fermentation. *Fermentation* 4 (4), 99. doi:10.3390/fermentation4040099

Palma, M., Iacono, R., SanninoBargagli, G. A., Bargagli, A., Carillo, A., Fekete, B. M., et al. (2020). Short-term, Linear, and Non-linear Local Effects of the Tides on the Surface Dynamics in a New, High-Resolution Model of the Mediterranean Sea Circulation. *Ocean. Dyn.* 70, 935–963. doi:10.1007/s10236-020-01364-6

Pantusa, D., Francone, A., and Tomasicchio, G. R. (2020). Floating Offshore Renewable Energy Farms. A Life-Cycle Cost Analysis at Brindisi, Italy. *Energies* 13, 6150. doi:10.3390/en13226150

Pantusa, D., and Tomasicchio, G. R. (2019). Large-scale Offshore Wind Production in the Mediterranean Sea. *Cogent Eng.* 6 (1), 1661112. doi:10.1080/23311916.2019.1661112

Paolinelli, G., Fortuna, L., Marinaro, L., and Valentini, A. (2022). On Marine Wind Power Expressiveness: Not Just an Issue of Visual Impact. *Front. Energy Res.* In press (this research topic).

Parker, R. P. M., Harrison, G. P., and Chick, J. P. (2007). Energy and Carbon Audit of an Offshore Wave Energy Converter. *Proc. Institution Mech. Eng. Part A J. Power Energy* 221, 1119–1130. doi:10.1243/09576509JPE483

Patrizi, N., Pulselli, R. M., Neri, E., Niccolucci, V., Vicinanza, D., Contestabile, P., et al. (2019). Lifecycle Environmental Impact Assessment of an Overtopping Wave Energy Converter Embedded in Breakwater Systems. *Front. Energy Res.* 7, 32. doi:10.3389/fenrg.2019.00032

Petit, V. (2018). *The New World of Utilities: A Historical Transition towards a New Energy System*. Springer.

Pisacane, G., Sannino, G., Carillo, A., Struglia, M. V., and Bastianoni, S. (2018). Marine Energy Exploitation in the Mediterranean Region: Steps Forward and Challenges. *Front. Energy Res.* 6. doi:10.3389/fenrg.2018.00109

Poujol, B., Prieur-Vernat, A., Dubranna, J., Besseau, R., Blanc, I., and Pérez-López, P. (2020). Site-specific Life Cycle Assessment of a Pilot Floating Offshore Wind Farm Based on Suppliers' Data and Geo-located Wind Data. *J. Industrial Ecol.* 24, 248–262. doi:10.1111/jiec.12989

Pulselli, R. M., Maccanti, M., Bruno, M., Sabbetta, A., Neri, E., Patrizi, N., et al. (2022). Benchmarking Marine Energy Technologies through LCA: Offshore Floating Wind Farms in the Mediterranean. *Front. Energy Res.* 10, 902021. doi:10.3389/fenrg.2022.902021

Pulselli, R. M., Marchi, M., Neri, E., Marchettini, N., and Bastianoni, S. (2018). Carbon Accounting Framework for Decarbonisation of European City Neighbourhoods. *J. Clean. Prod.* 208, 850–868.

Quero García, P., Chica Ruiz, J. A., and García Sanabria, J. (2020). Blue Energy and Marine Spatial Planning in Southern Europe. *Energy Policy* 140, 111421. doi:10.1016/j.enpol.2020.111421

Raadal, H. L., Vold, B. I., Myhr, A., and Nygaard, T. A. (2014). GHG Emissions and Energy Performance of Offshore Wind Power. *Renew. Energy* 66, 314–324. doi:10.1016/j.renene.2013.11.075

Rémouit, F., Chatzigiannakou, M.-A., Bender, A., Temiz, I., Sundberg, J., and Engström, J. (2018). Deployment and Maintenance of Wave Energy Converters at the Lysekil Research Site: A Comparative Study on the Use of Divers and Remotely-Operated Vehicles. *Jmse* 6, 39. doi:10.3390/jmse6020039

Salvador, S., Gimeno, L., and Sanz Larruga, F. J. (2019). The Influence of Maritime Spatial Planning on the Development of Marine Renewable Energies in Portugal and Spain: Legal Challenges and Opportunities. *Energy Policy* 128, 316–328. doi:10.1016/j.enpol.2018.12.066

Seapower scrl (2022). Horizontal Axis Marine Turbine. Available at: http://www.seapowerscrl.com/ocean-and-river-system/gem#slide_5 (Accessed on March 31, 2022).

Seghetta, M., Hou, X., Bastianoni, S., Bjerre, A.-B., and Thomsen, M. (2016). Life Cycle Assessment of Macroalgal Biorefinery for the Production of Ethanol, Proteins and Fertilizers - A Step towards a Regenerative Bioeconomy. *J. Clean. Prod.* 137, 1158–1169. doi:10.1016/j.jclepro.2016.07.195

Sklenicka, P., and Zouhar, J. (2018). Predicting the Visual Impact of Onshore Wind Farms via Landscape Indices: A Method for Objectivizing Planning and Decision Processes. *Appl. Energy* 209, 445–454. doi:10.1016/j.apenergy.2017.11.027

Soukissian, T., Denaxa, D., Karathanasi, F., Prospathopoulos, A., Sarantakos, K., Iona, A., et al. (2017). Marine Renewable Energy in the Mediterranean Sea: Status and Perspectives. *Energies* 10, 1512. doi:10.3390/en10101512

Spanos, P. D., Strati, F. M., Malara, G., and Arena, F. (2018). An Approach for Non-linear Stochastic Analysis of U-Shaped OWC Wave Energy Converters. *Probabilistic Eng. Mech.* 54, 44–52. doi:10.1016/j.probengmech.2017.07.001

Stančin, H., Pfeifer, A., Perakis, C., Stefanatos, N., Damasiotis, M., Magaudda, S., et al. (2022). Blue Energy Spearheading the Energy Transition: The Case of Crete. *Front. Energy Res.* 10, 863664. doi:10.3389/fenrg.2022.868334

Stival, C. A. (2014). "Methodological Approach for Recovery and Energetic Requalification of Historical Buildings. Fondazione Internazionale Trieste per il Progresso e la Libertà delle Scienze," in Proceedings of the Workshop on Geothermal Energy. Status and future in the Peri - Adriatic Area, Veli Losinj (HR), 25-27 August 2014. Available at: https://www.researchgate.net/publication/303507189.

Strömstedt, E., Svensson, O., and Leijon, M. (2012). A Set-Up of 7 Laser Triangulation Sensors and a Draw-Wire Sensor for Measuring Relative Displacement of a Piston Rod Mechanical Lead-Through Transmission in an Offshore Wave Energy Converter on the Ocean Floor. *ISRN Renew. Energy* 2012, 1–32. Article ID 746865. doi:10.5402/2012/746865

SWEL Sea Wave Energy Ltd (2022). SWEL Sea Wave Energy Ltd Research. Available at: https://swel.eu/research/(Accessed on March 31, 2022).

Takacs, B., and Goulden, M. C. (2019). Accuracy of Wind Farm Visualisations: The Effect of Focal Length on Perceived Accuracy. *Environ. Impact Assess. Rev.* 76, 1–9. doi:10.1016/j.eiar.2019.01.001

Tedesco, M., Brauns, E., Cipollina, A., Micale, G., Modica, P., Russo, G., et al. (2015). Reverse Electrodialysis with Saline Waters and Concentrated Brines: a Laboratory Investigation towards Technology Scale-Up. *J. Membr. Sci.* 492, 9–20. doi:10.1016/j.memsci.2015.05.020

Tedesco, M., Cipollina, A., Tamburini, A., and Micale, G. (2017). Towards 1 kW Power Production in a Reverse Electrodialysis Pilot Plant with Saline Waters and Concentrated Brines. *J. Membr. Sci.* 522, 226–236. doi:10.1016/j.memsci.2016.09.015

Tedesco, M., Scalici, C., Vaccari, D., Cipollina, A., Tamburini, A., and Micale, G. (2016). Performance of the First Reverse Electrodialysis Pilot Plant for Power Production from Saline Waters and Concentrated Brines. *J. Membr. Sci.* 500, 33–45. doi:10.1016/j.memsci.2015.10.057

Tethys (2022). Eco Wave Power Ltd. Available at: https://tethys.pnnl.gov/organization/eco-wave-power-ltd (Accessed on March 29, 2022).

Thomson, R. C., Chick, J. P., and Harrison, G. P. (2019). An LCA of the Pelamis Wave Energy Converter. *Int. J. Life Cycle Assess.* 24, 51–63. doi:10.1007/s11367-018-1504-2

Thomson, R. C., Harrison, G. P., and Chick, J. P. (2011). "Life Cycle Assessment in the Marine Renewable Energy Sector," in *LCA Report - Instruments for Green Futures Markets: Proceedings from the LCA XI International Conference* (Chicago, IL, United States: American Center for Life Cycle Assessment), 120–125. Available at: http://lcacenter.org/Data/Sites/1/lcaxi/LCA%20XI%20Proceedings%20Final%20Version.pdf.October 4-6, 2011LCA XI, Chicago, United States, 4/10/11.

Tsai, L., Kelly, J. C., Simon, B. S., Chalat, R. M., and Keoleian, G. A. (2016). Life Cycle Assessment of Offshore Wind Farm Siting: Effects of Locational Factors, Lake Depth, and Distance from Shore. *J. Industrial Ecol.* 20 (Number 6), 1370–1383. doi:10.1111/jiec.12400

Twomey, S., and O'Mahony, C. (2019). "Stakeholder Processes in Marine Spatial Planning: Ambitions and Realities from the European Atlantic Experience," in *Maritime Spatial Planning: Past, Present, Future*. Editors J. Zaucha and K. Gee (Cham: Palgrave Macmillan), 295–325. doi:10.1007/978-3-319-98696-8_13

Vannucchi, V., and Cappietti, L. (2016). Wave Energy Assessment and Performance Estimation of State of the Art Wave Energy Converters in Italian Hotspots. *Sustainability* 8, 1300. doi:10.3390/su8121300

Weinzettel, J., Reenaas, M., Solli, C., and Hertwich, E. G. (2009). Life Cycle Assessment of a Floating Offshore Wind Turbine. *Renew. Energy* 34, 742–747. doi:10.1016/j.renene.2008.04.004

Zaucha, J., and Kreiner, A. (2021). Engagement of Stakeholders in the Marine/maritime Spatial Planning Process. *Mar. Policy* 132, 103394. doi:10.1016/j.marpol.2018.12.013

Zhao, Y., Ma, L., Li, Z., and Ni, W. (2021). The Development of Regional Smart Energy Systems in the World and China: The Concepts, Practices, and a New Perspective. *Wiley Interdiscip. Rev. Data Min. Knowl. Discov.* 11 (6), e1409. doi:10.1002/widm.1409

Zheng, X., You, S., Yang, J., and Chen, G. (2014). Seepage and Heat Transfer Modeling on Beach Well Infiltration Intake System in Seawater Source Heat Pump. *Energy Build.* 68, 147–155. doi:10.1016/j.enbuild.2013.09.005

Conflict of Interest: RP and EN were employed by Indaco2. SM and VM were employed by U-space. VP, KS, and EV were employed by Geoimaging. LS was employed by Cyprus Energy Agency.

The remaining authors declare that the research was conducted in the absence of any commercial or financial relationships that could be construed as a potential conflict of interest.

Publisher's Note: All claims expressed in this article are solely those of the authors and do not necessarily represent those of their affiliated organizations or those of the publisher, the editors, and the reviewers. Any product that may be evaluated in this article, or claim that may be made by its manufacturer, is not guaranteed or endorsed by the publisher.

frontiers | Frontiers in Energy Research

TYPE Original Research
PUBLISHED 26 August 2022
DOI 10.3389/fenrg.2022.941606

OPEN ACCESS

EDITED BY
Biagio Fernando Giannetti,
Paulista University, Brazil

REVIEWED BY
Clemente Augusto Souza Tanajura,
Federal University of Bahia, Brazil
Zexun Wei,
Ministry of Natural Resources, China

*CORRESPONDENCE
E. Napolitano,
ernesto.napolitano@enea.it

†These authors have contributed equally to this work

SPECIALTY SECTION
This article was submitted to Sustainable Energy Systems and Policies,
a section of the journal
Frontiers in Energy Research

RECEIVED 11 May 2022
ACCEPTED 28 July 2022
PUBLISHED 26 August 2022

CITATION
Napolitano E, Iacono R, Palma M, Sannino G, Carillo A, Lombardi E, Pisacane G and Struglia MV (2022), MITO: A new operational model for the forecasting of the Mediterranean sea circulation.
Front. Energy Res. 10:941606.
doi: 10.3389/fenrg.2022.941606

MITO: A new operational model for the forecasting of the Mediterranean sea circulation

E. Napolitano*†, R. Iacono†, M. Palma†, G. Sannino†, A. Carillo†, E. Lombardi†, G. Pisacane† and M. V. Struglia†

Climate Modeling Laboratory, Division Model and Technologies for Risk Reduction, Department for Sustainability, ENEA, Rome, Italy

Availability of detailed short-term forecasts of the ocean main characteristics (circulation and waves) is essential for a correct management of the human activities insisting on coastal areas. These activities include the extraction of renewable energy, which has developed in recent years, and will play an important role in the context of future blue growth. The present work describes the implementation of a new ocean operational system, named MITO, that provides daily 5 days forecasts of the Mediterranean Sea circulation. Distinctive features of this system are the inclusion of the main effects of the tidal forcing, both local and propagating from the Atlantic, and the high spatial detail. The horizontal resolution is of 1/48° (about 2 km) in most of the computational domain, and is smoothly increased (down to few hundred meters) in key passages, such as the Gibraltar Strait and the Turkish Straits, to correctly resolve the complex local dynamics. Initial and boundary conditions for MITO are taken from the reference European operation model of Copernicus, which covers the Mediterranean Sea with a uniform resolution of 1/24°. A thorough validation of the new system is performed, analyzing the forecasts of the year 2020, whose results are compared with *in situ* and remote observational data (sea surface temperature, altimeter data, temperature and salinity profiles by floats, tide-gauge measurements, available through the Copernicus portal) using the same large-scale metrics applied in the validation of the Copernicus operational model. MITO results are generally found in very good agreement with the observations, despite the fact that the model does not make explicit use of data assimilation. We also give examples of the capability of the model to correctly describe complex local mesoscale dynamics, and point out aspects that need to be improved, which will be addressed in a future upgrade of the operational implementation.

KEYWORDS

numerical model, mediterranean, forecasting, validation, winds and tides

Introduction

Correct planning and management of the economic activities insisting on marine coastal areas is essential to reduce the impacts on the local ecosystems, and, in some cases, to preserve the resources being exploited. This is a key issue for a country like Italy, with more than 8,000 km of coastline, where a significant portion of the gross domestic product derives from activities taking place in coastal areas. Together with marine transportation, tourism, fishing, and aquaculture, these activities now include the extraction of renewable energy, which has developed in recent years, under the impulse of the "blue growth" policies adopted at the European level (https://blue-action.eu/policy-feed/blue-growth).

A recent assessment of the energy potential in the Mediterranean Sea, with focus on coastal areas, has been given by Nikolaidis et al. (2019), who presented results of the Interreg MED project Maestrale (https://maestrale.interreg-med.eu). It was found that the most promising fonts are the offshore wind energy and the wave energy, which can be extracted both offshore, using floating devices (see, e.g., Pisacane et al., 2018, and references therein), and on shore, with devices embedded in ports or wave-breakers (e.g., Barbarelli et al., 2018). Other potentially interesting fonts are the thermal energy (here temperature differences between air and sea, or between different ocean layers are exploited), and the energy residing in marine currents with a strong tidal component. Interesting locations for the latter font are in the Messina (Coiro et al., 2013) and Gibraltar Straits, and in a few coastal sites in the Aegean Sea. Another font of potential interest relies on the exploitation of salinity gradients due to river discharges, but the technologies in this field have not yet reached a mature stage.

It can be easily understood that activities aimed at harvesting energy from these fonts do require a detailed knowledge of the marine environment, both in terms of circulation and sea state (waves), on a variety of time scales. Multidecadal simulations of the past climate, and of future climate, under different emission scenarios, are necessary to assess the resources and their variability, and consequently to choose the best technological solutions. On the other hand, the optimization and management of the devices being deployed requires the availability of detailed and reliable short-term forecasts.

In the last 2 decades, forecasting of the marine circulation has received increasing attention, thanks to the development of the operational oceanography (e.g., Schiller and Brassington, 2011; Davidson et al., 2019), a branch of oceanography whose purpose is to develop observational networks and numerical forecasting systems to be used for an accurate prediction of the short-term evolution of the main ocean physical parameters (currents, temperature, salinity), similarly to what has been done for long time for the atmosphere (weather forecasting). A recent ample review of developments in this relatively new field, focusing on European seas, is given in Fernandez et al. (2021), which contains the Proceedings of the 9th EuroGOOS Conference (EuroGOOS is the European branch of GOOS, the intergovernmental Global Ocean Observing System), devoted to "Advances in operational oceanography: expanding Europe's ocean observing and forecasting capacity".

Current operational ocean forecasts are mainly "deterministic"; they are based on a single high-resolution simulation that starts from the "best" possible initial condition, that is, an initial three-dimensional sea state that is as close as possible to the available observations, in terms of some given metrics. *A posteriori*, simulations of reanalysis are also made, by constraining the numerical models with new observational data that have become available, through sophisticated numerical techniques of data assimilation analogous to those initially developed in the atmospheric context.

Models for the ocean forecast and reanalysis are being constantly improved, building on the advances in the numerical modelling techniques, on the developments in the field of high-performance computing, and on the growing amount of observations, both *in-situ* and from satellite. At European level, most of these observations are collected by the Copernicus Marine Environment Monitoring Service (CMEMS; https://marine.copernicus.eu/it), the marine component of the Copernicus Programme of the European Union, which makes these data freely available to the interested research community. The CMEMS repository also contains state of the art modelling products for the European seas, which can be used as reference in the development of new products, and for the nesting with regional models of higher spatial resolution.

In the Italian context, several operational models for the forecast of the circulation have been developed in the last 2 decades, both for the whole Mediterranean basin (Oddo et al., 2009), and for some Italian seas (Tyrrhenian Sea, Adriatic Sea, Western Mediterranean, Sicily Strait), which have been part of a national network coordinated by the National Group for Operational Oceanography (GNOO; see Napolitano et al., 2016). Some of these developments (see Napolitano et al., 2014), together with those that are the subject of the present paper, have been carried out at ENEA (the National Agency for New Technologies, Energy and Sustainable Economic Development), in the context of a long-term agreement with the Italian Ministry of Economic Development (MISE) that has promoted research activities in the energy sector.

In this work, we describe a new, high-resolution (horizontal grid spacing of 1/48°, or about 2 km) operational system for the forecasting of the Mediterranean Sea circulation we have recently developed, and perform a detailed assessment of its skills. The system is named MITO (MIT Operational), since its computational core is based on an implementation of the MITgcm ocean model (Marshall et al., 1997a; Marshall et al., 1997b) of the

Massachusetts Institute of Technology. An important new feature that we have added to the basic computational core in this implementation is the main tidal forcing, both local, as a body force, and propagating from the Atlantic through the Gibraltar Strait. This was one of the main motivations for the development of MITO, since, when this development started, there was no model for the forecast of the Mediterranean circulation including tidal effects. Moreover, in the first studies with the new model (Palma et al., 2020), we found that complex, nonlinear effects of the tides on the dynamics were present in several regions of the Mediterranean Sea. This means that tidal effects cannot be linearly superposed *a posteriori*; they need to be included in forecasting models at basin scale to have a correct description of the dynamics, and, eventually, to provide the correct boundary conditions to higher resolution regional models.

We shall assess the performance of MITO by comparing the results of the forecasts of the year 2020 with *in situ* and remote experimental observations (sea surface temperature, altimeter data, temperature and salinity profiles by floats, tide-gauge measurements) available through CMEMS. The comparison will make use of the same large-scale metrics applied in the validation of the reference Mediterranean operational model of CMEMS (NEMO; Clementi et al., 2021). The current version of the model produce forecasts at 1/24° of horizontal resolution with 141 vertical levels and includes current-wave interactions, and, from 2021 on, tidal forcing.

The paper is organized as follows. The main features of the model and of its operational implementation are described in *MITO system: Main model features and operational details* Section, whereas Sections 3-6 are concerned with the system validation and the analysis of some interesting aspects of the 2020 Mediterranean circulation. In particular, *Sea surface temperature* Section focuses on the sea surface temperature, and *Hydrological profiles* Section on the hydrological properties. *Circulation* Section examines the large-scale surface circulation patterns produced by the system, and gives some examples of the model capability of capturing small-scale mesoscale features. *Sea level* Section focuses on sea level, both in open sea and in coastal areas, and *Conclusion* Section presents the conclusions, indicating aspects that should be examined to further improve the skill of the system.

MITO system: Main model features and operational details

The MITO forecasting system is based on an innovative, tide-including, three-dimensional numerical model of the marine circulation, implemented on a domain that covers the whole Mediterranean Sea-Black Sea system. The model has 100 vertical z-levels, and a horizontal resolution of 1/48° (about 2 km) over most of the computational domain. MITO is therefore an eddy-resolving model, since the typical Rossby radius of deformation for the Mediterranean is of 10–15 km. Note that the horizontal resolution is higher than that of the current NEMO-CMEMS-Copernicus forecasting model of the Mediterranean Sea (Clementi et al., 2021). A key feature of MITO is the fact that the horizontal resolution is smoothly increased in some critical regions, namely the Strait of Gibraltar and the Turkish Straits. At the Gibraltar Strait, a very high horizontal detail is achieved (down to 200 m) that allows to adequately resolve the complex local dynamics, including the propagation of the Atlantic tidal signal into the Mediterranean basin. Further information on the model and its implementation can be found in Palma et al. (2020), where a first assessment of the main effects of tidal forcing on the circulation was performed. Tidal forcing includes both the tide generating potential as a body force in the momentum equations and the tidal signal propagating from the Atlantic Ocean (see Naranjo et al., 2014, and Sannino et al., 2015, for further details). The four main lunar, solar, and luni-solar tidal components (M2, O1, S2, K1) have been prescribed inside the computational domain.

The model is initialized and forced at the Atlantic boundary by temperature and salinity data from the NEMO-CMEMS model (details are given in *MITO system: Main model features and operational details* Section of Palma et al., 2020).

Data from the high-resolution (5 km), non-hydrostatic SKIRON/Eta regional atmospheric model (Kallos et al., 1997) are used to compute the atmospheric forcing at the sea surface (hourly wind stress, heat and fresh water fluxes). SKIRON is part of the POSEIDON forecast system, which is operational at the National and Kapodistrian University of Athens (http://forecast.uoa.gr/forecastnewinfo.php). The performances of the last version of the model, with respect to those of a previous implementation with horizontal resolution of 10 km have been assessed in Papadopoulos and Katsafados (2009). It is a well-established model that has been used in variety of investigations of atmosphere and ocean dynamics (see, e.g., Kallos et al., 2006; Stathopoulos et al., 2013; de Ruggiero et al., 2016) in the last 2 decades.

The current version of the system does not explicitly implement a data assimilation scheme, although the initial and boundary conditions from the NEMO-CMEMS model incorporate observed data of sea level, temperature and salinity, thus mildly constraining the forecast [the NEMO-CMEMS model solutions are corrected by a variational data assimilation scheme (3DVAR) of temperature and salinity vertical profiles and along track satellite Sea Level Anomaly observations; Clementi et al., 2021, also objective analysis of the SST is used to correct the surface heat fluxes]. We found that this is sufficient to keep the forecasts close to the observations, although future developments envisage the implementation of assimilation procedures, to further improve the skill.

The MITO operational system consists of a complex set of numerical codes, implemented on ENEA's High-Performance

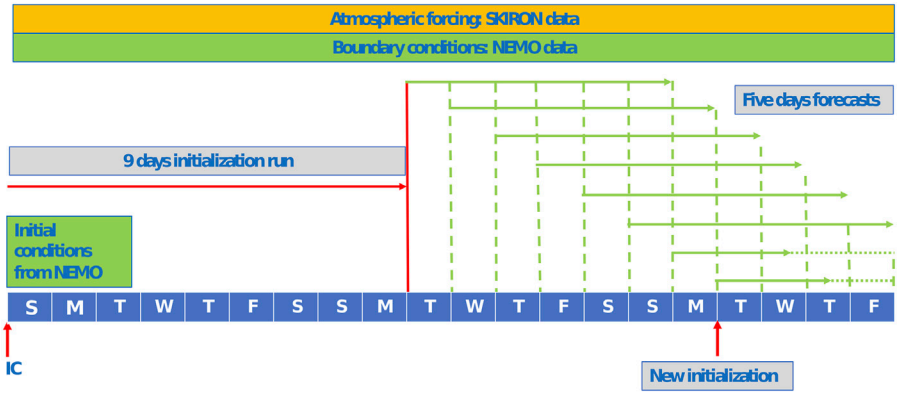

FIGURE 1
MITO operational chain.

Computing (HPC) infrastructures. The operational chain is schematized in Figure 1. Every Tuesday the model is initialized with data from the NEMO-CMEMS Mediterranean Sea and Black Sea forecast models, and a 14-days run is performed, of which the first 9 days represent the initialization phase (forced by SKIRON, here we use the first days of the Skiron forecasts that are assumed to have the best skills) and the last five are the actual forecast. In each of the following days (from Wednesday to next Monday) a 5 days forecast is performed, initialized with restart files from the previous run (see the scheme in Figure 1). The choice of 9 days for the initial adjustment results from an evaluation of the time needed for damping spurious barotropic waves in the different sub-basins. Such perturbations are unavoidable, because they result from the inconsistency between the initial conditions and MITO bathymetry. Nine days are sufficient to completely damp the initial perturbations, and allow for a correct development of the baroclinic velocity field (e.g., Ezer and Mellor, 1994; remember that we initialize with the hydrological fields). The whole operational chain is repeated every week.

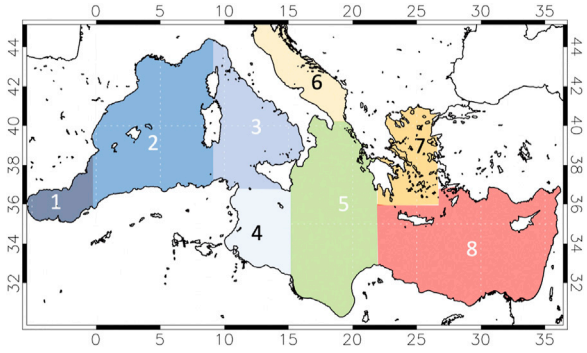

FIGURE 2
Regions on which statistical analyses for the SST, SSH and the hydrological variables have been carried out.

Data

The operational forecasting system produces every day hourly datasets of currents (3D), free surface height (SSH; 1D), and hydrological variables (temperature—T - and salinity—S; 3D), for the following 5 days. The datasets are in NetCDF-4 format, a format widely used in the ocean modelling community. The validation makes use of the first day of each forecast, which is expected to have the best skill. The following data from CMEMS are used to assess the skill of the system:

- Sea Surface Temperature (SST) measured from satellite; product SST_MED_SST_L4_NRT_OBSERVATIONS_010_004, which is provided on a regular grid at 1/16°, and represents the reconstruction of the daily SST based on the data measured at 0:00 UTC using various types of sensors (Buongiorno Nardelli et al., 2013);
- Vertical profiles of temperature and salinity obtained from Argo floaters (product INSITU_MED_NRT_OBSERVATIONS_013_035; data provided by the European Research Infrastracture Consortium);
- Absolute Dynamic Topography (ADT) measured from satellite altimeters, and corresponding geostrophic reconstructions of the circulation [product SEALEVEL_EUR_PHY_L4_MY_008_068; data

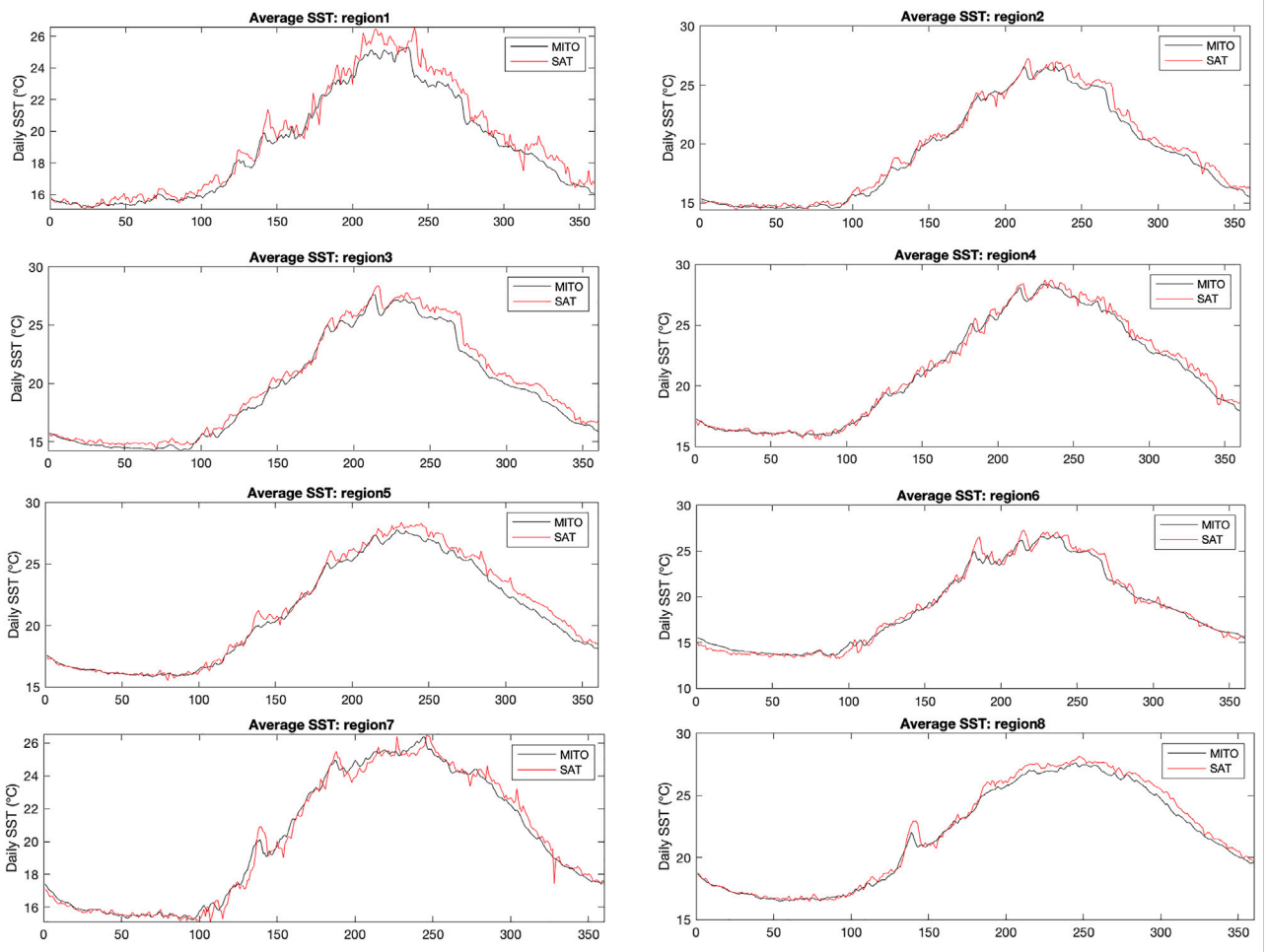

FIGURE 3
Comparison between time series of SST from MITO (black) and from satellite measurements (red), in the eight regions defined in Figure 2. Note that the MITO data are those from the first day of each forecast.

processed by SSALTO/DUACS and distributed by AVISO+ (https://www.aviso.altimetry.fr) with support from CNES (Centre national d'études spatiales; France)];
- Sea level data from coastal tide-gauge stations (product INSITU_MED_NRT_OBSERVATIONS_013_035);
- Turbidity data from satellite (product OCEANCOLOUR_MED_OPTICS_L3_REP_OBSERVATIONS_009_095).

The comparison between the model forecasts and the observations has been done for the whole 2020, for the eight regions shown in Figure 2, which are considered as dynamically coherent. The operational system has been validated via the same method adopted for the CMEMS forecasting system (Clementi et al., 2021), which makes use of the bias between the predicted and observed values, and of the corresponding root-mean-square deviation (RMSD), as the main statistical metrics to assess the reliability of the relevant predicted variables.

TABLE 1 Bias and RMSD of the SST [°C]–(MITO vs. satellite data).

Region	Mean	RMSD
1	−0.46	0.71
2	−0.31	0.51
3	−0.51	0.68
4	−0.19	0.42
5	−0.37	0.55
6	−0.06	0.55
7	0.01	0.42
8	−0.30	0.45

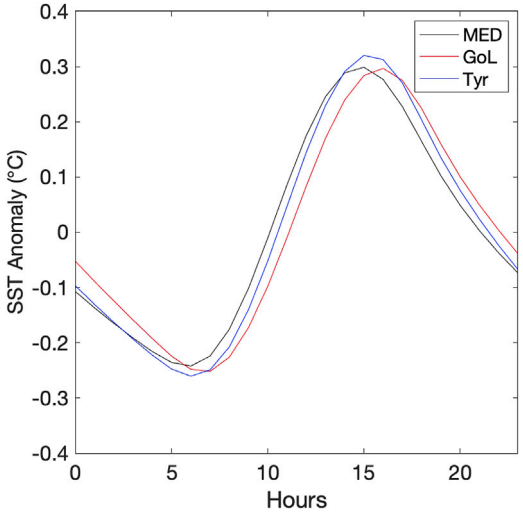

FIGURE 4
The SST diurnal Cycle for Mediterranean Basin Gulf of Lion and the Southern Tyrrhenian sea.

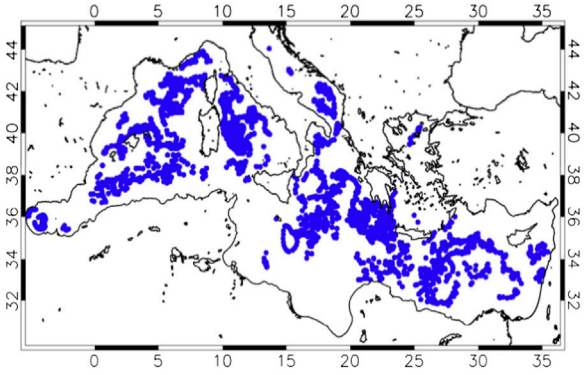

FIGURE 5
Spatial distribution of the Argo profiles available in 2020 (period March-December).

Sea surface temperature

The comparison between modeled and observed daily series of SST (values taken at 00 UTC for both) for the eight regions is shown in Figure 3. There is generally a good agreement between model data and observations, even though in some regions the model SST underestimates the observed one in the second half of the year.

The corresponding bias and RMSD values are reported in Table 1. The bias is always below 0.5°C, except for region 3 (Tyrrhenian-Ligurian), where it is slightly larger, and it is almost always negative. The best agreement is found in the Aegean Sea (7) and the Levantine basin (8). Discrepancies can be attributable to deficiencies either in the data (L4 data making use of climatologic values to fill missing data) or in the forecasts, as a consequence of the approximations implied by the use of vertical mixing parameterizations and bulk formulas.

The diurnal variation of the SST is a topic that has recently received considerable attention, since it has been shown that resolving this variation may have a non-negligible impact on the estimation of the total mean heat budget in the Mediterranean Sea (Marullo et al., 2016). The SST diurnal cycle also controls biogeochemical processes in the upper ocean and in coastal ecosystems (e.g., Doney et al., 1995; Zhang et al., 2022). Figure 4 shows the SST diurnal cycle as reproduced by the model for August 2020, averaged over the whole Mediterranean basin (black curve), which is in good qualitative agreement with that obtained by Marullo et al. (2016) for the summer of 2011. The red curve corresponds to the analogous cycle for the Gulf of Lion and the blue one to that of the southeastern Tyrrhenian Sea, with the latter displaying the largest amplitude. This is an area where diurnal warming events have been observed in the past (Marullo et al., 2016).

TABLE 2 Bias (MITO-observation) and RMSD for temperature (in °C) and salinity (psu).

	T		S	
Layer (m)	Bias	RMSD	Bias	RMSD
0–10	−0.224	1.049	−0.154	0.316
10–30	−0.079	1.573	−0.138	0.301
30–60	0.363	1.795	−0.140	0.297
60–100	0.275	1.067	−0.137	0.298
100–150	0.132	0.586	0.051	0.217
150–300	−0.006	0.390	0.020	0.173
300–600	−0.112	0.240	0.017	0.095
600–1,000	−0.098	0.175	0.020	0.096
1,000–2000	−0.188	0.202	0.014	0.090

Hydrological profiles

The vertical profiles of temperature and salinity produced by the model have been compared with Argo profiles The number of available profiles for 2020 is 2,993. These profiles are quite regularly distributed over the period from March to December; their spatial distribution is displayed in Figure 5. For each observed profile, the corresponding modelled one was extracted at the nearest grid point and output time.

The average bias and RSMD for temperature and salinity are reported in Table 2, for nine reference layers in the first 2000 m of

10.3389/fenrg.2022.941606

TABLE 3 Bias (MITO-observation) for temperature (A) and salinity (B): monthly variability. The nine reference layers considered are indicated in the first column.

A	Mar	Apr	May	Jun	Jul	Aug	Sept	Oct	Nov	Dec
0–10	−0.044	−0.246	−0.369	−0.347	−0.165	−0.205	−0.451	0.084	−0.299	−0.093
10–30	−0.007	−0.134	−0.118	−0.166	0.080	0.245	−0.339	0.102	−0.272	−0.085
30–60	0.117	0.063	0.311	0.711	0.670	1.009	0.404	0.523	−0.170	0.007
60–100	0.166	0.117	0.288	0.411	0.401	0.573	0.367	0.364	−0.051	0.140
100–150	0.136	0.094	0.217	0.214	0.199	0.246	0.222	0.116	−0.089	0.038
150–300	0.032	0.008	0.027	0.021	−0.017	−0.007	0.057	−0.001	−0.098	−0.044
300–600	−0.089	−0.098	−0.085	−0.104	−0.099	−0.115	−0.099	−0.128	−0.139	−0.138
600–1,000	−0.079	−0.082	−0.086	−0.100	−0.079	−0.098	−0.088	−0.124	−0.101	−0.123
1,000–2000	−0.191	−0.185	−0.182	−0.193	−0.181	−0.193	−0.187	−0.188	−0.188	−0.195
B	**Mar**	**Apr**	**May**	**Jun**	**Jul**	**Aug**	**Sept**	**Oct**	**Nov**	**Dec**
0–10	−0.155	−0.162	−0.122	−0.172	−0.166	−0.176	−0.128	−0.126	−0.087	−0.168
10–30	−0.141	−0.153	−0.135	−0.164	−0.159	−0.157	−0.137	−0.127	−0.091	−0.145
30–60	−0.146	−0.158	−0.170	−0.159	−0.150	−0.153	−0.092	−0.096	−0.083	−0.127
60–100	−0.139	−0.145	−0.147	−0.134	−0.118	−0.159	−0.084	−0.103	−0.016	−0.083
100–150	−0.047	−0.058	−0.092	−0.048	−0.020	−0.052	−0.030	−0.007	0.059	0.001
150–300	0.028	0.015	0.001	0.033	0.019	0.031	0.047	0.054	0.060	0.019
300–600	−0.013	0.013	0.027	0.033	0.021	0.014	0.022	0.012	0.014	0.011
600–1,000	0.016	0.014	0.022	0.025	0.020	0.013	0.018	0.004	0.013	0.007
1,000–2000	0.004	0.014	0.027	0.037	0.032	0.025	0.026	0.020	0.028	0.026

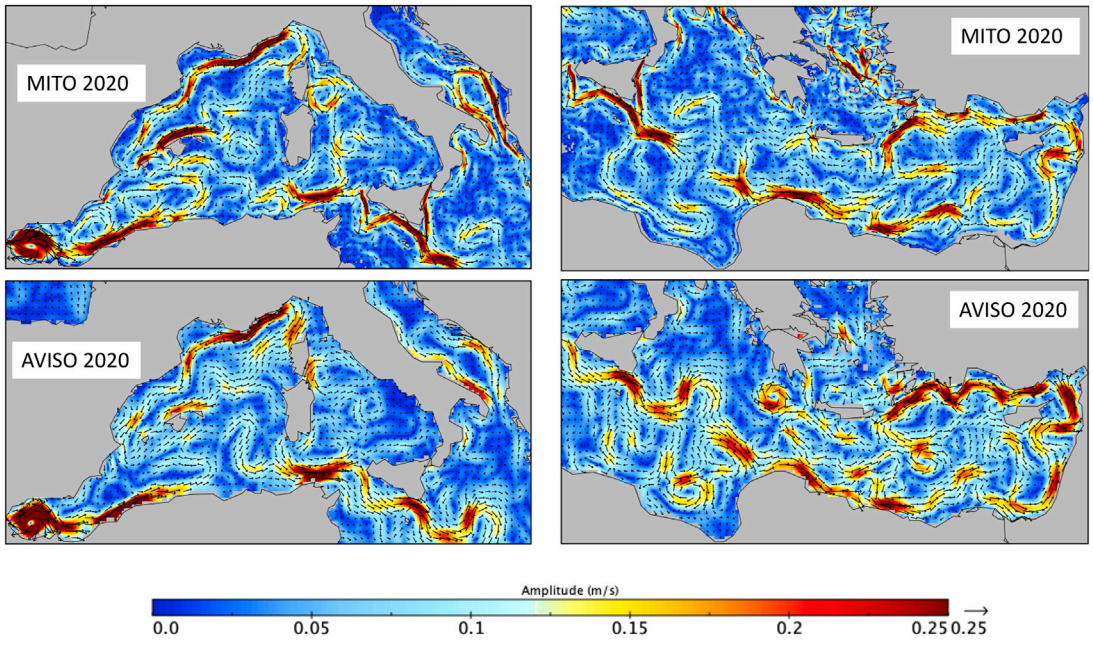

FIGURE 6
Average 2020 circulation in the western and central Mediterranean. MITO circulation at 30 m of depth in the left panels; geostrophic reconstruction from altimeter data (AVISO) in the right panels.

the water column. In the first 30 m model temperatures are lower than those observed, consistently with the results obtained for SST (Section 2.2). Between 60 and 150 m, the bias is slightly higher and changes sign, to reverse again in the deep layers. Model salinity is generally lower than the observations in the surface layers.

The monthly biases computed for temperature (A) and salinity (B) are shown in Table 3. The temperature bias exhibits moderate seasonal variability; it is higher in spring and summer and quite low in December and March. The corresponding values for salinity do not indicate significant variations along the year.

Circulation

Surface circulation

The annual averages of the surface circulation (30 m of depth) for the western and eastern basins are shown in Figure 6 (upper panels), and compared with the average geostrophic flow reconstruction by AVISO (lower panels). It can be seen that the model reproduces all the well-known circulation features of the western basin, namely: the Algerian Current, the Liguro-Provençal Current, the cyclonic gyre in the Gulf of Lion, the cyclone-anticyclone dipole in the north Tyrrhenian, the Atlantic Ionian Stream (AIS), which meanders in the channel of Sicily, the anticyclonic region in the south of the Ionian, and the cyclonic gyre of the south Adriatic. The model features are in very good agreement with those present in the average geostrophic flow. There are some differences, however. Currents tend to be stronger in the model circulation, which is something that could be expected, because the model resolution is much higher than that of the altimeter maps, and we can consequently resolve mesoscale dynamics that are not well captured in the latter. Moreover, the model includes ageostrophic dynamics induced by nonlinear advection and wind-driven dynamics that are missing in the altimetric reconstruction. There are also local details not resolved in the average geostrophic reconstruction. An example is the current, with a strong tidal component, that originates in the Messina Strait (the very narrow passage between the eastern tip of Sicily and the western tip of Calabria, in the southern Italy) and borders the eastern coast of Sicily.

Results for the eastern Mediterranean are also very good. Here we recognize the Ionian current that enters the Levantine and flows cyclonically along the coasts of the basin, forming large meanders including mesoscale structures. The model also reproduces well the cyclonic region represented by the gyre of Rhodes and the anticyclonic gyres such as Mersha Mathrut, Shikmona, and Ierapetra.

It is interesting to note that both the model circulation and the geostrophic reconstruction from satellite data indicate the presence of an overall cyclonic circulation in the northern Ionian. This region has recently been the focus of many investigations (e.g., Borzelli et al., 2009; Menna et al., 2019; Notarstefano et al., 2019), because of the presence of the so-called North Ionian Gyre (NIG) oscillation, a periodic reversal of the circulation, observed a few times in the last decades, which appears to have a nearly decadal time scale. This phenomenon, whose causes are not yet entirely clear, influences the transport of less salty surface water in the Levantine basin. ADT maps for the Ionian Sea, for the years from 2018 to 2020, with the corresponding geostrophic reconstructions of the circulation superimposed, are displayed in Figure 7. The figure shows that the anticyclonic cell intruding the north Ionian (above 36°N, and approximately in the range 16°–19°E), still present in 2018, becomes weak in 2019, where a cyclonic cell starts to grow. The latter becomes dominant in 2020, filling the whole north Ionian, and the Atlantic Ionian Stream (AIS) coming from the Sicily Channel directly flows in the middle Ionian, heading towards the Levantine basin. This indicates that the third anticyclonic phase of the NIG (Menna et al., 2019; Notarstefano et al., 2019) has apparently lasted only a few years.

Examples of local dynamics

An example of the effects of high resolution is given in Figure 8, where we compare the average circulation of July 2020 in the Gulf of Lion, at 10 m, produced by MITO (b) with the July average of the ADT in the area, with the corresponding geostrophic circulation superimposed (a).

The model surface circulation is very similar to that derived from ADT data. The main feature in both fields is a westward coastal current, with a wide cyclonic circulation on the offshore side. This current is part of the wide cyclonic cell present in the northern portion of the western Mediterranean (Ligurian-Provençal basin). The model field has more details in the inner portion of the gulf, revealing a cyclone-anticyclone pair, with a smaller anticyclone near coast, to the west. Indications of the presence of these small-scale structures can be found in the turbidity map (K490; data from the CMEMS portal) of July 18th, shown in panel (c) of the figure. The image shows the presence of two coastal plumes in the inner part of the gulf. The westernmost plume bifurcates while heading towards south, with a branch that veers towards the coast, exactly in the region in which is the boundary of a small coastal anticyclone present in the model map. This small structure could not be resolved in the altimeter maps. On the other hand, the small eastern branch may be consistent with the presence of the anticyclonic pole of the dipole previously noted. The strongest plume, which corresponds to the outflow of the Rhone river, is also initially directed southward, but then gets trapped by the westward current; the main branch veers towards south-west, and a small branch towards south-east, bordering the wide cyclonic circulation present both in the ADT and model maps.

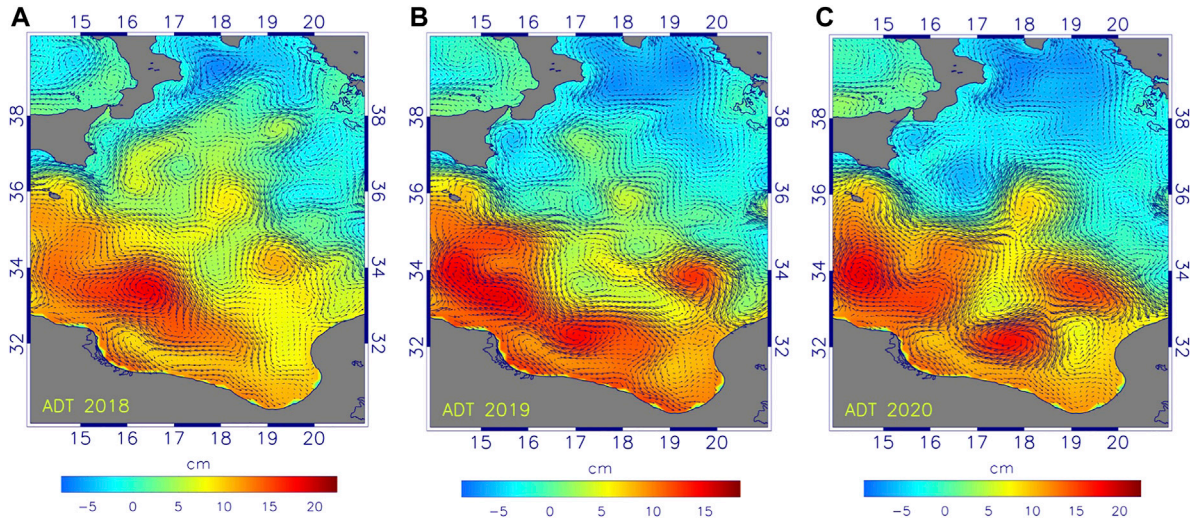

FIGURE 7
Average ADT maps in the Ionian region, for the years 2018 **(A)** 2019 **(B)** and 2020 **(C)**, with the corresponding geostrophic circulations superimposed. The anticyclonic cell still present in the northern Ionian in 2018 is rapidly destroyed.

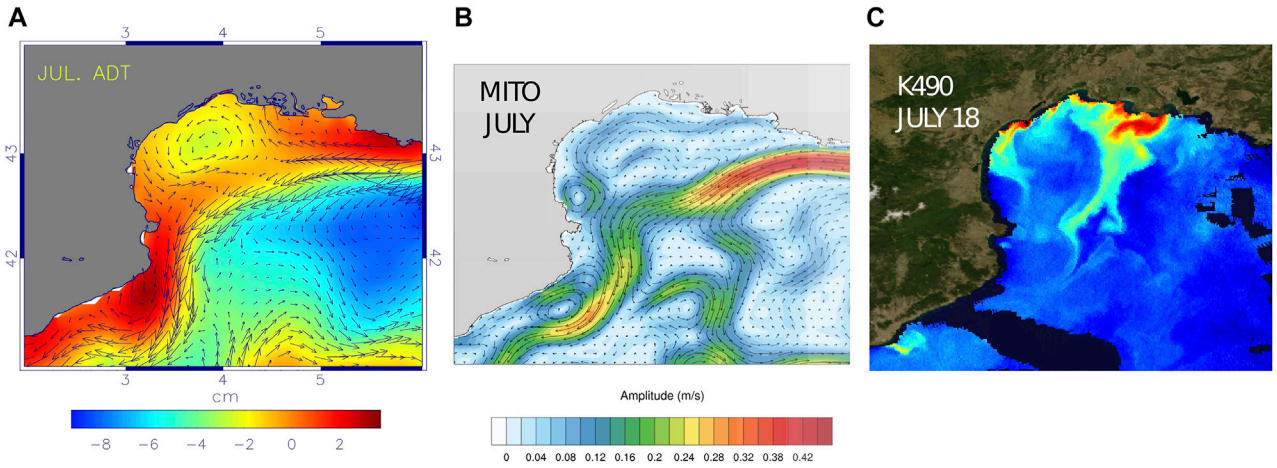

FIGURE 8
Average July surface circulation in the area of the Gulf of Lion: **(A)** ADT (colors), with a geostrophic reconstruction of the circulation superimposed (AVISO, satellite data); **(B)** MITO currents at 10 m; **(C)** map of K490 (coefficient of light extinction at 490 nm) measured from satellite, for July 18.

Overall, this example indicates that the model is indeed capable of capturing mesoscale structures with sizes of few tens of kilometers.

Another area in which the description of small-scale dynamics is crucial is the Messina Strait, where the dynamics are deeply influenced by the tidal forcing. It has been shown in Palma et al. (2020) that MITO correctly describes the tidal dynamics in the area, and, despite the non-optimal resolution, is capable of reproducing the strong currents observed inside the strait, which can exceed 2 m/s. Figure 9 shows maps of the circulation and temperature, at 25 m of depth, for 31 August 2020, in the area surrounding the strait, taken from the site in which results from the operational system are displayed, and constantly updated (https://climaweb.casaccia.enea.it/en/MITO/). The small red patch just south of the strait marks a strong tidally

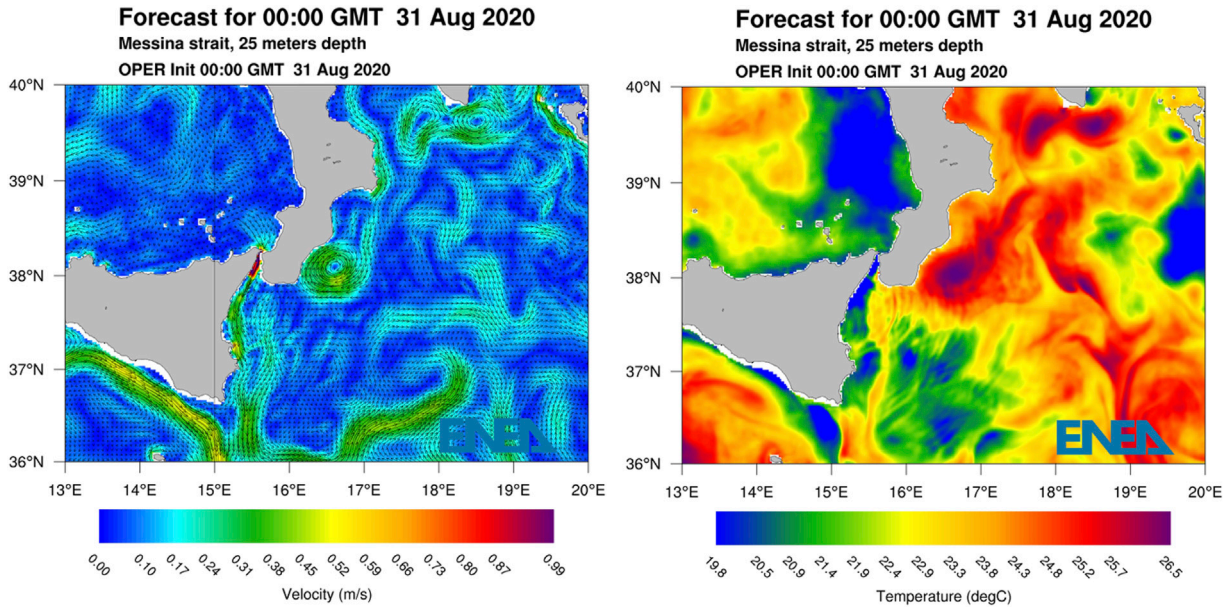

FIGURE 9
MITO maps of circulation and temperature at 25 m of depth, for 31 August 2020, in a wide region around the Messina Strait. The maps are taken from the website (climaweb.casaccia.enea.it/mito) where daily forecast data from the operational system are made available for visualization purposes.

modulated current that then flows along most of Sicily's eastern coast (see Bohm et al., 1987, for experimental observations of the dynamics in the area). In the same region, the map of temperature shows the presence of a cold tongue that appears to originate in the southeastern corner of the Tyrrhenian Sea. Another interesting feature revealed by the temperature map is the presence of a wave-train that propagates towards south-east in the Ionian Sea.

Sea level

Comparison with absolute dynamic topography data

The sea surface elevation predicted by the model was compared with the AVISO altimetric data, which integrates data from all the available altimeters on board of different satellites, to yield ADT maps covering the Mediterranean Sea and part of the Atlantic and of the North Sea, at a uniform spatial resolution of 1/8° (about 14 km), both in latitude and longitude.

We have compared the weekly series of modelled elevation anomalies (with respect to the annual mean) to the corresponding series of mean ADT anomalies. Although daily data are in fact available, we have chosen to use weekly averages, because spectral analysis of the ADT time series shows no significant component with periods below 7–10 days.

A quantitative measure of the agreement between the observed and modelled elevation is provided by the map of the pointwise time correlation between the two time series, which is displayed in the top panel of Figure 10. In the lower panel of the same figure is the map of the 2020 ADT error obtained from AVISO data. The figure shows that the correlation is high (about 0.6 or more) in most of the basin, and highest in the eastern Mediterranean. There are small areas, particularly in the western basin, with low values of the correlation, located along the paths of the main currents systems (Algerian Current, Tyrrhenian Northern Current, Liguro-Provencal current, Atlantic stream in the Sicily Strait). This indicates that significant high frequency mesoscale variability associated with these currents is not fully captured by the altimeter observations. It should also be noted that some regions of low correlation correspond to regions with higher values of the ADT error, e.g., Algerian basin). We finally note that another possible reason for low correlation is that the model does not include the steric component, which can be locally important. Considering all these limitations, the agreement with the observations can be considered as satisfactory.

Table 4 shows regional averages (over the eight regions defined in Figure 2) of the RMSD and of the time correlation, which show consistency, since lower values of the RMSD and higher values of the correlation are found in the eastern basin. The RMSD values are just a little higher than the typical values for the Copernicus operational model, where the comparison between observed and simulated values was made along the satellite tracks.

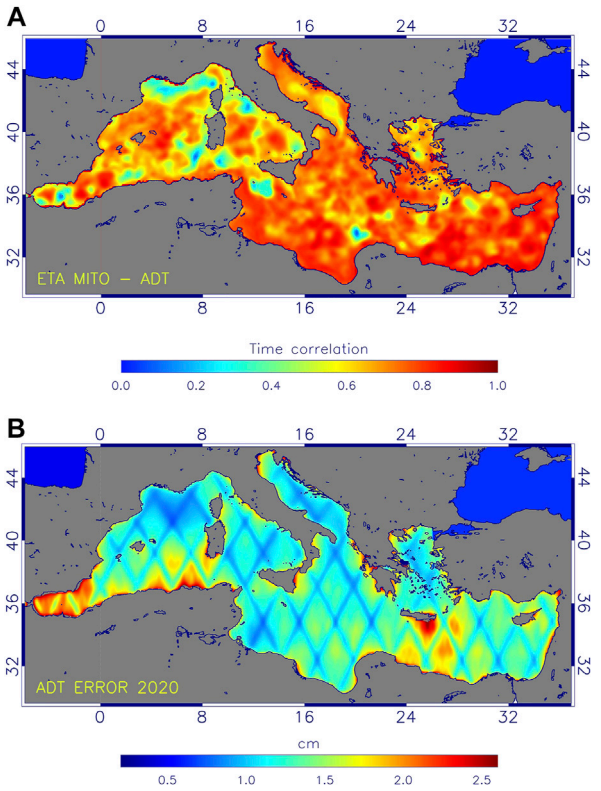

FIGURE 10
(A) SSH time correlation map between MITO and AVISO data. **(B)** AVISO error map for 2020 (units are in cm).

TABLE 4 RMSD between the free surface of MITO and AVISO data (SSH anomaly).

Region	RMSD (cm)	Time correl
1	6.01	0.62
2	5.67	0.63
3	5.33	0.62
4	5.12	0.71
5	5.41	0.74
6	6.34	0.67
7	5.85	0.70
8	5.46	0.76

Coastal sea level

The predicted sea level heights were compared with the tide gauge measurements available for 2020 (55 stations, see left top panel of Figure 11). The 2020 observations are concentrated in the western Mediterranean and all along the Italian coasts. Comparisons were made using the model grid point closest to the station, at the time closest to that measured.

The other panels of Figure 11 show histograms of the correlation coefficients between model and observed data, for the four seasons; in most of the cases the coefficients are higher than 0.85. This seems a very good result, considering that the model grid points can be quite far from the stations, and that the local bathymetry is not resolved with great detail.

By way of example, we show in the left lower panels of the figure the comparison between the time series of measured and observed elevation in four of the stations, for the month of January in SanBenedetto del Tronto and Sciacca, June in Porto Cristo, and July in Cagliari.

Tidal effects

The tidal behavior has been thoroughly investigated in Palma et al. (2020), where it has been shown that the model reproduces both the barotropic and the baroclinic tide very well. It was also shown in that work that tides significantly modulate the transport, not only through the Strait of Gibraltar and the Strait of Sicily, but also through the Corsica Channel and the Strait of Otranto. The tidal effects also modify some characteristics of the circulation inside the basin; in some cases, topographic waves are excited and get trapped by the bathymetry, producing diurnal rotations of the currents. Examples of this phenomenon have been found in the Sicily Channel (on the Adventure Bank and on the Malta Plateau), in the Corsica Channel and in the Strait of Otranto. Furthermore, in different areas of the basin (Channel of Sicily, Channel of Corsica, Strait of Messina, Northern Adriatic Sea), spectral analysis of the average kinetic energy reveals the presence of spectral peaks corresponding to periods of approximately 8 and 6 h, which can be interpreted as harmonics (overtides and compounds) of the diurnal and semi-diurnal tide components, generated through non-linear interactions.

We have found similar results analyzing the 2020 forecasts. For example, the mean kinetic energy power spectrum (not shown) for the region over the Adventure Bank shows dominant diurnal components, which are accompanied by significant semidiurnal components, and also by quite strong peaks corresponding to nonlinear harmonics (periods of 8 and 6 h).

Conclusion

We have described the main features of MITO, a new operational system for the forecasting of the Mediterranean circulation that is running since 2018, and performed a detailed evaluation of its performances, by comparing the forecasts of the year 2020 with a variety of experimental data.

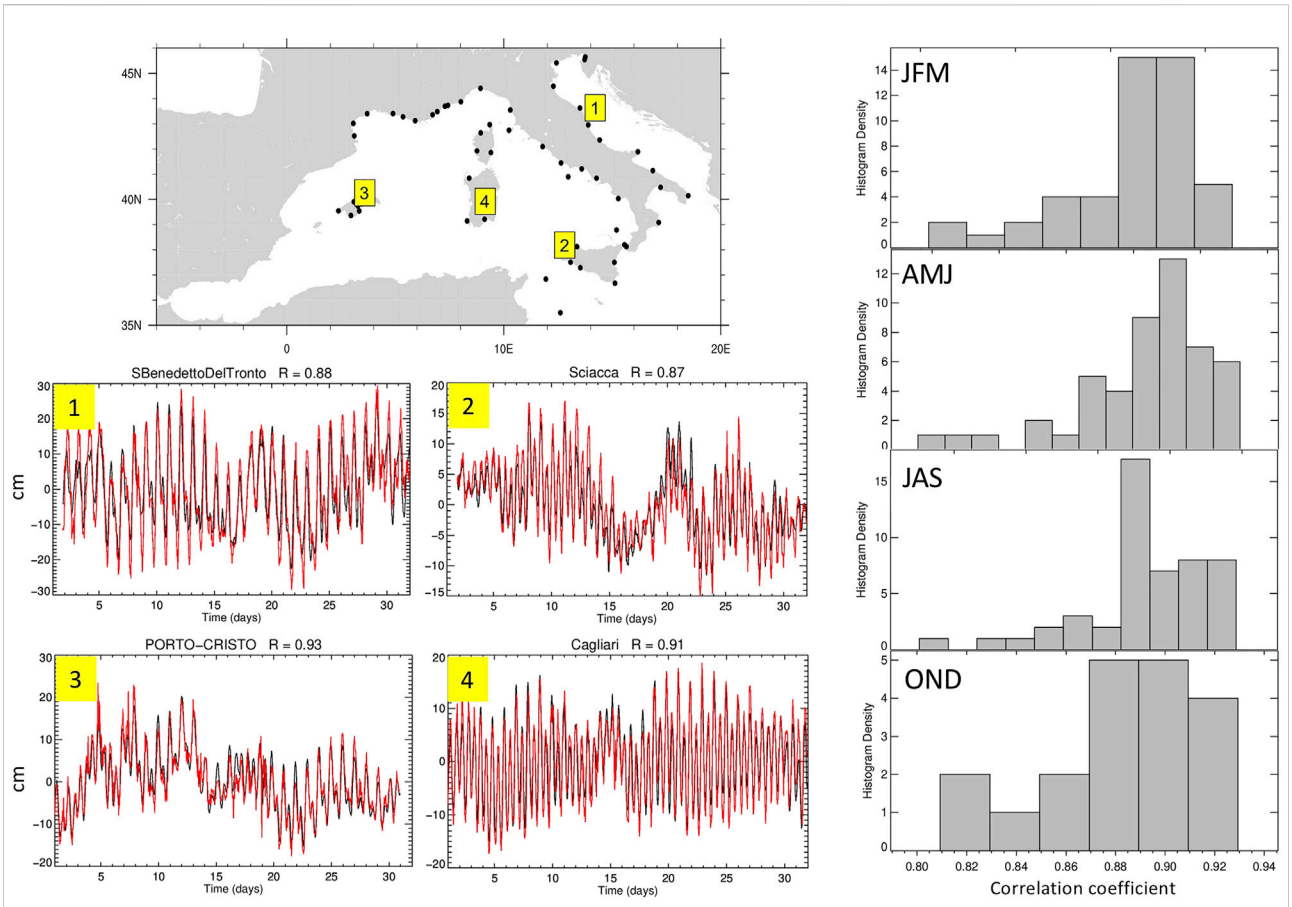

FIGURE 11
Left top panel: tidal stations for which elevation data are available for the year 2020 (not always with continuous coverage). The other panels show histograms of the correlation coefficients between model and observed data, for the four seasons (right) and January sea surface elevation time series at four stations (San Benedetto del Tronto, Sciacca, Porto-Cristo, and Cagliari, marked by the numbers 1,2,3, and 4 in the map. Observations are in black, and MITO data in red. Units are in cm.

The model-data comparison revealed that the hydrological structure and the circulation are generally in good agreement with the observations. The model was also found to correctly reproduce robust mesoscale structures, and the tide-induced sea level variability in coastal areas. This indicates that the MITO system could be successfully used to nest higher resolution coastal models.

There are aspects that could be improved, and will be the object of future development. The first naturally concerns the inclusion of data assimilation, which could improve the quality of the initial conditions. We have found that the surface temperature shows a larger bias (albeit generally well below 1°C) during the summer phase. This may be due to various problems, including for example the quality of the atmospheric forcing, especially for what concerns the short-wave radiation, which is the component of the total heat flux that modulates the diurnal variability of the SST. Other errors could contribute to the cold bias, such as atmospheric forecast errors due to a bad cloud cover representation or to numerical schemes. Note also that the diurnal SST cycle reproduced by the model is in qualitative agreement with the observation, but with a smaller range of variation. Another issue that could be interesting to consider is the fact that the extinction coefficient of short-wave radiation, which is here taken as constant, as it is usually done, may instead have seasonal and regional variability. Satellite products could be of help in addressing this issue. Salinity in the surface layer has also been found to have a bias with respect to experimental data in some regions, indicating that the components of the E-P-R budget should be further examined to improve the agreement with the observations. The inclusion of additional tidal components could also be envisaged, to have a more complete representation of the tidal forcing.

Nevertheless, we believe that the MITO system, thanks to its high resolution and to the capability of describing the linear and nonlinear dynamics induced by tidal forcing, may represent a useful tool in support of a wide spectrum of applications focusing on coastal areas, including energy extraction.

We finally note that the archive of short-term forecasts produced through the years, providing a long-term, high-resolution description of the evolution of the Mediterranean dynamics, will allow in the future for the investigation of the basin variability on time scales of climatic interest. Such archive could also be used as a training set for machine learning applications, for the exploration of alternative forecasting approaches.

Data availability statement

The raw data supporting the conclusions of this article will be made available by the authors, without undue reservation.

Author contributions

GS and AC: implemented the model. EL: performed the run, GS, RI, AC, EN, GP, MVS, and MP: designed the analysis, RI, AC, MP, and EN: performed the analysis. All the authors contributed to writing the paper.

Acknowledgments

The authors gratefully acknowledge the financial support from MISE, and from the EU-CEF DYDAS (Dynamic Data and Analytic Services) Project (https://www.dydas.eu/).

Conflict of interest

The authors declare that the research was conducted in the absence of any commercial or financial relationships that could be construed as a potential conflict of interest.

Publisher's note

All claims expressed in this article are solely those of the authors and do not necessarily represent those of their affiliated organizations, or those of the publisher, the editors and the reviewers. Any product that may be evaluated in this article, or claim that may be made by its manufacturer, is not guaranteed or endorsed by the publisher.

References

Barbarelli, S., Florio, G., Amelio, M., and Scornaienchi, N. M. (2018). Preliminary performance assessment of a novel on-shore system recovering energy from tidal currents. *Appl. Energy* 224, 717–730. doi:10.1016/j.apenergy.2018.05.029

Bohm, E., Magazzu, G., Wald, L., and Zoccolotti, M. L. (1987). Coastal currents on the Sicilian shelf south of Messina. *Oceanol. Acta* 10 (2), 137–142.

Borzelli, G., Gacic, M., and Civitarese, G. (2009). Eastern mediterranean transient and reversal of the Ionian Sea circulation. *Geophys. Res. Lett.* 36 (15). doi:10.1029/2009GL039261

Buongiorno Nardelli, B., Tronconi, C., Pisano, A., and Santoleri, R. (2013). High and ultra-high resolution processing of satellite Sea surface temperature data over southern European seas in the framework of MyOcean project. *Remote Sens. Environ.* 129, 1–16. doi:10.1016/j.rse.2012.10.012

Clementi, E., Aydogdu, A., Goglio, A. C., Pistoia, J., Escudier, R., Drudi, M., et al. (2021). *Mediterranean Sea analysis and forecast (CMEMS MED-currents, EAS6 system) (version 1) [data set]*. Copernicus Monitoring Environment Marine Service (CMEMS). doi:10.25423/CMCC/MEDSEA_ANALYSISFORECAST_PHY_006_013_EAS6

Coiro, D. A. P., Troise, G., Ciuffardi, T., and Sannino, G. (2013). "Tidal current energy resource assessment: the strait of Messina test case," in *International conferencs on clean electrical power (ICCEP)* (Alghero,Italy: IEEE), 213–220.

Davidson, F., Alvera-Azcárate, A., Barth, A., Brassington, G. B., Chassignet, E. P., Clementi, E., et al. (2019). Synergies in operational oceanography: The intrinsic need for sustained ocean observations. *Front. Mar. Sci.* 6, 450. doi:10.3389/fmars.2019.00450

de Ruggiero, P., Napolitano, E., Iacono, R., and Pierini, S. (2016). A high-resolution modelling study of the circulation along the Campania coastal system, with a special focus on the Gulf of Naples. *Cont. Shelf Res.* 122, 85–101. doi:10.1016/j.csr.2016.03.026

Doney, S. C., Nijar, R., and Stewart, S. (1995). Photochemistry, mixing and the diurnal cycles in the upper ocean. *J. Mar. Res* 53, 341–369.

Ezer, T., and Mellor, G. L. (1994). Diagnostic and prognostic calculations of the North Atlantic circulation and sea level using a sigma coordinate ocean model. *J. Geophys. Res.* 99 (7), 14159–14171. doi:10.1029/94JC00859

Fernandez, V., Lara-Lopez, A., Eparkhina, D., Cocquempot, L., Lochet, C., and Lips, I. (Editors) (2021). "Advances in operational oceanography: Expanding Europe's ocean observing and forecasting capacity," in Proceedings of the 9th EuroGOOS International Conference, Brussels, Belgium, May 3–5, 2021 (EuroGOOS), 574 pp. Available at: https://archimer.ifremer.fr/doc/00720/83160/ [Online].

Kallos, G., Papadopoulos, A., Katsafados, P., and Nickovic, S. (2006). Transatlantic saharan dust transport: Model simulation and results. *J. Geophys. Res.* 111, D09204. doi:10.1029/2005JD006207

Kallos, G., Nickovic, S., Papadopoulos, A., Jovic, D., Kakaliagou, O., Misirlis, N., et al. (1997). "The regional weather forecasting system SKIRON: An overview," in *Proceedings of the symposium on regional weather prediction on parallel computer environments* Editor B. George, V. Kallos, and K. Kotroni (Athens, Greece: Lagouvardos), 109–122.

Marshall, J., Hill, C., Perelman, L., and Adcroft, A. (1997a). Hydrostatic, quasi-hydrostatic, and nonhydrostatic ocean modeling. *J. Geophys. Res.* 102, 5733–5752. doi:10.1029/96jc02776

Marshall, J., Adcroft, A., Hill, C., Perelman, L., and Heisey, C. (1997b). A finite-volume, incompressible Navier Stokes model for studies of the ocean on parallel computers. *J. Geophys. Res.* 102, 5753–5766. doi:10.1029/96jc02775

Marullo, S., Minnet, P. J., Santoleri, R., and Tonani, M. (2016). The diurnal cycle of sea-surface temperature and estimation of the heat budget of the Mediterranean Sea. *J. Geophys. Res. Oceans* 121 (11), 8351–8367. doi:10.1002/2016jc012192

Menna, M., Reys Suarez, N. C., Civitarese, G., Gačić, M., Rubino, A., and Poulain, P. M. (2019). Decadal variations of circulation in the Central Mediterranean and its interactions with mesoscale gyres. *Deep Sea Res. Part II Top. Stud. Oceanogr.* 164, 14–24. doi:10.1016/j.dsr2.2019.02.004

Napolitano, E., Iacono, R., and Marullo, S. (2014). "The 2009 surface and intermediate circulation of the Tyrrhenian Sea as assessed by an operational model," in *The Mediterranean Sea: Temporal variability and spatial pat- terns, geophysical monograph*. Editors G. L. E. Borzelli, M. Gacic, P. Lionello, and P. Malanotte-Rizzoli. 1st ed. (Washington DC: American Geophysical Union, published by Wiley), 59–74.

Napolitano, E., Iacono, R., Sorgente, R., Fazioli, L., Olita, A., Cucco, A., et al. (2016). The regional forecasting systems of the Italian seas. *J. Operational Oceanogr.* 9, s66–s76. doi:10.1080/1755876X.2015.1117767

Naranjo, C., Garcia-Lafuente, J., Sannino, G., and Sanchez-Garrido, J. C. (2014). How much do tides affect the circulation of the Mediterranean Sea? From local processes in the strait of Gibraltar to basin-scale effects. *Prog. Oceanogr.* 127, 108–116. doi:10.1016/j.pocean.2014.06.005

Nikolaidis, G., Karaolia, A., Matsikaris, A., Nikolaidis, A., Nicolaides, M., and Georgiou, G. C. (2019). Blue energy potential analysis in the mediterranean. *Front. Energy Res.* 7, 62. doi:10.3389/fenrg.2019.00062

Notarstefano, G., Menna, M., and Legas, F. (2019). Reversal of the northern ionian circulation in 2017. *J. Ope. Oce* 1, 108–111. Copernicus Marine Service Ocean State Report, Issue 3. doi:10.1080/1755876X.2019.1633075

Oddo, P., Adani, M., Pinardi, N., FratianniTonani, C, M., and Pettenuzzo, D. (2009). A nested Atlantic-Mediterranean Sea general circulation model for operational forecasting. *Ocean. Sci.* 5, 461–473. doi:10.5194/os-5-461-2009

Palma, M., Iacono, R., Sannino, G., Bargagli, A., ACarillo, A., Fekete, M., et al. (2020). Short-term, linear, and non-linear local effects of the tides on the surface dynamics in a new, high-resolution model of the Mediterranean Sea circulation. *Ocean. Dyn.* 70, 935–963. doi:10.1007/s10236-020-01364-6

Papadopoulos, A., and Katsafados, P. (2009). Verification of operational weather forecasts from the POSEIDON system across the Eastern Mediterranean. *Nat. Hazards Earth Syst. Sci.* 9, 1299–1306. doi:10.5194/nhess-9-1299-2009

Pisacane, G., Sannino, G., Carillo, A., Struglia, M. V., and Bastianoni, S. (2018). Marine energy exploitation in the mediterranean region: Steps forward and challenges. *Front. Energy Res.* 6, 109. doi:10.3389/fenrg.2018.00109

Sannino, G., Carillo, A., Pisacane, G., and Naranjo, C. (2015). On the relevance of tidal forcing in modelling the Mediterranean thermohaline circula- tion. *Prog. Oceanogr.* 134, 304–329. doi:10.1016/j.pocean.2015.03.002

Schiller, A., and Brassington, G. B. (Editors) (2011). *Operational oceanography in the 21st century* (Dordrecht, Netherlands: Springer). doi:10.1007/978-94-007-0332-2

Stathopoulos, C., Kaperoni, A., Galanis, G., and Kallos, G. (2013). Wind power prediction based on numerical and statistical models. *J. Wind Eng. Industrial Aerodynamics* 112, 25–38. doi:10.1016/j.jweia.2012.09.004

Zhang, T. L., Xiao, R., Cao, Q., Zhang, Y., Qu, Q., Wang, Z., et al. (2022). Interactive effects of ocean acidification, ocean warming, and diurnal temperature cycling on antioxidant responses and energy budgets in two sea urchins Strongylocentrotus intermedius and Tripneustes gratilla from different latitudes. *Sci. Total Environ.* 824. doi:10.1016/j.scitotenv.2022.153780

frontiers | Frontiers in Energy Research

TYPE Original Research
PUBLISHED 29 August 2022
DOI 10.3389/fenrg.2022.944417

OPEN ACCESS

EDITED BY
Siamak Hoseinzadeh,
Sapienza University of Rome, Italy

REVIEWED BY
Mamdouh El Haj Assad,
University of Sharjah, United Arab Emirates
Shahin Shoeibi,
Islamic Azad University Semnan, Iran
Hamed Kariman,
Shahid Beheshti University, Iran
Farbod Esmaeilion,
K. N. Toosi University of Technology, Iran

*CORRESPONDENCE
Giovanna Pisacane,
giovanna.pisacane@enea.it

SPECIALTY SECTION
This article was submitted to Sustainable Energy Systems and Policies, a section of the journal Frontiers in Energy Research

RECEIVED 15 May 2022
ACCEPTED 27 July 2022
PUBLISHED 29 August 2022

CITATION
Carillo A, Pisacane G and Struglia MV (2022), Exploitation of an operative wave forecast system for energy resource assessment in the Mediterranean Sea.
Front. Energy Res. 10:944417.
doi: 10.3389/fenrg.2022.944417

Exploitation of an operative wave forecast system for energy resource assessment in the Mediterranean Sea

Adriana Carillo, Giovanna Pisacane* and Maria Vittoria Struglia

Climate Modeling Laboratory, Division Model and Technologies for Risk Reduction, Department for Sustainability, ENEA, Rome, Italy

Ocean Energy is now emerging as a viable long-term form of renewable energy, which might contribute around 10% of EU power demand by 2050, if sufficient support is guaranteed along its road to full commercialization, allowing to further demonstrate the reliability, robustness and overall economic competitiveness of technologies. Although wave energy is still less developed than other marine renewables, its high density, great potential and minimal environmental impact have renewed the interest of developers, investors and governments globally, also in view of the increasing awareness of climate change and of the necessity to reduce carbon emissions. In parallel with technological development, the reliable characterization of wave climate and of the associated energy resource is crucial to the design of efficient Wave Energy Converters and to an effective site-technology matching, especially in low-energy seas. The preliminary scrutiny of suitable technologies and the identification of promising sites for their deployment often rely on wave climatological atlases, yet a more detailed characterization of the local resource is needed to account for high-frequency spatial and temporal variability that significantly impact power generation and the economic viability of WEC farms. We present a high-resolution assessment of the wave energy resource at specific locations in the Mediterranean Sea, based on a 7-years dataset derived from the operative wave forecast system that has been developed at ENEA and has been running since 2013. The selected areas correspond to the target regions of the Blue Deal project, where energy resource estimates were combined with technical and environmental considerations, so as to identify optimal sites for Blue Energy exploitation, from a Maritime Spatial Planning perspective. The available resource at selected sites is analysed together with site theoretical productivity for three state-of-the art WECs, showing interesting potential for future deployment.

Abbreviations: CapEx, capital expenditure; C_f, capacity factor; CR-n, *n*th candidate site at Crete island; CY-n, *n*th candidate site at Cyprus island; CWR, capture width ratio; E_a, mean available wave energy; H_s, significant wave height; IEC, international electrotechnical commission; IRENA, international renewable energy agency; ISWEC, inertial sea wave converter; J, energy flux per meter of wave crest; LCOE, levelized cost of energy; ML-n, *n*th candidate site at Malta island; OpEx, operating expenditure; P, power matrix of WEC device; PTO, power take off; P_E, average power output; P_n, nominal power; P_w, omnidirectional mean wave power; T_e, energy period; T_p, peak period; TS, technical specifications; WAM, wave model; WEC, wave energy converter.

KEYWORDS

wave energy, energy resource assessment, Mediterranean sea, wave forecast system, marine spatial planning

1 Introduction

Except for the years of the pandemic, global energy demand has been steadily increasing in the last decades, still mainly relying on fossil fuels, which are currently responsible for around three-quarters of the global greenhouse gas emissions, while renewables appear to only meet around half the increase through 2022 (IEA 2021a). On the other hand, the political consensus has been growing on the necessity to reduce global carbon dioxide emissions to net zero by 2050, consistently with the Paris Agreement resolution to limit the long-term increase in average global temperatures below 2°C, and to pursue efforts to limit it to 1.5°C. Nevertheless, although pledges to achieve such goal have been made by countries that are responsible for around 70% of global emissions, such commitments are not yet accompanied by the necessary near-term policies and measures, and fail to envisage a radical and effective transformation of how we produce, transport and consume energy (IEA 2021b). As a matter of fact, production from renewable sources is indeed projected to meet most of the increase in global electricity demand in the near future (up to 2024), yet such positive trend would only result in a plateauing of emissions (IEA 2022).

In June 2021, the EU adopted a European Climate Law, establishing the aim of reaching net zero greenhouse gas emissions in the EU by 2050, thus committing itself to achieve the goal set out in the *European Green Deal* (EU Commission, 2019) for Europe's economy and society to become climate-neutral to that date. Intermediate targets are set, namely that of reducing net greenhouse gas emissions by at least 55% by 2030, compared to 1990 levels (EU Regulation, 2021). In this context, the *Renewables Directive 2018/2001/EU* (EU Directive, 2018) established a binding renewable energy target for the EU of at least 32% of renewable energy sources in the overall energy mix, to be reached by 2030. Such limit is currently being revised to at least 40% by 2030, which means doubling the current renewables share in just a decade, with the aim to also boost an economic sector with remarkable potential to create jobs, growth and trade (EU Proposal, 2021). In November 2020, the EU issued its Strategy to harness the potential of offshore renewable energy (EU Commission, 2020), recognizing the maturity that offshore wind technologies have reached since the first installation of an offshore wind farm off the southern coast of Denmark in 1991, as well as the ongoing rapid development of a range of promising energy converters, such as wave or tidal, floating photovoltaic installations and the use of algae to produce biofuels. The European Commission has committed to support the value chain of this now fully emerged sector, supporting the creation of industrial opportunities and green jobs across the continent, as the marine renewables industry is required to scale up 5 times by 2030 and 25 times by 2050 to support the Green Deal's objectives, at the same time meeting its environmental constraints.

Among marine renewables, ocean waves are recognized as one of the most promising sources of clean, reliable, and renewable energy, with an estimated potential that is theoretically equivalent to more than double the world's current electricity demand (IRENA 2020). Nevertheless, the full exploitation of Wave Energy Converters (WECs) is still hindered by deficiencies in wave resource assessments, often overlooking relevant non-linear processes that affect the reliability of theoretical estimates (Hong et al., 2021; Tran et al., 2021), as well as by the need to better characterize their performance in complex multi-device configurations and to develop efficient control systems (Gallutia et al., 2022). In general, WECs have yet to reach the level of commercial viability that would guarantee their competitiveness with alternative energy sources, especially in the absence of synergetic technologies with the potential for hybridization and/or co-location (Foteinis and Tsoutsos, 2017; Clemente et al., 2021; Petracca et al., 2022). Moreover, despite the considerable efforts in research and development, technological convergence (i.e., a shift towards a common "optimal" design on which to concentrate future research) is yet to be achieved (Hannon et al., 2017; Guo and Ringwood, 2021). One of the reasons for such diversity of WEC concepts is the significant temporal variability of wave energy, ranging from seconds to decades, and making it difficult to focus on a limited range of sea states for WEC optimization, in terms of PTO (Power Take Off), control, survivability, and power prediction and management (Guo and Ringwood, 2021). The current variety of technological options has in fact contributed to delaying the operative exploitation of WECs, through the resulting (i) lack of an adaptable taxonomy that is both analytical and capable of accommodating future technologies, (ii) absence of an agreed coherent and flexible cross-scale method to select optimal locations, from the initial large scale studies for generic feasibility assessments to the effective identification and quantification of costs and trade-offs across the installation, operativity and dismissal phases of a WEC farm, and (iii) difficulty to define a systematic site-technology matching procedure that allows the identification of the best devices to be deployed in a specific location (Bertram et al., 2020).

It should be underlined that filling each such gap represents a step towards the realistic implementation of wave energy farms, and should be considered to all effects as part of the value chain, from the initial concept all the way through its delivery to the

market, and to the constant upgrade of technological solutions. In particular, alongside the development of device-scaling roadmaps and energy-maximizing control systems, enhancing optimal site-technology matching would considerably help shifting the paradigm for wave energy exploitation from the current focus on higher density areas (>25 kW/m) to the due consideration of the so far undervalued milder environments (Lavidas and Blok, 2021).

Despite its mild climate, the Mediterranean Sea in fact offers substantial opportunities for wave energy production, provided the technologies are effectively downscaled to meet the local comparatively low-energy wave conditions (Dialyna and Tsoutsos, 2021). The latter also allow the affordable testing of scale devices designed for harsher environments, and stimulate solutions to increase device efficiency for optimal energy harvesting. (Pisacane et al., 2018). The accentuated vulnerability of the Mediterranean environment indeed demands that the effort be undertaken to pursue the transition towards higher shares of renewable energy, by implementing multi-purpose solutions that simultaneously address greenhouse-gas-emission reduction and climate adaptation. Here, marine energy solutions can in fact prove effective to both generate utility scale grid electricity and increase the value of climate-adaptive infrastructures, such as breakwaters, where WECs can be incorporated with the advantage of combining a limited increase in construction costs with ease of maintenance and coastal protection (Silva et al., 2018; Vicinanza et al., 2019). Besides its cost-effectiveness and low environmental impact, the combination of WECs with other technologies and across different economic sectors would also allow to reduce anthropic pressures on a heavily exploited marine space, for example, through the implementation of multi-functional offshore farms (Wan et al., 2016; Leira, 2017; Foteinis, 2022) that harmonize the needs of the tourism industry and of maritime transport, the exploitation of fisheries and aquaculture (Menicou and Vassiliou, 2010), and the emerging opportunities offered by marine renewables.

This work has been carried out within the Blue Deal Project (https://blue-deal.interreg-med.eu), which addressed many of the highlighted criticalities of WEC deployment in the environmentally sensitive Mediterranean region, by connecting experts from the different fields of engineering and environmental sciences, administrative bodies and citizen organizations, with the aim to both design viable pathways for marine energy exploitation and increase social awareness as to the opportunities offered by the sector. Specifically, the project designed a methodology to coherently address site-technology matching through (i) technology classification and assessment and (ii) preliminary site selection based on energy resource availability, also accounting for the issues posed by environmental protection and by the necessary governance of inter-sectorial competition (Pulselli et al., 2022). Together with the ongoing developmental assessment of devices, these constitute the complementary building blocks of the successful evaluation, selection and implementation of WEC systems, as schematically represented in Figure 1.

In Pulselli et al. (2022), the preliminary selection of the promising sites has mainly relied on monthly wave climatology maps, which were then confronted with the specific requirements of different technologies suitable for the Mediterranean conditions, and overlapped with the spatial distribution of protected areas and critical ecosystems (e.g., Posidonia Oceanica meadows), as well as of the areas reserved for marine traffic. Historical hindcast data are often used to quantify the wave energy resource. Nevertheless, while offering longer time coverage with respect to observations, they are often affected by biases in the estimation of climatological means, and fail to capture the high natural inter-annual variability that characterizes wave climate, as well as climate-change induced variations, due to both insufficient resolution and to the inadequate representation of relevant processes (Mackay et al., 2010a; Mackay et al., 2010b). However, for the Mediterranean Sea, sufficiently long reanalysis hourly time series of wave parameters are now available at a spatial resolution of 1/24° (Korres et al., 2021), which would further allow to characterize wave statistics, so as to better evaluate the projected omnidirectional wave power (P_w) and the expected productivity of a farm, via the performance metrics generally used to compare and rank the prospective operative devices (e.g., average power output, P_E, Capture Width Ratio, CWR, and capacity factor, C_f), ultimately allowing the assessment of their economic performance via the Levelised Cost of Energy (LCoE) (Astariz and Iglesias, 2015). Yet historical data, are not sufficient to support the operativity of offshore devices that need real-time calibration, such as the ISWEC (Inertial Sea Wave Energy Converter), a WEC developed at the Politecnico di Torino (Italy), which underwent full-scale testing offshore Pantelleria Island (Sicily, Italy) (Cagninei et al., 2015). Indeed, the conversion from wave energy to electricity can be affected by variations in the wave spectrum at the sub-daily to daily scales, affecting the efficiency of the power management system, which necessitates accurate high-resolution sea-state predictions up to a few days ahead (Widén et al., 2015). Wave forecasts are in fact crucial across all stages of WEC development, from the design and planning of the wave farm, to its commissioning, operation, maintenance and decommissioning (Mérigaud et al., 2017), and should be considered a permanent element of the industrial process. In addition, by being forced by atmospheric forecasts starting from a data-constrained initial condition, on the long run short-term operative wave forecasts also constitute an ever-expanding dataset, capable of capturing the long-term trends of wave climate that impact WEC optimization and commercial development (Atan et al., 2016; Ulazia et al., 2020). Similarly to historical hindcasts and reanalyses, long time series of operative forecasts can in fact allow the back-testing of climate variability

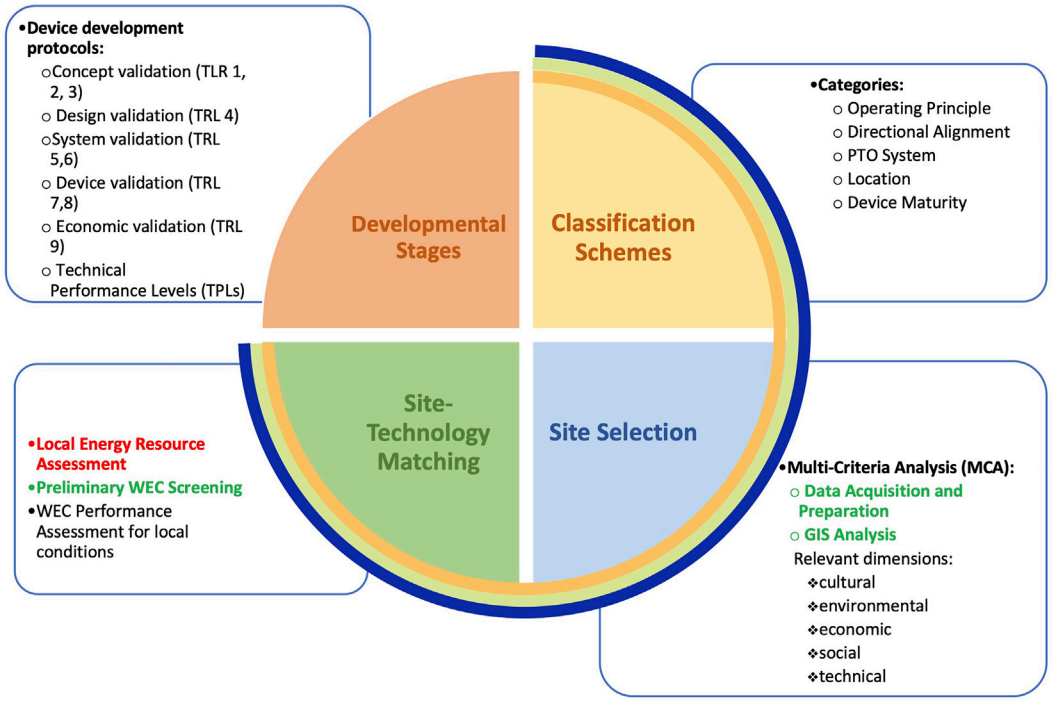

FIGURE 1
Schematic representation of the recommended systematic approach to the deployment of WECs in marine areas. Developmental stages are defined according to functional readiness, as established by the International Structured Development Plan of the International Energy Agency–Ocean Energy Systems (IEA–OES) group (Holmes and Nielsen, 2010). The complementary Technical Performance Levels (TPLs - Weber, 2012) are included in the list, despite their limited applicability, due to the difficulty of generally assessing supplementary cost drivers which are better evaluated in the context of site-specific implementation and are, in fact, usually covered within the site selection and site-technology matching components (e.g., environmental, social and legal acceptability, efficiency, survivability, capital expenditure and lifecycle operational costs). An alternative classification of WEC TRLs can be found in Fitzgerald and Bolund (2012), who also recommend accounting for lifecycle readiness. Classification schemes are based on the categories defined by Lehmann et al. (2017). The three bands in the Blue Deal logo colours encompass the components that have been addressed during the project lifetime, following the indications of the Blue Deal Methodology (Pulselli et al., 2022). The local resource assessment activities that are the object of this paper fall into the site-technology matching component, and are highlighted in red. They rely on results obtained in parallel project tasks (in green). Preliminary WEC screening made in its turn use of the device classification that was carried out during the project, allowing to narrow the number of promising technologies to those that can be effectively deployed in the Mediterranean environment.

and near-future extrapolations, yet with the competitive advantages of early availability and higher-resolution atmospheric forcing [for example, the Korres et al. (2021) reanalysis is forced by 0.25° horizontal-resolution ERA5 data, while ECMWF atmospheric forecasts are released at 0.1°]. On the other hand, mid- to long-term future variations in wave fields characteristics under climate change should be ideally projected via future climate scenario simulations (Reeve et al., 2011), which, however, still retain too large uncertainties from a variety of sources (Wolf et al., 2020) and entail high computational costs, as multiple realizations are needed to adequately sample the phase space of the climate system (Morim et al., 2019). Nevertheless, although this surely represents a critical issue for the sustainability of the energetic transition towards greater shares of marine renewables (Harrison and Wallace, 2005), its treatment is beyond the scope of this work, which only focuses on the present opportunities for WEC deployment in the Mediterranean Sea.

The wave forecast system developed at ENEA has been operatively running since 2014, and it has been extensively employed to provide the ISWEC developers with the necessary forecast for the device calibration (Mattiazzo, 2019). It is used here as a source of wave data over the period 2014–2020, to illustrate the added value of high spatial (1/32°) and time (hourly) resolution for the purpose of site-technology matching. To this end, detailed wave-energy spectra were constructed at selected locations, providing valuable information on the available resource and, after combination with illustrative device power matrices, allow the preliminary assessment of potential site productivity.

Following the description of the data and methods used (Section 2), the results obtained for test sites in Malta, Crete and Cyprus are presented in Section 3, covering mean wave

climate indicators, wave roses, and wave spectra. Section 4 summarizes the integral parameters that characterize wave energy availability at the test sites, as well as standard productivity indices for three state-of-the-art wave converters, allowing direct island inter-comparison; a preliminary analysis of the impact of seasonality on the wave energy resource is also presented. In Section 5, conclusions are drawn and future perspectives outlined.

2 Materials and methods

The presented results generally cover the two bottom sectors of Figure 1, from the preliminary large-scale characterization of the test case area, based on the climatological average of local wave height and period, to the interaction with local authorities aimed at narrowing site selection, to the joint analysis of wave parameters at specific sites and WEC requirements.

The reference framework for the analysis is the ongoing normative process for the wave energy sector synthesized in the International Electrotechnical Commission (IEC) Technical Specifications (TS) for marine energy, namely part IEC-62600-101, that has been specifically dedicated to the wave energy resource across three classes of assessment: reconnaissance (Class 1), feasibility (Class 2), and design (Class 3) (IEC 2015). IEC-62600-101 has been verified to constitute a robust and coherent methodology, providing a set of recommendations and rules that allow accurate wave resource characterization (Ramos and Ringwood, 2016). Nevertheless, the minimum requirements needed for the validation of classes 2 and 3 might prove excessively demanding and, therefore, could be subject to future change (Ramos and Ringwood 2016). The present study mainly focuses on Class 1 assessments for the deployment of offshore wave energy, by exploiting 7 years of projections from the operative wave forecast system for the Mediterranean Sea developed at ENEA (MED-ENEA - https://giotto.casaccia.enea.it/waves/), which has been continuously running since June 2013. The system is based on the WAM model, a third-generation wave model that numerically integrates the basic transport equation for the evolution of a 2D ocean wave spectrum, without resorting to any specific assumption as to the spectral shape (WAMDI-group, 1988). The Cycle 4.5.3 configuration (C4.5.3) was implemented, which improved that of WAM cycle 4 (Günther et al., 1992), by including a new semi-implicit integration scheme for the source function (Herbach and Janssen, 1996), the revised wave dissipation presented in (Bidlot et al., 2007), the wind generation function and dissipation terms described in (Janssen, 1982; Janssen, 1989; Janssen, 1991), and the evaluation of nonlinear interaction source functions through a discrete interaction approximation (Janssen, 2008). The detailed characteristics of WAM C4.5.3 are summarized in Günther and Behrens (2011), who also conducted a thorough validation exercise.

The model configuration meets almost all the TS101 requirements as to the physical processes that need to be explicitly accounted for in Class 1 assessments[1], while it also includes wave breaking and bottom friction (only recommended for Class 2 and 3), and it is even more stringent as to numerical specifications. However, the two neglected components, namely diffraction and wave-current interaction, appear to be especially important near-shore and in shallow waters, or when the interaction between the waves and the devices (possibly aligned in large farms) is to be modelled (Folley, 2017), and they are not critical for the present analysis. Indeed, in such cases the spatial scale of the assessment would need to be much more refined, of the order of tens, or at least hundreds, of meters, and the choice of devices to have already been restricted to a limited number of specific candidates. On the other hand, the temporal, directional and spectral characterization offered by MED-ENEA data is expected to be appropriate for offshore application (Folley, 2017). With respect to low- or intermediate-resolution climatologies based on historical data, the use of high-resolution operative forecasts offers an improved spatial and temporal characterization of wave fields for the preliminary screening of promising sites, and allows the real-time calibration and operability optimization of devices that are being tested at sea, providing effective support for the assessment of their productivity and, ultimately, of their economic sustainability.

The MED-ENEA operative system covers the whole Mediterranean Sea at a spatial resolution of 1/32° (approximately 3.5 km). Starting every day at 00 h from the +24 h sea state forecast from the previous run, hourly time series of wave parameters are predicted for the following 5 days. The system is forced with the wind fields predicted by the atmospheric circulation model SKIRON over the forecast time interval [00 h ÷ 00 h + 120 h], at a resolution of 0.05° × 0.05°, i.e. close to that of the wave model and considerably higher than that of standard reanalyses. SKIRON has been developed by the Atmospheric Modelling and Weather Forecasting Group of the National University of Athens, where it has been operatively running for over 20 years (Kallos, 1997; Papadopoulos et al., 2001).

Over its operating life, MED_ENEA has been validated against in situ-measurements (buoy data), satellite data and reanalyses products, with good results (Carillo et al., 2015a; Carillo et al., 2015b; Memè et al., 2020). The dataset used for this study is constituted by the +24 h forecast from each 5-days simulation, and covers the period 2014–2020. It includes significant wave height, H_s, mean wave power, P_w, energy period T_e, and wave direction, θ.

1 Namely: a) wind-wave growth; b) whitecapping; c) quadruplet interactions; d) triad interactions; e) diffraction; f) refraction; g) wave reflections; h) wave-current interactions.

3 Results

Basin-wide, climatological wave energy resource maps have been presented in Pulselli et al. (2022), who also describe the overall methodology of the Blue Deal systematic approach to marine energy exploitation in the Mediterranean. Here we will focus on the high-resolution results at locations where the feasibility of WEC deployment has emerged, for which the stakeholders manifested interest in exploring realistic viability during the Blue Deal Labs. These are Malta, Crete and Cyprus, which are all located in the least sheltered area of the Mediterranean Sea and are therefore exposed to both the waves generated by the local prevailing winds and to the longer period swell generated by distant weather systems. The following analyses will make use of the minimum H_s threshold for devices to efficiently operate (0.5 m), as indicated by the preliminary device screening exercise. The specific candidate sites have been identified through the multi-criteria analysis for site selection that has been applied to all potentially interesting marine renewable technologies, by jointly considering device requirements in terms of resource availability and depth installation range, environmental constraints, and exclusion zones (e.g., areas reserved for navigation routes). It should be noted that a major constraint for the deployment of marine renewables in the Mediterranean is its steep bathymetry, which causes the costs of WEC mooring systems to increase and forces wind energy technologies to also resort to costly floating structures, as the competing interests of landscape preservation and alternative sea-space use push prospective farms further offshore (Pisacane et al., 2018; Ghigo et al., 2020; Petracca et al., 2022). Together with wind data, accurate wave characterization is therefore also crucial in the design phase of floating platforms for offshore wind deployment at specific locations, also in combination with WECs, in order to optimize the stability of the platform and guarantee low inclination angles in any weather, without excessively inflating the costs (Fenu et al., 2020; Ghigo et al., 2020).

The impact of time-resolution on wave characterization was preliminarily tested, by computing the Probability Density Functions of H_s for different data aggregations (hourly, daily, monthly) over the analyzed period, and verifying that indeed the shape of the distributions significantly changes, in particular as to tail population, while using monthly data also affects the estimate of the mean expected values.

For the three selected islands, the following quantities have been analyzed, using hourly data:

1) Hs mean, standard deviation, and maximum over the entire analyzed period, as indicators of the mean expected productivity of a site (independent of seasonal fluctuations), of its variability, of the expected intermittent productivity peaks and of the possible occurrence of events when the operability threshold of the WEC is exceeded (i.e., when the device must be set in survivability mode, a configuration in which no power can be extracted), or when Operation & Maintenance activities might be impaired;
2) the percentage of time over which Hs exceeds the critical 0.5 m threshold, as an indicator of the overall time the device can be expected productive;
3) the distribution of wave direction θ at the candidate sites, as an indicator of the local variability of meteorological conditions;
4) omnidirectional wave power P_w at the candidate sites, as a function of H_s and T_e, whose bivariate distribution (scatterplot) is indicative of how the annually available energy resource is distributed among the typical local sea states.

3.1 Malta

Figure 2 shows the maps of significant-height time average (panel A), standard deviation (panel B) and maximum value achieved over the simulation period (panel C). It is worth noting that panel C is in fact a composite map, as maxima are not contemporarily attained at different locations. Due to its position in the middle of the Sicily Channel, Malta is subject to the channeling of the synoptic-scale Mediterranean winds—i.e., the Mistral and Tramontane from the north, the Sirocco from the south and the Bora from the northeast (Burlando, 2009; Omrani et al., 2016)—and it is exposed to waves propagating in either direction along a north-west/south-east axis. As a consequence, mean wave height is everywhere above the levels required for WEC exploitation, and characterized by significant variability, peaking up to $6 \div 7\,m$ on the eastern coast during extreme events. Consistently with the results of Omrani et al. (2016), H_s mean and standard deviation patterns indicate a predominant propagation from the northwest, with the exposed coast experiencing waves that are on average higher and more variable than in the rest of the island, and the southeastern coast in the lee of the island. Nevertheless, the analysis of geomorphological data carried out by Mottershead et al. (2020) has documented the significant impacts of the less frequent yet higher wind-waves from the southeast, associated with Sirocco winds, whose statistical relevance has been confirmed by the present analysis of wave intensity and direction at selected sites (Figures 3–4). In the research of absolute maxima over the specified period (Figure 2C), the spatial covariance of the two different H_s regimes is preserved west and east of the island, as local extremes are associated either with one or with the other, giving rise to coherent patterns, where the respective signatures coexist. Panel D maps the percentage of time spent above the minimum wave-height threshold for WEC deployment, as an indicator of the stability of wave energy resource. Operative

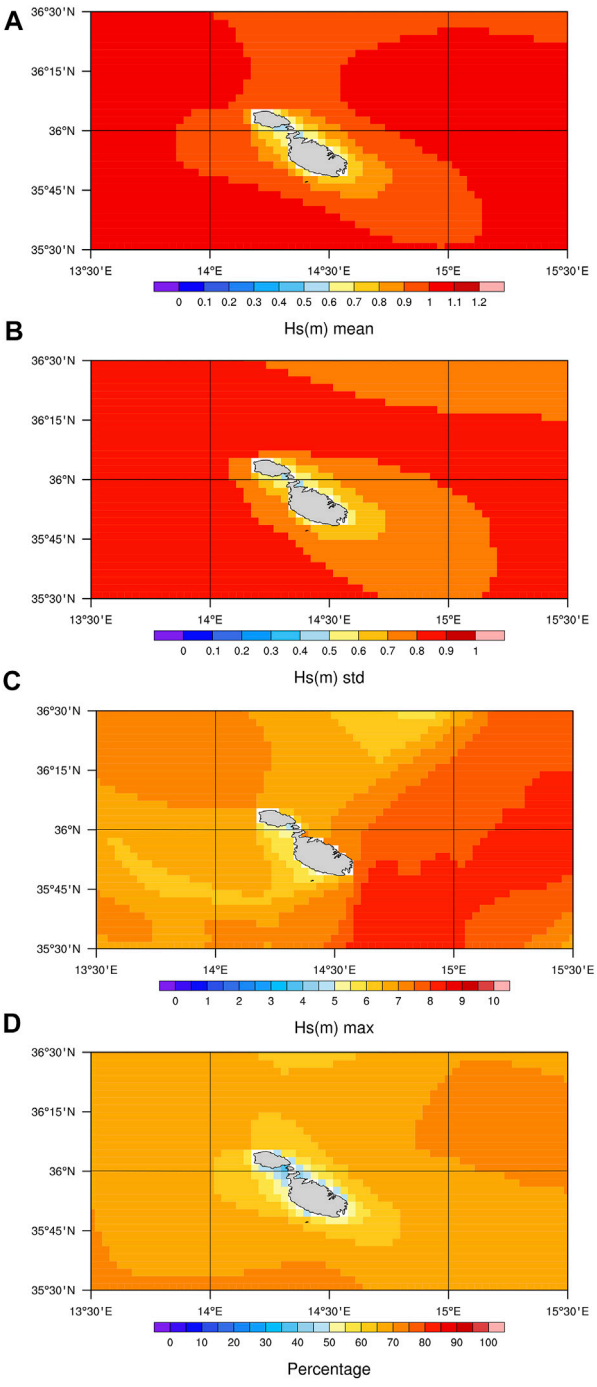

FIGURE 2
Malta Island—H_s average **(A)**, H_s SD **(B)**, and max of H_s over the period 2014–2020 **(C)**; all values are expressed in meters. Panel **(D)**: percentage of time spent over the threshold H_s = 0.5 m.

conditions are met for more than 60% of the examined period in offshore areas, while nearer-to-shore and more sheltered locations anyway guarantee sufficient wave motion for more than 50% of the time.

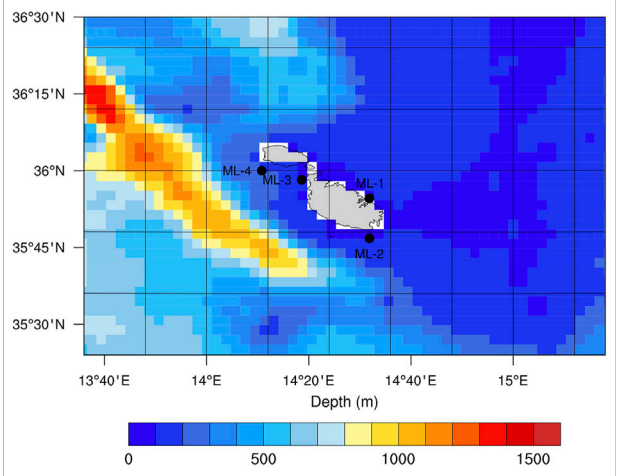

FIGURE 3
Wave model bathymetry for the area around Malta. Locations used for the specific analysis are also shown.

Figure 3 shows the candidate locations (ML-n) for this island and the surrounding bathymetry. A preliminary selection of sites was performed through the application of a GIS-based procedure, which allowed (i) to jointly assess the availability of promising wave energy resource (from climatology) and the fulfillment of basic WEC requirements (e.g., maximum installation depth, minimum wave height, wind-speed range if the combined exploitation of waves and offshore wind is foreseen), (ii) to account for environmentally sensitive, protected and/or restricted marine and coastal areas (e.g., for the presence of vulnerable ecosystems, valuable landscapes and cultural heritage, or maritime traffic hubs), and (iii) to map coastal infrastructures and human settlements and activities that can support the installation of devices, compete for the use of maritime space, and/or benefit from the energy produced.

In the case of Malta, the selection criteria for offshore WEC deployment limited site location to within 12 marine miles from the coastline (for operational affordability), and depth range to within the intervals $[7 \div 25]\,m$ and $[35 \div 50]\,m$ (depending on the device). Areas hosting Posidonia meadows, natural reserves and Natura 2000 sites were excluded, as well as ship maneuvering areas in the proximity of ports and main navigation routes. A 500 m buffer was prescribed around both sensitive and otherwise exploited areas. In addition, local stakeholders manifested a specific interest in combining wave and offshore wind energy exploitation. Therefore, the distance-from-coast, depth and wind-velocity (v) prescriptions for offshore wind farms ($[5 \div 80]\,km$, $[45 \div 159]\,m$ and $v \geq 4\,m$, respectively) were also considered, so as to identify prospective locations for multi-functional installations. Possible synergies with aquaculture farms were also examined. The candidate locations ML-n lie in proximity of the preliminarily selected

TABLE 1 Synthesis of the relevant parameters that characterize the locations considered in this study.

Site	Longitude (°E)	Latitude (°N)	Depth (m)	Mean power P_W (kW/m)	Mean Annual energy E_a (MWh/m)	AquaBuOY Average Electric power P_e (kW)	Pelamis Average Electric power P_e (kW)	Wave Dragon Average Electric power Pe (kW)	Capacity factor AquaBuOY	Capacity factor Pelamis	Capacity factor Wave Dragon
ML-1	14,53	35,92	90	2,28	19,95	18,1	33,5	471,8	0,07	0,04	0,12
ML-2	14,53	35,79	84	2,88	25,21	18,8	41,5	474,9	0,08	0,06	0,12
ML-3	14,31	35,98	82	2,10	18,43	18,9	43,2	481,7	0,08	0,06	0,12
ML-4	14,19	36,11	219	4,91	43,04	27,1	74,4	635,5	0,11	0,10	0,16
CR-1	23,31	35,20	2200	5,85	51,25	24,0	95,1	608,4	0,10	0,13	0,15
CR-2	24,72	35,01	48	0,82	7,22	15,3	22,6	430,1	0,06	0,03	0,11
CR-3	26,41	35,42	387	3,80	33,33	13,5	66,4	418,5	0,05	0,09	0,10
CR-4	23,41	35,70	404	5,32	46,56	24,2	88,1	605,1	0,10	0,12	0,15
CY-1	32,50	35,17	170	1,59	13,97	19,8	43,4	529,7	0,08	0,06	0,13
CY-2	32,50	34,64	143	2,43	21,29	19,6	36,9	521,5	0,08	0,05	0,13
CY-3	32,27	34,79	41	2,25	19,68	19,8	35,6	518,7	0,08	0,05	0,13
CY-4	34,00	34,92	304	1,14	9,99	21,9	34,8	561,5	0,09	0,05	0,14

10.3389/fenrg.2022.944417

offshore sites, with characteristics that are close to the above requirements, within the limits of the average cell bathymetry of the wave model used (Table 1). For the present Class 1 assessment, this limitation is not crucial, as the analysis is only intended to provide preliminary support to policy makers when the opportunity to resort to wave exploitation needs to be early evaluated, before engaging in detailed and costly feasibility studies.

The characterization of wave height across the different incoming directions is illustrated in Figure 4, for the differently exposed locations. Results are consistent with the overall dominance of northwesterly winds and with the wider spread of easterly winds, which are more evenly distributed among the two right-hand quadrants (Omrani et al., 2016).

The sheltering effect of topography is apparent, and was found to condition the sampling adequacy of the energy distribution shown in Figure 5, where the four scatter plots represent the distribution of the annual mean omnidirectional wave energy as a function of T_e and H_s, in correspondence of the four sites. For each hourly sea-state output, the energy flux per meter of wave-crest, $J(T_e, H_s)$, was computed, lumped into discrete elements $\Delta T_e \times \Delta H_s$ of area $0.25\,s \times 0.25\,m$ - corresponding to the pixels in the figure - and integrated in time to yield $E(T_e, H_s)$, i.e. the contribution from each sea-state (pixel) to the annual mean available wave energy, E_a. The latter results from integration over all possible sea states.

Contributions to wave power are obtained from the energy-flux formula for deep water

$$J = \frac{\rho g^2}{64\pi} T_e H_s^2 \tag{1}$$

where J is expressed in kW/m, $\rho = 1025\,kg/m^3$ is the sea water density, and g is the gravity acceleration. Under the assumption of linear super-position, T_e, can be estimated through the formula:

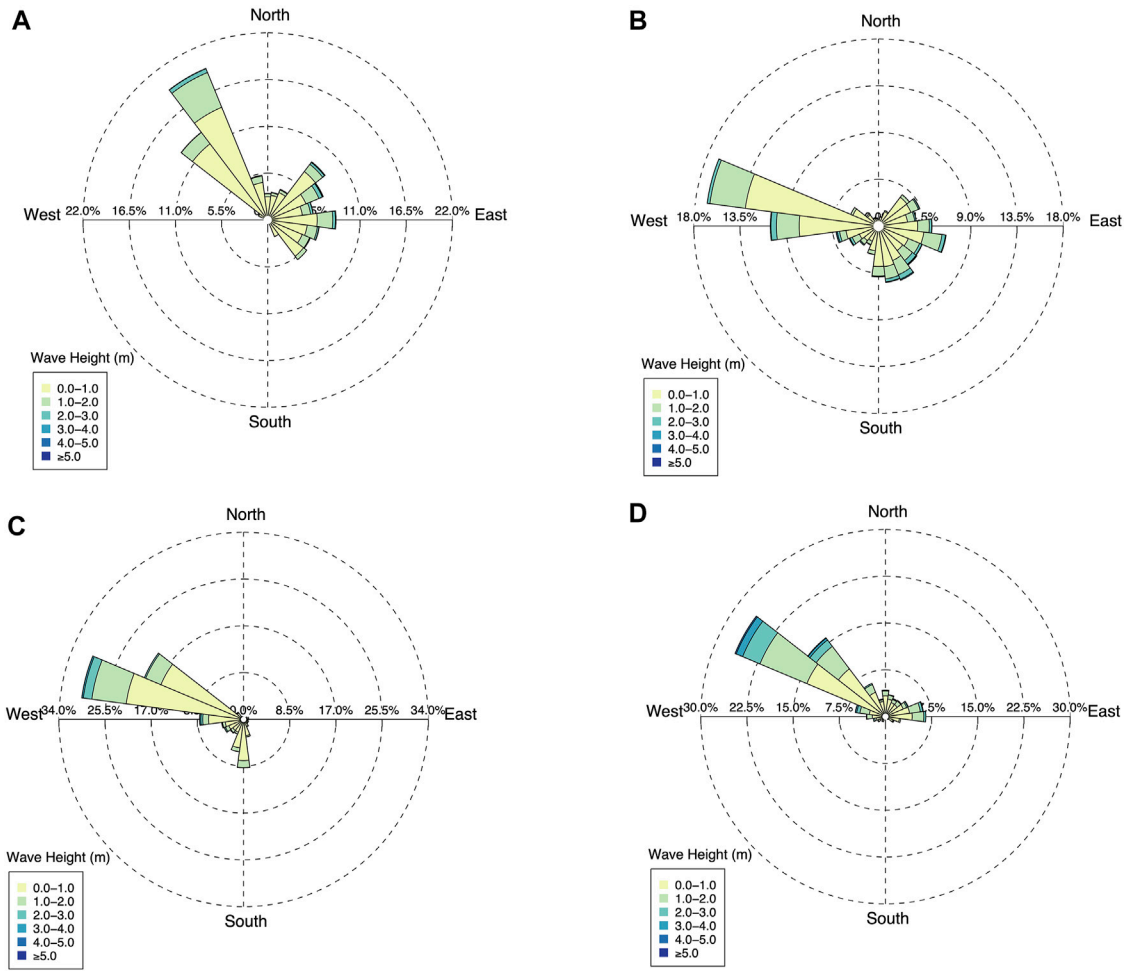

FIGURE 4
Rose plots of significant wave height distribution over wave incoming direction, for sites ML-1 **(A)**, ML-2 **(B)**, ML-3 **(C)**, ML-4 **(D)** of Figure 3.

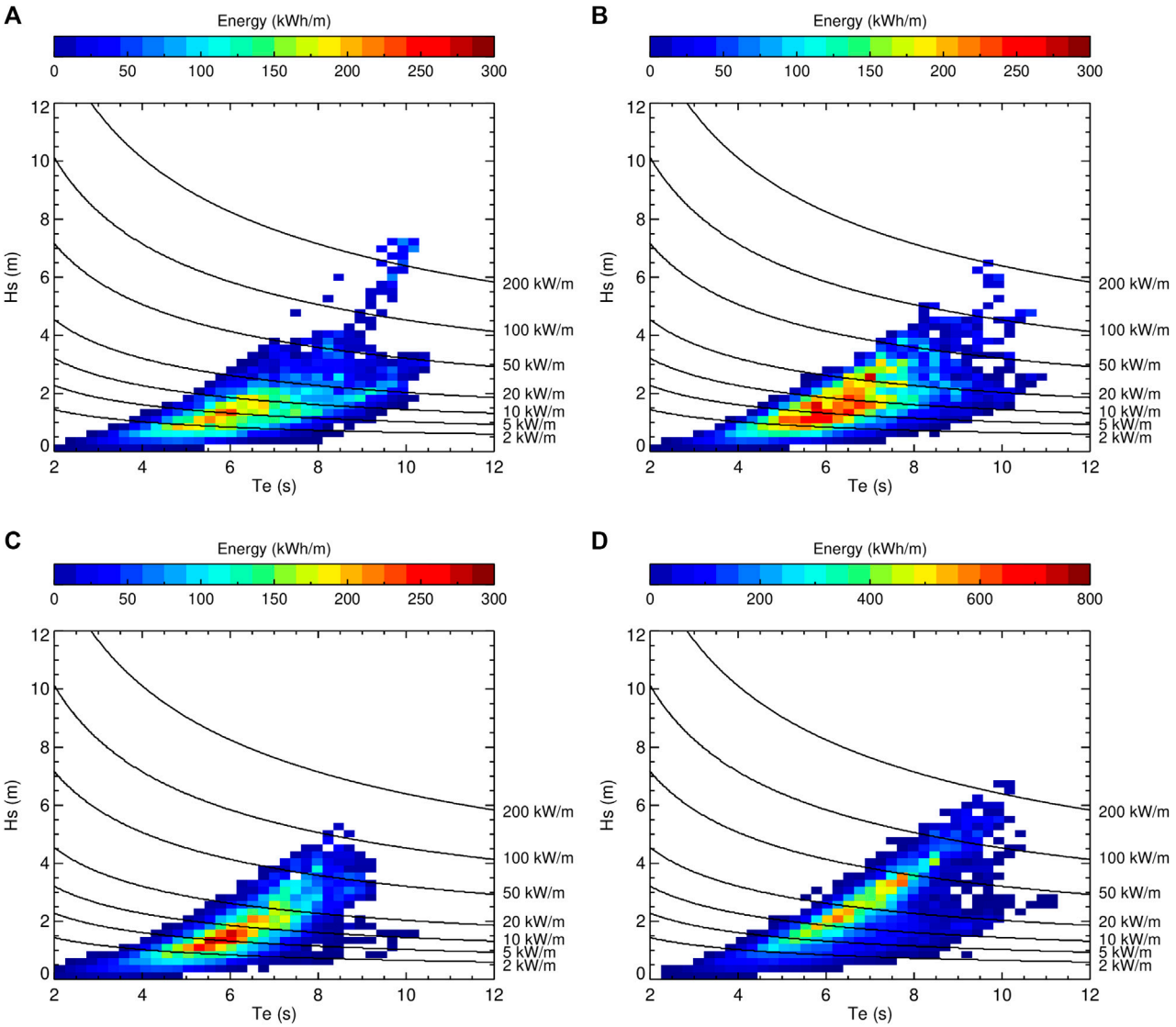

FIGURE 5
Distribution of average annual wave energy as a function of significant wave period and significant wave height, for sites ML-1 **(A)**, ML-2 **(B)**, ML-3 **(C)**, ML-4 **(D)** of Figure 3. Dotted lines mark reference power levels.

$$T_e = \frac{\int_0^{2\pi}\int_0^{\infty} f^{-1} S(f,\theta)\, df d\theta}{\int_0^{2\pi}\int_0^{\infty} S(f,\theta)\, df d\theta} \tag{2}$$

where $S(f,\theta)$ is the spectral variance density as a function of wave frequency (f) and direction (θ). In its turn, H_S is derived from the relationt

$$H_s = 4\sqrt{\int_0^{2\pi}\int_0^{\infty} S(f,\theta)\, df d\theta} \tag{3}$$

(Folley, 2017). T_e and H_s are direct output parameters of the WAM model.

Reference curves of constant energy flux J are also shown in the figure.

At ML-1 (A) and ML-3 (C), the right-leaning elongated core of the energy distribution (roughly corresponding to energy values exceeding $100\,kWh/m$) is centered around periods of $\sim 6\,s$ and wave heights of $\sim 1.5\,m$, with T_e generally confined within the interval $[4 \div 8]\,s$ and H_s ranging from $0.5\,to\,2\,m$ for ML-1, and from $0.5\,and\,4\,m$ for ML-3, with energy approximately comprised between 100 and $220\,kWh/m$ for ML-1, and between 100 and $250\,kWh/m$ for ML-3. The more energetic sea-states corresponding to higher (T_e, H_s) couples are sparsely populated, especially at ML-1,

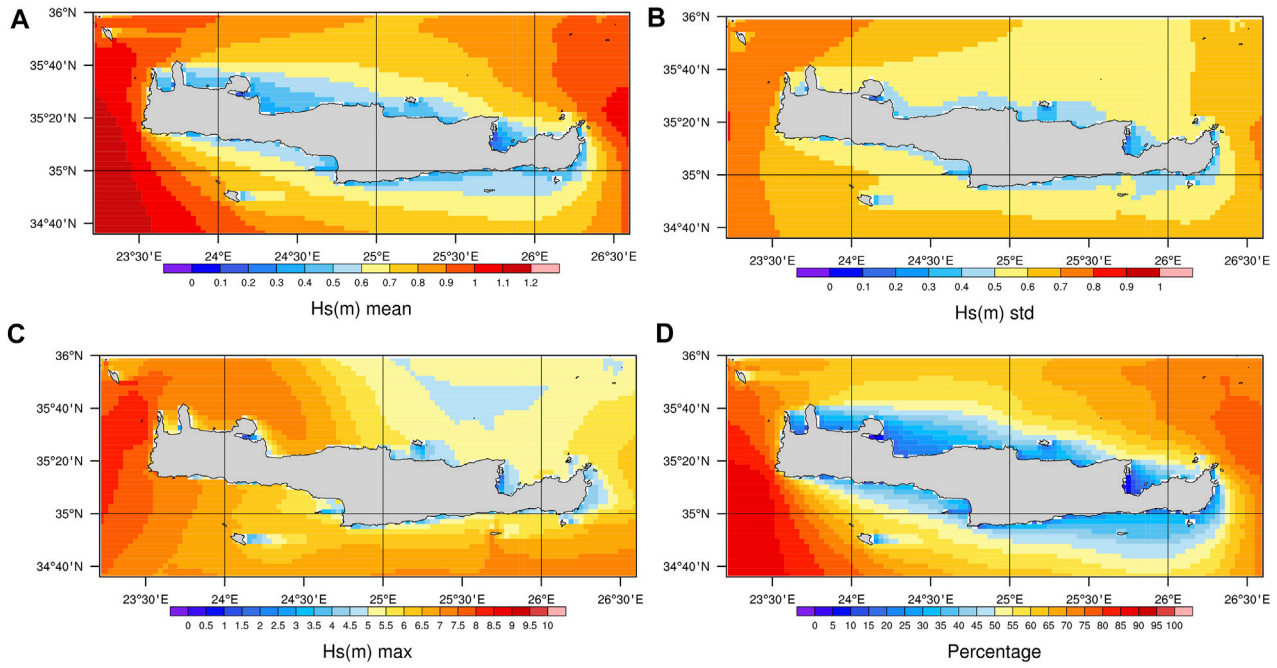

FIGURE 6
Crete Island – H_s average **(A)**, H_s SD **(B)**, and max of H_s over the period 2014–2020 **(C)**; all values are expressed in meters. Panel **(D)**: percentage of time spent over the threshold H_s = 0.5 m.

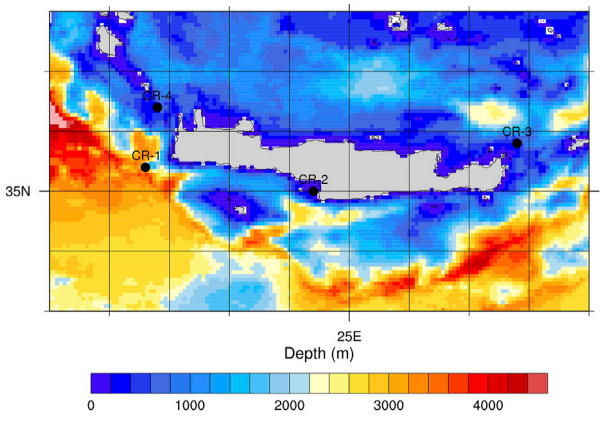

FIGURE 7
Wave model bathymetry for the area around Crete. Locations used for the specific analysis are also shown.

due to the lower occurrence rate of extreme weather in these less exposed locations, and would need longer time series to be adequately sampled. In particular, at ML-1 the patchy pattern in the statistical representation of high-energy extreme events is liable to be associated with the inadequate sampling of waves propagating from the northeast and characterized by high H_s and intermediate-to-long T_e, consistently with the results shown in Figures 4A, 2C. Gaps in the reconstruction at ML-3 seem to be less critical, as the length of the simulated period is sufficient to represent the spectrum of sea conditions in this location, which is mainly exposed to the prevailing northwesterlies, while it is comparatively sheltered from the less frequent waves travelling from other directions (Figure 4C), with local topography determining the damping and the slight counter-clockwise rotation with respect to the upstream location ML-4, and completely obstructing easterly propagation. By being fully exposed to the dominant northwesterly waves, ML-4 (D) in fact exhibits a better sampled and more outstretched energy distribution (note the different scale used for energy with respect to the other panels), with the core roughly located within the intervals $[3 \div 9]\,s$ and $[0.5 \div 6]\,m$, and the energy peaking up to $600\,kWh/m$, for $T_e \approx 8\,s$ and $H_s \approx 4\,m$. ML-2 is also characterized by a topography-induced counter-clockwise rotation of northwesterly waves, which have been significantly dumped along their track with respect to ML-4 (Figure 4), and it is unsheltered from the waves incoming from the two eastern quadrants, except for the higher H_s northeasterlies that fully impact ML-1. The under-sampling of these latter waves only mildly affects the local energy distribution (Figure 5B), which appears to combine the features of those observed at ML-1 and ML-4.

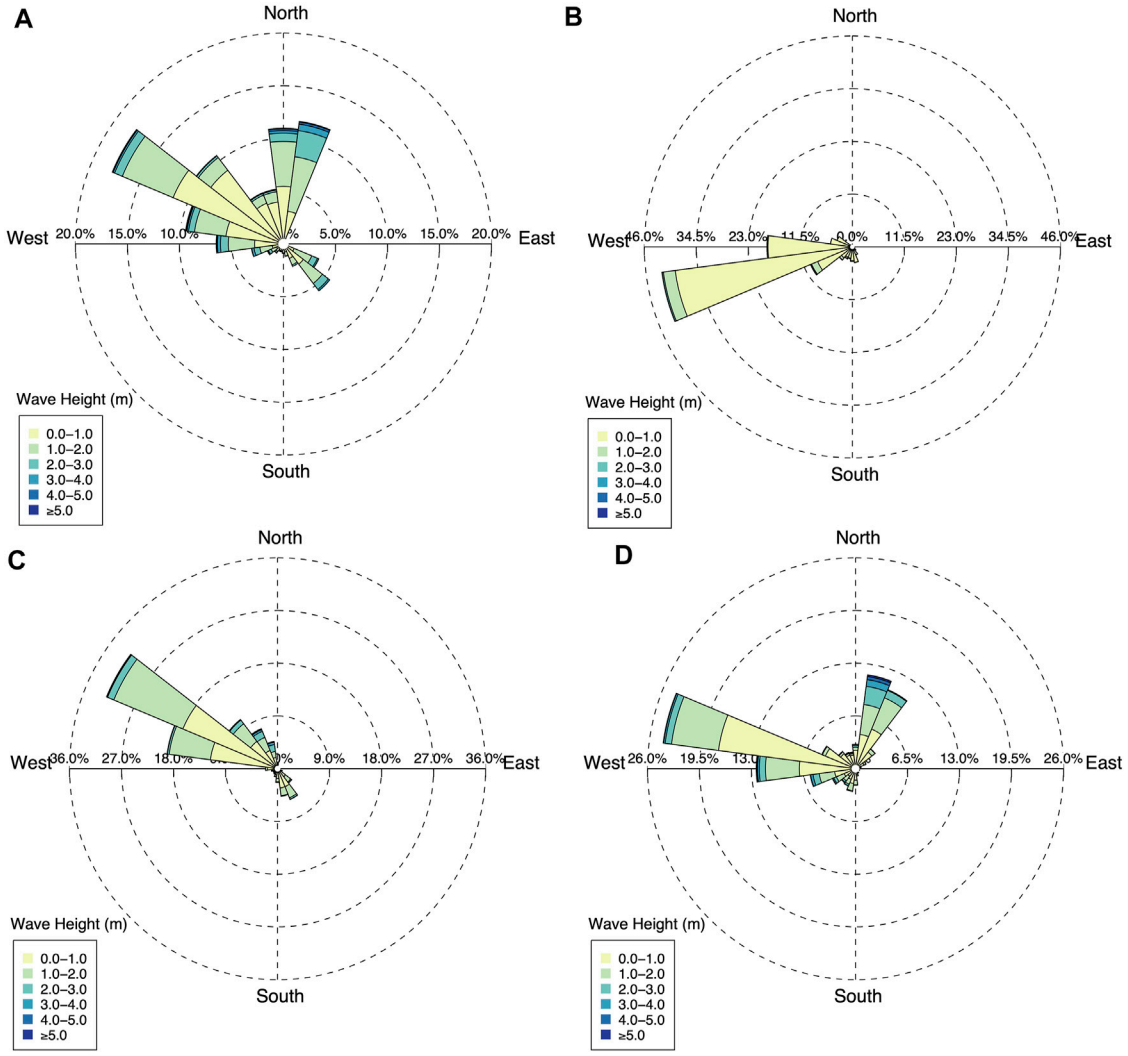

FIGURE 8
Rose plots of significant wave height distribution over wave incoming direction, for sites CR-1 **(A)**, CR-2 **(B)**, CR-3 **(C)**, CR-4 **(D)** of Figure 7.

3.2 Crete

Figure 6 shows the maps of Hs time averages (A), SD (B) and maximum value (C) in the area surrounding Crete, which extends from 23.21°E to 26.6°E in longitude and from 34.6°N to 36°N in latitude. H_s mean values range from 0.5 to 1.0 m, and are characterized by comparable variability. The most intense events range from 3 to 8 m. All patterns are consistent with the documented prevalence of the north-northwesterly Etesian winds in the southern Aegean Sea, across all seasons except winter (Zecchetto and De Biasio, 2007). In particular, panel A and B retain the signature of the intensification and increased variability of the Etesian flow over the west and east edges of Crete, as a result of the interaction between the flow and the topography, which also determines the wind deceleration upstream of the island (Koletsis et al., 2009). The Southern coast of the island is thus generally shielded, although an alternation of cyclones and anticyclones is produced in the lee of the island by the wind funneling through the mountain gaps and through the strait between Crete and Karpathos. The strong anti-cyclonic circulation south of the strait extends and intensifies in summer and autumn, following the seasonal cycle of Etesian winds, while the effects on the coast appear to be more moderate and fairly stable throughout the year (Zecchetto and De Biasio, 2007). Overall, the westernmost zone appears to be the most productive, as it is exposed to both the waves propagating from the Ionian Sea and to those locally generated by the prevailing northwesterly winds, but

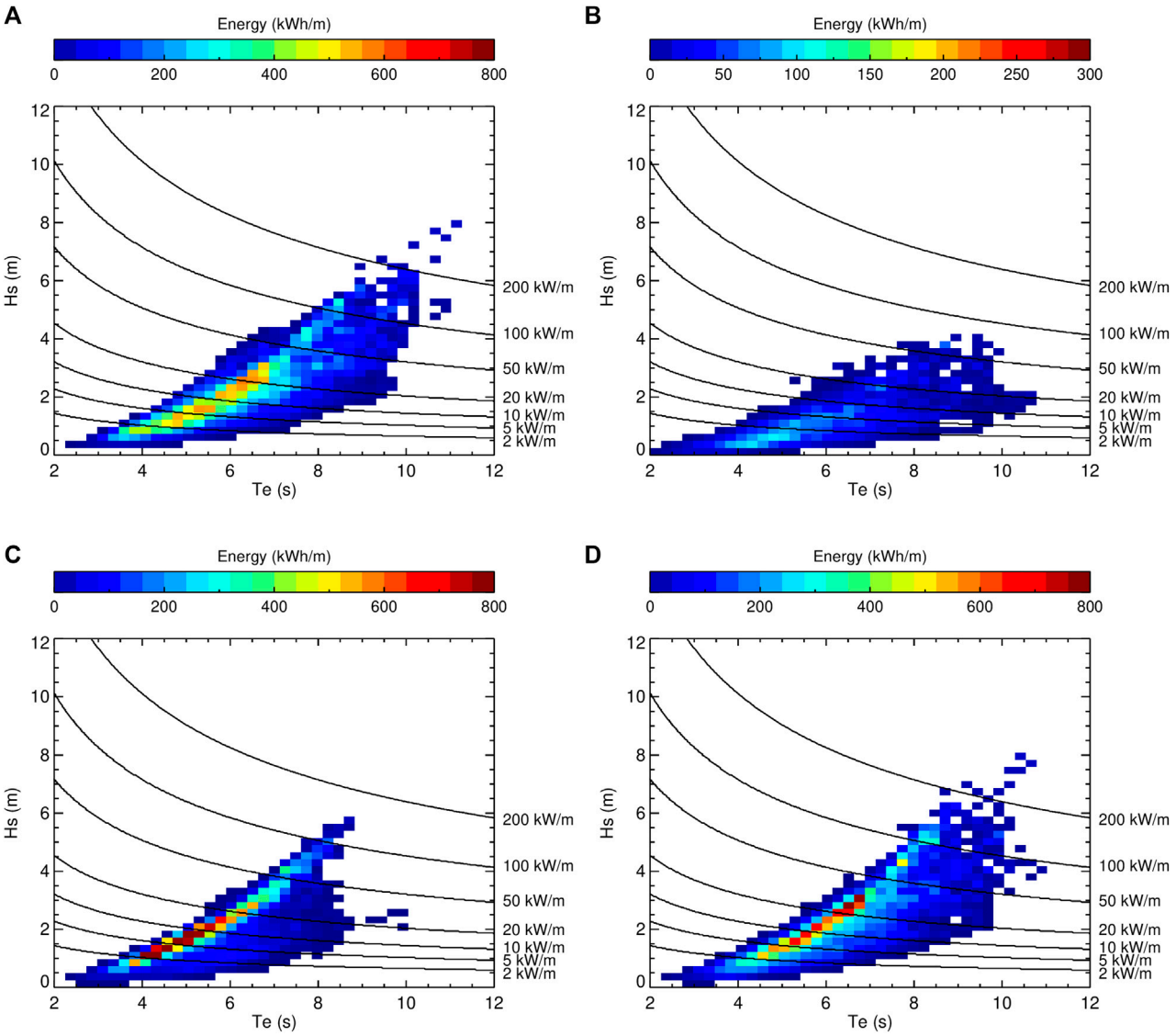

FIGURE 9
Distribution of average annual wave energy as a function of significant wave period and significant wave height, for sites CR-1 **(A)**, CR-2 **(B)**, CR-3 **(C)**, CR-4 **(D)** of Figure 7. Dotted lines mark reference power levels.

offshore location are above the minimum threshold for WEC deployment all around the island. The percentage of above-threshold time (Figure 6D) indicates that the most productive regions are also quite stable, peaking up to 70%–80% at the western edge, and exceeding 50% at the northeastern tip, while wave energy exploitation might be critical in other coastal regions.

Candidate sites (CR-n) are shown in Figure 7, together with the bathymetry of the area. Site selection followed the same procedure described for the Malta test-case, and identified CR-2 as a potentially suitable area for the installation of seabed-based and/or oscillating buoy technologies, while CR-3 and CR-4 offered good opportunities for the deployment of wave converters in association with offshore wind farms. According to the parameters reported in Table 1 and from the inspection of Figure 8, CR-1 is situated in a potentially more energetic open-sea region where blue energy exploitation is however impaired by excessive depth, and it only serves as a term of comparison for CR-3 and CR-4, to illustrate the trade-offs between the magnitude of high-energy events and their frequency and/or duration.

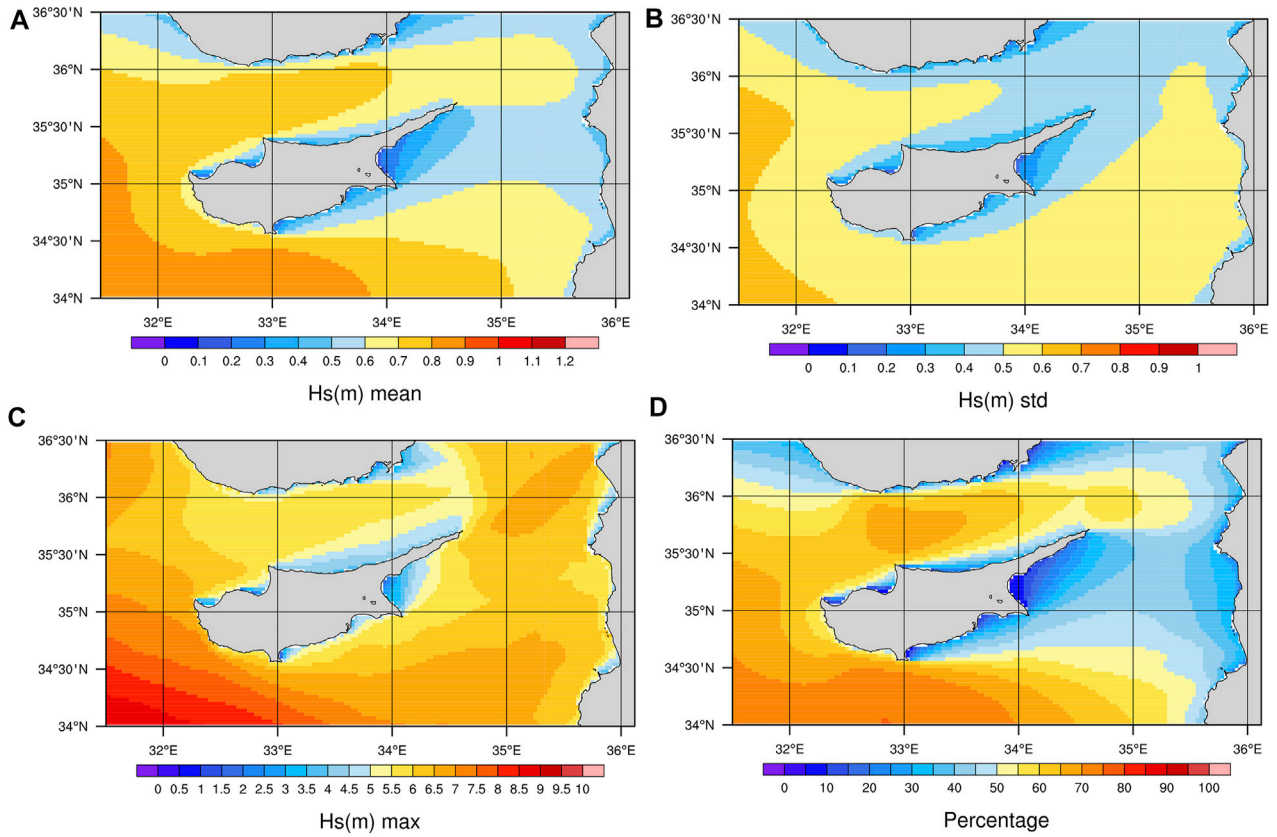

FIGURE 10
Cyprus Island—H_s average **(A)**, H_s SD **(B)**, and max of H_s over the period 2014–2020 **(C)**; all values are expressed in meters. Panel **(D)**: percentage of time spent over the threshold H_s = 0.5 m.

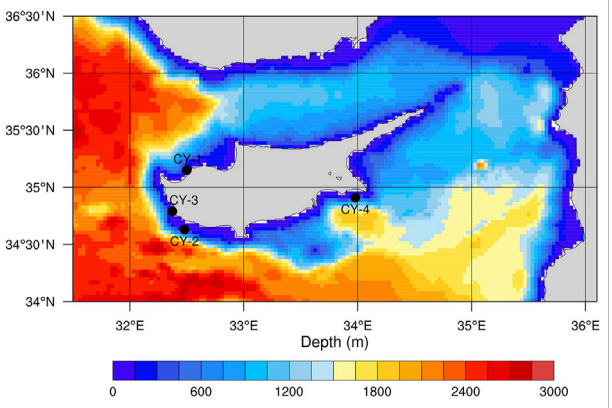

FIGURE 11
Wave model bathymetry for the area around Cyprus. Locations used for the specific analysis are also shown.

For each site, Figure 8 shows the significant wave height distribution over wave incoming direction. The predominance of northwesterly winds is apparent at all sites except CR-2, which is located on the southern coast of the island and therefore characterized by lower wave heights, mainly propagating from the west-southwest.

Figure 9 shows the scatter plots of average annual wave energy at the different locations, as a function of wave period and significant wave height. The average characteristics of each site can be found in Table 1. The distribution of energy differs across sites. The shallower, more sheltered and less energetic CR-2 (note the different energy scale used) attains its maximum values at wave heights lower than 1 m, while the well sampled extremes are anyway characterized by limited H_s and are too rare to rely on.

In terms of theoretical mean power, CR-1 is apparently the most energetic site (mean energy above 50 MWh/m), as a result of the local wider spread of sea states (i.e. energy appears to be more uniformly distributed over T_e values between 2 s and 10 s and H_s values between 0 m and 7 m), which is only comparable to that of the not-too-distant yet slightly less energetic CR-4 (Table 1). Nevertheless, the greater (yet under-sampled) occurrence of higher-energy sea states at CR-1 does not immediately translate into a greater abundance of

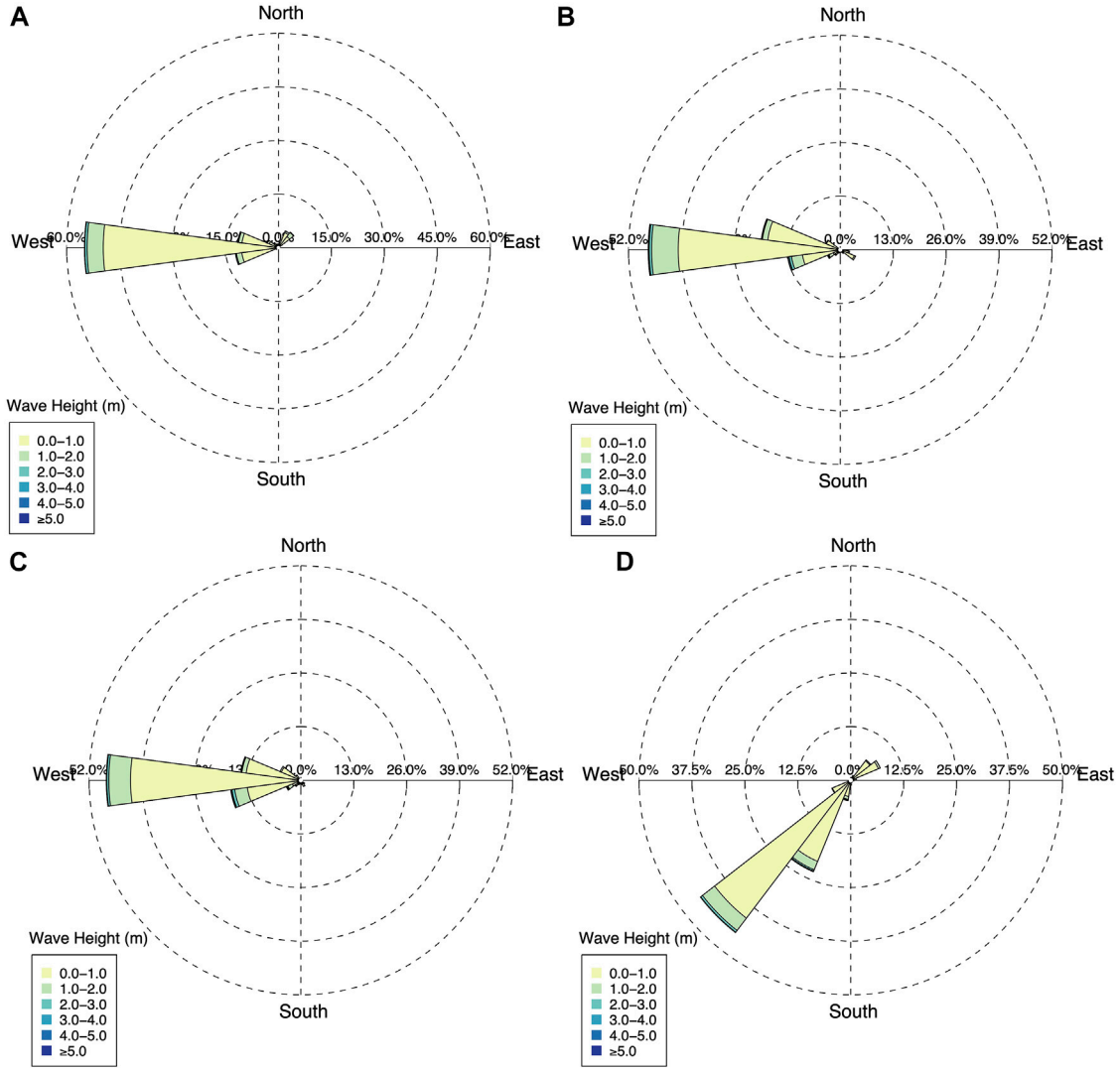

FIGURE 12
Rose plots of significant wave height distribution over wave incoming direction, for sites CY-1 **(A)**, CY-2 **(B)**, CY-3 **(C)**, CY-4 **(D)**, of Figure 11.

exploitable resource over time, CR-4 appearing to be more promising due to the substantial relative prevalence of intermediate energy-content sea states - with T_e and H_s respectively in the $[4.5 \div 7]\,s$ and in the $[1 \div 3]\,m$ range - accompanied by a high-end tail shape that is qualitatively less outstretched than at CR-1. In fact, higher energy concentrations over a limited cluster of sea conditions can in principle allow more effective design and calibration of devices, increasing their efficiency and guaranteeing better resource deployment. Similarly, at CR-3 the available energy is more concentrated in specific (T_e, H_s) intermediate classes, in the $[4 \div 6]\,s$ and $[1 \div 3]\,m$ ranges, over which to concentrate device optimization, whereas higher-energy sea states appear to be less frequent.

3.3 Cyprus

If compared to other areas of the Mediterranean basin, wave potential in the Levantine Sea appears to be lower, yet it still deserves attention as local wave height is quite stably above the critical 0.5 m threshold all year round. For Cyprus in particular, maps of the mean (A), the standard deviation (B) and the maximum (C) of H_s, computed over the period 2014–2020, are shown in Figure 10. Consistently with the steady influence of Etesian winds over the eastern Mediterranean, which in this region rotate further counter-clockwise with respect to the southern Aegean, to generally blow from the west (Zecchetto and De Biasio, 2007), the west and south coast are the most energetic, with average Hs equal to 0.8 m, its standard deviation close to 0.6 m, and a maximum of 7 m. The

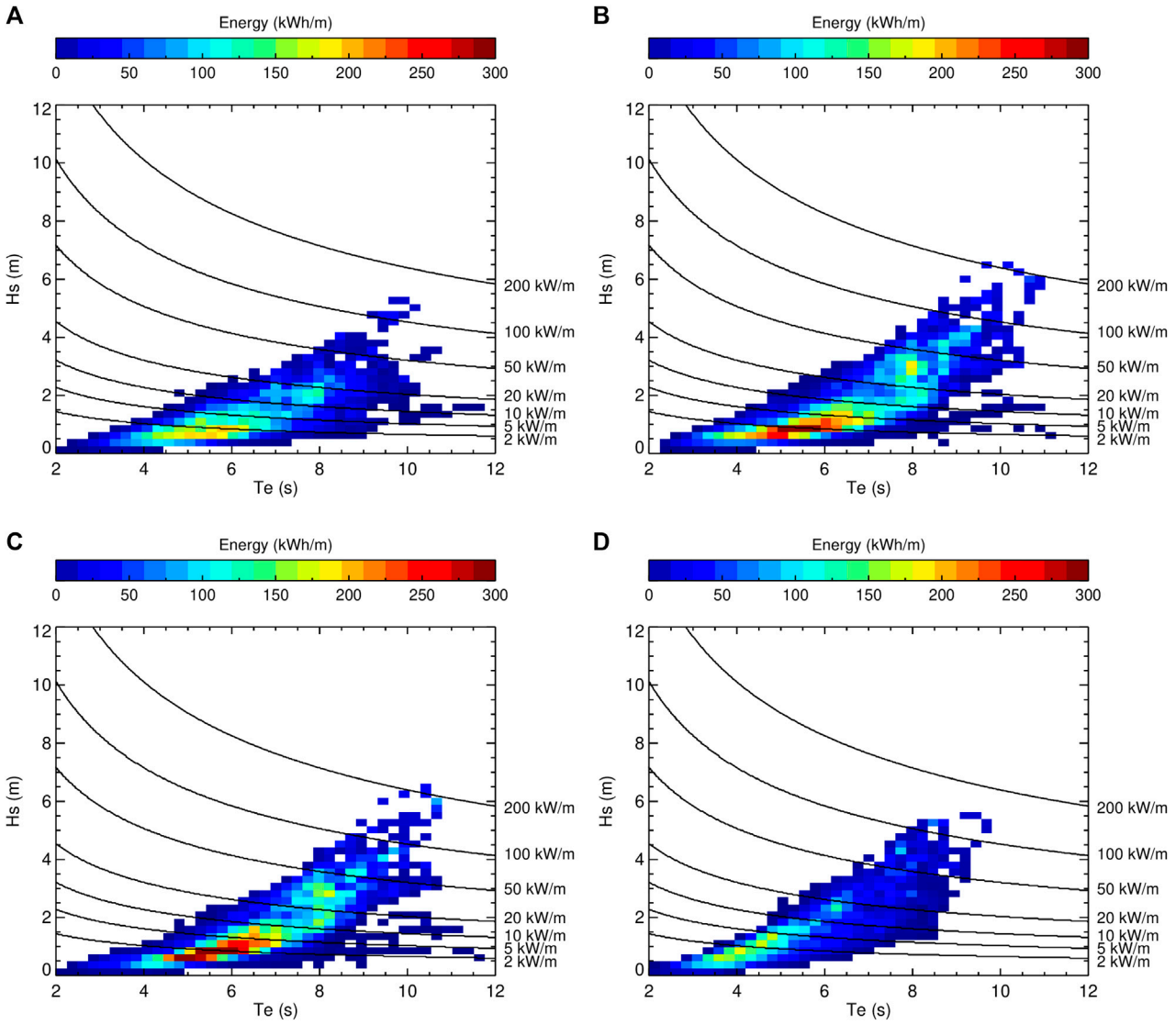

FIGURE 13
Distribution of average annual wave energy as a function of significant wave period and significant wave height, for sites CY-1 **(A)**, CY-2 **(B)**, CY-3 **(C)**, CY-4 **(D)**, of Figure 11. Dotted lines mark reference power levels.

percentage of time spent above the critical threshold of 0.5 m (D) is above 50% for the southwestern shores of the island, locally reaching 70% close to the Limassol region.

The BE planning activities carried out in collaboration with local stakeholders highlighted several possible pilot areas for the deployment of WECs in Cyprus. Figure 11 shows the most promising ones, resulting from the selection procedure already described and guided by a primary interest from the stakeholders for the deployment of oscillating and/or seabed-based buoys (at CY-1 and CY-2) and of onshore floaters (at CY-3 and CY-4).

As might be expected, candidate sites (CY-n) are all exposed to westerly waves, which rotate southward at CY-4 due to the shielding effect of the island (Figure 12).

The corresponding wave-energy scatterplots are shown in Figure 13, indicating moderate yet interesting potential for WEC deployment, mainly concentrated in persistent low-energy sea states. The high-end tail of the distribution appears to be generally well sampled, although coverage might still be improved.

3.4 Summary of site characteristic and theoretical productivity

For each site (column 1), Table 1 summarizes the values of the relevant geographic parameters (columns 1 ÷ 4) and of

two integral indicators of the available wave resource, P_w (annual mean available wave power—column 5) and E_a (mean wave energy per meter of wave crest, derived from P_w—column 6), condensing the results presented above and allowing direct island inter-comparison. In addition, the theoretical productivity was also computed for three state-of-the-art devices based on different functioning principles, whose nominal power matrices could be found in the literature (columns 7 ÷ 9) (Castro-Santos et al., 2018). The device capacity factor was also calculated (columns 10 ÷ 12), according to the relation

$$C_f = 100 * \frac{P_E}{P_N} \tag{4}$$

where P_E is the electric power produced by the WEC at a specific location, and P_N is its maximum rated power (nominal power) according to the developers.

The three devices selected for the present analysis are the AquaBuOY, the Pelamis and the Wave Dragon. The AquaBuOY is classified as a point absorber, and consist of a floating structure that converts the kinetic energy of the vertical motion of waves into electricity. The cylindrical buoy acts as the displacer, while the large water mass enclosed in the long vertical tube underneath the buoy is the reactor. It has a non-fixed bottom end (i.e., it is moored to the seabed), and it is characterized by small dimensions with respect to the longer wavelengths in which it can operate. A 250 kW buoy has a diameter of 6 m and a draught of 30 m. It has been designed to maximize power output under sustained moderate wave conditions rather than during less frequent extreme events. Its modularity allows deployment in arrays, so as to meet a potentially growing power demand with power plants that are scalable from hundreds of kilowatts to hundreds of megawatts, at the same time guaranteeing a consistent flow of power during maintenance cycles (Poullikkas, 2014).

The Pelamis converter is a floating device classified as an attenuator. It consists of three cylindrical hollow steel segments (diameter of 3.5 m), connected to each other by two degree-of-freedom hinged joints, with the central unit of each joint containing the complete power conversion system. Four hydraulic cylinders resist the wave-induced motion of these joints, both horizontal and vertical, acting as pumps which drive fluid through a hydraulic motor, in its turn driving an electrical generator. Each Pelamis is 120 m long, it is designed to operate in water depths of ~50 m and each of its three modules is rated at 250 kW power. It is allowed to orient itself to the predominant wave direction by its loose mooring system, while its length contributes to its survivability in harsh sea conditions, by automatically "detuning" from the longer-wavelength high-power waves. Pelamis P-750 machines can produce a total power of 2.25 MW (Drew et al., 2009).

Finally, the Wave Dragon is a floating, offshore Wave Energy Converter (WEC) based on the overtopping mechanism. A doubly-curved ramp conveys oncoming waves, which flow over the top into a reservoir placed above the mean water level, and are then released back to the sea through a set of low-head hydro-turbines. The size and rated energy production of a Wave Dragon unit depend on the wave climate (Soerensen et al., 2003; Parmeggiani et al., 2013).

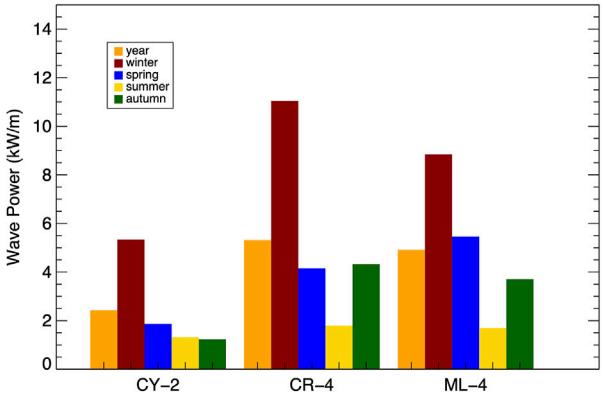

FIGURE 14
Comparison between average annual and seasonal wave power for three of the selected sites.

For each device, theoretical productivity was computed via the formula

$$P_e = \sum_{i=1}^{i=N_T} \sum_{j=1}^{j=N_H} P_{i,j} * p_{i,j} \tag{5}$$

where $P_{i,j}$ is the power matrix of each specific WEC (Castro-Santos et al., 2018) and $p_{i,j}$ is the normalized frequency (probability) of occurrence of each discrete sea state. When necessary, the discretization of sea states was re-computed, and T_e substituted with the Peak Period (T_p), in order to match the specifications of the power matrix.

Overall, the Mediterranean locations considered for this study appear to offer appreciable wave energy resource for the exploitation of currently available devices, whose productivity is still a sizeable fraction of that rated at more energetic Atlantic sites (Rusu, 2014). In particular, the expected electric power ranges between ~13 and ~27 kW for the AquaBuOY, between ~22 and ~95 kW for the Pelamis, and between ~418 and ~635 kW for the Wave Dragon, whereas the corresponding values for North Spain, the Portuguese continental shore, the Canary Islands, and Madeira Archipelago, respectively, are:

- AquaBuOY: [n.a.], [30÷36] kW, [24÷32 kW] and [40÷50 kW];
- Pelamis: [114÷127] kW, [90÷102] kW, [65÷90 kW] and [100÷135 kW];
- Wave Dragon: [2027÷2197] kW, [767÷956] kW, [n.a] and [1147÷1644] kW.

Values are computed for average annual sea states, except for Madeira, where estimates refer to winter conditions (October to March) (Rusu, 2014).

Both Malta and Crete host at least one location (ML-4 and CR-4) that is particularly suitable for wave energy exploitation, due to the comparatively high abundance of the resource, especially if deployment in combination with other marine renewables is envisaged. Nevertheless, also sites where average wave energy is lower are found to offer comparable electric power when the distribution of sea states is combined with device specifications.

The reference nominal power indicated by the manufacturer for the three devices is 0.25 MW (AquaBuOY), 0.75 MW (Pelamis), and 4 MW (Wave Dragon). The Wave dragon appears to be the most effective device, although such result should be weighted in the light of its dimensions, high cost and limited scalability for deployment in low energy sea (Previsic et al., 2004). As a matter of fact, the capacity factor of WECs generally increases with wave power, and their scaling-down is necessary to improve their performance (Guo and Ringwood, 2021; Foteinis, 2022).

In its turn, the relatively small, scalable and manageable AquaBuOY is expected to give a near-optimal economic value of electricity for $C_f \approx 40\%$, a condition that is hardly met in the Mediterranean, and that is still far from the value of around 12% provided by the manufacturer for more energetic seas ($25\ kW/m$) (Previsic et al., 2004).

As to the Pelamis, its scalability for low energy conditions is still to be fully assessed, despite its high tuneability to wave climate and conversion efficiency. Tests at sea have shown power output to scale to the power of 3.5 of the linear dimension, resulting in a power output at 1:7 scale of roughly 0.1% of the full-scale device (Previsic et al., 2004).

If appropriately scaled-down to between 1/4 and 1/3 of the full WEC size, the two latter devices have been theoretically estimated to reach capacity factors higher than 0.2 along 40% of the Mediterranean coastline, and higher than 0.3 at 8% of the scrutinized locations, including the Sicily Channel, Crete and Cyprus, with rated power ranging between 10 and 30 kW (Bozzi et al., 2018). Capacity factors higher than 0.2 should be regarded as encouraging, in consideration of the relative weight of the other factors that determine WEC viability (i.e. resource variability and device survivability), as well as of the smaller size, which is expected to potentially lower CapEx (Lavidas, 2020). The question remains open as to the opportunity of sub-optimal deployment of devices in the Mediterranean, in view of its extreme vulnerability and of the hidden costs of environmental hazards.

Theoretical productivity is anyway affected by a non-negligible degree of uncertainty, arising from deficiencies in the characterization of the wave climate and/or in the modeling of wave-device interactions, from the misrepresentation of possible external perturbations or from the involuntary omission of relevant dynamics (Guo and Ringwood, 2021). In particular, beside possible model deficiencies, the characterization of the resource only in terms of climatological annual averages cannot account for the inter- and intra-annual variability of wave climate, which has been found to affect the performance of devices, although the generated power appears to be less intermittent than the available wave energy flux, due to the filtering action of device power matrices (Folley, 2017; Guillou and Chapalain, 2018). Variability can indeed result in significantly different power generation across locations for the same annual average incident wave power, and in higher power generation in winter than in summer, ending up with being a strong cost driver in both capital and operational expenditures (Ringwood and Brandle, 2015). After first selecting prospective deployment sites based on their annual average characteristics, further analysis is therefore needed to assess the stability of the resource over time, possibly offsetting adverse short- to mid-term variations through technological improvement, i.e., by enhancing real-time control and power management systems (Guo and Ringwood, 2021).

As a first step in this direction, the most promising locations—one for each island—are compared in Figure 14, as to the overall annual amount of resource and its seasonality. Cyprus lags behind, while the two sites in Crete and Malta, although indeed similar as to average wave power, differ as to its seasonal distribution, with Crete exhibiting higher variability and larger differences between winter and spring with respect to Malta, where the resource is more consistent over the year. As might be expected, summer is the least energetic season in all three islands, as opposed to the increase in energy demand potentially induced by tourism fluxes.

4 Conclusion and outlook

In the context of the Blue Deal Project, this work represents a first step towards a systematic site-WEC technology matching in the Mediterranean Sea, where, notwithstanding the comparatively limited resource abundance with respect to the world oceans, wave energy deployment can effectively sustain the ongoing transition towards higher shares of renewables, at the same time reconciling the competing interests in the use of marine space and the necessary environmental protection.

For the specific sites selected during the Blue Deal Labs organized in Malta, Crete and Cyprus, the general characterization of the local wave climate via standard average parameters has been significantly improved by the use of the full time-series from high-resolution wave forecasts. Local wave characteristics have been described in terms of spatial and temporal averages and variability, and theoretical power generation has been estimated, highlighting the so far not fully explored potentialities of the Mediterranean region.

In particular, for each island:

- the local prevailing wave regimes have been analyzed;
- the rationale for preliminary site selection has been presented, based on multi-criteria analyses;
- at the selected sites, the distribution of the annual mean omnidirectional wave energy was described, as a function of T_e and H_s;
- the theoretical productivity of three WECs, the AquaBuOY, the Pelamis and the Wave Dragon, has been computed, as representative of the developmental stage of state-of-the-art technologies;
- opportunities for WEC deployment have been demonstrated.

Future developments critically depend on the definition of effective procedures to scale-down devices that have been designed for harsher sea conditions, as well as on the development of control strategies capable of maximizing power output in moderate-energy seas. Among these, the Mediterranean can indeed offer competitive advantages in terms of lower CapEx and OpEx, mainly due to local resource persistence and to the expected higher survivability of devices. Nevertheless, in order to assess the medium- to long-term economic performance of a wave energy project, the uncertainties in future resource availability should be reduced, inter- and intra-annual variability should be further characterized, and crucial external factors, such as the investment environment, market data and national incentives, should be soundly evaluated.

Data availability statement

The raw data supporting the conclusions of this article will be made available by the authors, without undue reservation.

Author Contributions

AC performed the numerical simulations used and collaborated to the analysis of data and to the writing of the manuscript. GP collaborated to the analysis of data and to the writing of the manuscript. MS coordinated the activities and collaborated to the analysis of the data and to the writing of the manuscript.

Funding

This study has been developed in the framework of the Interreg Med BLUE-DEAL (2019–2022) project co-financed by the European Regional Development Fund. Website: https://blue-deal.interreg-med.eu.

Conflict of interest

The authors declare that the research was conducted in the absence of any commercial or financial relationships that could be construed as a potential conflict of interest.

Publisher's note

All claims expressed in this article are solely those of the authors and do not necessarily represent those of their affiliated organizations, or those of the publisher, the editors and the reviewers. Any product that may be evaluated in this article, or claim that may be made by its manufacturer, is not guaranteed or endorsed by the publisher.

References

Astariz, S., and Iglesias, G. (2015). The economics of wave energy: A review,. *Renew. Sustain. Energy Rev.* 45, 397–408. doi:10.1016/j.rser.2015.01.061ISSN 1364-0321

Atan, R., Goggins, J., and Nash, S. (2016). A detailed assessment of the wave energy resource at the atlantic marine energy test site,. *Energies* 9, 967. doi:10.3390/en9110967

Bertram, D. V., Tarighaleslami, A. H., Walmsley, M. R. W., Atkins, M. J., and Glasgow, G. D. E. (2020). A systematic approach for selecting suitable wave energy converters for potential wave energy farm sites,. *Renew. Sustain. Energy Rev.* Vol. 132–110011, 0321. doi:10.1016/j.rser.2020.110011

Bidlot, J. R., Janssen, P. A. E. M., and Abdalla, S. A. (2007). *Revised formulation of ocean wave dissipation and its model impact; tech. Rep.* Memorandum 509. Reading, UK: ECMWF.

Bozzi, S., Besio, G., and Passoni, G. (2018). Wave power technologies for the Mediterranean offshore: Scaling and performance analysis. *Coast. Eng.* 136, 130–146. doi:10.1016/j.coastaleng.2018.03.001ISSN 0378-3839

Burlando, M. (2009). The synoptic-scale surface wind climate regimes of the Mediterranean Sea according to the cluster analysis of ERA-40 wind fields,. *Theor. Appl. Climatol.* 96, 69–83. doi:10.1007/s00704-008-0033-5

Cagninei, A., Raffero, M., Bracco, G., Giorcelli, E., Mattiazzo, G., and Poggi, D. (2015). Productivity analysis of the full scale Inertial Sea wave energy converter prototype: A test case in Pantelleria island. *J. Renew. Sustain. Energy.* 7, 061703. doi:10.1063/1.4936343

Carillo, A., Lombardi, E., and Sannino, G. (2015a). Validazione del sistema operativo per la previsione del moto ondoso nel Mediterraneo. Available at: https://www.enea.it/it/Ricerca_sviluppo/documenti/ricerca-di-sistema-elettrico/energia-dal-mare/2014/rds-par2014-238.pdf.RdS/PAR2014/238.

Carillo, A., Sannino, G., and Lombardi, E. (2015b). Wave energy potential: A forecasting system for the Mediterranean basin,. *Energ. Ambiente Innov.* 61 (2), 16–21. doi:10.12910/EAI2015-05

Castro-Santos, L., Silva, D., Bento, A. R., Salvação, N., and Guedes Soares, C. (2018). Economic feasibility of wave energy farms in Portugal. *Energies* 11, 3149. doi:10.3390/en11113149

Clemente, D., Rosa-Santos, P., and Taveira-Pinto, F. (2021). On the potential synergies and applications of wave energy converters: A review,. *Renew. Sustain. Energy Rev.* Vol. 135, 110162–110321. doi:10.1016/j.rser.2020.110162110162

Dialyna, E., and Tsoutsos, T. (2021). Wave energy in the Mediterranean Sea: Resource assessment, deployed WECs and prospects. *Energies* 14, 4764. doi:10.3390/en14164764

Drew, B., Plummer, A., and Sahinkaya, M. (2009). A review of wave energy converter technology. Proceedings of the Institution of Mechanical Engineers, Part

A:. *Proc. Institution Mech. Eng. Part A J. Power Energy* 223 (8), 887–902. doi:10.1243/09576509jpe782

EU Commission (2020). Communication from the commission to the European parliament, the council, the European economic and social committee and the committee of the regions: An EU Strategy to harness the potential of offshore renewable energy for a climate neutral future. Available at: https://eur-lex.europa.eu/legal-content/EN/TXT/?uri=CELEX:52020DC0741 (COM/2020/741 final.

EU Commission (2019). Communication from the commission: The European green deal, COM(2019) 640 final. Available at: https://eur-lex.europa.eu/legal-content/EN/TXT/?uri=CELEX%3A52019DC0640.

EU Directive (2018). Directive (EU) 2018/2001 of the European Parliament and of the Council of 11 December 2018 on the promotion of the use of energy from renewable sources, PE/48/2018/REV/1. Available at: https://eur-lex.europa.eu/legal-content/EN/TXT/?uri=uriserv:OJ.L_.2018.328.01.0082.01.ENG&toc=OJ: L:2018:328:TOC.

EU Proposal (2021). Proposal for a directive of the European parliament and of the council amending directive (EU) 2018/2001 of the European parliament and of the council, regulation (EU) 2018/1999 of the European parliament and of the council and directive 98/70/EC of the European parliament and of the council as regards the promotion of energy from renewable sources, and repealing council directive (EU) 2015/652, COM/2021/557 final Available at: https://eur-lex.europa.eu/legal-content/EN/TXT/?uri=CELEX:52021PC0557.

EU Regulation (2021). Regulation (EU) 2021/1119 of the European parliament and of the council of 30 June 2021: Establishing the framework for achieving climate neutrality and amending regulations (EC) No 401/2009 and (EU) 2018/1999 ('European climate Law'), PE/27/2021/REV/1. Available at: https://eur-lex.europa.eu/legal-content/EN/TXT/?uri=CELEX:32021R1119.

Fenu, B., Attanasio, V., Casalone, P., Novo, R., Cervelli, G., Bonfanti, M., et al. (2020). Analysis of a gyroscopic-stabilized floating offshore hybrid wind-wave platform. *J. Mar. Sci. Eng.* 8, 439. doi:10.3390/jmse8060439

Fitzgerald, J., and Bolund, B. (2012). "Technology readiness for wave energy projects; ESB and Vattenfall classification system," in Proceedings of the 4th International Conference on Ocean Energy (Dublin: Ireland), 17–19.

Folley, M. (2017). "The wave energy resource," in *Handbook of ocean wave energy*. Editors A. Pecher and J. Kofoed (Cham: Springer), *Ocean engineering & oceanography*, Vol. 7. doi:10.1007/978-3-319-39889-1_3

Foteinis, S. (2022). Wave energy converters in low energy seas: Current state and opportunities. *Renew. Sustain. Energy Rev.* 162 (112448), 1364–0321. doi:10.1016/j.rser.2022.112448

Foteinis, S., and Tsoutsos, T. (2017). Strategies to improve sustainability and offset the initial high capital expenditure of wave energy converters (WECs). *Renew. Sustain. Energy Rev.* 70, 775–785. doi:10.1016/j.rser.2016.11.258ISSN 1364-0321

Gallutia, D., Tahmasbi Fard, M., Gutierrez Soto, M., and He, J. (2022). Recent advances in wave energy conversion systems: From wave theory to devices and control strategies. *Ocean Eng.* 252. doi:10.1016/j.oceaneng.2022.111105

Ghigo, A., Cottura, L., Caradonna, R., Bracco, G., and Mattiazzo, G. (2020). Platform optimization and cost analysis in a floating offshore wind farm. *J. Mar. Sci. Eng.* 8, 835. doi:10.3390/jmse8110835

Guillou, N., and Chapalain, G. (2018). Annual and seasonal variabilities in the performances of wave energy converters. *Energy* 165 (B), 812–823. doi:10.1016/j.energy.2018.10.001ISSN 0360-5442

Guo, B., and Ringwood, J. V. (2021). A review of wave energy technology from a research and commercial perspective. *IET Renew. Power Gen.* 15, 3065–3090. doi:10.1049/rpg2.12302

Günther, H., and Behrens, A. (2011). The WAM model validation document version 4.5.3, tech. Rep. Institute of coastal research helmholtz-zentrum geesthacht (HZG)

Günther, H., Hasselmann, S., and Janssen, P. A. E. M. (1992). *The WAM model cycle 4.0, user manual*; Deutsches Klimarechenzentrum Hamburg: Hamburg, Germany, Vol. 4, 102pp

Hannon, M., van Diemen, R., and Skea, J. (2017). *Examining the effectiveness of support for UK wave energy innovation since 2000: Lost at sea or a new wave of innovation?* Glasgow: University of Strathclyde, International Public Policy Institute. doi:10.17868/62210

Harrison, G. P., and Wallace, A. R. (2005). Sensitivity of wave energy to climate change. *IEEE Trans. Energy Convers.* 4, 870–877. doi:10.1109/tec.2005.853753 2005.853753

Herbach, H., and Janssen, P. A. E. M. (1996). Improvement of the short-fetch behavior in the wave ocean model (WAM). *J. Atmos. Ocean. Technol.* 16, 884–892.

Holmes, B., and Nielsen, K. (2010). Guidelines for the development & testing of wave energy systems. OES-IA Annex II Task, 2.

Hong, J.-S., Moon, J.-H., Kim, T., Cho, I.-H., Choi, J., and Park, J. Y. (2021). Response of wave energy to tidal currents in the western sea of Jeju Island, Korea. *Renew. Energy* 172, 564–573. doi:10.1016/j.renene.2021.03.052

IEA (2022). Electricity market report january 2022. Available online at. https://www.iea.org/reports/electricity-market-report-january-2022.

IEA (2021a). Electricity market report july 2021. Available at: https://www.iea.org/reports/electricity-market-report-july-2021.

IEA (2021b). Net zero by 2050: A roadmap for the global energy sector. Available at: https://www.iea.org/reports/net-zero-by-2050.

IEC (2015). Marine Energy: Wave, tidal and other water current converters – Part 101: Tidal energy resource assessment and characterization (IEC TS 62600-101: 2015). International Electrotechnical Commission.

IRENA (2020). Innovation outlook: Ocean energy technologies, ISBN 978-92-9260-287-1. Available online at. https://www.irena.org/publications/2020/Dec/Innovation-Outlook-Ocean-Energy-Technologies.

Janssen, P. A. E. M. (2008). Progress in ocean wave forecasting. *J. Comput. Phys.* 227, 3572–3594. doi:10.1016/j.jcp.2007.04.029

Janssen, P. A. E. M. (1991). Quasi-linear theory of wind-wave generation applied to wave forecasting. *J. Phys. Oceanogr.* 21, 1631–1642. doi:10.1175/1520-0485(1991)021<1631:qltoww>2.0.co;2

Janssen, P. A. E. M. (1982). Quasilinear approximation for the spectrum of wind-generated water waves. *J. Fluid Mech.* 117, 493–506. doi:10.1017/s0022112082001736

Janssen, P. A. E. M. (1989). Wave-induced stress and the drag of air flow over sea waves. *J. Phys. Oceanogr.* 19, 745–754. doi:10.1175/1520-0485(1989)019<0745:wisatd>2.0.co;2

Kallos, G. (1997). "The regional weather forecasting system SKIRON," in Proceedings, symposium on regional weather prediction on parallel computer environments, October 1997, 15–17. Athens p. 9.

Koletsis, I., Lagouvardos, K., Kotroni, V., and Bartzokas, A. (2009). The interaction of northern wind flow with the complex topography of Crete Island – Part 1: Observational study. *Nat. Hazards Earth Syst. Sci.* 9, 1845–1855. doi:10.5194/nhess-9-1845-2009

Korres, G., Ravdas, M., Zacharioudaki, A., Denaxa, D., and Sotiropoulou, M. (2021). Mediterranean Sea waves reanalysis (CMEMS med-waves, MedWAM3 system) (version 1) [data set]. Copernicus monitoring environment marine service (CMEMS). doi:10.25423/CMCC/MEDSEA_MULTIYEAR_WAV_006_012

Lavidas, G. (2020). Selection index for wave energy deployments (siwed): A near-deterministic index for wave energy converters,. *Energy* 196 (117131), 0360–5442. doi:10.1016/j.energy.2020.117131

Lavidas, G., and Blok, K. (2021). Shifting wave energy perceptions: The case for wave energy converter (WEC) feasibility at milder resources,. *Renew. Energy* 170, 1143–1155. doi:10.1016/j.renene.2021.02.041ISSN 0960-1481

Lehmann, M., Karimpour, F., Goudey, C. A., Jacobson, P. T., and Alam, M. R. (2017). Ocean wave energy in the United States: Current status and future perspectives. *Renew. Sustain. Energy Rev.* 74, 1300–1313. doi:10.1016/j.rser.2016.11.101

Leira, B. J. (2017). "Multi-purpose offshore-platforms: Past, present and future research and developments," in Proceedings of the 36th International Conference on Offshore Mechanics and Arctic Engineering OMAE2017.

Mackay, E. B. L., Bahaj, A. S., and Challenor P. G. (2010a). Uncertainty in wave energy resource assessment. Part 1: Historic data. *Renew. Energy* 35 (8), 1792–1808. doi:10.1016/j.renene.2009.10.026ISSN 0960-1481

Mackay, E. B. L., Bahaj, A. S., and Challenor P. G. (2010b). Uncertainty in wave energy resource assessment. Part 2: Variability and predictability. *Renew. Energy* 35 (8), 1809–1819. ISSN 0960–1481. doi:10.1016/j.renene.2009.10.027

Mattiazzo, G. (2019). State of the art and perspectives of wave energy in the Mediterranean Sea: Backstage of ISWEC. *Front. Energy Res.* 7, 114. doi:10.3389/fenrg.2019.00114

Memè, S., Carillo, A., Antonioli, F., Pisacane, G., Struglia, M. V., Bargagli, A., et al. (2020). Previsioni operative dello stato del mare per il Mediterraneo e per 10 sotto-bacini italiani. Report Report RdS/PTR(2019)/163. Avaialable at: https://www.enea.it/it/Ricerca_sviluppo/documenti/ricerca-di-sistema-elettrico/adp-mise-enea-2019-2021/energia-elettrica-dal-mare/report-rds_ptr2019_163.pdf.

Menicou, M., and Vassiliou, V. (2010). Prospective energy needs in Mediterranean offshore aquaculture: Renewable and sustainable energy solutions. *Renew. Sustain. Energy Rev.* 14 (9), 3084–3091. doi:10.1016/j.rser.2010.06.013

Mérigaud, A., Ramos, V., Paparella, F., and Ringwood, J. (2017). Ocean forecasting for wave energy production. The sea: The science of ocean prediction. *Suppl. J. Mar. Res.* 75 (17), 459–505. doi:10.1357/002224017821836752

Morim, J., Hemer, M., Wang, X. L., Cartwright, N., Trenham, C., Semedo, A., et al. (2019). Robustness and uncertainties in global multivariate wind-wave climate projections. *Nat. Clim. Chang.* 9, 711–718. doi:10.1038/s41558-019-0542-5

Mottershead, D. N., Soar, P. J., Bray, M. J., and Hastewell, L. J. (2020). Reconstructing boulder deposition histories: Extreme wave signatures on a complex rocky shoreline of Malta. *Geosciences* 10, 400. doi:10.3390/geosciences10100400

Omrani, H., Arsouze, T., Béranger, K., Boukthir, M., Drobinski, P., Lebeaupin-Brossier, C., et al. (2016). Sensitivity of the sea circulation to the atmospheric forcing in the Sicily Channel. *Prog. Oceanogr.* 140, 54–68. doi:10.1016/j.pocean.2015.10.007ISSN 0079-6611

Papadopoulos, A., Katsafados, P., and Kallos, G. (2001). Regional weather forecasting for marine application. *Glob. Atmos. Ocean. Syst.* 8 (2–3), 219–237.

Parmeggiani, S., Kofoed, J. P., and Friis-Madsen, E. (2013). Experimental study related to the mooring design for the 1.5 MW Wave Dragon WEC demonstrator at DanWEC. *Energies* 6 (4), 1863–1886.

Petracca, E., Faraggiana, E., Ghigo, A., Sirigu, M., Bracco, G., and Mattiazzo, G. (2022). Design and techno-economic analysis of a novel hybrid offshore wind and wave energy system. *Energies* 15, 2739. doi:10.3390/en15082739

Pisacane, G., Sannino, G., Carillo, A., Struglia, M. V., and Bastianoni, S. (2018). Marine energy exploitation in the mediterranean region: Steps forward and challenges, Frontiers in energy research. https://www.frontiersin.org/article/10.3389/fenrg.2018.00109.6, DOI=10.3389/fenrg.2018.00109,

Poullikkas, A. (2014). Technology prospects of wave power systems. Electron. J. Energy environ. https://repositoriodigital.uct.cl/bitstream/handle/10925/1653/wave_power_ejee.pdf?sequence=3.24769DOI 10.7770/ejee-V2N1-art662.

Previsic, M., Bedard, R., and Hagerman, G. (2004). E2I EPRI assessment offshore wave energy conversion devices. *E2I EPRI WP–004–US–Rev* 1, 1–52.

Pulselli, R. M., Struglia, M. V., Maccanti, M., Bruno, M., Patrizi, N., Neri, E., et al. (2022). Integrating blue energy in maritime spatial planning of mediterranean regions. *Front. Energy Res. Sec.*. Sustainable Energy Systems and Policies. doi:10.3389/fenrg.2022.939961

Ramos, V., and Ringwood, J. V. (2016). Exploring the utility and effectiveness of the IEC (international electrotechnical commission) wave energy resource assessment and characterisation standard: A case study,. *Energy* 107, 668–682. doi:10.1016/j.energy.2016.04.053ISSN 0360-5442

Reeve, D. E., Chen, Y., Pan, S., Magar, V., Simmonds, D. J., and Zacharioudaki, A. (2011). An investigation of the impacts of climate change on wave energy generation: The Wave Hub, Cornwall, UK,. *Renew. Energy* 36 (9), 2404–2413. doi:10.1016/j.renene.2011.02.020ISSN 0960-1481

Ringwood, J., and Brandle, G. (2015). A new world map for wave power with a focus on variability, in: European wave and tidal energy conference, pp. 1–8. Nantes, France, rusu, E. (2014). Evaluation of the wave energy conversion efficiency in various coastal environments. *Energies* 7, 4002–4018. doi:10.3390/en7064002

Silva, D., Rusu, E., and Guedes Soares, C. (2018). The effect of a wave energy farm protecting an aquaculture installation,. *Energies* 11 (8), 2109. doi:10.3390/en11082109

Soerensen, H. C., Friis-Madsen, E., Panhauser, W., Dunce, D., Nedkvintne, J., Frigaard, P. B., et al. (2003). *Dev. Wave Dragon Scale* 1:50 to Prototype. In Proceedings from the fifth European wave energy conference: Cork, Ireland, 2003 (vol. Session 11)

Tran, N., Sergiienko, N. Y., Cazzolato, B. S., Ding, B., Wuillaume, P.-Y., Ghayesh, M. H., et al. (2021). On the importance of nonlinear hydrodynamics and resonance frequencies on power production in multi-mode WECs. *Appl. Ocean Res.* 117 (102924), 102924. 0141-1187. doi:10.1016/j.apor.2021.102924

Ulazia, A., Esnaola, G., Serras, P., and Penalba, M. (2020). On the impact of long-term wave trends on the geometry optimisation of oscillating water column wave energy converters. *Energy* 206 (118146). 0360-5442. doi:10.1016/j.energy.2020.118146

Vicinanza, D., Di Lauro, E., Contestabile, P., Gisonni, C., Lara, J., and Losada, I. J. (2019). Review of innovative harbor breakwaters for wave-energy conversion. *J. Waterw. Port. Coast. Ocean. Eng.* 145, 10. .1061/(ASCE)WW.1943-5460.0000519. doi:10.1061/(asce)ww.1943-5460.0000519

WAMDI-group (1988). The WAM model—a third generation ocean wave prediction ModelThe WAM model - a third generation ocean wave prediction model, in J. *J. Phys. Oceanogr.* 18, 1775–1810. doi:10.1175/1520-0485(1988)018<1775:twmtgo>2.0.co;2

Wan, L., Gao, Z., Moan, T., and Lugni, C. (2016). Comparative experimental study of the survivability of a combined wind and wave energy converter in two testing facilities. *Ocean. Eng.* 111, 82–94. doi:10.1016/j.oceaneng.2015.10.045

Weber, J. (2012)., WEC Technology Readiness and Performance Matrix–finding the best research technology development trajectory*Proc. 4th Int. Conf. Ocean Energy*, Ireland (Vol. 17). Dublin.

Widén, J., Carpman, N., Castellucci, V., Lingfors, D., Olauson, J., Remouit, F., et al. (2015). Variability assessment and forecasting of renewables: A review for solar, wind, wave and tidal resources,. *Renew. Sustain. Energy Rev.* 44, 356–375. doi:10.1016/j.rser.2014.12.019ISSN 1364-0321

Wolf, J., Woolf, D., and Bricheno, L. (2020). Impacts of climate change on storms and waves relevant to the coastal and marine environment around the UK10.14465/2020.arc07.saw. *MCCIP Sci. Rev.* 2020, 132–157.

Zecchetto, S., and De Biasio, F. (2007). Sea surface winds over the Mediterranean basin from satellite data (2000–04): Meso- and local-scale features on annual and seasonal time scales. *J. Appl. Meteorol. Climatol.* 46 (6), 814–827. doi:10.1175/jam2498.1

frontiers | Frontiers in Energy Research

TYPE Perspective
PUBLISHED 09 September 2022
DOI 10.3389/fenrg.2022.937828

OPEN ACCESS

EDITED BY
Maria Vittoria Struglia,
Energy and Sustainable Economic Development (ENEA), Italy

REVIEWED BY
Giuseppe Giorgi,
Politecnico di Torino, Italy

*CORRESPONDENCE
Gabriele Paolinelli,
gabriele.paolinelli@unifi.it

†These authors have contributed equally to this work

SPECIALTY SECTION
This article was submitted to Sustainable Energy Systems and Policies, a section of the journal Frontiers in Energy Research

RECEIVED 06 May 2022
ACCEPTED 28 July 2022
PUBLISHED 09 September 2022

CITATION
Paolinelli G, Fortuna L, Marinaro L and Valentini A (2022), On marine wind power expressiveness: Not just an issue of visual impact.
Front. Energy Res. 10:937828.
doi: 10.3389/fenrg.2022.937828

On marine wind power expressiveness: Not just an issue of visual impact

Gabriele Paolinelli[1*†], Lorenza Fortuna[2†], Ludovica Marinaro[3†] and Antonella Valentini[1†]

[1]Department of Architecture - Landscape Design Lab, University of Florence, Florence, Italy, [2]Ph.D. Programme in Landscape Architecture, University of Florence, Florence, Italy, [3]School of Architecture, University of Florence, Florence, Italy

Technological research for the exploitation of marine energy has produced significant advances which promise to expedite the process of transitioning to renewable resources. However, many issues hinder the effective exploitation of marine energy: among these are cultural concerns regarding the visual impacts of these technologies used. Assuming that "protecting" means preserving without banning evolutive changes, seascape protection and ecological transition are not alternatives because both converge toward sustainability. Even so, scientific concepts, technical practices, social perceptions, and the decisions and actions associated with them raise contradictions and conflicts. Within the complex challenge of ecological transition, clean energy availability arises as a necessary and imperative condition. This article proposes a critical landscape design perspective which focuses on the importance of understanding and expressing contemporaneity through the changes it brings to habitats and life. A focus on the visual impact of marine wind turbine is proposed as an example for a general discussion on technical and social perceptions in a context of both cultural and spatial transition. Site-specific critical visions have to be imagined and discussed to produce not business as usual transformations. This article aims to show that decisions predominantly influenced by issues of visual impact do not adequately express the cultural dimension of ecological transition.

KEYWORDS

ecological transition, blue energy, visual impact, expressiveness, seascape, Mediterranean Sea

Introduction: Ecological transition, today's challenge is one of a long series

Over 60 years ago Sylvia Crowe wrote "Tomorrow's Landscape" (Crowe, 1956), "The Landscape of Power," (Crowe, 1958) and "The Landscape of Roads" (Crowe, 1960). Something was changing in economies and societies, and landscapes were recording the ongoing transitions. Human beings have been using wood for over 120.000 years and coal for more than 800 years; over the last three centuries massive quantities of coal have been burnt to produce energy, and oil and gas have been used for the same purpose since the

early nineteenth century. Surface water, underground heat and nuclear reactivity have been in use for half a century or thereabouts, and (and) solar and wind power for a decade or so. Human societies have always been in transition, but in the last three centuries they have multiplied emissions and waste. In the 20th century the increasing demand for energy caused the electrification of countries and the expression of this in their landscapes. Nowadays we need technologies that will transform natural energies without producing greenhouse gases or generating radioactive waste. "Electrification of the Landscape," a research project the University of Florence is currently undertaking, explores the issue of expressing of contemporaneity, which is also the focus of this paper.

The processes that Crowe envisaged in her seminal books are today widely implemented. In Italy, electricity consumption has increased nearly 40 times from about 8 TWh in 1931 to about 314 TWh in 2011 (ISTAT, 2022). Since the end of the 1980s, internal production, although greatly increased, has not covered national consumption.

The impacts of marine technologies upon ecosystems, fishing, navigation, tourism and recreational activities, vary considerably and productivity levels depend on the available energy: these two factors, therefore will define specific potentials and limits of use. This makes the assessment of the environmental and economic-financial feasibility of such transformations is a priority. The visibility of marine technologies is mostly seen as an issue of visual impact, but landscapes and seascapes are expressions of societies and economies within environments, rather than just panoramas or images. So the ecological transition paradigm is challenging the aesthetics of contemporary cultures and the visibility of changes is affecting its social acceptance. To this general approach to landscape protection, the specific Italian context adds the controversial positions of the landscape authorities, mostly still focused on the 20th century concepts of the preeminence of aesthetic and panoramic values. Planning ecological transition in the Mediterranean region requires a systemic understanding of landscapes and how best to protect them. The care of natural richness and cultural heritage makes it possible to "achieve sustainable development based on a balanced and harmonious relationship between social needs, economic activity, and the environment" (CE, 2000). But we also have to consider that "public understanding of marine cultural landscapes and seascapes is limited yet" (Pungetti, 2012). Because cultural perceptions matter, a vision of the sea is not only just as the environment or territory but also as a special kind of space, with water-covered land and a meaningful liquid surface. This sensitive attention that the English (and German) word "seascape" denotes is missing in the Italian language (and culture); therefore, the commitment is that the word "paesaggio" should be fully inclusive of the dimension of the sea.

Seascape and blue energy

From a formal point of view, the use of certain words is indicative. The Convention on the Law of the Sea (UN General Assembly, 1982) does not use the terms "landscape" or "seascape," but "territory," "environment" and their derivatives do recur several times. With regard to the environment, a regional convention for the Mediterranean Sea was signed in 1976 and then amended to become the Convention for the Protection of the Marine Environment and the Coastal Region of the Mediterranean (UNEP/MAP, 1995). The Marine Strategy Framework Directive (EC, 2008) has the same profile. Although the Landscape Convention approved by the Council of Europe makes no reference to "sea" or "seascape," the text is explicit and demanding when it "includes land, inland water and marine areas" (CE, 2000). The scientific literature identifies seascape with regard to specific features. "(...) the concept of seascape, initially meaning a picture or view to the sea, or a view of an expanse of sea (Oxford English Dictionary), has been broadened to mean the coastal landscape and adjoining areas of open water, including views from land to sea, from sea to land and along the coastline. As it can describe the effect on landscape at the confluence of sea and land, seascape becomes an area of intervisibility between land and sea, with three defined components: sea, coastline, and land" (Pungetti, 2012). So with regard to the sea it is evident that there are not only territorial, environmental and blue energy issues, that beyond environmental and economical issues, there is not only the social issue of visual impact.

According to European Commission communications on Blue Energy (EC, 2012; EC, 2014), offshore wind and marine technologies can generate electricity and contribute towards sustainable development. In fact, technological developments can positively impact the supply of sustainable electricity, even though average potentials in the Mediterranean Sea are lower than those found in the North Sea and the oceans (Golfetti et al., 2018; Nikolaidis et al., 2019). Research into the exploitation of marine energy has produced significant advances which have the potential to expedite the process of ecological transition (Pisacane et al., 2018) but there are still issues that need to be explored (Golfetti et al., 2018).

Regarding the visibility of energetic changes, we consider the development of offshore wind plants as a key to understanding landscape relationships brought into existence by the visibility of sustainable energy generating infrastructure. With regard to the impact of this type of infrastructure on visual resources and the stewardship required, the literature makes it clear that a dominat issue is how the impact is classified (Golfetti et al., 2018). Some researches (Haggett, 2010; Jones and Eiser, 2010; Walker et al., 2014) highlight how sensitivities towards visible changes along coastal landscapes and seascapes are not only caused by exterior attachments to their images but also depend on people's sense of places, be they insiders or outsiders, tourists or workers, and

independently of their ages and social ranks. Technocratic approaches are characterised by a lack of public participation and unfortunately this is widespread in the decision-making and design processes for offshore wind plants (Breukers and Wolsink, 2007; Wolsink, 2007). Effective engagement with local stakeholders is likely to result in a fuller, and more meaningfullikely to result in a fuller, and more meaningful understanding of the issues involved (Van Hooijdonk et al., 2007). Wind turbines can easily seem contradictory and unrelated to the consolidated image of marine landscape: they provide new perceptions and change the relationship between the landscape and the observer (Pasqualetti, 2011; Sullivan et al., 2012a; Donaldson, 2018; Colafranceschi and Manfredi, 2021). Most studies are about to move away from what is identified as a visual problem (O'Keeffe and Haggett, 2012), or at least from the solution of making that which is impossible to hide seem smaller. This prevailing perspective makes the need for mitigation arise as a key point if there is to be a general acceptance of wind farm implementation (Sullivan et al., 2012b; Walker et al., 2014; Donaldson, 2018), bringing into play several aspects of the design process.

By only evaluating the visual impact of a wind farm with a view to pushing it further offshore, its expressive potential is denied before it has been critically investigated. The visibility of marine wind turbines needs to be discussed in a context that does not only seek to mitigate the effect of their presence but also identifies what they can add to seascapes in terms of aesthetic meaning and scenic value. In such conceptual framework the transitioning of the landscape emerges as a sensitive matter, to be evaluated and framed taking into account people's attachment to places and their sense of landscape's identity loss (Jones and Eiser, 2009; Gee, 2010; Haggett, 2010; Pasqualetti, 2011; Walker et al., 2014; DeWan, 2018). Social perceptions, though, depend on cultures and attitudes which change over time: turbines could become inherent to seascapes. Moving energy generating plants offshore for tens of kilometers requires the laying of submarine cables which increases their environmental impacts and makes their construction and management less economically viable (Green and Vasilakos, 2011). If the intention of hiding wind farms is replaced with a willingness to consider their expressive potential the point of view could shift towards an understanding of sustainable aesthetics (Nohl, 2001; Meyer, 2008; Paolinelli, 2018).

Position: Expressing versus hiding

While most contributions focus on how to hide or reduce disturbance and visual disamenity of marine wind farms (Ladenburg and Dubgaard, 2009; Krueger et al., 2011; Donaldson, 2018), it is worth trying to change this perspective and consider energy transition as an opportunity to design something which will have an effect on aesthetics. In fact hiding anthropic changes is a strange, non-evolutionary way of expressing their meanings.

With regard to Blue Energy, some features of the sea matter. It is a wide-open surface, for the most part uniform and flat, which hosts few anthropic structures, mostly perceived from on-shore points of view and less frequently from off-shore, and it has a straight continuous horizon that distinguishes its surface from the sky. Seascapes express unique scale factors in terms of objects-background and object-surface relations.

Thus, we could argue that the width of the sea surface probably makes large turbines more suitable than smaller ones, and that the almost total absence of human structures could significantly reduce scale concerns for such huge technological devices (Scottish Natural Heritage, 2014). Visual perceptions also depend upon distances. A short distance produces an imbalance of scale between the observer and the power plants. These dominate the scene, making it seem disharmonious and disturbing the comprehensibility of the seascape's new connotation. If the power plants are too far from any potential point of view their connoting capacity decreases, and the low comprehensibility of the images generates disturbance. Thus, it is worth evaluating distances as key factors when designing wind farms, in order to balance environmental and visual impacts, and construction and management costs. Some authors (Ladenburg and Dubgaard, 2007; Haggett, 2010) however argue that it is worth moving the power plants as far away as possible to reduce their visual impact, despite the higher cost. Power plant planning must provide congruous coastal marine corridors to safeguard the many human activities which depend on seascapes; it must also allow for large marine fields, in order to alternate the visibility of smaller areas of changed seascape with larger ones that maintain the horizon intact.

According to Sullivan et al. (2012a) and Colafranceschi and Manfredi (2021), rotational motion is sometimes perceived as a factor of visual disturbance, unrelated, and detached from the seascape scenery, because it contrasts with backgrounds' stillness. This perspective recalls the notion of panorama: a view to be observed as a canvas with fixed images whereas in seascapes everything is actually in constant movement, both in the sea and in the sky, with natural changing speeds and rhythms. Seascape reveals the power of nature and our ability to exploit it: wind turbines are just human inventions that highlight natural forces.

For engineering reasons wind farms are generally designed in regular patterns with clusters prevailing over one-line patterns. We suggest that, independently of their orientation, extended lines of turbines should also be avoided for visual reasons because they could adversely affect the view of the horizon making it uniform and continuously disturbed by structures.

Looking for a seascape planning position on the issue of offshore wind plant visibility, here we propose a preliminar focus on distances from the shore, the main focus in the literature on visual impact and social acceptance. This literature clearly

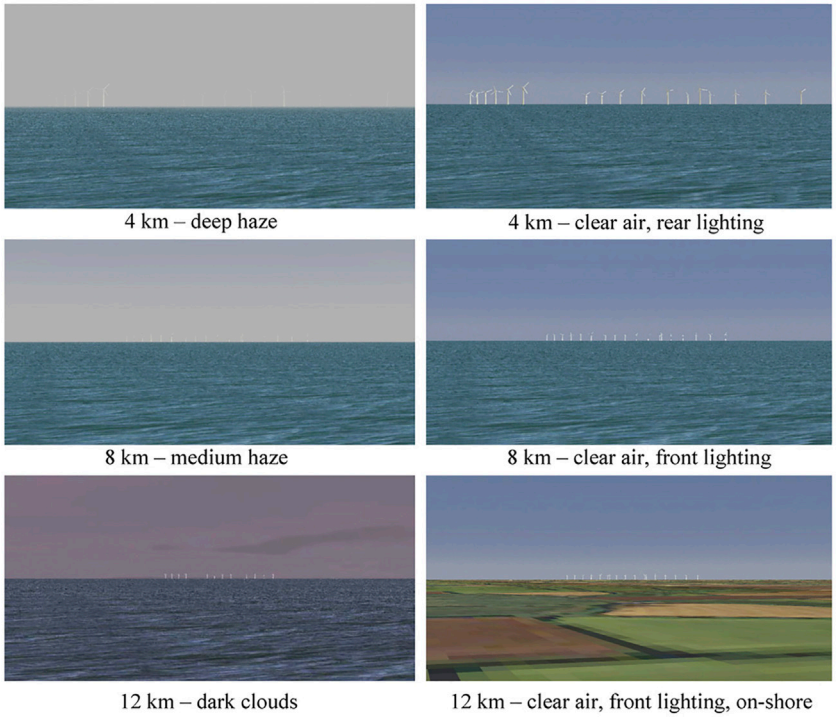

FIGURE 1
Simulation of visibility as a variable of distance: the visual recognition of turbines appears weak at around 8 km and compromised at around 12. Source of image: Bishop and Miller (2007, page 819).

demonstrates that opinions on these issue depend primarily on social perceptions and indicates the need to identify basic topics that can be culturally shared. Here, we are not defining visual dimensional planning standards but just posing a concept: expressing versus hiding. So we have consulted available visual data to reflect on the topic, but parametric digital simulations will need to be elaborated to test the hypothesis.

Some simulations carried out by Bishop and Miller (2007) about turbines of a 2.0 MW commercial facility with a 100 m tower and 40 m blades show that at 4 km from the coast both the turbine formations and the marine horizon which they interfere with are legible. Around 8 km, the legibility weakens and at around 12 km it appears compromised (Figure 1). This fits in with the findings of Sullivan et al. (2012b) as we can also see in Figure 2: at about 12 km from the coast turbines are still visible, but at such a distance it is no longer possible to perceive the composition of the clusters or to enjoy the alternation of seascape with intact horizon. So, we can hypothesize the need for a distance at least 20 km to avoid visual interference with the horizon. Conversely, close to the shoreline wind plants not only interfere with many activities but also produce heavy scale imbalances of the scenery. Regarding turbines for commercial plants with heights of between 100 and 200 m approx., a distance of 2 km is just a dimension with a 10 factor for heights till up to 200 m and a 20 factor for heights up to 100 m. Here, the hypothesis regards the visual inadequacy of the strip lying between the shoreline and 2–5 km out to sea, with the exception of small wind farms with only a few turbines that can become landscape identity factors expressing the ecological energy transition.

Between the distances of 2–5 km from the coast and 20 km from it, the visual effects of inserting wind farms change. In the area closest to the coast, clusters and their compositions may be legible both compared with the spatial fields without turbines and with the horizon visibility within the clusters, while in the furthest area there are the conditions of visibility and illegibility mentioned earlier. A distinction of the two bands may be assumed as from 2–5 km from the shore up to 5–10 km, and 5–10 km up from the shore to 20 km.

These topics should be investigated with regard to the dynamics of social perceptions by submitting simulations as photorealistic images (rendering) or as immersive experiences (augmented reality) and by holding discussions within participatory processes, which also enhance cultural awareness of ecological transition in the same context as care of seascapes. In a general hypothesis about the changes in seascape expressivity the suitable plant options for large 2 MW industrial turbines from 100 to 200 m high are probably two of the four possible:

– Far away from the shore (d > 20 Km approx.) - a recommended alternative: the turbines are far enough to away eliminate visibility

FIGURE 2
A sample of low visual impact with lack of expressiveness of changes. In such a situation, the infrastructures are not far enough away to eliminate their visibility on the horizon and not close enough to be perceived from the coast. Source of image: Sullivan et al., 2012b, page 6 of the conference paper.

on the horizon but offer a comprehensible and expressive visual of sustainable energy generation to passing ships;
– A medium distance from the shore (5–10 Km approx. < d < 20 Km approx.) - an inadvisable alternative: the turbines are not far enough away to eliminate their visibility on the horizon and are not close enough to be comprehended from the coast line therefore thereby denying expression to the energy transformation process;
– Not far from the shore (2–5 Km approx. < d < 5–10 Km approx.) - a recommended alternative: the turbines are far enough to avoid scale imbalances but close enough for comprehensibility from the coast and therefore for giving expression to the energy transformation process;
– Close to the shoreline (d < 2–5 Km approx.) - an inadvisable alternative: the distance is insufficient to avoid scale imbalances.

Discussion: Ecological transition in seascapes

Protecting a seascape means preserving its essence without preventing changes. This means that seascape protection and ecological transition are complementary to achieving the goal of sustainability. Scientific concepts, technical practices, social perceptions, and the consequent evaluations, decisions, and actions can help prevent contradictions and conflicts.

In every age and geographical area, landscapes and seascapes express the relationships between nature and culture in space and time: the present was once a future and it is going to become a past. The sustainability balances of energy transition interventions need to consider cultural as well as environmental and economic–financial issues. Visual impact is not the only issue if we seek to "express" changes rather than "hiding" them. It is not feasible to reduce these issues to a binary form: yes vs. no, close vs. far, and very visible vs. barely visible. Rather, there is a need to calibrate certain quantities, which are essential quality factors. Visual impact assessments are not enough, we need to design comparisons of expressible scenic properties. Nor are purely technical comparisons sufficient: we need iterative participatory processes to produce more meaningful results.

Because environmental issues are essential for sustainability, they must be *a priori* considered and satisfied, with increasing

recourse to multi-scale balances which also take into account the ecological impacts of non-transition scenarios. With regard to the three linked goals of the New European Bauhaus promoted by the European Commission, it is essential to build not only more sustainable but also more beautiful and inclusive landscapes. Moreover aesthetics are included among the non-material cultural services in the Millennium Ecosystem Assessment (Swaffield and McWilliam, 2013). So we need to constantly bear in mind that sustainability is the comprehensive key of contemporaneity and to understand that beauty cannot exist without it. Ecological transition is stressing our societies with essential challenges that have to be dealt with by thinking together about ecology, economy, ethics, and aesthetics.

In Italy, 64 projects for floating offshore wind farms have recently been proposed and 40 of those have been examined (MiTE, 2021). At least 20 of the expressions of interest have proposed detailed projects, which in many cases include floating plants located over 12 miles from the coast. Of the 40 floating offshore wind farm projects that have been examined, many are located off the coast of Sicily and Sardinia (more than 20), others are located along the Adriatic coast (more than 10) and the remainder are distributed between the Ionian and Tyrrhenian (MiTE, 2021). If the reason for this propensity to float the wind farms offshore lies in the search for the best environmental and economic cost-benefit ratios, this is the right way to proceed. If, on the other hand, the predominant reason is to move the wind farms as far away as possible so they are seen as little as possible, then the choice is inspired by an obsolete concept of landscape and it will limit the development of the essential cultural dimension of ecological transition and compromise the expression of natural energies through human imagination and action. In the official communication of the Ministry of Ecological Transition, we read that it is continuing its work aimed at encouraging the development of a new generation of floating offshore plants, located off the Italian coast and therefore devoid of any impact on the landscape (MiTE, 2021). Once again, visual-impact based positions seem to prevail. As considering landscapes and seascapes as panoramas is simplistic, there need to be changes to this banal approach. Critical scenarios need to be developed and compared using expert design processes and then discussed and selected through participation processes in which the local communities involved are actively engaged. The more ecological transition remains unexpressed or poorly expressed, the less it will be understood both by living and future generations.

A century after the Mumford proposal, we again need utopia to look for "a reconstituted environment, which is better adapted to the nature and aims of the human beings who dwell within it than the actual one; and not merely better adapted to their actual nature, but better fitted to their possible development" (Mumford, 1922). Such planning, mostly intended as a "strong forward looking action" (CE, 2000), can bring forth the beauty inherent in sustainability and stimulate the understanding of its meaning (Paolinelli, 2018). "The intrinsic beauty of landscape resides in its change over time. Landscape architecture's medium (...) is material and tactile; it is spatial. But more than its related fields, the landscape medium is temporal" (Meyer, 2008).

Transition means change and we cannot expect landscapes to defy evolution and not express this change. Landscapes sediment the effects of what we do and represent who we are, our participation in life on Earth. Removing the things we make from our backyards and hiding them far away and out of sight or coloring them green, does not erase them, but it does erase our will to express ourselves. Another problem that this transition poses is therefore to avoid hiding and to express the human intervention in the landscape well.

Data availability statement

The original contributions presented in the study are included in the article/Supplementary Material; further inquiries can be directed to the corresponding author.

Author contributions

All authors listed have made a substantial, direct, and intellectual contribution to the work and approved it for publication.

Funding

The publication is funded by the University of Florence, Department of Architecture, as part of the research "Electrification of the Landscape" and of the Landscape Design Lab activities.

Conflict of interest

The authors declare that the research was conducted in the absence of any commercial or financial relationships that could be construed as a potential conflict of interest.

Publisher's note

References

Bishop, I. D., and Miller, D. R. (2007). Visual assessment of off-shore wind turbines: The influence of distance, contrast, movement and social variables. *Renew. Energy* 32, 814–831. doi:10.1016/j.renene.2006.03.009

Breukers, S., and Wolsink, M. (2007). Wind power implementation in changing institutional landscapes: An international comparison. *Energy policy* 35, 2737–2750. doi:10.1016/j.enpol.2006.12.004

CE (2000). *Council of Europe landscape convention*. Florence: European Treaty Series n°176. 20.10.2000, amended by the 2016 Protocol.

Colafranceschi, D. Sala P., and Manfredi, F. (2021). Nature of the wind, the culture of the landscape: Toward an energy sustainability project in catalonia. *Sustainability* 13, 7110. doi:10.3390/su13137110

Crowe, S. (1958). *The landscape of power*. London: The Architectural Press.

Crowe, S. (1960). *The landscape of Roads*. London: The Architectural Press.

Crowe, S. (1956). *Tomorrow's landscape*. London: The Architectural Press.

DeWan, T. (2018). "The Maine wind energy act. In a time of change," in *2018. Visual resource stewardship conference proceedings: Landscape and seascape management in a time of change. Gen. Tech. Rep. NRS-P-183*. Editors P. H. Gobster and R. C. Smardon (Newtown Square, PA: U.S. Department of Agriculture, Forest Service). Northern Research Station, Visual Case Studies.

Donaldson, J. J. (2018). in *Mitigating visual impacts of utility-scale energy projects*. Editors P. H. Gobster and R. C. Smardon (cit.), Newtown Square, PA, 237–243.

EC (2014). *Communication from the commission to the European parliament, the Council, the European economic and social committee and the committee of the regions, blue energy action needed to deliver on the potential of ocean energy in European seas and oceans by 2020 and beyond*. Bruxelles: European Commission.

EC (2012). *Communication from the commission to the European parliament, the Council, the European economic and social committee and the committee of the regions, blue growth opportunities for marine and maritime sustainable growth*. Bruxelles: European Commission.

EC (2008). Directive 2008/56/EC of the European Parliament and of the Council of 17 June 2008 establishing a framework for community action in the field of marine environmental policy (Marine Strategy Framework Directive). *OJ L* 164, June 25, 2008.

Gee, K. (2010). Offshore wind power development as affected by seascape values on the German North Sea coast. *Land Use Policy* 27, 185–194. doi:10.1016/j.landusepol.2009.05.003

Golfetti, G., Montini, M., Volpe, F., Gigliotti, M., Pulselli, F. M., Sannino, G., et al. (2018). Disaggregating the SWOT analysis of marine renewable energies. *Front. Energy Res.* 6, 138. doi:10.3389/fenrg.2018.00138

Green, R., and Vasilakos, N. (2011). The economics of offshore wind. *Energy Policy* 39, 496–502. doi:10.1016/j.enpol.2010.10.011

Haggett, C. (2010). Understanding public responses to offshore wind power. *Energy Policy* 39 (2), 503–510. doi:10.1016/j.enpol.2010.10.014

ISTAT (2022). *Produzione lorda e consumo di energia elettrica in Italia - anni 1883-2014*. Serie Storiche. Roma: Istituto Nazionale di Statistica (Accessed March 30, 2022).

Jones, C. R., and Eiser, R. (2009). Identifying predictors of attitudes towards local onshore wind development with reference to an English case study. *Energy policy* 37, 4604–4614. doi:10.1016/j.enpol.2009.06.015

Jones, C. R., and Eiser, R. (2010). Understanding 'local' opposition to wind development in the UK: How big is a backyard? *Energy policy* 38, 3106–3117. doi:10.1016/j.enpol.2010.01.051

Krueger, A. D., Parsons, G. R., and Firestone, J. (2011). Valuing the visual disamenity of offshore wind power projects at varying distances from the shore: An application on the Delaware shoreline. *Land Econ.* 87 (2), 268–283. doi:10.3368/le.87.2.268

Ladenburg, J., and Dubgaard, A. (2009). Preferences of coastal zone user groups regarding the siting of offshore wind farms. *Ocean Coast. Manag.* 52, 233–242. doi:10.1016/j.ocecoaman.2009.02.002

Ladenburg, J., and Dubgaard, A. (2007). Willingness to pay for reduced visual disamenities from offshore wind farms in Denmark. *Energy Policy* 35, 4059–4071. doi:10.1016/j.enpol.2007.01.023

Meyer, E. K. (2008). Sustaining beauty. The performance of appearance. *J. Landsc. Archit.* 3 (1), 6–23. doi:10.1080/18626033.2008.9723392

MiTE (Italian Government, Ministry of Ecological Transition) (2021). *Eolico offshore: Pervenute 64 manifestazioni di interesse*. Rome: Official press communication. Available at: https://www.mite.gov.it/comunicati/eolico-offshore-pervenute-64-manifestazioni-di-interesse (Accessed April 29, 2022).

Mumford, L. (1922). *The story of utopias*. New York: Boni and Liveright, 21.

Nikolaidis, G., Karaolia, A., Matsikaris, A., Nikolaidis, A., Nicolaides, M., and Georgiou, G. C. (2019). Blue energy potential analysis in the mediterranean. *Front. Energy Res.* 7, 62. doi:10.3389/fenrg.2019.00062

Nohl, W. (2001). Sustainable landscape use and aesthetic perception - preliminary reflections on future landscape aesthetics. *Landsc. Urban Plan.* 54, 223–237. doi:10.1016/s0169-2046(01)00138-4

O'Keeffe, A., and Hagget, C. (2012). An investigation into the potential barriers facing the development of offshore wind energy in Scotland: Case study - firth of Forth offshore wind farm. *Renew. Sustain. Energy Rev.* 16, 3711–3721. doi:10.1016/j.rser.2012.03.018

Paolinelli, G. (2018). *Landscape design in a changing world*. Florence: DIDAPress, 182.

Pasqualetti, M. J. (2011). Opposing wind energy landscapes. A search for common cause. *Ann. Assoc. Am. Geogr.* 101, 907–917. doi:10.1080/00045608.2011.568879

Pisacane, G., Sannino, G., Carillo, A., Struglia, M. V., and Bastianoni, S. (2018). Marine energy exploitation in the mediterranean region: Steps, forward and challenges. *Front. Energy Res.* 6, 109. doi:10.3389/fenrg.2018.00109

Pungetti, G. (2012). Islands, culture, landscape and seascape. *J. Mar. Isl. Cult.* 1, 51–54. doi:10.1016/j.imic.2012.11.007

Scottish Natural Heritage (2014). Siting and designing wind farms in the landscape. Version 2. 2014. Available at: https://www.nature.scot/siting-and-designing-wind-farms-landscape-version-2.

Sullivan, R. G., Cothren, J., Winters, S. L., Cooper, C., and Ball, D. (2012b). "An assessment of offshore wind turbine visibility in the United Kingdom," in Oceans, conference paper, Hampton Roads, VA, USA, 14-19 October 2012 (IEEE). doi:10.1109/OCEANS.2012.6405138

Sullivan, R. G., Kirchler, L., Roche, S., Beckman, K., and Richmond, P. (2012a). "Wind turbine visibility and visual impact threshold distances in Western landscapes," in Proceedings, National Association of Environmental Professionals, 37th Annual Conference, Portland, Or, May 21-24, 2012.

Swaffield, S. R., and McWilliam, W. J. (2013). "Landscape aesthetic experience and ecosystem services," in *Ecosystem services in New Zealand – conditions and 349 trends"*. Editor J. R. Dymond (Lincoln, New Zealand: Manaaki Whenua Press).

UN General Assembly (1982). Convention on the Law of the sea. Available at: https://www.refworld.org/docid/3dd8fd1b4.html (Accessed May 3, 2022).

UNEP/MAP (1995). *Convention for the protection of the marine environment and the coastal region of the mediterranean*. Barcelona: United Nations.

Van Hooijdonk, E., Barrot, J., and Gallanti, G. (2007). *Soft values of seaports. A Strategy for the restoration of public support for seaports*. Antwerpen: Garant Publishers.

Walker, B. J. A., Wiersma, B., and Bailey, E. (2014). Community benefits, framing and the social acceptance of offshore wind farms: An experimental study in England. *Energy Res. Soc. Sci.* 3, 46–54. doi:10.1016/j.erss.2014.07.003

Wolsink, M. (2007). Planning of renewables schemes: Deliberative and fair decision-making on landscape issues instead of reproachful accusations of non-cooperation. *Energy policy* 35, 2692–2704. doi:10.1016/j.enpol.2006.12.002

frontiers | Frontiers in Energy Research

TYPE Original Research
PUBLISHED 29 September 2022
DOI 10.3389/fenrg.2022.980557

OPEN ACCESS

EDITED BY
Muhammad Shafique,
Brunel University London,
United Kingdom

REVIEWED BY
Sheng Xu,
Jiangsu University of Science and Technology, China
Mohd Rosdzimin Abdul Rahman,
National Defence University of Malaysia, Malaysia
Mark Mba Wright,
Iowa State University, United States

*CORRESPONDENCE
Riccardo Maria Pulselli,
riccardomaria.pulselli@unifi.it

SPECIALTY SECTION
This article was submitted to Sustainable Energy Systems and Policies, a section of the journal Frontiers in Energy Research

RECEIVED 28 June 2022
ACCEPTED 04 August 2022
PUBLISHED 29 September 2022

CITATION
Bruno M, Maccanti M, Pulselli RM, Sabbetta A, Neri E, Patrizi N and Bastianoni S (2022), Benchmarking marine renewable energy technologies through LCA: Wave energy converters in the Mediterranean.
Front. Energy Res. 10:980557.
doi: 10.3389/fenrg.2022.980557

Benchmarking marine renewable energy technologies through LCA: Wave energy converters in the Mediterranean

Morena Bruno[1], Matteo Maccanti[1], Riccardo Maria Pulselli[2,3]*, Alessio Sabbetta[2], Elena Neri[2], Nicoletta Patrizi[1] and Simone Bastianoni[1]

[1]Department of Physical, Ecodynamics Group, Earth and Environmental Sciences, University of Siena, Siena, Italy, [2]INDACO2 srl, Colle di Val d'Elsa, Siena, Italy, [3]Department of Architecture, University of Florence, Florence, Italy

The present work evaluates the environmental performance of three wave energy converters including on-shore oscillating water columns and oscillating floaters embedded in piers, and near-shore seabed-based buoys in the Mediterranean Basin. The life cycle assessment methodology was used to account for their potential environmental impact, in terms of carbon footprint (t CO_2eq), considering four main phases, i.e., manufacturing of material components, assembling and installation on site, maintenance in time, and decommission end of life. Results show the greenhouse gas emission from different lifecycle processes, based on the inventory of main energy inputs and materials, highlighting the major impact of the manufacture of the structural components (52 %), especially due to the limited durability of materials. In order to compare the performances of the three different wave energy converters, the carbon intensity of electricity was evaluated considering a range of electricity production per technology based on data available in scientific literature. The results obtained for a single device (203–270 g CO_2eq·kWh^{-1} for the oscillating water column system; 94–374 g CO_2eq·kWh^{-1} for oscillating floater and 105–158 g CO_2eq·kWh^{-1} for the seabed-based buoy) highlight that wave energy converters are promising solutions to harvest wave energy, showing lower carbon intensity of electricity values compared to fossil energy sources; nevertheless, technological improvements are needed to increase efficiency and achieve the performances of other renewable energy sources. Moreover, the combination of wave energy converters with other solutions, such as offshore wind turbines, represents a valuable option in the future to increase productivity and foster energy transition of the Mediterranean regions.

Abbreviations: CF, Carbon Footprint; CIE, Carbon Intensity of Electricity; EC, European Commission; EoL, End of Life; FU, Functional Unit; GHG, Greenhouse gas; GWP, Global Warming Potential; LCA, Life Cycle Assessment; LCOE, Levelized Cost of Energy; MRE, Marine Renewable Energy; OWC, Oscillating Water Column; PTO, Power Take-Off; WEC, Wave Energy Converter.

KEYWORDS

ocean energy, energy transition, life cycle assessment, carbon footprint, carbon intensity of electricity

1 Introduction

Blue economy includes all those activities that are marine-based or marine-related (European Commission (EC), 2021); particularly, one of the emerging and innovative sectors is Marine Renewable Energy (MRE). Marine energy, also called ocean energy, is seawater-based renewable energy in which the kinetic and potential energies in tides, waves, and currents are used to drive systems to produce electricity (Mohamed, 2021). Climate change and environmental degradation are an existential threat to Europe and the world; for this reason, MRE could be a key in meeting the European green deal targets supporting economic growth, energy transition, and job opportunities (Pirttimaa and Cruz, 2020).

The European Commission (EC) proposed to raise the European Union's ambition on reducing greenhouse gas (GHG) emissions to at least 55 % below the levels of 1990 by 2030 and to achieve climate neutrality by 2050 (European Commission (EC), 2022). To this purpose, the transition to a competitive economy with low carbon emissions requires higher rates of renewable energy and ocean energy can play a relevant role (Appiott et al., 2014).

Ocean energy technologies are currently being developed and tested to exploit the vast source of energy that seas and oceans have to offer (European Commission (EC), 2021), theoretically over 30,000 TWh·year^{-1} globally (Liu et al., 2017). Although in many cases they are still at the early stage of development and not yet commercially available, wave and tidal energy converters have been widely tested in the last years (Falcão, 2010; Douziech et al., 2016).

Wave power represents a considerable source of renewable energy, nevertheless, most of the Wave Energy Converters (WECs) developed still require further research and demonstration tests (Apolonia and Simas, 2021). As highlighted by Esteban et al. (2017), the technology behind WECs is not mature enough to be developed industrially and the Levelized Cost of Energy (LCOE) remains too high. According to International Renewable Energy Agency (IRENA) (2020), currently, 33 WECs with a combined capacity of 2.3 MW are deployed in 9 projects across 8 countries and 3 continents. France, Gibraltar, Greece, Israel, Italy, Portugal, and Spain are examples of Mediterranean locations in which these projects are activated.

Since the real-life applications of WECs are currently limited (Zhai et al., 2018), their environmental performance and potential impacts are not well known. In this context, the Life Cycle Assessment (LCA) can be a proper methodology to account for the potential environmental impacts characterizing WECs throughout the value chain. From the extraction of raw materials to the production of structural elements, their assembling on site, maintenance in time, end-of-life management, recycling, and final disposal, the LCA examines and quantifies the amount of GHG emissions from the different stages. The results allow for evaluating the environmental performance of different devices, identifying solutions to improve efficiency and address choices. At the same time, it permits the comparison with other technologies with equivalent functions in order to select those with lower environmental impacts (Paredes et al., 2019).

In recent years, LCA was applied to assess the environmental performances of different WEC technologies, each able to harvest wave energy and generate electricity. Generally, WECs are conceptualized to absorb kinetic energy, mainly through moving bodies, potential energy, through overtopping devices or attenuators, or both through point absorbers (International Renewable Energy Agency (IRENA), 2020). These systems are classified according to different criteria such as location, device size, orientation, conversion principle, energy capture, energy use, and installation site (Koca et al., 2013; Khan et al., 2017).

The aim of this study is to evaluate, through an LCA-based analysis, the Carbon Footprint (CF), expressed in ton of carbon dioxide equivalent (t CO_2eq) of three WECs and their adaptability to the Mediterranean contest. These include two onshore devices embedded in piers or docks, namely Oscillating Water Column (OWC) and Oscillating Floater, and a near-shore seabed-based buoy.

A literature review of the most relevant LCA studies of onshore and offshore WECs was conducted (Table 1). To allow an easy comparison among WECs, the corresponding Carbon Intensity of Electricity (CIE) was reported as well, namely the CO_2eq emissions generated by the life cycle of each WEC with its average annual productivity (MWh). This performance indicator permits to compare the GHG emission mitigation effect of different solutions, as lower CIE values indicate lower impacts per unit of energy produced. Calculating the CIE allows us to highlight the profitability, in the long run, of those projects that enable producing clean energy with lower emissions. CIE is, in fact, an intensive indicator that allows for adding information to the mere environmental cost assessment of any technology. Results of CIE should complement the information that drives the decision on these plant installations, such as the type of construction technique, the operating principle, and the meteorological characteristics of the hypothetical installation site.

Table 1 also gives information on the technical characteristics, nominal power (in MW), and LCA phases considered (system boundary) to account for the CIE values per each WEC.

10.3389/fenrg.2022.980557

TABLE 1 Literature review of previous LCA studies on WECs and focus on the Carbon Intensity of Electricity (CIE) (g CO_2eq·kWh^{-1}) evaluation.

Nominal Power	CIE (g CO_2eq·kWh^{-1})	Lifetime (yr)	References	Device type	System boundary	Notes and other Info
1 MW	47	20	Dalton et al. (2014)	Wavestar WEC	From the extraction of raw materials to the disposal of waste ("cradle-to-grave")	**Design:** Wave Star Energy ApS. Located 1.5 km from the coast. **Outcomes:** Embodied energies, energy intensity, embodied CO_2 and CO_2e emissions, carbon intensity, energy and carbon payback, cost of electricity
750 kW	23.0	20	Parker et al. (2007)	Pelamis WEC	Extraction of the raw materials, manufacturing, assembly and installation, operation and maintenance (O&M), end-of-life (EoL) ("cradle to grave")	**Design:** Edinburgh-based Ocean Power Delivery Ltd. The first versions were 120 m long, 3.5 m in diameter and rated at 750 kW. Designed for water depths of 50–100 m. **Outcomes:** Embodied energy, embodied CO_2, energy payback, CO2 payback.
	30.0		Thomson et al. (2011)		Material extraction, processing, manufacture, assembly, installation, O&M, decomissioning in landfill or recycling ("cradle-to-grave")	**Design:** Modeled based on Parker et al. (2007). **Outcomes:** Embodied energy, global warming 100a, ozone depletion, ozone formation (vegetation), ozone formation (human), acidification, terrestrial eutrophication, aquatic eutrophication EP(N), aquatic eutrophication EP(p), human toxicity air, human toxicity water human toxicity soil, ecotoxicity water chronic, ecotoxicity water acute, ecotoxicity soil chronic, hazardous waste, slags/ashes, bulk waste, radioactive waste, resources (all).
	20.0		Banerjee et al. (2013)		Raw material impacts ("cradle-to-gate")	**Design:** Based on Taylor (2006). Lifetime follows Parker et al. (2007). **Outcomes:** Global warming potential, energy payback period.
	44.0		Uihlein, (2016)		Extraction of raw material, assembly and manufacturing, installation and maintenance, use and EoL ("cradle-to-grave")	**Design:** Weight ranges depend on device type (103 wave devices from 50 developers). **Outcomes:** Global warming potential.
	35.0		Thomson et al. (2019)		Extraction of the raw materials, manufacturing, assembly and installation, operation and maintenance, EoL ("cradle to grave")	**Design:** Based on Parker et al. (2007). **Outcomes:** Climate change, ozone depletion, photochemical oxidant formation, terrestrial acidification, freshwater eutrophication, marine eutrophication, particulate matter formation, human toxicity, terrestrial ecotoxicity, freshwater ecotoxicity, marine ecotoxicity, ionising radiation, agricultural land occupation, urban land occupation, natural land transformation, water depletion, metal depletion, fossil depletion, cumulative energy demand, and embodied Energy
315 kW	25.0	15	Walker and Howell, (2011)	Oyster WEC	Material extraction, manufacturing, transport, installation, O&M and decommissioning (including recycling)	**Design:** Aquamarine Power Ltd. **Outcomes:** Energy use and carbon emissions.
-	64.0	20	Uihlein, (2016)		Extraction of the raw materials, manufacturing, assembly and installation, O&M, EoL ("cradle to grave")	**Design:** Weight ranges depend on device type (103 wave devices from 50 developers). **Outcomes:** Global Warming Potential
800 kW	65.5	20	Douziech et al. (2016)		Construction, transport, O&M, EoL ("cradle to grave")	**Design:** Aquamarine Ltd. Efficiency 40%, annual expected power generation of 2.8 GWh. **Outcomes:** Climate change

(Continued on following page)

TABLE 1 (*Continued*) Literature review of previous LCA studies on WECs and focus on the Carbon Intensity of Electricity (CIE) (g CO_2eq·kWh^{-1}) evaluation.

Nominal Power	CIE (g CO_2eq·kWh^{-1})	Lifetime (yr)	References	Device type	System boundary	Notes and other Info
wave power farm of 20 MW	39–126	20	Dahlsten, (2009)	Point absorber WEC	From the extraction of raw materials to the disposal of waste ("cradle-to-grave")	**Design:** Seabased Industry AB. **Outcomes:** Global Warming Potential, Ozone Depletion potential, acidification, eutrophication, non-renewable energy, water use, and energy payback time
-	105.0	20	Uihlein, (2016)	-	All life cycle steps 'from cradle to grave', including device assembly and manufacturing, installation and maintenance, use and EoL	**Design:** Weight ranges depend on device type (103 wave devices from 50 developers). **Outcomes:** Global Warming Potential
wave power farm of 20 MW	30–80	5	Zepeda, (2017)	-	Material extraction, processing, manufacture, assembly, installation, O&M, decomissioning in landfill or recycling ("cradle-to-grave")	**Design:** Based on Holmgren (2016) for the buoy specifications, the generator was developed according to the Electric Power Systems department at the Royal Institute of Technology and Bjørnsen (2014) was followed for the mooring system module. **Outcomes:** Climate Change
7 MW	13.0	50	Sørensen et al. (2006)	Wave Dragon WEC	Extraction of raw materials, manufacturing and assembly, use and disposal ("cradle-to-grave")	**Design:** Demonstration project. **Outcomes:** Global Warming, Ozone Depletion, Acidification, Nutrient enrichment, Human Toxicity Water, Human Toxicity Soil, Human Toxicity Air, Photochemical oxidation, Ecotoxicity Water Chronic, Ecotoxicity Water Acute, Ecotoxicity Soil Chronic, Slag and Ashes, Nuclear Waste, Hazardous Waste, Bulk Waste
	28.0		Banerjee et al. (2013)		Raw material impacts ("cradle-to-gate")	**Design:** Based on Russel (2007). **Outcomes:** Global Warming Potential, Energy Payback Period
10 kW	89.0	20	Zhai et al. (2018)	Buoy-rope-drum WEC	Raw materials extraction and manufacturing, component manufacturing, module production, system assembly, installation, O&M, decommissioning and recycling	**Design:** Shandong University. Located 2 km from the shore. **Outcomes:** Climate Change, Ozone Depletion, Terrestrial Acidification, Freshwater Eutrophication, Marine Eutrophication, Human Toxicity, Photochemical Oxidant Formation, Particulate Matter Formation, Terrestrial Ecotoxicity, Freshwater Ecotoxicity, Marine Ecotoxicity, Ionising Radiation, Agricultural and Occupation, Urban Land Occupation, Natural Land Transformation, Water Depletion, Metal Depletion and Fossil Depletion
3 kW	37.0	60	Patrizi et al. (2019)	OBREC WEC	Production of components, on site installation including transport, O&M ("cradle-to-gate")	**Design:** Department of Engineering, University of Campania. **Outcomes:** Global Warming Potential, Carbon Intensity of Electricity
1 MW	33.8	20	Apolonia and Simas, (2021)	MegaRoller WEC	Production of each component part, assembly, transport and installation, O&M, decommissioning and disposal ("cradle to grave")	**Design:** Based on WaveRoller design. Installed at approximately 8–20 m of depth and 400 m from shore. **Outcomes:** Global Warming Potential, Stratospheric ozone depletion, Ionizing radiation, Ozone formation, Human health, Fine particulate matter formation, Ozone formation, Terrestrial ecosystems, Terrestrial acidification Freshwater eutrophication, Marine Eutrophication, Terrestrial ecotoxicity, Freshwater ecotoxicity Marine ecotoxicity, Human carcinogenic toxicity, Human non-carcinogenic toxicity, Land use, Mineral resource scarcity, Fossil resource scarcity, Water Consumption, Cumulative Energy Demand

10.3389/fenrg.2022.980557

Paredes et al. (2019) conducted a systematic review of LCA of ocean energy technologies and highlighted that the manufacture of structural materials (e.g., steel), mooring and foundations, and the shipping operations have the greatest impact on the total CO_2 emissions (between 40–95 % of the total emissions).

Uihlein (2016) carried out the LCA of 180 ocean energy technologies, which confirmed that environmental impacts were closely linked to the material inputs for mooring, foundations, and structural components while the impacts from assembly, installation, and use were negligible for all types.

Through the LCA of a near-shore WEC tested in Sweden, namely Seabased, Dahlsten (2009) highlighted that the potential environmental impact of the buoy that mainly stemmed from the manufacturing phase. In particular, the production of steel parts makes a large contribution (around 50 %) to the overall results.

In addition, the LCA of the WEC buoy conducted by Zepeda (2017) observed the highest contribute to the climate change impact category which was due to the mooring system (16 %) and the polyurethane buoy (60 %).

Walker and Howell (2011) evaluated the CO_2 emissions of the *Oyster* WEC in Scotland, analyzing all stages involved in its life cycle from cradle-to-grave, taking raw materials as a starting point, and disposal of waste as an end point (Walker and Howell, 2011). The study has shown that the material manufacture phase represents more than 95 % of the total emission.

Douziech et al. (2016) quantified the potential environmental impacts of three tidal stream devices, one tidal range plant, and the *Oyster* wave energy system and concluded that the construction and end of life (EoL) burden phases dominated the values of the impact categories assessed, including climate change.

The LCA of the *Wavestar* technology, studied for the Irish site of Belmullet, confirmed that the phase that covered the extraction of the raw materials up to the manufacturing and assembly of the device was the most intensive one with the greatest impact (Dalton et al., 2014).

Zhai et al. (2018) conducted a LCA for a buoy–rope–drum WEC installed 2 km off the shore at Weihai, Shandong (China), and demonstrated that the most significant environmental impact contributor was the manufacturing stage, due to the consumption of energy and materials.

Patrizi et al. (2019) evaluated the overtopping breakwater WEC, named *OBREC*, installed in the Naples harbor (Italy), showing that 82 % of the total CO_2 emissions was due to the use of materials for the construction components (including structural elements, ramp, foundations, and cables for the connection to the grid).

A preliminary LCA of the Portuguese *MegaRoller* WEC conducted by Apolonia and Simas (2021) also confirmed the main environmental contribution of material use and the manufacture stage.

Thomson et al. (2019) presented a full LCA of the first-generation *Pelamis* WEC, designed for the northwest coast of Scotland. The assessment built on previous studies carried out on the same device (Parker et al., 2007; Thomson et al., 2011; Banerjee et al., 2013) showed the greatest impacts of steel manufacture and diesel for sea vessel operations, particularly for maintenance. The study also highlighted the opportunities to reduce environmental impacts considering the reduction of steel quantity in future design developments or increasing the recycled content of this material. Moreover, refining the *Pelamis* design and selecting an installation site nearer to a port could reduce the impacts of sea vessel operations.

As the aim of our research was not focused on devices designed for targeted locations and produced by specific companies, but dedicated to the identification of a design benchmark for WECs, 3D digital models were created according to Pulselli et al. (2022). Their work created a benchmark for the design of two models of offshore floating wind turbines, and instead of specific devices with many variables, technological standards for the type, size, installed power, and use were elaborated. Based on a systematic comparison with what already exists in the literature, our study tried to apply the same *modus operandi* for the wave energy sector. Therefore, this work can contribute to overcoming the variability between deployed and planned projects which, in addition to providing energy security to countries located close to the sea, can help to reduce GHG emissions (Sgobbi et al., 2016).

The second part of the study was focused on the assessment of CIE values, measured in g CO_2eq·kWh^{-1}, for each WEC. The range of electricity production values, based on tested devices like those modeled and suited to the Mediterranean context, were assumed to obtain data comparable with the performance of other technologies that produce energy both from renewable and fossil sources.

2 Materials and methods

The WEC systems analyzed convert wave-induced oscillations from mechanical energy to electricity, through the core component named power take-off (PTO) mechanism.

The first device is an onshore air compression system capable of capturing wave energy using an OWC-operating principle (Figure 1A). The basic unit is a reinforced concrete caisson that can be incorporated into a traditional breakwater or, according to Curto et al. (2021), integrated into a floating device. In this article, the first case is considered. This system transforms harbor dams, from passive structures for the protection of the port, into active structures for energy production. Each caisson hosts an absorption chamber in which a sea wave produces a vertical water oscillation (Curto et al., 2021). This movement generates an air pocket that compresses and decompresses cyclically driving an air turbine–generator pair with consequent electricity production. According to Ibarra-Berastegi et al. (2018), the self-rectifying *Wells* turbine 2.83 m high, weighs

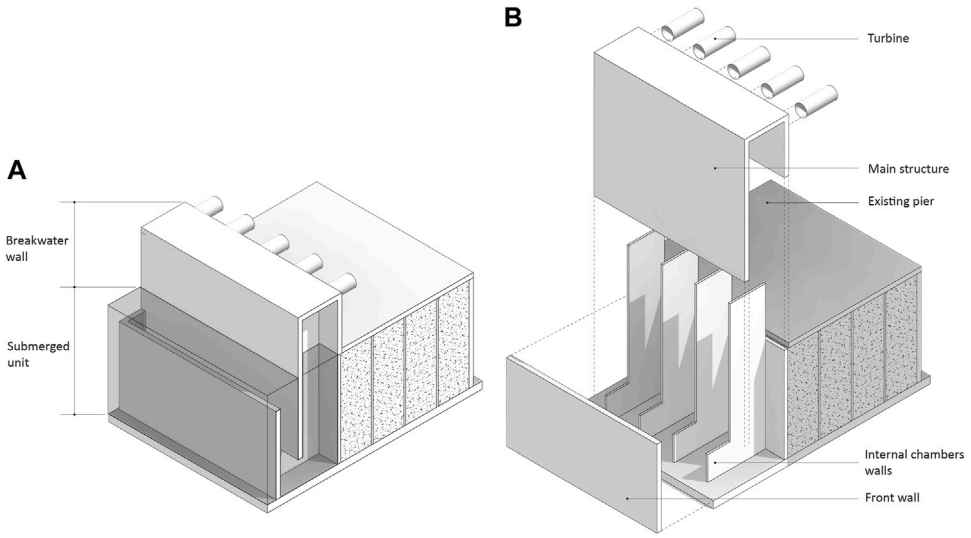

FIGURE 1
The onshore OWC 3D model **(A)** and its main construction elements **(B)**. Legend and values: breakwater wall height = 6 m; submerged unit height = 10 m.

around 1,200 kg, and a diameter of 1.25 m was assumed. To ensure the stability of the structure, the dredged material from the excavations (i.e., gravel) for the insertion of the caissons was used for the ballast. The installation procedures can be carried out in safer environmental conditions and with reduced maintenance costs due to the onshore location. The proximity to the power grid and the absence of deep-water moorings are further advantages for its implementation. In order to find an average value of materials and determine an estimate of productivity, one reference for the present study was a 296 kW OWC plant composed of 16 chambers with a length of 100 m, inaugurated in the bay of Mutriku (Spain) in 2011 (Lacasa et al., 2019). Another one was the full-scale plant *REWEC 3* (*REsonant Wave Energy Converter*) developed in Italy by the University of Reggio Calabria and installed in the port of Civitavecchia. It is composed of 136 chambers and has a rated power of 2.5 MW (Cascajo et al., 2019). In addition, *WHT* (*Wave Hydro Turbine*) is another example of an onshore solution working inside an OWC. In contrast to the first two cases, *WHT* is a prototype system installed and tested on the breakwaters of the port of Cartagena (Spain) (BLUE DEAL MED, 2022a).

The second WEC considered in this benchmarking assessment is the onshore oscillating floater (Figure 2A) which converts the rising and falling motions of waves into energy. The floater, designed based on existing real cases, was assumed to be anchored to an existing pier or dock. Its movement actives a hydraulic piston with moving valves and a linear alternating motion conversion system that moves the internal generators to produce energy (BLUE DEAL MED, 2022b). This energy conversion system follows the example of the *Seadamp FX* ® technology designed by Seareas Company. Electricity produced is further transferred into the grid. This WEC can be potentially installed in series to generate electricity from waves having a height between 0.5 and 3 m. As for the previous case, the installation, operation, and maintenance activities do not require divers, underwater cabling, and mooring. One important reference for the floater's modeling was the *EWP* (*Eco Wave Power*) system installed in Gibraltar with a rated power of 100 kW that was planned to achieve 5 MW of installed power (Cascajo et al., 2019). A second example was the pilot technology called *EDS* (*Energy Double System*), a near-shore point absorber WEC composed of a heaving float and a surging paddle developed by the Politecnico of Milan and Tecnomac Company (Marchesi et al., 2020). In addition, *Wavestar* is another example of a plant composed of 20 buoys (10 m diameter), arranged in two lines, and being able to extract until 6 MW according to the climatic conditions of the North Sea (Curto et al., 2021).

The last WEC examined is a near-shore seabed-based buoy (Figure 3A) located 2 km from the coast in shallow waters, as described by Short (2012). The main reference device was the third generation of *Seabased*'s patented technology developed at Uppsala University (Sweden), with a rated power of 30 kW (Leijon et al., 2008; Hultman et al., 2014). The system is composed of a floating body connected via a steel wire to a linear PTO generator lying on the seabed. This submerged unit anchored with a gravity-based foundation converts the buoy kinetic energy to electricity through an enclosed piston that moves up and down driven by the oscillating motion of waves

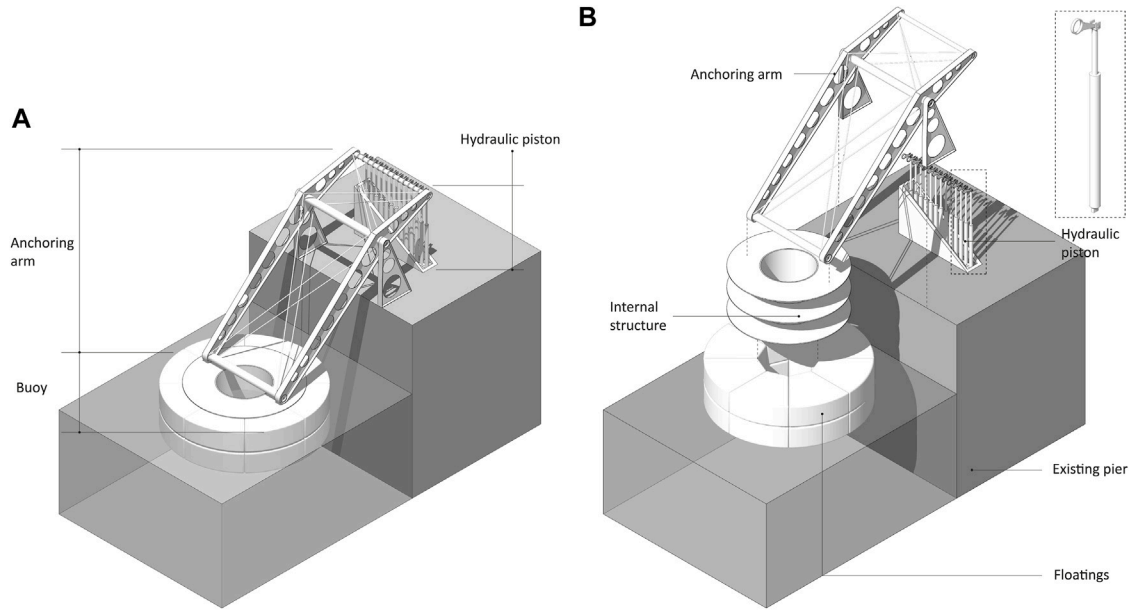

FIGURE 2
The onshore oscillating floater 3D model **(A)** and its main construction elements. **(B)** Legend and values: buoy diameter = 5 m; anchoring arm height = 6 m.

(Lissandrom, 2010). The composition of the direct driven magnetic part of the generator, the translator, was modeled following the study of Dahlsten (2009). To promote the reduction of material and production costs, the translator was assumed to be designed with a ferrite magnet, replacing the previous neodymium (NdFeB) magnet, which was less impactful and cheaper, even if less stronger (Chatzigiannakou et al., 2014; Hultman et al., 2014). The device works as a point absorber able to exploit energy independently of wave direction due to the small sizes in comparison with the wavelength (Curto et al., 2021). The modular design allows the implementation of wave energy power parks, where several buoys are interconnected in a marine substation that pulls the generated electricity and transmits it to the shore (Hong et al., 2013). For the installation activities, buoys can be assembled on-shore and transported on-site by a specialized vessel equipped with a crane to be arranged in clusters. The work of a diver's crew permits is to make the proper underwater cable connections and disconnect slings and shackles attached to the foundation (Chatzigiannakou et al., 2017).

In compliance with International Standard Organisation 14040 (ISO, 2006) and 14044 (ISO, 2020), LCA was used to account for the input and output flows and evaluate the potential environmental impacts of the three WECs from their production to the disposal stage. The CF of each device was assessed using the SimaPro 9.1.1 software (PRé Consultants, 2020) to model the inventory and carry out the Life Cycle Impact Assessment. According to Pulselli et al. (2022), the data inventory for each technology was based on the combined use of digital 3D models and literature data. Particularly, 3D models were developed to obtain a more precise quantification of the material volumes involved constituting the different components of each system. The models explored in Figure 1B, Figure 2B, Figure 3B show the characteristics and dimensions of the WECs analyzed including the details of each component, while Table 2, Table 3, and Table 4 describe the related Life Cycle Inventory data.

For background data, Ecoinvent v3.6 (Ecoinvent, 2022) datasets were used. The Intergovernmental Panel on Climate Change (IPCC) (2013) characterization method was selected to quantify the GHG emissions through a standardization based on Global Warming Potentials (GWPs). These characterization factors were expressed for a period of 100 years (GWP 100), in CO_2eq per ton of emission and hereafter expressed as CF values.

As reported in the flow chart in Figure 4, the "cradle-to-grave" LCA considered four main phases common to all WECs: 1) manufacturing; 2) transport, assembly, and installation; 3) maintenance and material replacement; and 4) EoL. The life cycle impacts of the main energy inputs and materials that make up the technological components were considered, starting from the mass of the materials used and therefore neglecting the impact of the specific industrial process of producing the technological component in its final form (Pulselli et al., 2022).

The functional unit (FU) was 1 year of operation of each device. As a precaution, the service lifetime of the OWC was 50 years even if Patrizi et al. (2019) considered 60 years for the

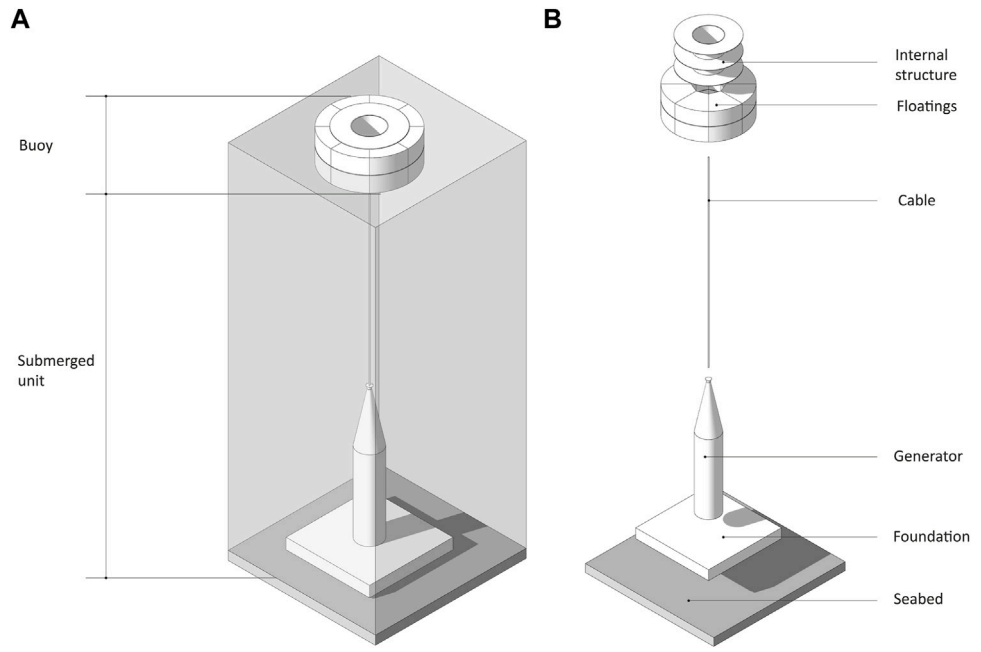

FIGURE 3
The near-shore seabed-based buoy 3D model **(A)** and its main construction elements. **(B)** Legend and values: buoy height = 1.5 m; buoy diameter = 5 m; submerged unit (cable and generator) height = 22 m.

onshore overtopping breakwater WEC. The expected lifetime of 25 years was assumed for both oscillating floater and seabed-based buoy (Rémouit et al., 2018; BLUE DEAL MED, 2022c). For specific elements (e.g., PTO mechanism, electrical connections), the lifetimes were differentiated to consider the maintenance and substitution operations. As an example, according to Bruschi et al. (2019), the average lifespan of an air turbine of an OWC is lower than that of wind turbines (20 years; Chipindula et al., 2018), in this article, it was assumed to be 15 years considering work under non-constant conditions. According to Zhai et al. (2018), the system boundary excluded small mechanical components used for the upstream module and system assembly as well as downstream maintenance, such as bolts, nuts, and studs, which account for a negligible portion of weight and minimal environmental impacts.

Specific data of materials and energy needed to manufacture the structural components (Phase 1) were estimated by calculation procedures to quantify relevant inputs and outputs of the product system starting from scientific literature sources. For example, the external electricity generator system for the OWC was modeled according to Faÿ et al. (2020).

Regarding the assembly and installation stage (Phase 2), the study assumed different time frames for each system. For the OWC system, the whole deployment spot took about 17 working days; for the oscillating floater, 4 working days were needed, while for the seabed-based buoy, about 3 working days per device were required. The study assumed the onshore assembly and installation for the OWC and the floater, while the buoy needed to be transported by boat to the installation site after its assembly on the port. For all technologies assessed, the materials and construction components were transported by lorry for an assumed distance of 200 km to the assembly site. The research of Chatzigiannakou et al. (2017) was taken as reference to quantify the installation time per device and the construction site machineries involved (e.g., cranes, forklifts, generators, ships, etc.). The consumption of diesel was required for assembly on land and the operational activities on site, which was estimated based on Chipindula et al. (2018). For the installation of the marine substation, the study of Chatzigiannakou et al. (2015) was considered.

Since the port systems already have connections to the national grid and in the absence of detailed information regarding the necessary terrestrial electric cables, for all WECs, they were excluded from the analysis. On the other hand, the study estimated the material composition of the submarine cables for the transmission of the electricity produced by the seabed-based buoy. Particularly, the composition of the 33 kV submarine cables was modeled following Birkeland (2011). The present study was limited to evaluate the connection cable between the buoy and the marine substation, having a length equal to 70 m, and an addition submarine cable with a length of 2 km to allow the energy transmission from the marine substation to the coast (Leijon et al., 2008).

TABLE 2 Life Cycle Inventory data for a 20 m breakwater hosting 5 generic OWC systems. Values in bold represent totals and subtotals.

Element	Technical specification	Unit	Value	%	Lifetime (yr)	Notes and References
Phase 1 - MANUFACTURING						
Foundations	Concrete	t	632.1	8.1%	50	The values for the pier structure hosting the OWC derive from a 3D model that was built on the basis of the following literature: Arena et al. (2013); Arena (2016); Curto et al. (2021); De Girolamo (2015); Malara et al. (2017); Spanos et al. (2018)
	Steel	t	55.3	0.7%	50	
Alveolar structure	Concrete	t	1,150.9	14.8%	50	
	Steel	t	23.0	0.3%	50	
	Gravel	t	5,122.8	66.0%	50	
OWC superstructure	Concrete	t	502.7	6.5%	50	
	Steel	t	28.3	0.4%	50	
Roof covering	Concrete	t	236.8	3.1%	50	
Self-rectifying turbines	Steel	t	6.0	0.1%	15	The turbine taken as example (and its weight) is the one described in Ibarra-Berastegi et al. (2018)
Electric generator	Steel	t	0.2	0.003%	20	For the electric generator composition we consider the one described in Faÿ et al. (2020) (it is assumed to be made up of 80% steel and 20% copper)
	Copper	t	0.05	0.001%	20	
Mass balance Total Phase 1		t	**7758.1**	100.0%	—	
Phase 2 - ASSEMBLY and INSTALLATION						
Truck Mixer	Diesel	t	1.9	4.2%	50	For the construction of the pier and the OWC structure, 17 working days were assumed (of which 10 for the construction of the floating caissons, as suggested by Cejuela et al., 2018 and Magallanes et al., 2016), on the basis of what is described in Arena et al. (2013). The hourly fuel values are derived from Chipindula et al. (2018)
Crane	Diesel	t	39.9	89.5%	50	
Excavation digger	Diesel	t	0.5	1.2%	50	
Tugboat	Diesel	t	1.6	3.5%	50	
Track gravel	Diesel	t	0.5	1.1%	50	
Forflift	Diesel	t	0.2	0.5%	50	
Total Phase 2		t	**44.6**	100.0%	—	
Phase 3 - MAINTENANCE and MATERIAL REPLACEMENT						
Van	Transport, passenger, car (medium size)	km	360	—	1	It is assumed that a monthly check is carried out for a distance of 30 km with a medium-sized work vehicle (van)
Self-rectifying turbines	Steel	t	1.3	—	15	On the basis of what reported by Bruschi et al. (2019), the replacement of the Wells turbine is hypothesized, assuming a lifetime of 15 years, given the level of erosion to which the wells turbines are subjected in the marine environment
Phase 4 - END OF LIFE						
Materials	**Unit**	**Recycling**	**Landfill**	**Wast-to-Energy**	**Notes**	**References**
Concrete	t	—	2522.5	—	Landfill 100%	The scenarios for the end of life of the different materials have been built based on Raadal et al. (2014) and Tsai et al. (2016)
Steel	t	101.5	11.3	—	Recycling 90% Landfill 10%	
Copper	t	0.045	0.005	—	Recycling 90% Waste-to-Energy 10%	

For the maintenance and material replacement stage (Phase 3), for the OWC system, the study considered the replacement of the *Wells* turbine approximately 3 times over the life of the device (15 years, Bruschi et al., 2019). In addition, emissions related to the diesel consumption for periodic monitoring inspections (12 times per year) to check the status of the system were considered. For the floater system, the study assumed that hydraulic pistons would be replaced (12.5 years; Seares, 2022), and diesel consumption for monitoring the trips (12 times per year) was accounted as well. According to Strömstedt et al. (2012), the seabed-based buoy is maintenance-free, meaning that no maintenance should be needed during the whole lifetime (20–25 years) of the system. It may need to be monitored to detect possible damage or malfunctioning and

TABLE 3 Life Cycle Inventory data for a 20 m breakwater hosting 3 generic oscillating floater devices. Values in bold represent totals and subtotals.

Element	Technical specification	Unit	Value	%	Lifetime (yr)	Notes and References
Phase 1 - MANUFACTURING						
Support arms	Steel	t	8.0	16.5%	25	The dimensions are based on the existing literature concerning structures similar to the one considered, see for example Cascajo et al. (2019); Curto et al. (2021); Marchesi et al. (2020)
Hydraulic system	Aluminium	t	2.2	4.5%	12.5	The pistons of the hydraulic system were modeled based on the Seadamp Fx device, developed by Seares Srl (we assumed 13 pistons with a unit weight of 70 kg). See: BLUE DEAL MED (2022a) and Seares (2022); detailed and specific information on dimensions and materials derived from direct communication with Seares
	Steel	t	0.5	1.1%	12.5	
Buoy	Steel	t	8.3	17.2%	25	The dimensions are based on the existing literature concerning structures similar to the one considered, see for example Cascajo et al. (2019); Curto et al. (2021); Marchesi et al. (2020). Furthermore, it is based on buoy models developed by Resinex Trading Srl (Resinex, 2007) and from direct communications with the company
	Polyethylene	t	4.4	9.1%	25	
	Polyurethane foam	t	24.9	51.5%	25	
Total mass balance of Phase 1		t	**48.3**	100.0%	—	
Phase 2 - ASSEMBLY and INSTALLATION						
Forklift	Diesel	t	0.4	3.4%	25	Following personal communication with Seares company, 4 working days are assumed. They include the assembly of the main components on the pier and their anchoring through the use of land vehicles and a support boat. The hourly fuel values are taken from Chipindula et al. (2018)
Crane	Diesel	t	6.2	50.1%	25	
Auxiliary boats	Diesel	t	3.0	24.0%	25	
Generator	Diesel	t	2.8	22.5%	25	
Total Phase 2		t	**12.4**	**100%**	—	
Phase 3 - MAINTENANCE and MATERIAL REPLACEMENT						
Van	Transport, passenger, car (medium size)	km	360	—	1	12 trips per year are assumed for the inspection and maintenance of the structure, with a unitary distance of 30 km
Pistons	Aluminium	t	2.2	—	12.5	Based on what suggested by Seares Srl, it is assumed that the pistons are replaced once in the life span of the system, as they are subjected to wear due to their continuous use
	Steel	t	0.5	—	12.5	

Phase 4 - END OF LIFE

Materials	Unit	Recycling	Landfill	Wast-to-energy	Notes	References
Steel	t	15.6	1.7	—	Recycling 90% Landfill 10%	The scenarios for the end of life of the different materials have been built based on Raadal et al. (2014) and Tsai et al. (2016)
Aluminium	t	3.9	0.2	—	Recycling 90% Landfill 10%	
Polyethylene	t	—	—	4.4	Waste-to-Energy 100%	
Polyurethane foam	t	—	—	24.9	Waste-to-Energy 100%	

TABLE 4 Life Cycle Inventory data for a wave park hosting 25 generic seabed-based buoys. Values in bold represent totals and subtotals.

Element	Technical specification	Unit	Value	%	Lifetime (yr)	Notes and References
Phase 1 - MANUFACTURING						
Foundation	Concrete	t	2350.1	76.3%	50	The data comes from 3D models developed in this study and from literature. Foundation from: Andersen et al. (2009); Chatzigiannakou et al. (2017); De Girolamo (2015); Strömstedt et al. (2012). Capsule, superstructure and funnel from Strömstedt et al. (2012). For the buoy: Resinex (2007) and direct communications with the company
	Steel	t	205.6	6.7%	25	
	Steel	t	4.4	0.1%	25	
Capsule and superstructure	Steel	t	43.3	1.4%	25	
	Steel	t	20.5	0.7%	25	
	Steel	t	3.1	0.1%	25	
Funnel	Steel	t	13.0	0.4%	25	
Buoy	Steel	t	47.2	1.5%	25	
	Steel	t	21.4	0.7%	25	
	Polyethylene	t	37.8	1.2%	25	
	Polyurethane	t	152.7	5.0%	25	
Translator	Cast iron	t	45.0	1.5%	25	The translator's internal component data comes from Dahlsten (2009); the original $Nd_2Fe_{14}B$ magnet is replaced with a Ferrite one, as suggested by Hultman et al. (2014) and Chatzigiannakou et al. (2017)
	Copper	t	4.7	0.2%	25	
	Ferrite magnet	t	4.5	0.1%	25	
	Plastic and rubber	t	4.2	0.1%	25	
	Zinc	t	1.0	0.0%	25	
	Aluminium	t	0.4	0.0%	25	
	Paint	t	1.9	0.1%	25	
Substation	Steel	t	6.0	0.2%	25	Mechanical characteristics of the substation derived from Chatzigiannakou et al. (2015)
	Copper	t	1.3	0.0%	25	
	Concrete	t	3.2	0.1%	25	
Submarine power cable	Lead	t	30.0	1.0%	40	A 33 kV sub-marine cable was chosen for connecting the buoys to the substation (Assumed 70 m for each of the 25 buoys - based on Chatzigiannakou et al., 2015) and for the connection to the coast (2 km - Based on nearshore definition available in Leijon et al., 2008 and Short, 2012). Data from Birkeland (2011). Cable lifetime was assumed as 40 years (Huang et al., 2017)
	Copper	t	22.5	0.7%	40	
	Polyethylene	t	7.5	0.2%	40	
	Steel	t	45.0	1.5%	40	
	Polypropylene	t	3.8	0.1%	40	
Total Phase 1		t	**3079.9**	100.0%	—	
Phase 2 - ASSEMBLY and INSTALLATION						
Forklift	Diesel	t	5.3	3.3%	25	Based on Chatzigiannakou et al. (2015; 2017 - Sotenäs site example) it was hypothesized that both the device and the substation are assembled in port and then transported to the plant site where they are lowered and anchored to the seabed. Based on these, 3 working days were assumed for the buoy and substation assembly and installation The hourly fuel values are considered as in Chipindula et al. (2018)
Crane	Diesel	t	81.3	49.7%	25	
Generator	Diesel	t	69.8	42.7%	25	
Workboat	Diesel	t	7.1	4.3%	25	
Total mass balance of Phase 2		t	**163.5**	**100%**	—	
Phase 3 - MAINTENANCE						
Crew Transfer vessel	Diesel	t	6.3	—	1	As suggested by Rémouit et al. (2018) this technology is designed to not need components replacement during its lifetime. However, biofouling cleaning operations are periodically carried out through the use of a Crew Transfer Vessels (hourly fuel consumption derived from Acta Marine, 2017)
Phase 4 - END OF LIFE						
Materials	**Unit**	**Recycling**	**Landfill**	**Wast-to-energy**	**Notes**	**References**
Concrete	t	—	2353.3	—	Landfill 100%	

(Continued on following page)

TABLE 4 (*Continued*) Life Cycle Inventory data for a wave park hosting 25 generic seabed-based buoys. Values in bold represent totals and subtotals.

Element	Technical specification	Unit	Value	%	Lifetime (yr)	Notes and References
Steel	t	368.5	40.9	—	Recycling 90% Landfill 10%	The scenarios for the end of life of the different materials have been built based on Raadal et al. (2014) and Tsai et al. (2016)
Polyethylene	t	—	—	45.3	Waste-to-Energy 100%	
Polyurethane	t	—	—	152.7	Waste-to-Energy 100%	
Cast iron	t	40.5	4.5	—	Recycling 90% Landfill 10%	
Copper	t	25.7	—	2.9	Recycling 90% Waste-to-Energy 10%	
Ferrite magnet	t	—	4.5	—	Landfill 100%	
Plastic and rubber	t	—	—	4.2	Waste-to-Energy 100%	
Zinc	t	0.9	0.1	—	Recycling 90% Landfill 10%	
Aluminium	t	0.4	0.04	—	Recycling 90% Landfill 10%	
Paint	t	—	—	1.9	Waste-to-Energy 100%	
Lead	t	27	—	3	Recycling 90% Waste-to-Energy 10%	
Polypropylene	t	—	—	3.8	Waste-to-Energy 100%	

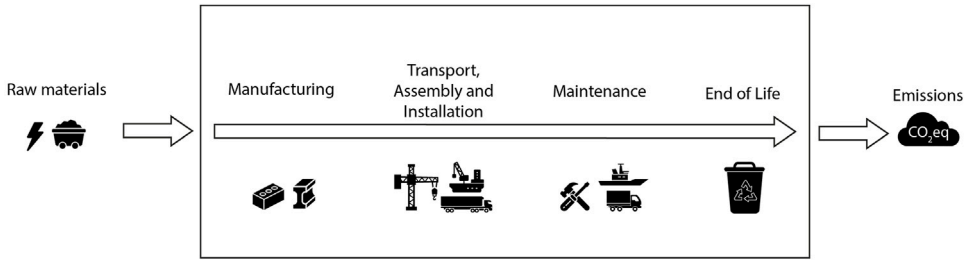

FIGURE 4
Flow chart representing the main life cycle phases involved in the assessment ("cradle-to-grave").

for biofouling prevention and observation (Rémouit et al., 2018). Also, for the marine substation, it was assumed that no maintenance should be needed, except for inspection activities to verify its functionality. For this reason, the diesel consumption for the use of a crew transfer vessel for inspection activities (2 times per year) was accounted for in accordance with Acta Marine (2017) for both cases.

Regarding the decommissioning and EoL (Phase 4), following Raadal et al. (2014) and Tsai et al. (2016), different scenarios were assumed considering recycling and landfill or energy recovery treatments. The destinations of the various materials assumed were: 90 % recycling and 10 % landfill for steel, aluminum, cast iron, and zinc; 90 % recycling and 10 % waste-to-energy for copper and lead; 100 % landfill for cement;

and 100 % waste-to-energy for paint and plastic materials (i.e., polyethylene, polyurethane, and polypropylene). The gravel removed during the installation activities for the OWC system was assumed to be reused in place. According to Pulselli et al. (2022), regarding recyclable metal components, the study considered emissions for their transport to a hypothetical waste management centre (200 km by truck for all WECs and 2 km by boat only for the seabed-based buoy case).

The impacts of subsequent management and recycling of metals to produce secondary raw materials were assigned to the future process that would use those materials (Pulselli et al., 2022).

Based on the LCA results, the CIE per kWh generated by each WEC system was calculated. As reference energy productions and consequently energy potential data from Arena (2016) and Ibarra-Berastegi et al. (2018) for the OWC model; BLUE DEAL MED (2022c) and BLUE DEAL MED (2022d) for the oscillating floater and Bozzi et al. (2013) for the near-shore seabed-based buoy were considered.

3 Results and discussion

CF results for each WEC were analyzed and values for individual components are shown in Table 5, Table 6, Table 7. The OWC system has a total CF of 4.2 t CO_2eq per unit, which increases to 21.1 t CO_2eq if a 20 m breakwater is considered (able to host up to 5 chambers) (Table 5). On the other hand, if it is considered a traditional 20 m breakwater without an OWC system, the associated CF is estimated to be around 17.9 t CO_2eq. This lower value is due to the avoided use of concrete for the OWC chamber walls and steel for the *Wells* turbines. In addition, the higher amount of gravel filling the concrete structure justify the lower emissions, as the corresponding weight in terms of CF is not relevant to the total result. It should highlight that the traditional breakwater remains a passive structure not able to produce energy, but rather dissipates it.

The oscillating floater shows a CF per unit of 5 t CO_2eq and, considering a breakwater of the same length as the previous one, the CF is around 15 t CO_2eq (3 installable systems) (Table 6). Regarding the seabed-based buoy, the CF per unit is 6.3 t CO_2eq and hypothesizing a wave park of 25 devices, the total results is 157.6 t CO_2eq (Table 7).

The main GHG emission sources per life cycle phase and process are shown in Figure 5. Overall, the results are in line with previous studies highlighting that the large majority of the environmental impacts associated with this type of devices are due to Phase 1, the manufacturing stage (Sørensen et al., 2006; Dahlsten, 2009; Walker and Howell 2011; Uihlein, 2016; Zhai et al., 2018). Particularly, this phase covered 54 % (2.3 t CO_2eq), 56 % (2.8 t CO_2eq), and 47 % (2.9 t CO_2eq) of the total CF for the OWC, oscillating floater, and seabed-based buoy, respectively. These percentages are in line with the range between 40 and 90 % emerged in previous assessments (Dahlsten, 2009; Thomson et al., 2011; Uihlein, 2016; Zhai et al., 2018). The potential environmental impacts assessed are mainly due to the WEC's material structural components such as concrete, steel, and polyurethane. Concrete and steel were involved in the structure of the OWC system and represented the 29 and 19 % of the total GHG emissions, respectively (Table 5). Polyurethane played a key role in the manufacturing stage of the oscillating floater and seabed-based buoy, covering the 36 and 21 %, respectively, of the GWPs evaluated (Table 6, Table 7).

Phase 2 (transport, assembly, and installation) covered 42 % (1.8 t CO_2eq) of the total CF of the OWC system, which is mainly due to the transport of material components by lorry (26 %) to the assembly site and the diesel consumption for the crane operation activities (14 %) (Table 5). Regarding the oscillating floater and seabed-based buoy performances, Phase 2 accounted for 14 and 24 %, respectively (Table 6, Table 7). In the former case, the diesel consumption for the crane use (6.2 %) is once again decisive, while in the latter, the percentage weight of emissions is divided between the transport of the material components by lorry (8.2 %) and diesel consumption for the crane (8 %) and the electricity generator (7 %).

Phase 3 (maintenance and material replacement) is negligible for OWC, covering 1.2% of the overall CF results (Table 5), while, for the other two WECs, it is responsible for the 10 and 15% of the emissions for the oscillating floater and seabed-based buoy, respectively (Table 6, Table 7). For the floater, the main input responsibility is the aluminum involved in the replacement of the hydraulic piston (around 9.6%), while for the buoy, the diesel consumption for the crew transfer vessel is the only responsibility.

Phase 4 (EoL) is not significant for the OWC (3%) (Table 5), while for the oscillating floater and seabed-based buoy, it represents 20 % and 15 % of the potential GHG emissions, respectively (Table 6, Table 7), due to the different fates of the materials involved (mainly metals recycling and waste-to-energy of plastics).

The CFs evaluated for each WEC were compared to an estimated range of electricity production (MWh·yr^{-1}), giving the CIE, expressed in g CO_2eq·kWh^{-1}. Considering wave energy potentials for Mediterranean marine areas, extrapolated from the scientific literature available, the CIE values for the OWC system fall in the range of 270–203 g CO_2eq·kWh^{-1} (hypothesizing 15.6–20.8 MWh per device, respectively, according to Arena, 2016 and Ibarra-Berastegi et al., 2018); for the oscillating floater they vary between 374 and 94 g CO_2eq·kWh^{-1} (considering 13.3–53.3 MWh per device, according to BLUE DEAL MED, 2022c and BLUE DEAL MED, 2022d), respectively, and for the buoy, the values fall in the range of 158–105 g CO_2eq·kWh^{-1} (assumed 60–40 MWh per device, respectively, according to Bozzi et al., 2013).

TABLE 5 Total GWP (t CO_2eq) impact category results for the OWC system and values for individual components. Values in bold represent totals and subtotals.

Element	Technical specification	Carbon footprint 20 m breakwater device (t CO_2eq)	Carbon footprint 1 chamber (t CO_2eq)	%
Phase 1 – MANUFACTURING				
Foundations	Concrete	1.6	0.3	7.4
	Steel	1.8	0.4	8.3
Alveolar structure	Concrete	2.8	0.6	13.4
	Steel	0.7	0.1	3.5
	Gravel	1.1	0.2	5.3
OWC superstructure	Concrete	1.2	0.2	5.9
	Steel	0.9	0.2	4.2
Roof covering	Concrete	0.6	0.1	2.8
Self-rectifying turbines	Steel	0.6	0.1	3.0
Electric generator	Steel	0.016	0.0	0.08
	Copper	0.002	0.0	0.01
	Total Phase 1	**11.4**	**2.3**	**53.9**
Phase 2 - TRANSPORT, ASSEMBLY, and INSTALLATION				
Transport, freight, lorry	—	5.5	1.1	25.9
Truck Mixer	Diesel	0.1	0.0	0.7
Crane	Diesel	3.0	0.6	14.1
Excavation digger	Diesel	0.0	0.0	0.2
Tugboat	Diesel	0.1	0.0	0.6
Track gravel	Diesel	0.04	0.0	0.18
Forflift	Diesel	0.02	0.0	0.08
	Total Phase 2	**8.8**	**1.8**	**41.8**
Phase 3 - MAINTENANCE and MATERIAL REPLACEMENT				
Van	Transport, passenger, car (medium size)	0.1	0.0	0.5
Self-rectifying turbines	Steel	0.1	0.0	0.7
	Total Phase 3	**0.3**	**0.1**	**1.2**
Phase 4 - END OF LIFE				
	Total Phase 4	0.67	0.1	**3.2**
Total		**21.1**	**4.2**	**100.0**

In general, the range of the CIE values calculated for each WEC system shows better performance than any fossil source for electricity production: natural gas (443 g CO_2eq·kWh^{-1}), petroleum products (778 g CO_2eq·kWh^{-1}), and solid fossil fuels (mainly coal) (1,050 g CO_2eq·kWh^{-1}), as reported by Sovacool (2008). The same is true for some alternative energy carriers and sources such as: hydrogen (664 g CO_2eq·kWh^{-1}; Sovacool, 2008) and geothermal (380 g CO_2eq·kWh^{-1}; Pulselli et al., 2019). It is a different situation if the comparison is made with the CIE values of solar photovoltaic panels (32 g CO_2eq·kWh^{-1}), hydroelectric (12 g CO_2eq·kWh^{-1}), onshore wind (10 g CO_2eq·kWh^{-1}) (Sovacool, 2008), offshore bottom fixed wind (32 g CO_2eq·kWh^{-1}), and offshore floating wind (49 g CO_2eq·kWh^{-1}) (Pulselli et al., 2022), which due to a higher technology readiness level, turn out to be more performing and advantageous, and thus more widespread.

Comparison with other WEC systems (Figure 6) is limited to the CIE results obtained for buoy technology, as LCA studies on OWC or oscillating floater technologies are not yet available in the literature. For this reason, particularly for the seabed-based

TABLE 6 Total GWP (t CO_2eq) impact category results for the oscillating floater and values for individual components. Values in bold represent totals and subtotals.

Element	Technical specification	Carbon footprint 20 m breakwater device (t CO_2eq)	Carbon footprint 1 floater (t CO_2eq)	%
Phase 1 – MANUFACTURING				
Support arms	Steel	0.5	0.2	3.4
Hydraulic system	Aluminium	1.4	0.5	9.6
	Steel	0.1	0.0	0.5
Buoy	Steel	0.5	0.2	3.5
	Polyethylene	0.3	0.1	2.1
	Polyurethane foam	5.5	1.8	36.4
	Total Phase 1	**8.3**	**2.8**	**55.5**
Phase 2 - TRANSPORT, ASSEMBLY, and INSTALLATION				
Transport, freight, lorry	—	0.2	0.1	1.3
Forklift	Diesel	0.1	0.0	0.4
Crane	Diesel	0.9	0.3	6.2
Auxiliary boats	Diesel	0.4	0.1	3.0
Generator	Diesel	0.4	0.1	2.8
	Total Phase 2	**2.1**	**0.7**	**14**
Phase 3 - MAINTENANCE and MATERIAL REPLACEMENT				
Van	Transport, passenger, car (medium size)	0.1	0.04	0.8
Pistons	Aluminium	1.4	0.5	9.6
	Steel	0.4	0.1	2.4
	Total Phase 3	**1.5**	**0.5**	**10.3**
Phase 4 - END OF LIFE				
	Total Phase 4	3.05	1.0	**20.4**
Total		**15.0**	**5.0**	**100.0**

buoy case study, the results obtained are close to the average values found in the literature for floating body converters (83 g CO_2eq·kWh^{-1} considering Dahlsten, 2009; 105 g CO_2eq·kWh^{-1} according to Uihlein, 2016; and 90 g CO_2eq·kWh^{-1} calculated by Zhai et al., 2018).

Based on the results obtained and from the comparison with the aforementioned literature, it is evident that encouraging research and development of such WEC systems, integrating them with already established technologies, and the implementation and deployment of new MRE solutions foster a conscious use of resources. Despite the need for targeted structural improvements, ocean energy technologies could still contribute to making energy systems more sustainable through synergies with other renewable energy sources (International Renewable Energy Agency (IRENA), 2020). To promote a hybrid electricity generation, for example, WECs can be coupled with offshore wind turbines. In this regard, Elginoz and Bas (2017) carried out an LCA of a multi-use offshore platform, designed for Atlantic Ocean Cantabrian conditions, which unites wave and wind energy converters. The research showed the manufacturing processes as the main source of environmental burdens. Nevertheless, the sensitivity and scenario analyses highlighted the significant effect of estimated recycling ratios and location of the energy farm on environmental impacts of the structure in the early design stage. Moreover, a feasibility and LCA study of a WEC platform, called *Wave Dragon*, combined with wind turbines, conducted by Sørensen et al. (2016), showed a 17 % lower LCOE attributed to the wave–wind combination unit compared to WEC alone.

4 Sensitivity analysis

A sensitivity analysis was carried out to assess variations in terms of CF and consequently CIE, postulating changes in the

TABLE 7 Total GWP (t CO_2eq) impact category results for the seabed-based buoy and values for individual components.

Element	Technical specification	Carbon footprint wave park (t CO_2eq)	Carbon footprint 1 buoy (t CO_2eq)	%
Phase 1 - MANUFACTURING				
Foundation	Concrete	5.8	0.2	3.7
	Steel	13.0	0.5	8.3
	Steel	0.3	0.0	0.2
Capsule and superstructure	Steel	2.7	0.1	1.7
	Steel	1.3	0.1	0.8
	Steel	0.2	0.0	0.1
Funnel	Steel	0.8	0.0	0.5
Buoy	Steel	3.0	0.1	1.9
	Steel	1.4	0.1	0.9
	Polyethylene	2.7	0.1	1.7
	Polyurethane	33.4	1.3	21.2
Translator	Cast iron	3.4	0.1	2.1
	Copper	0.1	0.0	0.1
	Ferrite magnet	0.3	0.0	0.2
	Plastic and rubber	0.4	0.0	0.2
	Zinc	0.2	0.0	0.1
	Aluminium	0.1	0.0	0.1
	Paint	0.2	0.0	0.1
Substation	Steel	0.4	0.0	0.2
	Copper	0.04	0.0	0.0
	Concrete	0.02	0.0	0.0
Submarine power cable	Lead	1.0	0.0	0.6
	Copper	0.45	0.0	0.3
	Polyethylene	0.3	0.0	0.2
	Steel	1.8	0.1	1.1
	Polypropylene	0.2	0.0	0.1
Total Phase 1		**73.5**	**2.9**	**46.6**
Phase 2 - TRANSPORT, ASSEMBLY and INSTALLATION				
Transport, freight, lorry	—	13	0.5	8.2
Forklift	Diesel	0.8	0.0	0.5
Crane	Diesel	12.2	0.5	7.7
Generator	Diesel	10.4	0.4	6.6
Workboat	Diesel	1.1	0.0	0.7
Total Phase 2		**37.4**	**1.5**	**24**
Phase 3 - MAINTENANCE				
Crew Transfer vessel	Diesel	23.7	0.9	15.1
Total Phase 3		**23.7**	**0.9**	**15.1**
Phase 4 - END OF LIFE				
Total Phase 4		23.0	0.9	**14.6**
Total		**157.6**	**6.3**	**100.0**

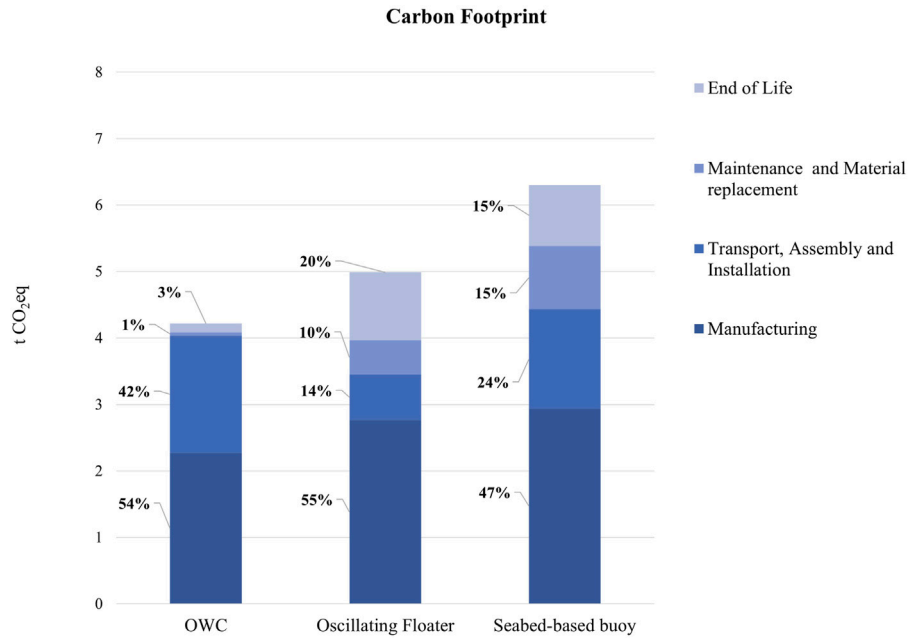

FIGURE 5
Carbon Footprint (t CO_2eq) results in the three WECs in relation to the different LCA phases analyzed.

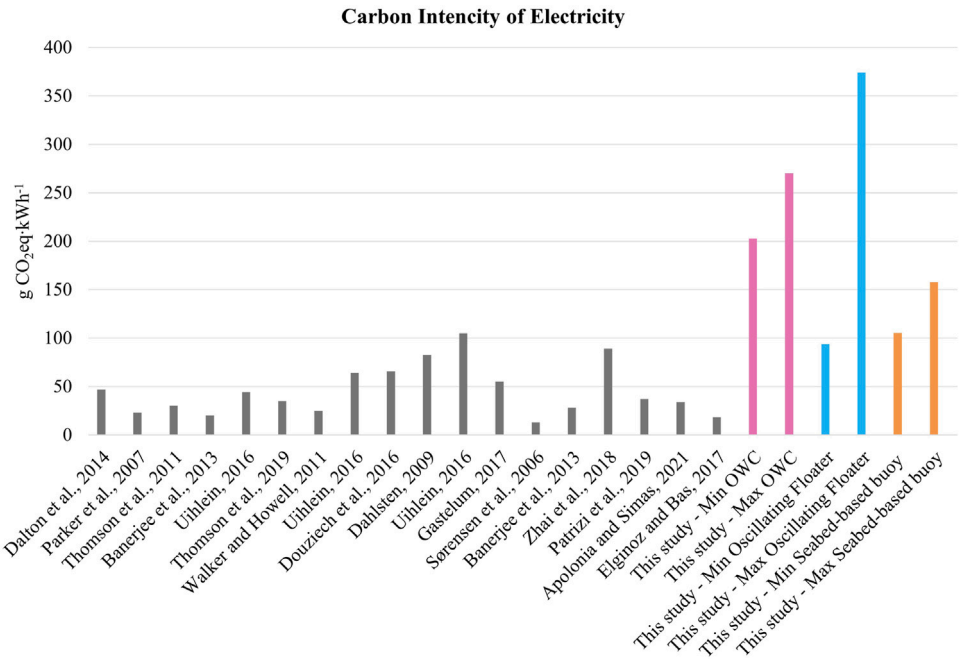

FIGURE 6
CIE values of the WEC systems available in the literature (grey columns) and results obtained from the present study (colored columns).

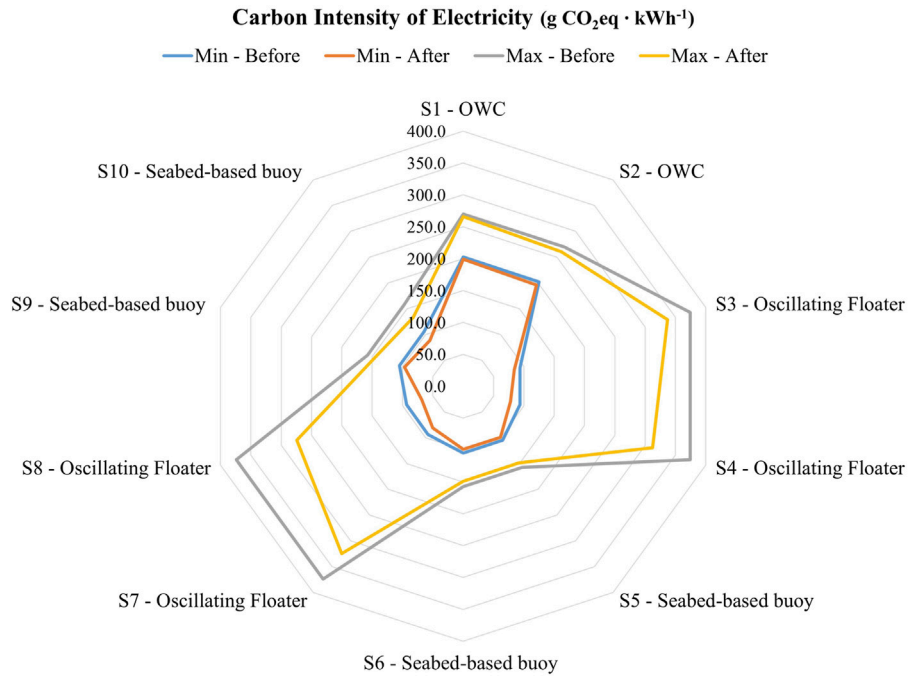

FIGURE 7
Results of the sensitivity analysis for each scenario analyzed.

parameters that most influence the results of the study (Figure 7 and Supplementary Table S1 in the supplementary material).

According to Paredes et al. (2019), the manufacture of materials used in the WEC structures showed the greatest impact on total GHG emissions. For this reason, using appropriate emission factors, it was hypothesized that 30 and 50 % of primary steel involved in the manufacturing phase should be recycled (Scenarios S1 and S2, respectively) for the OWC construction. Although in this system, concrete carries the greatest burden in terms of CF, there are currently no fates other than landfilling for this material. In addition, for a device such as the OWC, further studies would be needed to verify the possibility of reducing the amount of concrete involved or its replacement with other materials such as steel or wood to build the caisson structure. Moreover, various recycling methods can be applied to give a second life to polyurethane, avoiding disposing such a valuable polymer (Cannon, 2021). As it has the highest contribution in the manufacturing stage of the other two WEC structures, four scenarios (S3 and S4 for the oscillating floater; S5 and S6 for the seabed-based buoy) with 30 and 50 % of recycled polyurethane were postulated, respectively. To address the lack of background data on SimaPro to model the polyurethane recycling, the high-density polyethylene recycling process was assumed as "proxy", since the treatment processes can be assumed to be similar, and the raw material is not explicit.

As the development of new plastic materials with better environmental performances compared to the traditional fossil-based counterpart is a priority toward sustainable production processes (Manzardo et al., 2019), it was assumed that the substitution of polyurethane parts with a bio-based solution by following what is reported in Bioplastics (2015). This assumption considered that the parts in question were not in direct contact with the marine environment but constituted the internal structure of the WEC. It therefore considered an additional four scenarios (S7 and S8 for the oscillating floater; S9 and S10 for the seabed-based buoy) in which 50 and 100 % of the polyurethane was substituted with a bio-based polyurethane, respectively.

The sensitivity analysis showed that for the OWC model, scenarios S1 and S2 (with 30 and 50% of recycled steel, respectively) did not significantly decrease the impact (-0.3 % and -0.6 % of total CF). Indeed, the CF values remained almost unchanged in each scenario (around 4 t CO_2eq).

The implementation of recycled polyurethane in the oscillating floater structure, instead, is responsible for -6 % and -10 % of the total CF values variation, which decrease to

4.5 and 4 t CO_2eq in S3 and S4, respectively. Also, in the seabed-based buoy model, the use of recycled polyurethane improves the overall environmental performance, with lower CF values of 6 t CO_2eq in S5 and in S6 (-6%). Regarding the application of bio-based polyurethane for both oscillating floater and seabed-based buoy models, the substitution of 50 % (S7 and S9) and 100 % (S8 and S10) of traditional polyurethane is responsible for -8 % and -16 % of the emission variance. This means that the CF values of the floater decrease to 4.3 and 5.8 t CO_2eq, respectively; while the CF results of the buoy come to 3.6 and 5.3 t CO_2eq, respectively.

Likewise, the variations in terms of CIE show that the implementation of recycled materials can improve the performance of the systems analyzed. Regarding the OWC system, the values of CIE for S1 and S2 decrease to 199.4–266 g CO_2eq·kWh^{-1} and 196–261 g CO_2eq·kWh^{-1}, respectively. The CIE range values associated to the oscillating floater are 84–337 g CO_2eq·kWh^{-1} in S3 and 78–312 g CO_2eq·kWh^{-1} in S4, while for the seabed-based buoy are 99–148.5 g CO_2eq·kWh^{-1} in S5 and 99.2–149 g CO_2eq·kWh^{-1} in S6 (Figure 7 and Supplementary Table S1 in the supplementary material).

Finally, also the hypostatized application of bio-based polyurethane for the oscillating floater and the seabed-based buoy turns out to be an interesting choice that would allow for a range of CIE values of: 81.1–324.3 g CO_2eq·kWh^{-1} in S7; 68.6–274.5 g CO_2eq·kWh^{-1} in S8; 97–145.4 g CO_2eq·kWh^{-1} in S9; and 89–133 g CO_2eq·kWh^{-1} in S10 (Figure 7 and Supplementary Table S1 in the supplementary material).

5 Conclusion

One of the greatest challenges of this century is to find an alternative energy source to fossil fuels (Owusu and Asumadu-Sarkodie, 2016). A major boost to the ecological transition could therefore come from harnessing wave energy by avoiding leaving out the 70 % of the Earth surface (i.e., ocean and seas).

In this field, this study was aimed to define a benchmark of three WECs able to overcome the variability between specific technologies and provide a preliminary assessment of the potential environmental performance, following homogeneous evaluation criteria.

The LCA methodology was used to evaluate their environmental impact and in particular, the CF, considering the main materials and energy flows involved in the different lifecycle phases, i.e., manufacturing: transport, assembly, and installation; maintenance; and EoL. For each WEC, the LCA confirmed that the potential impacts, in terms of CF, stemmed from the manufacturing stage. Consequently, future studies and research studies should enhance the knowledge concerning the materials used in the construction of such technologies. For example, by reducing, where possible, the quantities of components having a high GWP, selecting those with better performances in terms of structural and environmental characteristics, and evaluating the possibility of extending their lifetime.

Although the productivity values were not related to direct monitoring activities of these systems in real sites, but relied on the productivity ranges valid for the Mediterranean according to literature sources, the results of this study showed that WEC technologies have high potential to be implemented with high rates of efficiency improvement. Each WEC exploits the same resource (the wave energy potential), but they are different technologies, characterized by different designs and operating systems. Moreover, their performance depends on where these technologies are installed. It is therefore not possible to recommend one technology with respect to the others. Nevertheless, given the results shown in this study, WECs can be taken seriously into account for energy policies at national and local scales (European Commission (EC), 2014) from administrations and public authorities. These systems are more competitive than those using fossil energy sources, and in some cases, even compared with other technologies able to deploy different renewable energy sources, such as hydrogen and geothermal.

Results refer to 3D model systems (even inspired by existing prototypes) and are based on assumptions (such as material mass, installation–maintenance operations, and expected lifetime of certain structural components); nevertheless, they provide useful information to understand current performances and figure out potential improvements. According to Pirttimaa and Cruz (2020), more research in the field of MRE and a better exchange of information on the potential environmental impacts will be required to understand and mitigate any adverse effects that ocean energy installations may have on marine ecosystems. Coherently, this study showed how LCA can inform the design of innovative WEC technologies dealing with their production yield, but also their lifecycle processes. Based on the information obtained (e.g., constructive technique used, functional principle, and marine energy potentials of the hypothetical implementation site), WEC look like a promising solution to exploit the MRE potential in the Mediterranean and clearly show the opportunity to further investigate and foster their deployment. Moreover, the creation of synergies between WECs and other solutions, such as offshore wind turbines, encourage hybrid electricity generation and sustain the detachment from fossil fuels.

Data availability statement

The original contributions presented in the study are included in the article/Supplementary Material; further inquiries can be directed to the corresponding author.

Author contributions

MB, MM, RMP, EN and NP conceived the manuscript and processed and discussed data. AS elaborated the 3D models and extracted inventory data. RMP and SB supervised the writing of the manuscript. All authors discussed reviewer feedback and contributed to the final manuscript.

Funding

This study was conducted in the framework of the Interreg Med BLUE-DEAL (2019–2022) project, co-financed by the European Regional Development Fund. Website: https://blue-deal.interreg-med.eu.

Conflict of interest

Authors RMP, AS, and EN were employed by 2INDACO2 srl.

The remaining authors declare that the research was conducted in the absence of any commercial or financial relationships that could be construed as a potential conflict of interest.

Publisher's note

All claims expressed in this article are solely those of the authors and do not necessarily represent those of their affiliated organizations, or those of the publisher, the editors, and the reviewers. Any product that may be evaluated in this article, or claim that may be made by its manufacturer, is not guaranteed or endorsed by the publisher.

Supplementary material

The Supplementary Material for this article can be found online at: https://www.frontiersin.org/articles/10.3389/fenrg.2022.980557/full#supplementary-material

References

Acta Marine (2017). Offshore response I south boats 12 m catamaran crew transfer vessel. Available at: https://www.actamarine.com/documenten/specs/ctv_s_17-05-2017/vessel_specifications_offshore_response.pdf (Accessed March 15, 2022).

Andersen, K., Chapman, A., Hareide, N. R., Folkestad, A. O., Sparrevik, E., and Langhamer, O. (2009). Environmental monitoring at the maren wave power test site off the island of runde, western Norway: Planning and design. Available at: https://www.researchgate.net/publication/228877739 (Accessed March 15, 2022).

Apolonia, M., and Simas, T. (2021). Life cycle assessment of an oscillating wave surge energy converter. *J. Mar. Sci. Eng.* 9, 206. doi:10.3390/jmse9020206

Appiott, J., Dhanju, A., and Cicin-Sain, B. (2014). Encouraging renewable energy in the offshore environment. *Ocean Coast. Manag.* 90, 58–64. doi:10.1016/j.ocecoaman.2013.11.001

Arena, F. (2016). Resonant wave energy converters REWEC3: Primi prototipi nei porti di Civitavecchia e di Salerno. Available at: http://www.eugeniopc.it/investigacion/seminari/EnergiaMareNSW16/PRESENTAZIONI/PresentazioneArena.PDF (Accessed April 15, 2022).

Arena, F., Romolo, A., Malara, G., and Ascanelli, A. (2013). "On design and building of a U-owc wave energy converter in the mediterranean sea: A case study," in ASME 2013 32nd International Conference on Ocean, Offshore and Arctic Engineering, Nantes, France, June 9-14, 2013. doi:10.1115/OMAE2013-11593

Birkeland, C. (2011). *Assessing the life cycle environmental impacts of offshore wind power generation and power transmission in the North Sea* (Trondheim (N): Norwegian University of Science and Technology). [dissertation/Master's thesis].

Banerjee, S., Duckers, L., and Blanchard, R. E. (2013). An overview on green house gas emission characteristics and energy evaluation of ocean energy systems from life cycle assessment and energy accounting studies. *J. Appl. Nat. Sci.* 5, 535–540. doi:10.31018/jans.v5i2.364

Bioplastics (2015). Just how environmentally friendly are biobased materials actually? Available at: https://www.bioplasticsmagazine.com/en/news/meldungen/20150814-Biobased-production-should-become-more-efficient.php (Accessed June 08, 2022).

Bjørnsen, E. (2014). *Chains in mooring systems* (Trondheim (N): Norwegian University of Science and Technology). [dissertation/Master's thesis].

BLUE DEAL MED (2022c). Eco wave power: Generating clean electricity from ocean waves for giglio island. Available at: https://bluedealmed.eu/colab/proposals/eco-wave-power-generating-clean-electricity-from-ocean-waves-for-giglio-island (Accessed April 15, 2022).

BLUE DEAL MED (2022d). EDS: The energy Double system for harnessing wave energy in the nearshore zone. Available at: https://bluedealmed.eu/colab/proposals/eds-the-energy-double-system-for-harnessing-wave-energy-in-the-nearshore-zone-2 (Accessed April 15, 2022).

BLUE DEAL MED (2022a). HYDRA WHT for the giglio island. Available at: https://bluedealmed.eu/colab/proposals/hydra-wht-for-the-giglio-island (Accessed April 15, 2022).

BLUE DEAL MED (2022b). Seadamp FX – the anchorage system that harvests energy from the sea. Available at: https://bluedealmed.eu/colab/proposals/seadamp-fx-the-anchorage-system-that-harvests-energy-from-the-sea-3 (Accessed April 15, 2022).

Bozzi, S., Miquel, A. M., Antonini, A., Passoni, G., and Archetti, R. (2013). Modeling of a point Absorber for energy conversion in Italian seas. *Energies* 6, 3033–3051. doi:10.3390/en6063033

Bruschi, D. L., Fernandes, J. C. S., Falcão, A. F. O., and Bergmann, C. P. (2019). Analysis of the degradation in the Wells turbine blades of the Pico oscillating-water-column wave energy plant. *Renew. Sustain. Energy Rev.* 115, 109368. doi:10.1016/j.rser.2019.109368

Cannon (2021). Recycled polyurethane: The second life of the polymer. Available at: https://www.cannonplastec.com/blog/recycled-polyurethane-the-second-life-of-the-polymer/ (Accessed May 6, 2022).

Cascajo, R., García, E., Quiles, E., Correcher, A., and Morant, F. (2019). Integration of marine wave energy converters into seaports: A case study in the port of valencia. *Energies* 12, 787. doi:10.3390/en12050787

Cejuela, E., Negro, V., del Campo, J. M., Martín-Antón, M., Esteban, M. D., and López-Gutiérrez, J. S. (2018). Recent history, types, and future of modern caisson technology: The way to more sustainable practices. *Sustainability* 10, 3839. doi:10.3390/su10113839

Chatzigiannakou, M. A., Dolguntseva, I., and Leijon, M. (2015). "Offshore deployment of marine substation in the lysekil research site," in Proceedings of the Twenty-fifth International Ocean and Polar Engineering Conference Kona, Big Island, Hawaii, USA, June 21-26, 2015, 1098–6189. ISBN 978-1-880653-89-0; ISSN.

Chatzigiannakou, M. A., Dolguntseva, I., and Leijon, M. (2014). Offshore deployment of point absorbing wave energy converters with a direct driven linear generator power take-off at the Lysekil test site. Available at: https://citeseerx.ist.psu.edu/viewdoc/download?doi=10.1.1.656.3662&rep=rep1&type=pdf (Accessed April 16, 2022).

Chatzigiannakou, M. A., Dolguntseva, I., and Leijon, M. (2017). Offshore deployments of wave energy converters by seabased industry AB. *J. Mar. Sci. Eng.* 5, 15. doi:10.3390/jmse5020015

Chipindula, J., Botlaguduru, V. S. V., Du, H., Kommalapati, R. R., and Huque, Z. (2018). Life cycle environmental impact of onshore and offshore wind farms in Texas. *Sustainability* 10, 2022. doi:10.3390/su10062022

Curto, D., Franzitta, V., and Guercio, A. (2021). sea wave energy. A review of the current technologies and perspectives. *Energies* 14, 6604. doi:10.3390/en14206604

Dahlsten, H. (2009). *Life cycle assessment of electricity from wave power* (Uppsala Sweden: Swedish University of Agricultural Sciences). [dissertation/Master's thesis] https://stud.epsilon.slu.se/5364/1/dahlsten_h_130321.pdf (Accessed March 15, 2022).

Dalton, G., Madden, D., and Daly, M. C. (2014). "Life cycle assessment of the wavestar," in 2014 Ninth International Conference on Ecological Vehicles and Renewable Energies (EVER), Monte-Carlo, Monaco, 25-27 March 2014, 1–9. doi:10.1109/EVER.2014.6844034

De Girolamo, P. (2015). Opere verticali o a parete o a muro. Available at: https://web.uniroma1.it/masterprogeo/sites/default/files/allegati_notizie/03_DIGHE%20A%20PARETE%20IN%20CASSONI%20%20CELLULARI.pdf (Accessed April 5, 2022).

Douziech, M., Hellweg, S., and Verones, F. (2016). Are wave and tidal energy plants new green technologies? *Environ. Sci. Technol.* 50, 7870–7878. doi:10.1021/acs.est.6b00156

Ecoinvent (2022). (For the availability of envorinmetal data worldwide. Available at: https://ecoinvent.org/(Accessed April 15, 2022).

Elginoz, N., and Bas, B. (2017). Life Cycle Assessment of a multi-use offshore platform: Combining wind and wave energy production. *Ocean. Eng.* 145, 430–443. doi:10.1016/j.oceaneng.2017.09.005

Esteban, M. D., López-Gutiérrez, J.-S., and Negro, V. (2017). Classification of wave energy converters. *Recent Adv. Petrochem Sci.* 2, 4. doi:10.19080/rapsci.2017.02.555593

European Commission (EC) (2022). 2030 climate target plan. Available at: https://ec.europa.eu/clima/eu-action/european-green-deal/2030-climate-target-plan_en#:~:text=With%20the%202030%20Climate%20Target,below%201990%20levels%20by%202030 (Accessed March 20, 2022).

European Commission (EC) (2014). Blue Energy. Action needed to deliver on the potential of ocean energy in European seas and oceans by 2020 and beyond. Available at: https://eur-lex.europa.eu/legal-content/EN/TXT/PDF/?uri=CELEX:52014DC0008&from=EN (Accessed March 10, 2022).

European Commission (EC) (2021). The EU blue economy report. 2021. Available at: https://blueindicators.ec.europa.eu/sites/default/files/2021_06_BlueEconomy_Report-2021.pdf (Accessed March 102022.]

Falcão, A. (2010). F.de OWave energy utilization: A review of the technologies. *Renew. Sustain. Energy Rev.* 14 (3), 899–918. doi:10.1016/j.rser.2009.11.003

Faÿ, F. X., Henriques, J. C., Kelly, J., Mueller, M., Abusara, M., Wanan Sheng, W., et al. (2020). Comparative assessment of control strategies for the biradial turbine in the Mutriku OWC plant. *Renew. Energy* 146, 2766–2784. doi:10.1016/j.renene.2019.08.074

Holmgren, R. (2016). *Modeling and concept design of wave energy device*. Stockholm: Royal Institute of Technology.

Hong, Y., Hultman, E., Castellucci, V., Ekergård, B., Sjökvist, L., Soman, D. E., et al. (2013). Status update of the wave energy research at Uppsala University. https://www.researchgate.net/publication/258999251 (Accessed March 10, 2022).

Huang, Y. F., Gan, X. J., and Chiueh, P. T. (2017). Life cycle assessment and net energy analysis of offshore wind power systems. *Renew. Energy* 102, 98–106. doi:10.1016/j.renene.2016.10.050

Hultman, E., Ekergård, B., Kamf, T., Salar, D., and Leijon, M. (2014). Preparing the Uppsala university wave energy converter generator for large-scale production. https://www.icoe-conference.com/publication/preparing-the-uppsala-university-wave-energy-converter-generator-for-large-scale-production/ (Accessed April 5, 2022).

Ibarra-Berastegi, G., Sáenz, J., Ulazi, A., Serras, P., Esnaola, G., and Garcia-Soto, C. (2018). Electricity production, capacity factor, and plant efficiency index at the Mutriku wave farm (2014–2016). *Ocean. Eng.* 147, 20–29. doi:10.1016/j.oceaneng.2017.10.018

Intergovernmental Panel on Climate Change (IPCC) (2013). Fifth assessment report. The physical science 469 basis. Available at: https://www.ipcc.ch/report/ar5/wg1/(Accessed June 08, 2022).

International Renewable Energy Agency (IRENA) (2020). Innovation outlook: Ocean energy technologies. Available at: https://www.irena.org/-/media/Files/IRENA/Agency/Publication/2020/Dec/IRENA_Innovation_Outlook_Ocean_Energy_2020.pdf (Accessed March 08, 2022).

International Standard Organization (ISO) (2006). *Environmental Management and Life Cycle Assessment e principles and Framework, Goal and Scope Definition and Life Cycle Inventory Analysis, Life Cycle Impact Assessment and Life Cycle Interpretation*. Geneva: International Organization for Standardization. ISO 14040: 2006.

International Standard Organization (ISO) (2020). *Environmental Management and Life Cycle Assessment e requirements and Guidelines*. Geneva: International Organization for Standardization. ISO 14044:2020.

Khan, N., Kalair, A., Abas, N., and Haider, A. (2017). Review of ocean tidal, wave and thermal energy technologies. *Renew. Sustain. Energy Rev.* 72, 590–604. doi:10.1016/j.rser.2017.01.079

Koca, K., Kortenhaus, A., Angelelli, E., Zanuttigh, B., Kirca, O., Bas, B., et al. (2013). *Wave Energy Convert. Energy Convert. MERMAID Deliv.* D3, 3.

Lacasa, M. C., Esteban, M. D., López-Gutiérrez, J. S., Negro, V., and Zang, Z. (2019). Feasibility study of the installation of wave energy converters in existing breakwaters in the north of. *Spain. Appl. Sci.* 9, 23. doi:10.3390/app9235225

Leijon, M., Boström, C., Danielsson, O., Gustafsson, S., Haikonen, K., Langhamer, O., et al. (2008). Wave energy from the North Sea: Experiences from the lysekil research site. *Surv. Geophys.* 29, 221–240. doi:10.1007/s10712-008-9047-x

Lissandrom, S. (2010). *Energia dal moto ondoso – wave energy* (Padova (IT): Università degli Studi di Padova). [dissertation/Bachelor's thesis].

Liu, Y., Li, Y., He, F., and Wang, H. (2017). Comparison study of tidal stream and wave energy technology development between China and some Western Countries. *Renew. Sustain. Energy Rev.* 76, 701–716. doi:10.1016/j.rser.2017.03.049

Magallanes, A., Sullivan, B., Moores, A., and Singh, A. (2016). Submerged concrete caisson breakwater construction. Available at: https://www.researchgate.net/publication/317842948 (Accessed April 15, 2022).

Malara, G., Romolo, A., Fiamma, V., and Arena, F. (2017). On the modelling of water column oscillations in U-OWC energy Harvesters. *Renew. Energy* 101, 964-972. doi:10.1016/j.renene.2016.09.051

Manzardo, A., Marson, A., Roso, M., Boaretti, C., Modesti, M., Scipioni, A., et al. (2019). Life cycle assessment framework to support the design of biobased rigid polyurethane foams. *ACS Omega* 4 (9), 14114–14123. doi:10.1021/acsomega.9b02025

Marchesi, E., Negri, M., and Malavasi, S. (2020). Development and analysis of a numerical model for a two-oscillating-body wave energy converter in shallow water. *Ocean. Eng.* 214, 107765. doi:10.1016/j.oceaneng.2020.107765

Mohamed, T. (2021). "Marine energy," in *Distributed renewable energies for off-grid communities. Empowering a sustainable, competitive, and secure twenty-first century* (Amsterdam, NL: Elsevier Science Publishing Co Inc), 231–245. doi:10.1016/B978-0-12-821605-7.00012-X

Owusu, P. A., and Asumadu-Sarkodie, S. (2016). A review of renewable energy sources, sustainability issues and climate change mitigation. *Cogent Eng.* 3, 1167990. doi:10.1080/23311916.2016.1167990

Paredes, M. G., Padilla-Rivera, A., and Güereca, L. P. (2019). Life cycle assessment of ocean energy technologies: A systematic review. *J. Mar. Sci. Eng.* 7, 322. doi:10.3390/jmse7090322

Parker, R. P. M., Harrison, G. P., and Chick, J. P. (2007). Energy and carbon audit of an offshore wave energy converter. *Proc. Institution Mech. Eng. Part A J. Power Energy* 221 (8), 1119–1130. doi:10.1243/09576509jpe483

Patrizi, N., Pulselli, R. M., Neri, E., Niccolucci, V., Vicinanza, D., Contestabile, P., et al. (2019). Life cycle environmental impact assessment of an overtopping wave energy converter embedded in breakwater systems. *Front. Energy Res.* 7, 32. doi:10.3389/fenrg.2019.00032

Pirttimaa, L., and Cruz, E. (2020). Ocean energy and the environment: Research and strategic actions. Review of environmental impacts and consenting processes for ocean energy. European Technology & Innovation Platform for Ocean Energy. Available at: https://www.oceanenergy-europe.eu/wp-content/uploads/2020/12/ETIP-Ocean-Ocean-energy-and-the-environment.pdf (Accessed June 16, 2022).

PRé Consultants (2020). SimaPro 9.1.1. Available at: https://simapro.com/ (Accessed June 15, 2022).

Pulselli, R. M., Maccanti, M., Bruno, M., Sabbetta, A., Neri, E., and Patrizi, N. (2022). Benchmarking marine energy technologies through LCA: Offshore floating wind farms in the mediterranean. *Front. Energy Res.* 10, 902021. In press (this research topic). doi:10.3389/fenrg.2022.902021

Pulselli, R. M., Marchi, M., Neri, E., Marchettini, N., and Bastianoni, S. (2019). Carbon accounting framework for decarbonisation of European city neighbourhoods. *J. Clean. Prod.* 208, 850–868. doi:10.1016/j.jclepro.2018.10.102

Raadal, H. L., Vold, B. I., Myhr, A., and Nygaard, T. A. (2014). GHG emissions and energy performances of offshore wind power. *Renew. Energy* 66, 314–324. doi:10.1016/j.renene.2013.11.075

Rémouit, F., Chatzigiannakou, M. A., Bender, A., Temiz, I., Sundberg, J., and Engström, J. (2018). Deployment and maintenance of wave energy converters at the lysekil research site: A comparative study on the use of divers and remotely-operated vehicles. *J. Mar. Sci. Eng.* 6, 39. doi:10.3390/jmse6020039

Resinex (2007). Support and Mooring Buoys - the widest range of floating equipment. Available at: https://www.resinextrad.com/en/wp-content/uploads/2007/06/Support-and-Mooring-Buoys.pdf (Accessed April 20, 2022). [Personal communication from Business development manager of Resinex].

Russel, I., (2007). Inventory materials of 7 MW wave dragon [personal communication from business development manager of wave dragon firm].

Seares (2022). SEADAMP FX. [Personal communication from Business development manager of Seares].

Sgobbi, A., Simões, S. G., Magagna, D., and Nijs, W. (2016). Assessing the impacts of technology improvements on the deployment of marine energy in Europe with an energy system perspective. *Renew. Energy.* 89, 515–525. doi:10.1016/j.renene.2015.11.076

Short, A. D. (2012). Coastal processes and beaches. *Nat. Educ. Knowl.* 3 (10), 15. Available at: https://www.nature.com/scitable/knowledge/library/coastal-processes-and-beaches-26276621/(Accessed April 5, 2022).

Sørensen, H. C., Friis-Madsen, E., Russel, I., Parmeggiani, S., and Fernández-Chozas, J. (2016). Feasibility and LCA for a Wave Dragon platform with wind turbines. Available at: https://onepetro.org/ISOPEIOPEC/proceedings-abstract/ISOPE16/All-ISOPE16/ISOPE-I-16-546/17011 (Accessed March 27, 2022).

Sørensen, H. C., Naef, S., Anderberg, S., and Hauschild, M. Z. (2006). "Life cycle assessment of the wave energy converter: Wave Dragon," in Proceedings of the International Conference on Ocean Energy, Bremerhaven, Germany, 23–24 October, 2016.

Sovacool, B. (2008). Valuing the greenhouse gas emissions from nuclear power: A critical survey. *Energy Policy* 36, 2950–2963. doi:10.1016/j.enpol.2008.04.017

Spanos, P. D., Strati, F. M., Malara, G., and Arena, F. (2018). An approach for non-linear stochastic analysis of U-shaped OWC wave energy converters. *Probabilistic Eng. Mech.* 54, 44–52. doi:10.1016/j.probengmech.2017.07.001

Strömstedt, E., Svensson, O., and Leijon, M. (2012). "A set-up of 7 laser triangulation sensors and a draw-wire sensor for measuring relative displacement of a piston rod mechanical lead-through transmission in an offshore wave energy converter on the ocean floor," in *International scholarly research notices* London, United Kingdom: Hindawi. doi:10.5402/2012/746865

Taylor, C. (2006). Inventory materials of 750 kW Pelamis [personal communication from chief engineer of Pelamis farm, OPD].

Thomson, R. C., Chick, J. P., and Harrison, G. P. (2019). An LCA of the Pelamis wave energy converter. *Int. J. Life Cycle Assess.* 24, 51–63. doi:10.1007/s11367-018-1504-2

Thomson, R. C., Harrison, G. P., and Chick, J. P. (2011). "Full life cycle assessment of a wave energy converter," in Proceedings of the IET Conference on Renewable Power Generation (RPG 2011), Edinburgh, UK, 6–8 September. doi:10.1049/cp.2011.0124

Tsai, L., Kelly, J. C., Simon, B. S., Chalat, R. M., and Keoleian, G. A. (2016). Life cycle assessment of offshore wind farm siting - effects of locational factors, lake depth, and distance from shore. *J. Industrial Ecol.* 20, 1370–1383. doi:10.1111/jiec.12400

Uihlein, A. (2016). Life cycle assessment of ocean energy technologies. *Int. J. Life Cycle Assess.* 21, 1425–1437. doi:10.1007/s11367-016-1120-y

Walker, S., and Howell, R. (2011). *Life cycle comparison of a wave and tidal energy device* (Sheffield (UK): University of Sheffield). [dissertation/Ph. D's thesis].

Zepeda, L. G. (2017). *Life cycle assessment of a wave energy converter*. (Stockholm (S): KTH Royal Institute of Technology). [dissertation/Bachelor's thesis]

Zhai, Q., Zhu, L., and Lu, S. (2018). Life cycle assessment of a buoy-rope-drum wave energy converter. *Energies* 11, 2432. doi:10.3390/en11092432

frontiers | Frontiers in Energy Research

TYPE Original Research
PUBLISHED 02 November 2022
DOI 10.3389/fenrg.2022.973952

OPEN ACCESS

EDITED BY
Siamak Hoseinzadeh,
Sapienza University of Rome, Italy

REVIEWED BY
Shahin Shoeibi,
Islamic Azad University Semnan, Iran
Carlos Pérez-Collazo,
University of Vigo, Spain
Amir Hassanzadeh,
Urmia University, Iran
Ali Sohani,
University of Rome Tor Vergata, Italy
Al-Janabi,
Sultan Qaboos University, Oman

*CORRESPONDENCE
Nicoletta Patrizi,
patrizi2@unisi.it

SPECIALTY SECTION
This article was submitted to Sustainable Energy Systems and Policies, a section of the journal Frontiers in Energy Research

RECEIVED 20 June 2022
ACCEPTED 14 September 2022
PUBLISHED 02 November 2022

CITATION
Betti G, Cervellera GP, Gagliardi F, Gioia C, Patrizi N and Bastianoni S (2022), Perceptions and attitudes toward blue energy and technologies in the Mediterranean area: ASKYOURCITIZENSONBE. *Front. Energy Res.* 10:973952. doi: 10.3389/fenrg.2022.973952

Perceptions and attitudes toward blue energy and technologies in the Mediterranean area: ASKYOURCITIZENSONBE

Gianni Betti[1], Gian Piero Cervellera[1], Francesca Gagliardi[1], Carmela Gioia[2], Nicoletta Patrizi[2]* and Simone Bastianoni[2]

[1]Department of Economics and Statistics, University of Siena, Siena, Italy, [2]Ecodynamics Group, Department of Earth, Environmental and Physical Sciences, University of Siena, Siena, Italy

An energy transition is needed in order to meet the European pledge of reaching climate neutrality by 2050. This transition cannot ignore the renewable resources available from 70% of the Earth (namely, the oceans and seas). This concept is fundamental for the planet, especially for the Mediterranean area. Marine renewable energies are still under-deployed in the Mediterranean area for many reasons, including legislative constraints, lower energy availability, and technological readiness. An appropriate participatory process including all actors (e.g., policymakers, firms, citizens, and researchers) is necessary for a correct path toward decarbonization. The BLUE DEAL project was conceived and implemented by 12 Mediterranean partners to tackle these issues and set the route for blue energy deployment in the Mediterranean area. Activities already conducted include a survey to probe the perceptions and attitudes of citizens toward blue energy. The survey targeted about 3,000 persons in 12 Mediterranean sites with the aim of bringing citizens into the discussion on future technologies. The results showed that although blue energy is still relatively unknown to the general public (only 42% of respondents were aware of these technologies), there was a general willingness (70%) to host one or more such installations in their areas. Here, we describe our survey method and some empirical results with suggestions for replicability and recommendations on how to use it for policymaking purposes.

KEYWORDS

marine renewable energies (MREs), blue energy, citizen engagement, citizen perception, social acceptance

1 Introduction

Renewable energy, in particular the deployment of marine renewable energy, is a key to fighting climate change. In November 2020, the European Commission issued an "EU Strategy to harness the potential of offshore renewable energy for a climate-neutral future" (EC, 2020). This strategy lays the foundations for replacing fossil fuels with offshore renewables, thus creating industrial opportunities and green jobs across the continent. It

recognizes the fundamental role that seas and oceans can play in EU decarbonization due to their untapped potential as clean energy sources. It underlines that the marine renewable energy industry will need to grow by a factor of five by 2030 and a factor of 25 by 2050 to sustain the goals of the Green Deal (EC, 2020). The readiness of renewable energy technologies to offer variegated alternative solutions is gradually improving (see for example Gilani et al., 2021; Shoeibi et al., 2021; Shoeibi et al., 2022a; Shoeibi et al., 2022b; Dhivagar et al., 2022). The same path, coupled with broad stakeholder involvement, should be followed by so-called blue energy to become a viable solution and be considered in coastal energy planning.

A sustainable blue economy is, therefore, critical for achieving the goals of the European Green Deal (EC, 2019a) and securing a green and inclusive recovery from the pandemic. This was recognized by the adoption of a new EU sustainable blue economy strategy in May 2021, entitled "transforming the EU's blue economy for a sustainable future." The strategy sets the agenda for the transformation needed in the whole bioeconomy sector and for the integration of the blue economy in the Green Deal (EC, 2021).

Seventy percentage of the Earth's surface is sea and ocean. In order to meet EU targets and become carbon neutral by 2050, marine energy production is necessary. The marine renewable strategy can be a stepping stone for the energy transition. Energy independence is also important for local community development since it eases and promotes social inclusion. Through the Clean Energy Package (CEP) (EC, 2019b), the European Commission empowers citizens to push for the energy transition in order to facilitate that transition (Wahlund and Palm, 2022). According to the CEP, the "clean energy transition must benefit everyone—no citizen and no region should be left behind." Lennon et al. (2019) pointed out that the social dimension is just as important as technology in the debate on how to foster the energy transition. The current energy transition cannot use past models of exploitation of new energy sources, ignoring the environmental and social consequences (Lennon et al., 2019). The transition needs to be implemented differently: no longer top-down decisions but a participative process that includes all stakeholders (Lennon et al., 2019; Lange and Cummins, 2021; O'Connor et al., 2022). It is important to understand public perceptions of energy technologies in order to build a more sustainable future (Sutterlin and Siegrist, 2017; O'Connor et al., 2022).

Interpreting the results of the Interreg MED projects MAESTRALE, PELAGOS, InnoBlueGrowth, and BLUE DEAL, Bastianoni et al. (2020) highlighted four key elements to avoid conflicts with other uses and public opposition to blue energy implementation: 1) sustainability assessments; 2) inclusion of the public and local communities from the earliest stages of energy planning; 3) participatory energy planning; and 4) making technological solutions more attractive and compatible with the landscape.

Since public support for renewable energy is generally high, Marine Renewable Energy (MRE) could be viewed positively by citizens and policymakers (Goffetti et al., 2018; Karasmanaki and Tsantopoulos, 2021). To promote social acceptance, people need an overview of blue energy and the technologies deployed to harness it.

Various studies have been conducted on citizen perceptions and attitudes toward renewable energy installations (e.g., Peterson et al., 2015; Tampakis et al., 2017; Djurisic et al., 2020; Fisher et al., 2021; Macht et al., 2022); some include MREs (e.g., de Groot and Bailey, 2016; Howell, 2019; Lange and Cummins, 2021; Billing et al., 2022).

With respect to other areas and seas, the deployment of marine renewable energy by means of so-called blue energy (BE) technologies in the Mediterranean is in an early stage, and work is still needed on the best way to involve all actors and stakeholders and to remove barriers to its development. A key element of this process is public opinion, considered a determinant for blue energy exploitation in the Mediterranean. Agnew and coauthors (2022) demonstrated that the involvement of citizens and the broad stakeholder community is crucial for addressing social-environmental issues in coastal research. As demonstrated in other regions and countries (de Groot and Bailey, 2016; Howell, 2019; Hazboun and Boudet, 2020; Brandt, 2021), public participation is imperative for developing marine renewable energy.

The BLUE DEAL project (https://blue-deal.interreg-med.eu), funded by the Interreg Med 2014–2020 program and cofinanced by the European Regional Development Fund and the Instrument for Pre-Accession Assistance Fund, aims to promote the deployment of blue energy in the Mediterranean area. Twelve partners from six Mediterranean countries tested a set of solutions for raising awareness about the potential of Mediterranean marine energy resources and fostering their deployment. The guiding principle behind all the activities implemented by the BLUE DEAL project can be summed up in one concept: participation. Under this principle, the partnership addressed activities of the local government, SMEs, and citizens and provided guidelines for marine energy planning in marine areas and business development. The present survey on public perception of blue energy was conducted to involve citizens and to allow them to take an active part in planning and owning the installations. By knowing citizen perceptions of BE, policies can be tailored for acceptance of BE and for raising awareness to all the actors involved, thus favoring BE deployment.

With this aim, we developed and conducted a statistical survey on perceptions and attitudes of the general public to blue energy and technologies to harness it in 12 Mediterranean sites in the framework of BLUE DEAL project activities. The results were first used to draw lessons and suggestions for fine-tuning project activities locally (including communication with the general public) and second, to understand how BE technologies are perceived in different countries/regions and

to what extent local communities are inclined to invest in BE (e.g., through popular shareholding). The results also outlined a model for a general understanding of the perceptions of Mediterranean populations toward blue energy.

In addition to the BLUE DEAL activity, the data from the survey can give policymakers and stakeholders (regional and local authorities, SMEs, and research centers) an overview of concerns to be considered in spatial planning and energy projects.

Here, we present the results of the survey on perceptions of BE gathered during the BLUE DEAL project in specific Mediterranean coastal areas of partner countries. It is the first harmonized survey on BE in a multi-country contest, a novelty in this domain and for current statistical databases. The data were used to understand the opinions of the public on renewable energy deployment, in the hope of raising awareness of marine energy potential, in addition to its main purpose of informing decision makers. The specific website with the scientific results of the survey and guidelines for replication can be visited at http://askyourcitizenonbe.unisi.it.

Unlike the literature mentioned previously, which used various statistical methods and carried out assessments in one or more countries, the present study describes results obtained by interviewing almost 3,000 citizens, analyzed with the same statistical method in all 12 locations. The survey was created for extensive application (not specifically for the 12 locations), in order to ensure replicability. The datasets can be further increased by including the southern shore and the whole MENA region, to obtain a complete picture of how the Mediterranean population perceives BE. The main novelty and outcomes of this research are, however, the methodology used, the representative nature of the opinions sampled, and the fact that anyone can access the data and replicate the survey.

Section 2 of the study describes the rationale and method used for the survey; Section 3 gives the empirical results, and outlines the utility and key characteristics of the portal. The last section sets out the main conclusions and learning outcomes.

2 Materials and methods

Studying attitudes toward MRE and using them in decision-making calls for an approach that explores how people perceive and evaluate MRE in different environmental, economic, and social circumstances (Ede Groot and Bailey, 2016). Biermann (2007) suggested that research methods should be integrative and use qualitative, case-based, contextual, and thoughtful approaches.

In the present research, our aim was to produce highly comparable results. Our first step was to create a common questionnaire with guidelines. The guidelines helped partners of the BLUE DEAL project to select the sample of persons to interview, the locations, and how to conduct the interviews. The questionnaire and guidelines ensured that the results could be compared and interpreted as a whole.

In the recent literature, there are some sample survey formats on sustainable agriculture (Verma et al., 2010) and other surveys on sustainable development in general. This study presents the first format on BE, to be conducted in four phases:

1) choosing the areas to conduct the survey;
2) preparing the prototype questionnaire and translating it into local languages;
3) selecting the gross sample by stratified systematic sampling of addresses;
4) fieldwork.

2.1 Choosing the study area

The first basic decision was to choose the areas for the survey. The areas had to be candidates for marine energy installations. They could be islands or parts of islands, coastal areas, cities, or parts thereof. The chosen areas need to have populations between 1,500 and 15,000. The upper limit is recommended when analyzing larger cities with a focus on coastal neighborhoods or harbor areas. For example, in Tuscany, Italy, we chose the Giglio Island, which has a population of 1,500, so the whole island was sampled.

2.2 Preparing the prototype questionnaire

At the same time, we prepared a prototype questionnaire on the basis of the questionnaire used in the MAESTRALE project. The survey was designed to collect the opinions of the coastal populations regarding marine energy installations, their knowledge of blue energy, and the new technologies for its deployment. The active participation of citizens in the energy transition is a crucial element of blue energy planning. This is why we investigated the social acceptance of blue energy.

The survey questionnaire consisted of 14 questions in a closed-scale form and was divided into three sections aimed to determine the following:

- The social and demographic metrics of respondents: sex, age, place of residence, and employment status, to define their profile (questions 1–6);
- How much they knew about climate change, marine renewable technologies, and environmental issues (questions 7–10);
- Whether respondents had a positive attitude toward certain technologies to harness blue energy. Questions 11–14 concerning willingness to accept floating monopile horizontal-axis wind turbines, submarine kites, oscillating water column plants, floaters fixed to piers, and

clusters of oscillating buoys, as well as their perception of negative impacts and their expectation of a better future due to the implementation of technologies for the deployment of renewable energy resources. Questions 12 and 13 investigated respondents' perceptions about strengths, weaknesses, opportunities, and threats associated with such technologies and their level of concern about the impacts of such technologies on the environment and socio-economic context. The last question (14) investigated the perceived impacts of the deployment of blue energy with regard to future job opportunities and socio-economic and environmental benefits.

The questionnaire was then translated into local languages.

2.3 Gross sample selection and fieldwork

In almost all international surveys, such as those of Eurostat, general implementation rules are defined at the central level in order to obtain comparable data; the single countries that partake in the surveys apply them according to their particular situations. In this survey, we proceeded in the same manner. We now describe the general sampling method with some numerical examples for clarification. Every single site applied the implementation rules according to their specific geographical diversity.

The sampling method chosen for the survey was two-stage sampling: in the first stage, addresses were selected by stratified systematic sampling; in the second stage, one member of the household was chosen to be the respondent.

Stratification (Verma, 1991) means dividing the Primary Sampling Units (PSUs) of the population into groups and then selecting a sample independently from each group. The PSUs of the first stage were addresses, and there was a one-to-one correspondence with the persons selected, which were our Secondary Selection Units (SSUs). This made it possible to separate control over the design and selection of the sample in each stratum. The PSUs have to be divided into homogeneous, mutually exclusive, and collectively exhaustive subgroups or strata, using some stratification variable, in order to have homogeneous elements in each stratum. However, a high degree of heterogeneity exists between strata. So far, as the strata represented relatively homogeneous groupings of units, the resulting sample was made more efficient by ensuring that units from each grouping were appropriately represented in a controlled way. The most common type of stratification is geographic stratification according to the type of place (urban-rural or by the degree of urbanization or size of locality or types of dwelling, etc.), location (province, region, or other administrative division), and climatic or ecological zone. Such stratification is simple and requires little auxiliary information. Once the strata are defined, an independent sample is collected from each stratum and the final sample is formed by consolidating all sample elements chosen in each stratum. With stratified sampling, greater precision than for simple random sampling can be gained with smaller sample sizes. Most frequently, the selection of the PSUs in each stratum is proportionate such that the ratio of sample elements from each stratum to sample size equals the ratio of the population elements in each stratum to the total number of population elements.

Within each stratum, the selection of PSUs was carried out by systematic sampling. Systematic sampling (Verma, 1991) is a type of probability sampling in which sample units from a population are selected according to a random starting point but with a fixed, periodic interval. This interval, called the sampling interval, is calculated by dividing the population size by the desired sample size. Figure 1 shows an example of systematic sampling where one in every three units is selected.

Systematic sampling from ordered lists is cheap and efficient; in particular, when the order of selection is geographical, systematic sampling introduces additional (implicit) stratification and therefore, improves its efficiency. During implementation, the procedure tends to be much simpler than selection using random numbers.

Addresses were the PSUs of the proposed sampling method. This meant that in each separate stratum, systematic sampling

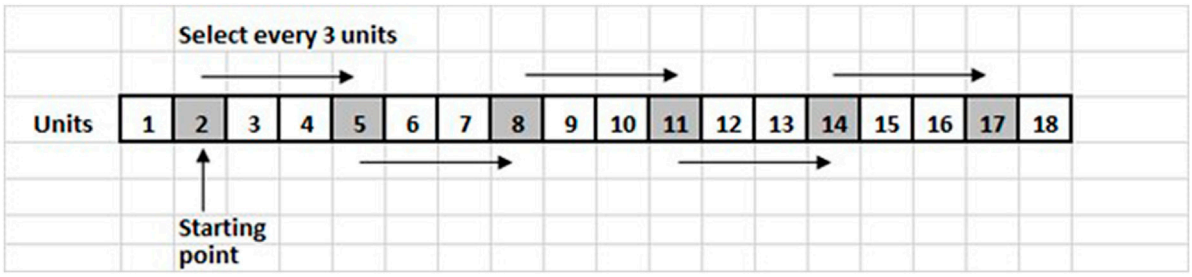

FIGURE 1
Selection of one unit in three.

had to be applied to all the addresses in the stratum so that the selection was of addresses. The result of the first stage of this sampling strategy is a sample of addresses.

The second stage of sampling was the selection of one person to interview at each address [examples of similar sampling can be found in Jaenson et al. (1992) and McMichael et al. (2013)]. The first adult in the house who agreed to be interviewed was selected.

2.4 Fieldwork: Practical description

The chosen coastal/island area was divided into ten blocks or strata. Each stratum had as nearly as possible the same population (e.g., Figure 2).

Each stratum should contain homogeneous units, i.e., similar types of dwellings; it may be an urban or rural area, a village, different neighborhoods of a city, a residential or commercial neighborhood, and an area with only condos or with contiguous or independent houses. It is important that the boundaries of each stratum are clearly defined (EUROSTAT, 2018).

$$N = 5000$$

$$n1 \approx n2 \approx n3 \approx n4 \approx n5 \approx n6 \approx n7 \approx n8 \approx n9 \approx n10 \approx 500$$

$$n1 + n2 + n3 + n4 + n5 + n6 + n7 + n8 + n9 + n10 = 5000.$$

Subdivision of the area may be performed using maps, such as satellite or street maps. The map should be as accurate as possible with a scale appropriate for the size of the area. An example of stratification is reported for the Giglio Island.

Giglio is a very small island with a population of about 1,500. It was divided into 10 strata with populations of about 150 each. The sat map (Figure 3) shows that there are about four residential areas and the rest of the island is rural. We first identified urban/rural strata; two rural areas (north and south) were identified.

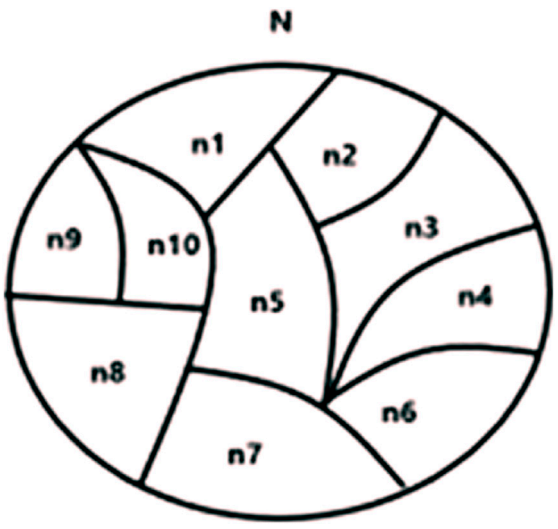

FIGURE 2
If the area chosen has a population of 5,000, the 10 strata must each have a population of about 500.

Then, each of the four urban areas was divided into a total of eight strata. The example of Giglio Porto divided into four strata is shown in Figure 3.

The next step was the selection of addresses by systematic sampling, independently for each stratum. The final sample chosen for each site involved about 200 interviews; to allow for nonresponses, we doubled the sample size. A total of 400 addresses were selected, i.e., 40 addresses per stratum. So for an area with a population of about 5,000, 500 per stratum, we had to select roughly one in every five addresses.

The next step was choosing a starting point for the selection of addresses. Once the first address in a stratum is chosen, the person doing the fieldwork has to cover all the streets of the stratum on foot, selecting one address in every five addresses (e.g., Figure 4, left side). Different paths are possible, as shown in Figure 4, right side.

Each address that was selected was recorded on a template database with the name of the family that appeared at the location and the full address. A letter was left in the mailbox of the selected family, informing its members about the survey and that an interviewer would contact them in the following days.

After this step, the fieldwork began. Trained and supervised interviewers with official badges visited the selected addresses and conducted computer-assisted personal interviews. To enhance response rates, the interviewers behaved as suggested by Hox and Leeuw (2002): 1. appear trustworthy; 2. appear friendly; 3. adapt to the situation at the doorstep; 4. react to the respondent.

A template with the full list of selected addresses and names of the families was provided to the interviewers. On the template, the interviewers recorded the outcome of the interviews as follows: interview completed, interview rejected, and family not present. In the latter case, the interviewer tried to contact the family three times at different hours and on different days: once in the morning, once in the evening, and once on the weekend. If the family was never found, it was recorded as 'not present.'

3 Results and discussion

The survey was conducted in 12 Mediterranean locations: Civitavecchia (IT), Giglio Island (IT), Livorno (IT), Valencia (ES), Granada (ES), Malta (MT), Crete (GR), Durres (AL), Larnaca (CY), Ciovo Island (HR), Dubrovnik (HR), and Koper (SI). The sample size was about 200 units per area; at the end of the fieldwork, 2,843 answers had been collected (Table 1).

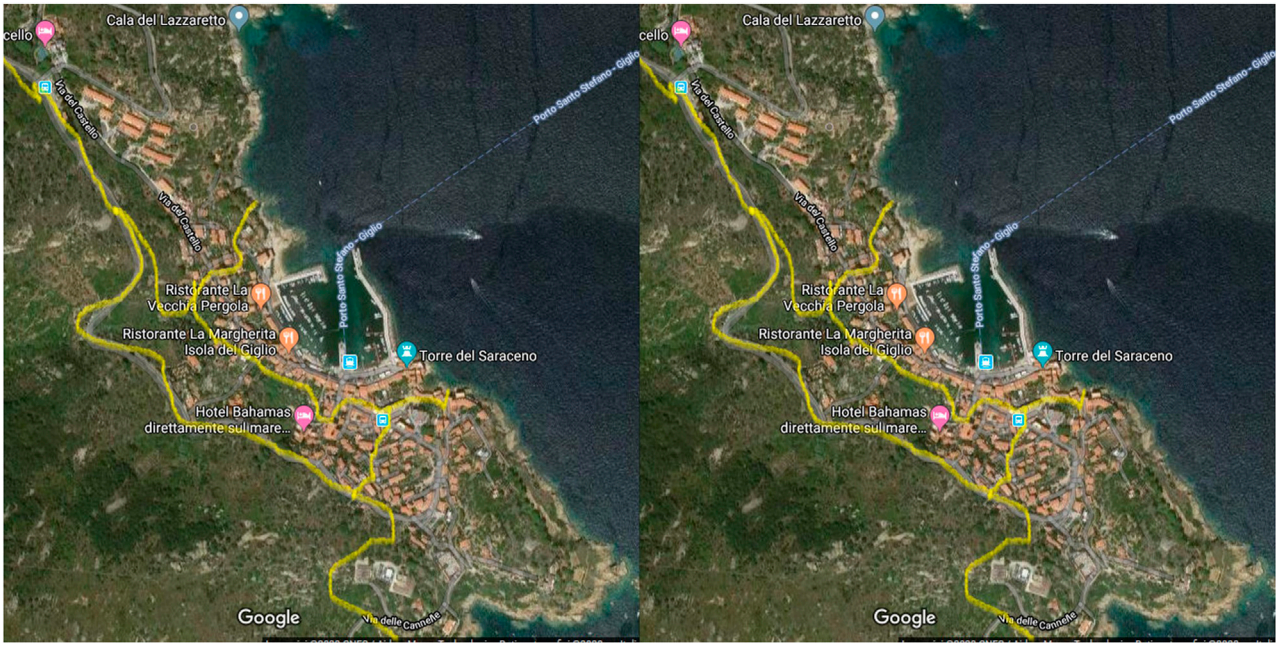

FIGURE 3
Identification of urban and rural areas of the Giglio Island and division of the urban area of Giglio Porto into four strata.

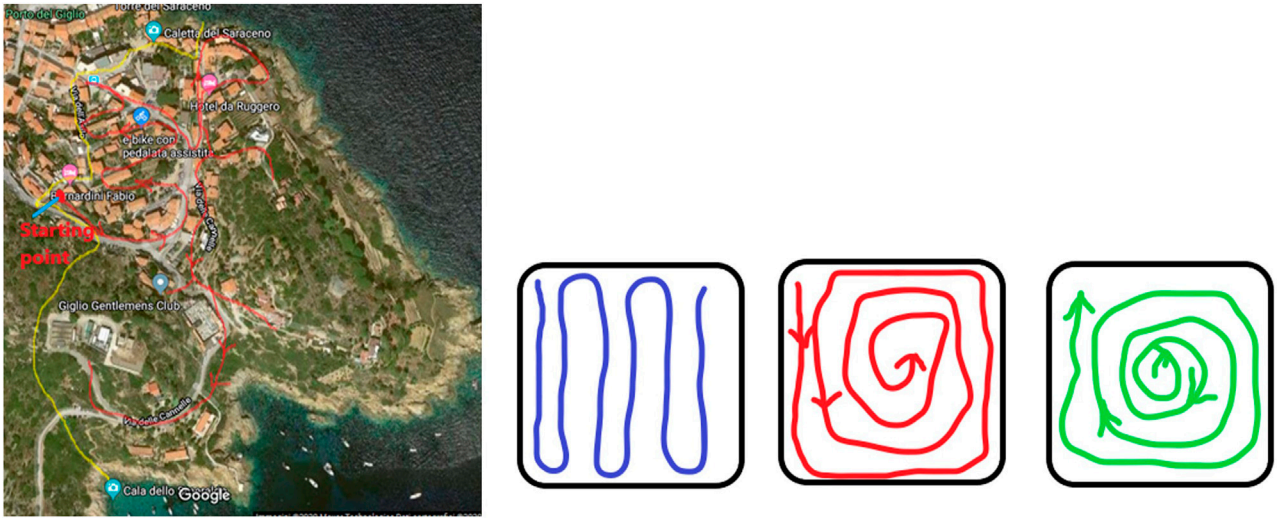

FIGURE 4
Example of a path for a stratum of the Giglio Island and examples of different paths that could be chosen for the same area.

Respondents were nearly equally distributed by gender and quite similarly by age classes (32% 18–39 years, 38% 40–59, and 28% over 60); 48.5% worked but not in the maritime industry, nearly 39% did not work, and about 13% worked in the maritime industry.

Regarding respondent awareness of climate change issues, 65% were aware and believed something needed to be implemented; this percentage was higher for young respondents, confirming a known trend: young people are

TABLE 1 Sample sizes by site.

Site	Achieved sample size (PSUs and SSUs)
Civitavecchia (IT)	200
Giglio Island (IT)	145
Livorno (IT)	198
Pobla de Farnals (ES)	202
Granada (ES)	200
Malta (MT)	204
Crete (GR)	200
Durres (AL)	452
Larnaca (CY)	208
Ciovo Island (HR)	300
Dubrovnik (HR)	302
Koper (SI)	232

more susceptible to climate change concerns. Surprisingly, respondents who worked in the maritime industry scored the lowest awareness of climate change issues.

Regarding the environmental impact of current use and production of energy, two-thirds of respondents believed it is necessary to reduce household energy consumption and to produce energy from renewable resources in order to reduce environmental impact, while one-quarter of respondents only believed it is necessary to produce energy from renewable resources.

Regarding knowledge and perceptions of blue energy among respondents, more than half did not know about marine renewable energy. The percentage was higher among women, about two-thirds of whom did not know about blue energy. Again, a higher percentage of young respondents knew about blue energy, confirming their higher awareness of this topic.

Then, a set of five blue energy technologies was proposed to respondents, and their support for such installations was investigated: 1. a floating wind turbine to harness wind energy; 2. submarine kites to harness the energy of marine currents; 3. an oscillating water column plant installed on a pier to harness wave energy; 4. a set of floaters fixed to a pier to harness wave energy; 5. a cluster of oscillating buoys to harness the energy of waves offshore (see Figure 5).

All the technologies found strong support (Figure 6), especially the oscillating water column plant installed on a pier. They also considered this installation the least invasive.

The two preceding results showed that there could be a visual impact issue concerning support for blue energy installations. The next question investigated this point. Five issues of blue energy installations were suggested to respondents: noise, impact on fauna and flora, visual impact, negative effects on tourism, and negative effects on fishing. All issues were chosen by nearly half the

FIGURE 5
Proposed blue energy installations.

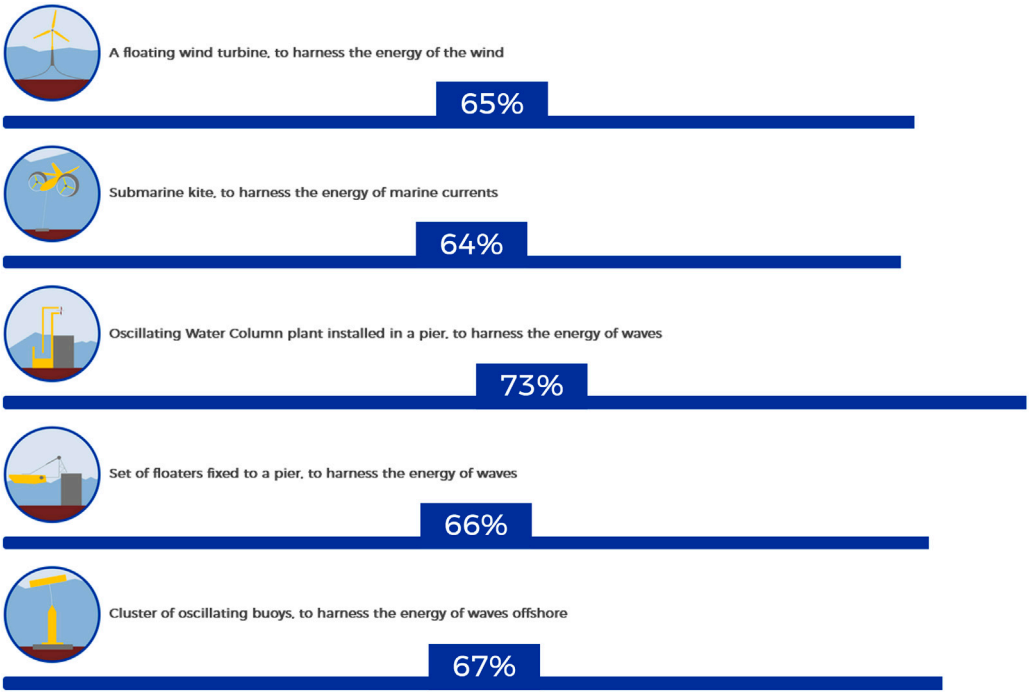

FIGURE 6
Support for technologies.

respondents. The highest concern was the impact on fauna and flora (54%), followed by negative effects on fishing (52%), noise (49%), visual impact (47%), and negative effect on tourism (40%); no significant differences were found between males and females.

The last question concerned hopefulness about the positive effect of BE installations. Here, the five options presented to respondents were new jobs, energy independence, climate change mitigation, reduction of local pollution, and impetus for innovative start-ups. Quite strong expectations were found for all: nearly 77% were hopeful about new jobs and energy independence, and about two-thirds of respondents were hopeful about climate change mitigation, reduction of pollution, and innovative start-ups.

Results of the present survey cannot be directly compared with results of other similar studies because different sampling methods and questionnaires were developed and adopted. Nevertheless, lessons learned can be compared and drawn. Lange and Cummins (2021) suggested the need to find a proper framework closer to local communities to accommodate large infrastructure development. In this light, the survey implemented by the BLUE DEAL project could be read as an example of the involvement of local and coastal communities in the decision-making process to be widely replicated. Findings of Howell (2019) for Scotland (United Kingdom) are on the same line, describing that blue energy technologies that were perceived as a positive benefit for local areas were welcomed by local communities. One of the questions included in the BLUE DEAL questionnaire is devoted to understanding which technology is the most preferred, thus demonstrating that focusing on the opinion of citizens is considered the starting point for energy planning. Billing et al. (2022) investigated the public perception of a peculiar integration between blue energy technologies and fish farming in Italy and Scotland (United Kingdom). Nevertheless, their main findings confirm the importance of correct information about the local communities and their involvement as a milestone to have a positive reply from the citizens. Devine-Wright (2011), de Groot and Bailey (2016), and Brandt (2021), assessing the public perception of blue energy technology in Oregon (United States), Ireland (IE), and the United Kingdom, highlighted the role of the communities' perception of local landscape value as one of the drivers for acceptance of blue energy. The BLUE DEAL questionnaire indirectly addressed this issue by asking citizens which technology is felt as less invasive, thus recognizing the importance of the preservation of the local landscape as of fundamental importance. Hazboun and Boudet (2020) carried out a comparative study to understand the public opinion and preference across a broad suite of energy sources, including both renewable and nonrenewable resources in British Columbia, Canada, and Washington and Oregon, United States. Even though the main aim of their research was broader than the survey

carried out in the BLUE DEAL project, their main finding is aligned with the lesson learned by the BLUE DEAL project. In fact, as a final recommendation for policymakers, the authors stressed the importance of raising awareness and community involvement during the planning process.

Even a numerical comparison among the results obtained by the BLUE DEAL project for the Mediterranean countries and other studies and territories was not possible. Lessons learned and the main outcomes demonstrated the alignment of general findings and recommendations.

3.1 The portal

The site http://askyourcitizenonbe.unisi.it, which publishes the results, is an important product of the survey. An interface with the site includes one- and multi-dimensional statistical indicators and data processing using artificial intelligence techniques. The results are reported in the specific dashboard section with the details of the 12 sites. A data section by the macro-area is included in the dashboard. There is a "BUILD MY GRAPHS" section for a dynamic database. The tools for the main statistics and synthesis of the results for each location have a graphic interface, including a freely downloadable pdf.

The dashboard section was designed to be as simple as possible with predisposed processing and custom graphic options. On the first page (Figure 7), the first main overall statistics are available, such as the number of respondents and the percentage of respondents who were aware of climate change and believe something needs to be implemented. Users simply click symbols such as those shown in Figure 8.

FIGURE 7
First page of the dashboard.

FIGURE 8
Symbols on the dashboard.

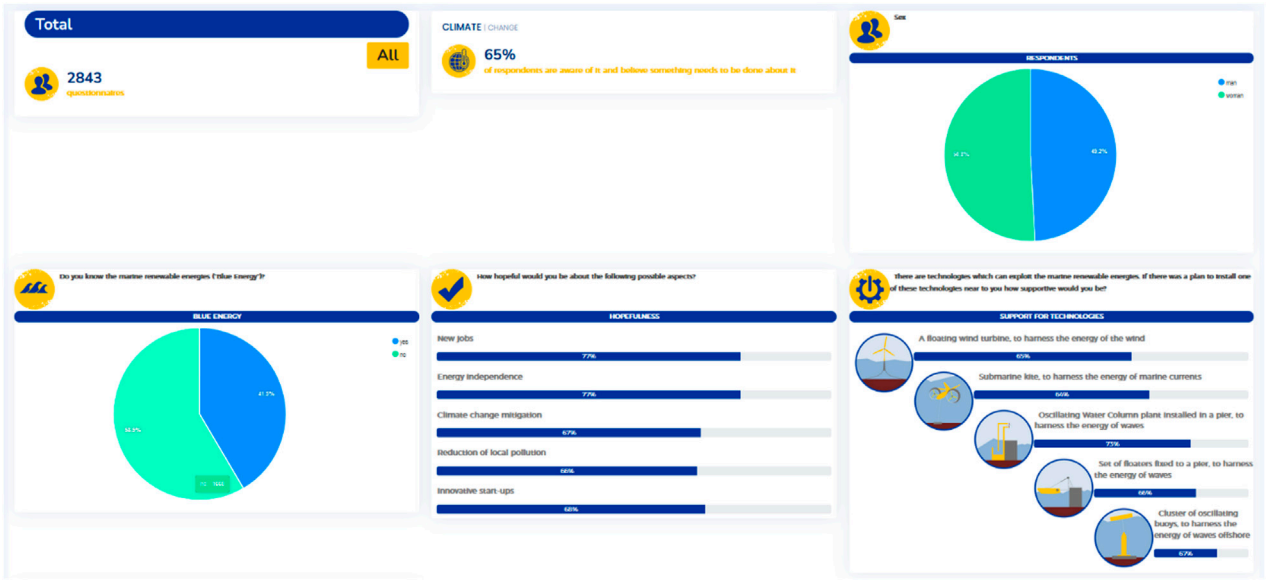

FIGURE 9
Screenshot of the short report and pdf.

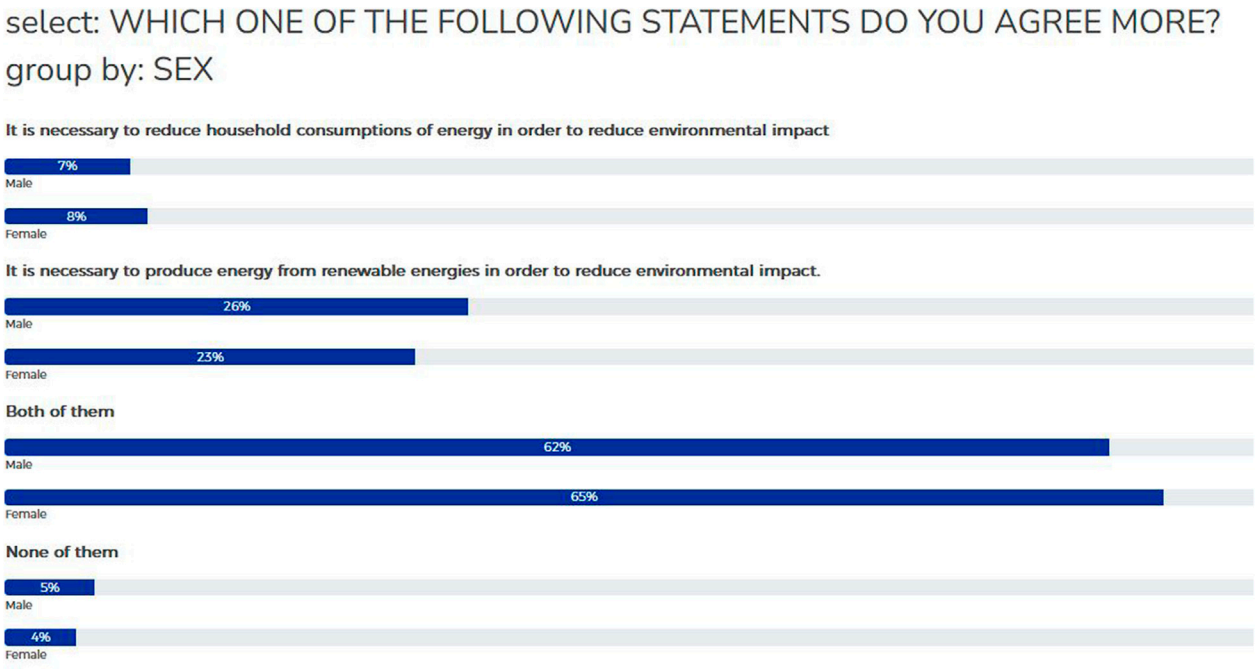

FIGURE 10
Example of selection from MyDashboard.

Although the overall statistics appear on the first page of the dashboard, the site is designed to have the same graphs at site and area levels.

It is also possible to create selected short reports *ad hoc* at overall, site, or area levels and to download them in the pdf format. There is also an option to create a standard report with graphs at an aggregate level for each section (Figure 9).

The online dashboard is designed so that users can create graphs and perform selected analyses. In the section MyDashboard (e.g., Figure 10), it is possible to build all sorts of charts and double-entry tables. Users can even group sites or create customized areas and download all the reports. With a single click, all the graphs of the answers to the entire questionnaire can be visualized at the same time. There is also the possibility to analyze the correlation between two variables with double-entry tables: the user simply chooses the question of interest (select), grouping it (group by) by variable to find correlations, and the result is a graph made up of as many bar graphs as there are characteristics of the second variable. All analyses can be downloaded in the pdf format.

4 Conclusion

This study presents the empirical results of a survey on the general public's perceptions and attitudes toward blue energy technologies in nine regions involved in the BLUE DEAL project. The results underline that a small majority of respondents do not know what blue energy is, albeit with differences according to the target site. However, although citizens were relatively unaware of blue energy, respondents were generally favorable to the installation of technologies to harness marine energy. Of the five technologies mentioned, oscillating water columns installed in piers were the most widely accepted, followed by oscillating buoys. Regarding concerns about the possible installation of one or more blue energy plants in their area, respondents expressed concern about all the impacts investigated, especially the impact on flora and fauna. Regarding local opportunities that the implementation of blue energy technologies could offer, respondents were hopeful about new jobs and energy independence.

To a certain extent, this survey in the first phase of the BLUE DEAL project tackled all the main aspects highlighted by the European Commission in its communication regarding strategies to harness potential offshore renewable energy for a climate-neutral future (EC, 2020). Indeed, it exemplifies the involvement of local people from the very start of energy planning with new technologies.

The results of the survey are an instrument to enable policymakers to obtain more knowledge on public perception of blue energy, set up concrete actions for developing blue energy in the Mediterranean area, and reach a wider audience. The scientific approach used to implement the survey showed that citizens are willing to participate in local planning and be involved in the energy transition from the earliest stages. In other words, the implementation of the survey put the social dimension of sustainability into practice. The social dimension is key to the success of any policy aimed at environmental sustainability.

The survey implemented in the framework of the BLUE DEAL project and the creation of the digital platform will allow other policymakers to implement the questionnaire in their regions of interest, increasing the dots on the Mediterranean map and making it possible to map Mediterranean citizens' perceptions of blue energy.

Data availability statement

The datasets presented in this study can be found in online repositories. The names of the repository/repositories and accession number(s) can be found at: http://askyourcitizenonbe.unisi.it/dashboard/Aindex.php?F=fase1&VAR=T&TYPEVAR=TOTAL.

Author contributions

All authors listed have made a substantial, direct, and intellectual contribution to the work and approved it for publication.

Funding

The study was conducted in the framework of the Interreg Med BLUE DEAL (2019–2022) project, co-financed by the European Regional Development Fund and the Instrument for Pre-Accession Assistance Fund. Website: https://blue-deal.interreg-med.eu.

Conflict of interest

The authors declare that the research was conducted in the absence of any commercial or financial relationships that could be construed as a potential conflict of interest.

Publisher's note

References

Agnew, S., Kopke, K., Power, O. P., Troya, M. D. C., and Dozier, A. (2022). Transdisciplinary research: Can citizen science support effective decision-making for coastal infrastructure management? *Front. Mar. Sci.* 9, 809284. doi:10.3389/fmars.2022.809284

Bastianoni, S., Praticò, C., Damasiotis, M., and Pulselli, R. M. (2020). Perspectives for marine energy in the mediterranean area. *Front. Energy Res.* 209. doi:10.3389/fenrg.2020.00209

Biermann, F. (2007). 'Earth system governance' as a crosscutting theme of global change research. *Glob. Environ. Chang.* 17 (3-4), 326–337. doi:10.1016/j.gloenvcha.2006.11.010

Billing, S. L., Charalambides, G., Tett, P., Giordano, M., Ruzzo, C., Arena, F., et al. (2022). Combining wind power and farmed fish: Coastal community perceptions of multi-use offshore renewable energy installations in Europe. *Energy Res. Soc. Sci.* 85, 102421. doi:10.1016/j.erss.2021.102421

Brandt, D. (2021). *A current look at marine renewable energy in Oregon: Oregon MRE and the role of public perception and participation in Oregon's MRE future*. [Master Thesis], Corvallis, OR: Oregon State University.

de Groot, J., and Bailey, I. (2016). What drives attitudes towards marine renewable energy development in island communities in the UK? *Int. J. Mar. Energy* 13, 80–95. doi:10.1016/j.ijome.2016.01.007

Devine-Wright, P. (2011). Place attachment and public acceptance of renewable energy: A tidal energy case study. *J. Environ. Psychol.* 31 (4), 336–343. doi:10.1016/j.jenvp.2011.07.001

Dhivagar, R., Shoeibi, S., Kargarsharifabad, H., Ahmadi, M. H., and Sharifpur, M. (2022). Performance enhancement of a solar still using magnetic powder as an energy storage medium-exergy and environmental analysis. *Energy Sci. Eng.* doi:10.1002/ese3.1210

Djurisic, V., Smolovic, J. C., Misnic, N., and Rogic, S. (2020). Analysis of public attitudes and perceptions towards renewable energy sources in Montenegro. *Energy Rep.* 6, 395–403. doi:10.1016/j.egyr.2020.08.059

European Commission (2019a). *Communication from the commission to the European parliament*. Brussels: European Council, the CouncilFIN. the European Economic and Social Committee and the Committee of the Regions: The European Green Deal. Communication no. COM/2019/640. Brussels: European Commission. Available online at: https://eur-lex.europa.eu/legal-content/EN/TXT/?uri=COM:2019:640.

European Commission (2019b). *Clean energy for all Europeans*. Luxembourg: Publications office of the European Union.

European Commission (2020). Communication from the commission to the European parliament, the European council, the council, the European economic and social committee and the committee of the regions: An EU strategy to harness the potential of offshore renewable energy for a climate neutral future. Available at: https://eur-lex.europa.eu/legal-content/EN/TXT/PDF/?uri=CELEX:52020DC0741&from=EN.

European Commission 2021. Communication from the commission to the European parliament, the European council, the council, the European economic and social committee and the committee of the regions: Transforming the EU's blue economy for a sustainable future. Available online at: EUR-Lex – COM:2021:240:FIN – EN – EUR-Lex (europa.eu)

EUROSTAT (2018). European social survey round 9 sampling guidelines: Principles and implementation. *ESS Sampl. Weight. Expert Panel.*

Fischer, B., Gutsche, G., and Wetzel, H. (2021). Who wants to get involved? Determining citizen willingness to participate in German renewable energy cooperatives. *Energy Res. Soc. Sci.* 76, 102013. doi:10.1016/j.erss.2021.102013

Gilani, H. A., Hoseinzadeh, S., Karimi, H., Karimi, A., Hassanzadeh, A., and Garcia, D. A. (2021). Performance analysis of integrated solar heat pump VRF system for the low energy building in Mediterranean island. *Renew. Energy* 174, 1006–1019. doi:10.1016/j.renene.2021.04.081

Goffetti, G., Montini, M., Volpe, F., Gigliotti, M., Pulselli, F. M., Sannino, G., et al. (2018). Disaggregating the SWOT analysis of marine renewable energies. *Front. Energy Res.* 138. doi:10.3389/fenrg.2018.00138

Hazboun, S. O., and Boudet, H. S. (2020). Public preferences in a shifting energy future: Comparing public views of eight energy sources in north America's pacific northwest. *Energies* 13 (8), 1940. doi:10.3390/en13081940

Howell, R. J. (2019). *In sight and in mind: Social implications of marine renewable energy*. [PhD thesis]. Edinburgh (UK)]: The University of Edinburgh.

Hox, J., and De Leeuw, E. (2002). "The influence of interviewers attitudes and behaviour in household non-response," in *Survey nonresponse*. Editors R. Groves, D. Dillman, J. Eltinge, and R. Little (London: Wiley).

Jaenson, R., Bassuk, N., Schwager, S., and Headley, D. (1992). A statistical method for the accurate and rapid sampling of urban street tree populations. *J. Arboric.* 18 (4), 171–183.

Karasmanaki, E., and Tsantopoulos, G. (2021). Public attitudes toward the major renewable energy types in the last 5 years: A scoping review of the literature. *Low. Carbon Energy Technol. Sustain. Energy Syst.*, 117–139. doi:10.1016/B978-0-12-822897-5.00004-3

Lange, M., and Cummins, V. (2021). Managing stakeholder perception and engagement for marine energy transitions in a decarbonising world. *Renew. Sust. Energy Rev.* 152, 111740. doi:10.1016/j.rser.2021.111740

Lennon, B., Dunphy, N. P., and Sanvicente, E. (2019). Community acceptability and the energy transition: A citizens' perspective. *Energy Res. Soc. Sci.* 9, 35. doi:10.1186/s13705-019-0218-z

Macht, J., Klink-Lehmann, J. L., and Simons, J. (2022). German citizens' perception of the transition towards a sustainable bioeconomy: A glimpse into the rheinische revier. *Sustain. Prod. Consump.* 31, 175–189. doi:10.1016/j.spc.2022.02.010

McMichael, J., Shook-Sa, B., Ridenhour, J., and Harter, R. (2013). "Chum: A frame supplementation procedure for address-based sampling," in Fed. Comm. Stat. Methodol. Res. Conf. Washington. D.C, November 4, 2013.

O'Connor, C. D., Fredericks, K., and Kosoralo, K. (2022). People's perceptions of energy technologies in an era of rapid transformation. *Environ. Innov. Soc. Trans.* 43, 331–342. doi:10.1016/j.eist.2022.04.010

Peterson, T. R., Stephens, J. C., and Wilson, E. J. (2015). Public perception of and engagement with emerging low-carbon energy technologies: A literature review. *MRS Energy Sustain* 2. doi:10.1557/mre.2015.12

Shoeibi, S., Ali Agha Mirjalily, S., Kargarsharifabad, H., Panchal, H., and Dhivagar, R. (2022a). Comparative study of double-slope solar still, hemispherical solar still, and tubular solar still using Al2O3/water film cooling: A numerical study and CO_2 mitigation analysis. *Environ. Sci. Pollut. Res.*, 1–17. doi:10.1007/s11356-022-20437-1

Shoeibi, S., Kargarsharifabad, H., Mirjalily, S. A. A., and Zargarazad, M. (2021). Performance analysis of finned photovoltaic/thermal solar air dryer with using a compound parabolic concentrator. *Appl. Energy* 304, 117778. doi:10.1016/j.apenergy.2021.117778

Shoeibi, S., Kargarsharifabad, H., Sadi, M., Arabkoohsar, A., and Mirjalily, S. A. A. (2022b). A review on using thermoelectric cooling, heating, and electricity generators in solar energy applications. *Sustain. Energy Technol. Assess.* 52, 102105. doi:10.1016/j.seta.2022.102105

Sütterlin, B., and Siegrist, M. (2017). Public acceptance of renewable energy technologies from an abstract versus concrete perspective and the positive imagery of solar power. *Energy Policy* 106, 356–366. doi:10.1016/j.enpol.2017.03.061

Tampakis, S., Arabatzis, G., Tsantopoulos, G., and Rerras, I. (2017). Citizens' views on electricity use, savings and production from renewable energy sources: A case study from a Greek island. *Renew. Sust. Energy Rev.* 79, 39–49. doi:10.1016/j.rser.2017.05.036

Verma, V., Ghellini, G., and Betti, G. (2010). "Area sampling for small-scale economic units," in *Agricultural survey methods*. Editors R. Benedetti, M. Bee, G. Espa, and F. Piersimoni (John Wiley & Sons, Ltd), 85–106.

Verma, V. (1991). *Sampling methods*. Tokyo: Statistical Institute for Asia and Pacific.

Wahlund, M., and Palm, J. (2022). The role of energy democracy and energy citizenship for participatory energy transitions: A comprehensive review. *Energy Res. Soc. Sci.* 87, 102482. doi:10.1016/j.erss.2021.102482

Frontiers in Energy Research

Advances and innovation in sustainable, reliable and affordable energy

Explores sustainable and environmental developments in energy. It focuses on technological advances supporting Sustainable Development Goal 7: access to affordable, reliable, sustainable and modern energy for all.

Discover the latest Research Topics

See more →

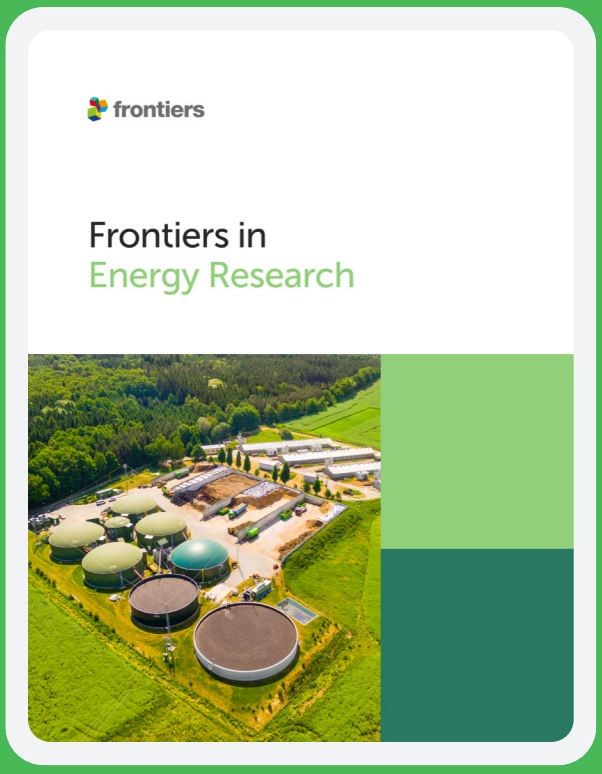

Frontiers

Avenue du Tribunal-Fédéral 34
1005 Lausanne, Switzerland
frontiersin.org

Contact us

+41 (0)21 510 17 00
frontiersin.org/about/contact